Universidade de Lisboa

Faculdade de Medicina de Lisboa

MICROCIRCULATION AND INFLAMMATION IN A NUMERICAL SIMULATION APPROACH

Ana Rosa Miranda dos Santos Silva Herdade

Orientador: Professor Doutor Ângelo Miguel Silva Calado

Tese especialmente elaborada para a obtenção do grau de Doutor em Ciências Biomédicas

Especialidade de Ciências Funcionais

2017

Universidade de Lisboa

Faculdade de Medicina de Lisboa

MICROCIRCULATION AND INFLAMMATION IN A NUMERICAL SIMULATION APPROACH

Ana Rosa Miranda dos Santos Silva Herdade

Orientador: Professor Doutor Ângelo Miguel Silva Calado

Tese especialmente elaborada para a obtenção do grau de Doutor em Ciências Biomédicas
Especialidade de Ciências Funcionais

Júri:
Presidente:

Professor Doutor José Luís Bliebernicht Ducla Soares, Professor Catedrático em regime de *tenure* e Vice-presidente do Conselho Científico da Faculdade de Medicina de Lisboa

Vogais:

Doutor Sayon Roy, *Professor of Medicine and Ophthalmology* da Boston University, School of Medicine, Estados Unidos da América;
Doutor Flávio Nelson Fernandes Reis, Investigador Principal da Faculdade de Medicina da Universidade de Coimbra;
Doutora Adélia da Costa Sequeira dos Ramos Silva, Professora Catedrática do Instituto Superior Técnico da Universidade de Lisboa;
Doutor Miguel Augusto Rico Botas Castanho, Professor Catedrático da Faculdade de Medicina da Universidade de Lisboa;
Doutora Maria Carlota Saldanha Lopes, Professora Associada com Agregação da Faculdade de Medicina da Universidade de Lisboa;
Doutor Ângelo Miguel Silva Calado, Professor Auxiliar da Faculdade de Medicina da Universidade de Lisboa; (*Orientador*).

2017

A impressão desta tese foi aprovada pelo Conselho Cientifico da Faculdade de Medicina de Lisboa em reunião de 18 de Outubro de 2016.

As opiniões expressas nesta publicação são da exclusiva responsabilidade do seu autor, não cabendo qualquer responsabilidade à Faculdade de Medicina de Lisboa pelos conteúdos nele apresentados.

Agradecimentos

“Aprender é a única coisa que a mente nunca se cansa, nunca tem medo e nunca se arrepende” by *Leonardo da Vinci*

E aprendemos em cada dia e com cada um com quem nos cruzamos. E é por isso que estes agradecimentos vão para todos aqueles que comigo cruzaram caminho e que por um motivo ou outro me ajudaram a aprender.

Agradeço de forma especial à Professora Carlota Saldanha que no meu estágio de licenciatura me recebeu no Instituto de Bioquímica e que sempre com uma grande vontade de transmitir conhecimento despertou em mim novos interesses de investigação e até capacidades que eu desconhecia ter.

Agradeço ao Professor Miguel Castanho pela confiança que em mim depositou a nível pedagógico e também pela ajuda na entrega deste trabalho.

À Professora Adélia Sequeira, com quem a estreita colaboração permitiu a realização de todo este trabalho e a minha constante busca de mais desenvolvimentos nesta temática de investigação.

Agradeço ao Ângelo, meu orientador, pelo apoio científico, por sua paciência ao longo de todo este tempo e por todas as revisões destes textos.

À Vanda pela sua ajuda enquanto esteve perto e pelo seu constante apoio já mais ao longe.

A todos os meus outros colegas mais diretos, Teresa, Patrícia, Sofia e Henrique agradeço toda ajuda que por diferentes motivos me deram quando necessário.

Agradeço à minha mãe, por todo o apoio, insistência, carinho e amizade com que me ajudou ao longo destes anos. Aos meus filhos, Carolina, Sebastião, Mateus e Afonso, que não percebendo do que se trata são também parte desta história e por fim ao Tiago por tudo aquilo que é e me faz ser!

Abbreviations

Acronym	
ACh	Acetylcholine
AChE	Acetylcholinesterase
DAMP	Damage Associated Molecular Patterns
EEI	Erythrocyte elongation index
Ht	Hematocrit
i.p.	Intraperitoneal
i.s.	Intrascrotal
i.v.	Intravenous
ICAM	Intracellular Adhesion Molecule
IL-1β	Interleukin-1 beta
LFA-1	Leukocyte Function-Associated Molecule 1/ $\alpha_L \beta_2$
LPS	Lipopolysaccharide
NO	Nitric Oxide
PAF	Platelet Activating Factor
PAMP	Pathogen Associated Molecular Patterns
PMN	Polymorphonuclear Neutrophilic Granulocytes/ Neutrophil
PSGL-1	P-Selectin Glycoprotein Ligand-1
RBC	Red Blood Cell
TNF-α	Tumor Necrosis Factor-alpha
VLN	Velnacrine maleate
WBC	White Blood Cell

Contents

Resumo

A inflamação é a resposta do organismo para erradicar o agente de lesão ou infeção de modo a repor a homeostasia. Esta resposta requer a migração de populações leucocitárias específicas a partir da circulação sanguínea até à área inflamada. O recrutamento leucocitário constitui um processo celular complexo pelo qual os leucócitos são inicialmente recrutados para a parede endotelial das vénulas pós-capilares, através das quais extravasam posteriormente para os tecidos intersticiais. O recrutamento é mediado por interações celulares entre leucócitos e o endotélio e envolve uma série de etapas: *tethering*, rolamento, rolamento lento, detenção, rastejamento, adesão e transmigração. A adesão ou não dos leucócitos ao endotélio depende não só da interação entre moléculas de adesão na superfície dos leucócitos e das células endoteliais, mas também das forças físicas que atuam sobre estas. Nesta perspetiva, tem sido correntemente sugerido que o *shear stress* resultante do fluxo sanguíneo controla a atividade leucocitária, fazendo com que as propriedades de dinâmica de fluídos da circulação sanguínea sejam determinantes para o recrutamento e migração dos leucócitos durante a resposta inflamatória. A maioria dos estudos da resposta inflamatória, e em particular do recrutamento leucocitário, baseiam-se em modelos animais e têm envolvido a quantificação de mediadores inflamatórios e de células inflamatórias e/ou a análise das interações leucócito-célula endotelial por microscopia intravital. Porém, a contribuição da hemodinâmica para o recrutamento leucocitário tem sido raramente abordada devido ao facto do seu estudo em modelos animais não ser facilmente exequível e de não ser possível a determinação experimental de vários parâmetros hemodinâmicos devido a limitações técnicas. Estas limitações podem, porém, ser obviadas através do desenvolvimento e posterior utilização de simulações numéricas que descrevam o recrutamento leucocitário.

Muitos processos biológicos que ocorrem nos seres vivos podem ser expressos por formulações matemáticas. Este conceito é extensível ao recrutamento leucocitário para o qual existiam muito poucos modelos numéricos à data do começo deste trabalho de Doutoramento. De salientar, porém que as simulações matemáticas existentes então foram concebidas sem se considerarem simultaneamente todos os intervenientes no processo,

nomeadamente, o vaso sanguíneo, o fluxo sanguíneo e os leucócitos. Por outro lado, a maioria desses estudos são estudos bidimensionais, que não foram realizados com base em dados experimentais e em que o sangue é simplisticamente considerado como um fluido newtoniano com viscosidade constante.

Desta forma, este trabalho teve como objetivo principal compreender a contribuição da hemodinâmica para o recrutamento leucocitário na resposta inflamatória através do desenvolvimento e utilização de modelos matemáticos capazes de reproduzir adequadamente este processo. Para tal, desenvolveram-se modelos animais de inflamação de forma a obter os dados experimentais necessários ao desenvolvimento dessas simulações numéricas, que foram por fim utilizadas como ferramentas para o estudo da função da hemodinâmica no recrutamento leucocitário na resposta inflamatória.

A nossa abordagem inicial foi a de desenvolver simulações numéricas mais simplificadas, que assumissem os leucócitos como esferas rígidas e o sangue como um fluido não-newtoniano. Para tal, começou por se desenvolver um modelo animal de inflamação em ratos *Wistar* através da administração local de um lipopolissacárido (LPS) de modo a desencadear uma resposta inflamatória. Neste modelo, avaliou-se o número de leucócitos em rolamento e aderentes ao longo de 15 minutos por microscopia intravital e colheu-se sangue para a determinação da concentração sérica de TNF-α. ‘elativamente a este último parâmetro, verificou-se um aumento significativo das concentrações de TNF-α ao fim de 15 minutos, o que assegurou o normal desenvolvimento da resposta inflamatória, como esperado. Em relação ao estudo do recrutamento leucocitário, observou-se um aumento significativo do número de leucócitos em rolamento e adesão ao fim de 15 minutos. As imagens e parâmetros medidos por microscopia intravital foram posteriormente utilizados, em colaboração com grupo de matemáticos, para o desenvolvimento de uma ferramenta numérica capaz de descrever o recrutamento de leucócitos na microcirculação.

Considerando então o sangue como um fluido não-newtoniano e o leucócito como uma esfera rígida, utilizou-se o modelo de rede de *Boltzmann* para descrever a dinâmica de

fluídos. Para tal, utilizaram-se ainda os dados experimentais de viscosidade sanguínea, de modo a descrever o sangue como um fluido não-newtoniano, ou seja, dependente do *shear stress*. A partir das simulações numéricas obtidas foram analisados os perfis de velocidade e *shear stress* na superfície dos leucócitos e junto à parede endotelial em duas situações discretas, nomeadamente aquando do recrutamento para a parede vascular de um leucócito isolado ou de um conjunto de leucócitos. Na primeira situação, as simulações numéricas obtidas permitiram identificar na superfície do leucócito, regiões com *shear stress* distintos: uma região de *shear stress* elevado próxima da parede endotelial e duas regiões de *shear stress* baixo localizadas numa posição oposta na célula. Estas regiões de *shear stresses* distintos na superfície do leucócito parecem estar relacionadas com o necessário direcionamento dos leucócitos em relação à parede endotelial no decorrer da resposta inflamatória. A zona de *shear stress* mais elevado junto à parede vascular é consistente com os mecanismos moleculares responsáveis pelo rolamento dos leucócitos dado que corresponderá muito provavelmente à zona de ligação do leucócito ao endotélio. Por seu turno, as zonas de *shear stress* mais baixo poderão constituir áreas da superfície do leucócito em que não existe ligação ao endotélio e que permitem o rolamento da célula por este. Verificou-se ainda que na presença de um conjunto de leucócitos, o *shear stress* na parede do vaso aumenta. Este resultado sugere que a presença de um conjunto de leucócitos poderá gerar condições para que novos leucócitos possam ser recrutados e iniciem o seu rolamento em direção ao local da inflamação.

Embora possam ter permitido uma descrição aproximada do recrutamento leucocitário, as nossas simulações numéricas iniciais foram obtidas considerando-se os leucócitos como esferas rígidas. Pese embora os leucócitos mantenham a sua forma esférica em circulação, o seu formato é, no entanto, alterado em rolamento de modo a que possam aderir posteriormente à parede endotelial. Assim de modo a ter em conta as variações da deformabilidade do leucócito que ocorrem durante o seu recrutamento na resposta inflamatória, foi necessário obterem-se novas imagens de microcirculação em que se conseguisse diretamente captar o perfil de deformabilidade dos leucócitos de forma independente dos restantes tipos celulares em circulação. Para tal, efetuou-se microscopia intravital no cremáster de ratinhos transgénicos Lys-EGFP-ki, nos quais os neutrófilos apresentam sinal de fluorescência que permite que os seus movimentos possam ser monitoriza-

dos individualmente. Usando o Fator Ativador de Plaquetas (PAF) como agente inflamatório, a partir da análise das interações entre leucócitos e a parede endotelial observou-se um aumento significativo do número de neutrófilos em rolamento até cerca de 4 horas após a indução da inflamação, o que corrobora a existência de uma resposta inflamatória. O número de neutrófilos aderentes quantificado foi também superior 4 horas após a administração do estímulo inflamatório. Uma vez que as características do fluxo sanguíneo também influenciam o recrutamento leucocitário face à sua relação com a viscosidade sanguínea, estudou-se ainda o efeito da inflamação na deformabilidade eritrocitária neste modelo animal. Observou-se assim um contínuo decréscimo na deformabilidade eritrocitária ao longo do período de tempo em análise. A diminuição deste parâmetro eritrocitário originará consequentemente um aumento da viscosidade sanguínea, que será acompanhado por uma menor velocidade do fluxo. Estas condições hemodinâmicas deverão favorecer a migração dos neutrófilos para a parede endotelial durante o processo inflamatório, dado que uma menor velocidade de fluxo irá também contribuir para uma menor velocidade de rolamento, como esperado numa resposta inflamatória.

Como expectável, as imagens obtidas por microscopia intravital neste modelo de inflamação aguda permitiram-nos observar de forma direta a deformação dos neutrófilos ao longo da parede endotelial durante o seu rolamento, sendo ainda possível observar-se a formação de *tethers*. A partir destas imagens capturaram-se então as trajetórias dos neutrófilos, mediram-se as suas velocidades e diâmetros e estes dados foram depois aplicados a simulações numéricas. Usando um modelo matemático já validado que descreve a deformação de um leucócito em fluxo no interior de um microcanal, foram produzidas várias simulações numéricas considerando diferentes velocidades para o recrutamento de um leucócito individual ou de dois leucócitos e uma viscosidade sanguínea constante. A análise das simulações produzidas permitiu comprovar que a velocidade tem um papel importante no movimento, deformação e atração dos leucócitos, pois diferentes velocidades iniciais dão origem a padrões de rolamento diferentes. Em concreto, uma maior velocidade de rolamento origina uma quebra mais rápida das ligações nos locais de contacto com o endotélio, não favorecendo o rolamento dos leucócitos. Sugere-se assim que, durante o processo inflamatório, deva existir uma modificação das condições hemodinâmicas, nomeadamente um aumento do *shear stress*, capaz de "orientar" a célula para a

parede endotelial. Este processo levará a uma diminuição das velocidades de fluxo e consequentemente das velocidades de rolamento. Estes resultados são corroborados no nosso modelo experimental pela diminuição da deformabilidade eritrocitária que conduz necessariamente a uma diminuição da viscosidade sanguínea e por esta razão, a uma menor velocidade do fluxo sanguíneo. Este modelo numérico vem assim demonstrar que as características hemodinâmicas do fluxo e das células em circulação influenciam amplamente o rolamento e adesão dos leucócitos à parede endotelial e que eventuais alterações nas propriedades hemodinâmicas do fluxo irão influenciar diretamente a eficácia da resposta inflamatória. A partir da análise de dois leucócitos em fluxo foi possível verificar que a presença de um leucócito aderente leva à diminuição da velocidade do leucócito em rolamento em comparação com a situação em que se simula o recrutamento apenas de um leucócito. Sugere-se assim que a presença próxima de leucócitos aderentes deva diminuir a velocidade de rolamento de um dado leucócito, e assim promover o seu abrandamento e a sua captura pelo endotélio.

Globalmente, os nossos resultados experimentais e as simulações numéricas obtidas suportam a hipótese subjacente ao presente trabalho de que as propriedades hemodinâmicas do fluxo e das células em circulação desempenham uma função essencial na marginação e rolamento de leucócitos para a parede vascular, e que por essa forma, têm um impacto no sucesso da resposta inflamatória. Em particular, os nossos resultados sugerem fortemente que alterações nas condições hemodinâmicas como, a diminuição da velocidade de fluxo e o aumento do *shear stress,* contribuem para direcionar os leucócitos para a parede endotelial. A partir destes dados, propomos que quaisquer variações das propriedades hemodinâmicas deverão certamente influenciar a progressão e resultado final de uma resposta inflamatória. Como tal, a adesão dos leucócitos ao endotélio deverá depender não só da magnitude relativa das forças químicas geradas pela interação das moléculas de adesão entre os leucócitos e as células endoteliais, mas também das forças físicas que atuam sobre os primeiros. A este respeito, os nossos resultados sugerem que alterações do fluxo sanguíneo, como por exemplo na velocidade de fluxo, deverão ocorrer na resposta inflamatória de forma a potenciar um mais amplo recrutamento leucocitário para a área inflamada e assim contribuir para o sucesso da resposta inflamatória.

No cômputo final, as simulações numéricas produzidas neste trabalho permitiram-nos contribuir para a melhor compreensão da contribuição das propriedades hemodinâmicas do fluxo na progressão da resposta inflamatória e para aprofundar o nosso conhecimento sobre o recrutamento leucocitário na inflamação. De salientar que este trabalho permitiu obter ferramentas numéricas que num futuro próximo, nos permitiram estudar e modular os mais variados parâmetros hemodinâmicos envolvidos na resposta inflamatória. Em particular, estas simulações numéricas possibilitarão no imediato determinar e estimar um vasto conjunto de parâmetros que dificilmente seriam obtidos apenas por intermédio da experimentação in vivo e por outro lado, seguir a sua evolução ao longo da resposta inflamatória. Globalmente, os nossos resultados permitem ainda reforçar a noção de que o desenvolvimento de modelos animais e ferramentas numéricas pode fornecer à comunidade médica e científica um conjunto importante de ferramentas para o estudo do recrutamento leucocitário na inflamação. Ao reproduzirem a microcirculação e o processo inflamatório, estas ferramentas serão cruciais no futuro para se compreender de forma mais detalhada a complexidade do processo inflamatório e dos mecanismos subjacentes às mais diversas patologias de natureza inflamatória.

Palavras-chave

Leucócitos, microcirculação, inflamação, hemodinâmica, simulações numéricas

Abstract

Inflammation is the response of the organism to eradicate the agent of lesion or infection in order to achieve hemostasis. This response requires the migration of specific leukocyte populations from the blood circulation towards the inflamed area. Leukocyte recruitment constitutes a complex cellular process by which leukocytes are first recruited to the endothelial vascular wall of *post*-capillary venules across which they further extravasate into the interstitial tissue. Recruitment is mediated via cell-cell interactions between the leukocyte and the endothelium and occurs through a multi-step cascade: tethering, rolling, slow rolling, arrest, crawling, adhesion and transmigration. However, whether or not the leukocytes adhere to the endothelium depends not only on the chemical forces generated by adhesion molecules on leukocytes and endothelial cells, but also on the physical forces that act on those cells. It has been suggested that fluid shear stress resulting from blood flow also regulates leukocyte activity which makes the fluid dynamic environment of the circulation to be considered an important aspect for leukocyte recruitment and migration during the inflammatory response. Most of the studies on the inflammatory response and in particular on leukocyte recruitment are based on animal models and involve, among others, the quantification of inflammatory mediators and cellular players, and/or the analysis of the leukocyte-endothelial cell interactions by intravital microscopy. However, the contribution of hemodynamics for leukocyte recruitment has been seldom addressed in those studies. This is mostly due to the fact that the study of hemodynamics in *in vivo* animal models is not straightforward and moreover, that several hemodynamic parameters cannot be experimentally determined due to technical constraints. In this work, we reasoned that these limitations could be circumvented by the development and use of numerical simulations to describe leukocyte recruitment.

Many of the processes, which take place in living organisms, can be expressed as mathematical equations. This applies to leukocyte recruitment, for which scarce numerical models existed before the beginning of this work. Importantly, these mathematical simulations were performed without considering simultaneously all the players in the process, namely the vessel, the blood flow and the leukocytes. Moreover,

most of these studies were two dimensional, assumed blood as a Newtonian fluid with constant viscosity and did not take into account *in vivo* experimental data.

Taken this, our major goal with this work was to understand the contribution of hemodynamics to leukocyte recruitment in inflammation. For such purpose, we aimed here at developing numerical simulations that more adequately reproduced this process. For such, we set up animal models of inflammation to obtain the experimental data required for the development of those numerical simulations. Finally, we used these models to investigate the role of hemodynamics in leukocyte recruitment in inflammation.

First, we considered the simpler case of a numerical simulation that assumed leukocytes to be rigid spheres and blood, a non-Newtonian fluid. For such, we initially developed an animal model of inflammation in Wistar rats using a lipopolysaccharide (LPS) as an inflammatory agent. Blood samples were collected for determination of TNF-α levels to ensure the triggering of the inflammatory process. Importantly, the number of rolling and adherent leukocytes in *post*-capillary venules was monitored using an intravital microscopy approach. As expected, our results showed that there is an increase in TNF-α concentrations after 15 minutes of LPS administration and a significant increase in the number of rolling and adherent leukocytes. The recorded intravital microcopy images, along with other recorded parameters, were then used, in collaboration with a group of mathematicians, to develop a numerical model capable of describing leukocyte recruitment in the microcirculation.

To evaluate the contribution of hemodynamics, the localized velocity fields and shear stresses on the surface of leukocytes and near the vessel wall contact points have been computed in two discrete situations, namely as a single leukocyte or when a cluster of them are recruited towards the vessel wall. In the first situation, our numerical results showed the presence of one region of maximum shear stress on the surface of the leukocyte close to the endothelial wall and of two regions of minimum shear stress on the opposite side of the cell. The different areas of shear stress observed in the surface of the leukocyte may be important in directing it towards the endothelial wall during an inflam-

matory response. The identification of a region of maximum shear stress is consistent with the molecular mechanisms that govern leukocyte rolling because it may actually correspond to the area that supports the interaction with the endothelium. On the other hand, the relatively lower shear stress regions may correlate with leukocyte surface areas where binding to the endothelium is not occurring at the moment, thus enabling the rolling of the cell along the endothelium. It was also observed that the shear stress at the endothelium gets higher as a cluster of leukocytes moves in the main stream. This suggests that the presence of a cluster of leukocytes may potentiate leukocyte rolling, as the increase in the shear stress promoted by the recruited leukocytes may support the migration and recruitment of additional cells.

Despite closely simulating leukocyte recruitment, our initial numerical simulation considered the simple case of leukocytes as rigid spheres. However, while circulating leukocytes maintain an approximately spherical shape, rolling leukocytes are known to deform. In order to account for the leukocyte deformability changes that occur during its recruitment in inflammation, we needed to assess the deformability profile of the leukocytes under flow and therefore, to "directly" observe them regardless of the other blood cells. For such, intravital microscopy was performed in the mouse cremaster of a transgenic mice strain (Lys-EGFP-ki) in which fluorescent neutrophils can be individually tracked. By using PAF as an inflammatory agent, the analysis of the leukocyte-endothelial cell interactions showed a continuous increase in the number of rolling and adherent neutrophils up to 4 hours after the introduction of the inflammatory stimuli, thus confirming the development of an inflammatory response. As the properties of the red blood cells modulate blood flow properties, erythrocyte deformability was also addressed in this model. A continuous decrease of this parameter was observed throughout time. The decrease in the erythrocyte deformability will most probably lead to an increase in the blood viscosity and to the decrease of the blood flow velocity. These conditions should facilitate the migration of leukocytes from the mainstream to the endothelial wall and promote leukocyte slow rolling and adhesion during the inflammatory response.

Importantly, in the intravital microcopy images obtained with this latter model, we clearly observed the deformation of neutrophils along the endothelial wall during rolling, as well

as the formation of tethers. As such, in these images, leukocyte trajectories were tracked and their velocities and diameters were measured and further applied to the numerical simulations. Using a recent validated mathematical model describing the coupled deformation-flow of an individual leukocyte and the respective experimental results, numerical simulations of the recruitment of an individual leukocyte and of two leukocytes under different velocities were performed, considering a constant blood viscosity. The mathematical models obtained showed that under conditions of increased velocity the cell movement is accelerated along the endothelial layer, favouring the dissociation of leukocyte-endothelium interactions at designated attraction points. These observations lead us to propose that, in order to attain an efficient inflammatory response, the blood flow velocity needs so as to decrease to facilitate slow rolling and subsequent adhesion. These results are corroborated by the decrease in the erythrocyte deformability observed in our animal model, which will ultimately have an impact on the blood flow velocity. Our results further showed that in the vicinity of an adherent leukocyte there is an early slight deceleration of the rolling leukocyte when compared with the case of an individual leukocyte. As such, these observations strongly suggest that the presence of an adherent cell in the vicinity should decrease the velocity of another leukocyte that is being recruited, thus promoting its slow rolling, and contributing to its capture by the endothelial cells.

Altogether, our experimental data and numerical simulations support our working hypothesis that the hemodynamic properties of the flow and of the cells in circulation should play an essential role in the margination and rolling of the leukocytes to the endothelial wall, which in turn will impact the success of the inflammatory response. In particular, our results strongly suggest that changes in hemodynamic conditions, such as decreased flow velocities and the increase of the shear stress, will contribute to target leukocytes to the endothelial wall. Given our results, we propose that any change in the hemodynamic properties will certainly influence the outcome of the inflammatory response. As such, the adherence of the leukocytes to the endothelium should depend not only on the relative magnitude of the chemical forces generated by the interaction of adhesion molecules between leukocytes and endothelial cells, but also on the physical forces that act on the leukocytes. In this respect, our results suggest that alterations in the blood flow, for example in the flow velocity, will occur during an inflammatory process, thus

potentiating the recruitment of more leukocytes towards the inflamed area and contributing to a successful inflammatory response.

Overall, the numerical simulations allowed us to better understand the contribution of the hemodynamic properties of the flow to the progression of an inflammatory response and to deepen our knowledge on leukocyte recruitment in inflammation. Importantly, our work provided numerical tools that can be used for the subsequent study and modulation of the hemodynamic parameters involved in an inflammatory response. In particular, these numerical simulations will surely enable us, in the near future, to determine or estimate a large set of parameters which are unlikely to be recoverable by *in vivo* experiments. Moreover, our methods will allow us to analyze how the parameters evolve over time. Altogether our results further reinforce the notion that the improvement and development of animal models and numerical tools will certainly provide the medical and biological community with useful tools to study leukocyte recruitment in inflammation. By closely reproducing the microcirculation and the inflammatory process, these tools will be critical for a better comprehension of the inflammatory process and of the mechanisms underlying a multitude of inflammatory pathological conditions.

Keywords

Leukocytes, microcirculation, inflammation, hemodynamics, numerical simulations

Objectives

The main goal of this thesis was to address the contribution of hemodynamics to leukocyte recruitment in inflammation.

To achieve this we aimed in generic terms at:

- Developing numerical simulations that adequately mimic the leukocyte recruitment.
- Developing animal models of inflammation to obtain experimental data required for the development of those numerical simulations.

In particular and to address the role of hemodynamics in leukocyte recruitment, we aimed at developing animal and mathematical models to simulate the recruitment of leukocytes in the microcirculation specifically by either accounting for the non-newtonian fluid behavior of the blood or for the deformability of the leukocyte.

PART ONE

I. General introduction

1. Microcirculation

The microcirculation, which includes all vessels with a diameter of <100μm, blood cells, endothelium and microparticles, plays a central role in tissue oxygenation because it is across the walls of the microvessels that oxygen diffuses from the blood to the cells within each tissue. At microscopic level blood is regarded as a suspension in which solid blood cells, such as red blood cells, white blood cells and platelets are suspended in fluid plasma. Blood is fluid with viscoelastic properties which flows in a pulsatile way through resistant vessels in dependence of heartbeat timing (1). Due to the non-linear relationship between shear stress and shear rate, blood is classified as a non-Newtonian fluid. Accordingly, erythrocyte aggregation tendency and erythrocyte deformability change with different shear rates (2). In the microcirculation, the ability of the RBC to deform is particularly crucial because these cells must pass through narrow capillaries that have diameters half the size of their own.

Leukocytes, circulating in the blood stream, also change their rheological properties such as the deformability, when activated by inflammatory mediators or by the presence of foreign organisms (1,2). Their activation generates a complex cascade of rolling along the vessel wall, induces adhesion to the microvascular endothelium and, ultimately, leads to extravascular migration into the surrounding tissue. Importantly, it is believed that these processes are influenced by the interaction of leukocytes with surrounding erythrocytes, as these deform and support the pushing of the leukocytes to the wall.

1.1 The blood

Whole blood is a concentrated suspension of formed cellular elements that includes red blood cells (RBCs) or erythrocytes, white blood cells (WBCs) or leukocytes and platelets or thrombocytes. These cellular elements are suspended in an aqueous polymer solution, called plasma, containing electrolytes and organic molecules such as metabolites, hormones, enzymes, antibodies and other proteins. Plasma is defined as a nearly Newtonian fluid, because it has a constant viscosity. However, whole blood exhibits marked non-Newtonian characteristics, particularly at low shear rates and is classified as a shear-thinning fluid with a decreased viscosity at higher shear stress. The non-Newtonian behavior of blood (Figure 1) is mainly explained by three phenomena: the erythrocytes' tendency to form a three-dimensional microstructure at low shear rates, their deformability and their tendency to align with the flow field at high shear rates (3,4). Erythrocytes have been shown to exert the most significant influence on the mechanical properties of blood, mainly due to their presence in very high concentration compared to the other formed elements (approximately $4–6\times10^6$ RBCs/mm3), comprising about 40 to 45% of its volume in healthy subjects. This volume percentage of RBCs in blood is defined as the hematocrit (Ht) (4).

As is well known, erythrocytes are biconcave cells that change their shape according to the vessel lumen diameter and have a key role in the oxygen transport in the body (5). The capacity of a reversible change of erythrocytes shape in response to a deforming force is called erythrocyte deformability. This property is an important determinant of blood viscosity, and therefore of the blood flow resistance in the vascular system. Since it is an essential property of blood flow it will also affect oxygen uptake or donation (6). The erythrocyte deformability largely influences blood viscosity, as the more the RBCs are deformed the lower the blood viscosity is.

Among other factors, some authors (7) suggest that nitric oxide (NO) may have a regulatory effect on RBC deformability. Human RBCs express both inducible (iNOS) and constitutive (eNOS) forms of NO synthase (NOS), and thus are capable of synthesizing their own NO. Besides this, NO has also been shown to play significant roles in the regulation of the function of individual cells and organs (8,9). For instance, when synthesized by endothelial cells it is able to diffuse to the smooth muscle where it triggers vasodilation.

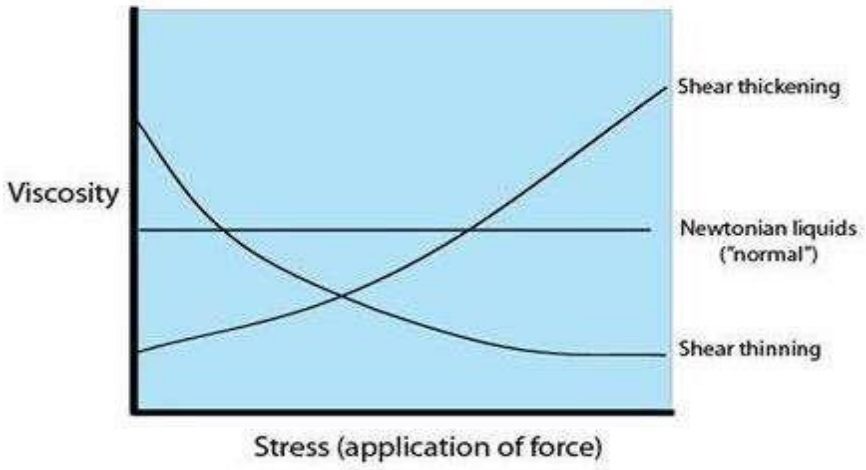

Figure 1 – Shear thinning and shear thickening liquids. Some liquids behave differently when stress is applied (application of force). Shear thickening liquids increase in viscosity as stress increases. Shear thinning liquids decrease in viscosity as stress increases.
Adapted from (10).

2. Inflammation

Inflammation is a disease process characterized by the recruitment of leukocytes from the blood stream to an organ or tissue that has been injured by trauma, infection or autoimmune reaction. Despite the focus on the leukocyte function in inflammation, endothelial cells are also critical in this process as already recognized by Elie Metchnikoff in the 19th century: “Next to leukocytes, the vessels and their endothelial lining play the most important role in inflammation”. Overall, the inflammatory response comprises a series of vascular and cellular events set into motion to destroy, dilute or isolate the causative agent and further to reconstitute the damaged tissue and regain tissue homeostasis.

An inflammatory response can have two different patterns and can thus be classified as an acute or chronic inflammation. The acute inflammation process constitutes a rapidly elicited response (in seconds or minutes) with a relatively short duration, lasting from minutes to several hours or few-days. Exudation of fluid and plasma proteins (edema) and the emigration of leukocytes, predominantly neutrophils and monocytes towards the affected tissue are its main characteristics. On the other side, chronic inflammation is a longer duration response of the organism that normally arises from an acute inflammation that is not completely turned off or extinguished (11). This is the case for a variety of chronic diseases, including atherosclerosis and autoimmune diseases such as rheumatoid arthritis.

2.1 Acute inflammation: a multistep process

Anyone who has experienced an injury knows from common sense that redness (rubor), heat (calor), swelling (tumor) and pain (dolor) are usually observed in an inflammatory response. As a consequence of the process, loss of tissue function may appear subsequently. These are the cardinal signs of acute inflammation and were already described by Celsius in the first century. These signs are the result of the complex action of different pro-inflammatory and anti-inflammatory mediators both at the molecular and cellular level.

An acute inflammatory response is triggered by the detection of a noxious agent by specialized cells, such as tissue resident macrophages or even by neighboring host cells. Such detection is based on the recognition of specific molecular patterns expressed by the invading pathogens, communally designated as pathogen-associated molecular patterns (PAMPs), such as lipopolysaccharide, which is a component of the bacteria's membrane. An acute inflammatory response can also be triggered by the recognition of intracellular proteins released by the dead host cells, the damage-associated molecular patterns (DAMPs). These include proteins, as the cytokine HMGB-1 (High Mobility Group Box-1) or metabolites like ATP or uric acid. The detection of PAMPs and DAMPs is achieved by specific receptors, the pattern recognition receptors (PRRs), expressed in the diverse immune and non-immune cells. Among the diverse groups of PRRs, Toll-like receptors (TLRs) stand as the best-known and more extensively studied (12).

The detection of the inflammatory agent raises a pro-inflammatory response mediated by the action of pro-inflammatory biochemical mediators and different cellular types that are mobilized to the inflamed area. Among other mediators, pro-inflammatory cues are expressed, such as the cytokines tumor necrosis factor-alpha (TNF-α) and interleukin-1β (IL-1β), which will further activate the endothelium and lead to the activation of vascular and cellular process in 3 different ways: (i) alterations in the diameter of the vessels adjacent to the inflamed area which enables the increase of blood flow in the region; (ii) structural alterations in the microvasculature that will enable the efflux of plasmatic proteins and leukocytes in the blood; and (iii) the migration of specific leukocytes to the

inflamed tissue where they accumulate and are activated to address essential functions against the inflammatory agent.

Importantly, acute inflammatory processes are characterized by a differential recruitment of leukocytes towards the inflamed area. Neutrophils, or polymorphonuclear leukocytes (PMNs), are the most common leukocyte in humans and dominate the initial efflux of leukocytes to the inflamed area where, once activated, they act towards the elimination of the inflammatory agent. Their recruitment and subsequent transmigration into inflamed tissue is the earliest cell adhesion event following tissue insult and occurs in every organ. Once at the site of inflammation the neutrophils can eliminate the inflammatory agent both by intra and extracellular mechanisms. The most common mechanisms are phagocytosis, degranulation (by releasing antibacterial proteins), and NETosis (by the release of extracellular traps that immobilize the pathogens) (13). At a later stage of the process, monocyte extravasation in preferred. Once in the inflamed area, monocytes differentiate into macrophages with: (i) either a pro-inflammatory functional profile, termed as classically-activated macrophages or (ii) anti-inflammatory and pro-resolving functions, the alternatively-activated macrophages, that ensure the clearance of apoptotic neutrophils and cellular debris, mediate the resolution of the inflammatory process and further favor the subsequent tissue healing and regeneration.

2.2 Leukocyte recruitment: the case of neutrophils

In most tissues, the leukocyte recruitment cascade involves the following recognized steps: tethering, rolling, adhesion, crawling and finally transmigration (13). Neutrophil recruitment is initiated by changes on the surface of endothelial cells that result from stimulation by inflammatory mediators.

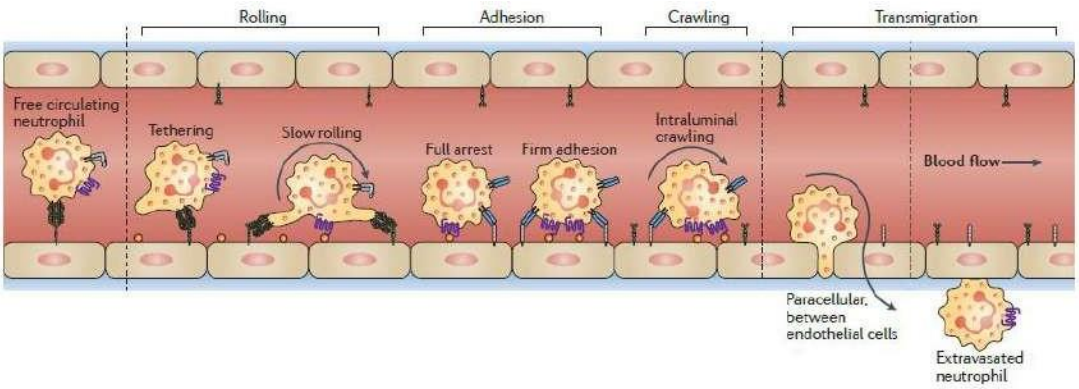

Figure 2 – The classical neutrophil recruitment cascade. Adapted from reference (13).

The leukocyte recruitment takes place largely at *post*-capillary venules. Here, the vessel wall is rather thin and the diameter of the vessel is adequate to sustain the recruitment process. In fact, the diameter of these venules is, on one hand, sufficiently small to enable leukocytes to contact the endothelial wall and, on the other hand, large enough so that venules are not occluded by leukocytes arresting on or adhering to the endothelium.

2.2.1 Neutrophil rolling

The attachment of neutrophils to the vascular wall is determined by the activation of the endothelial cells. Neutrophil rolling is then supported on the endothelial cells by E- and P-selectins (CD62E and CD62P) upregulated on the endothelial cell plasma membrane in response to cytokines or histamine stimulation. These two selectins have partially overlapping functions and maximize neutrophil recruitment by promoting the tethering of the free-flowing cells to the surface of the endothelium and their subsequent rolling in the direction of blood flow. The interaction of the constitutively expressed leukocyte selectin, L-selectin (CD62L), with the glycoprotein ligands upregulated on the activated endothelium, may also contribute to neutrophil tethering, and thus to the deceleration of already rolling cells (13).

Leukocyte rolling requires rapid formation and breakage of adhesive bonds. To support the slow rolling of the leukocytes, the dissociation of a P-selectin–PSGL1 bond at the rear of the cell should be balanced with the formation of another bond at the leading edge. However, the front bond does not allow any load until it is shifted to the rear of the

rolling neutrophil, where it is force bearing. Indeed, it was discovered that shear-resistant rolling involves the formation of long membrane tethers at the rear of the cell that catapult or 'sling' to the front of the rolling cell (Figure 3).

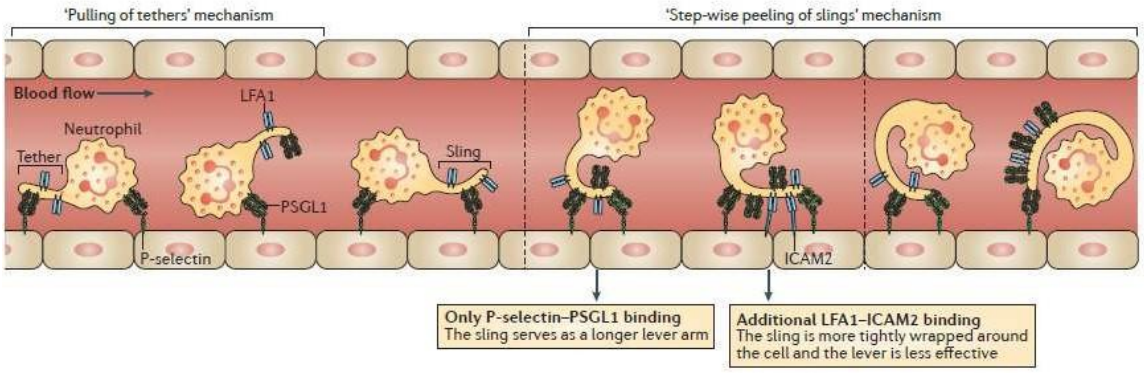

Figure 3 - Formation and engagement of tethers and "slings" by rolling neutrophils. Adapted from (13)

2.2.2 Neutrophil adhesion

Rolling along the vessel wall is thought to facilitate neutrophil contact with the endothelium and elicit the activation of neutrophil's integrins. Upon activation, these bind to their receptors on endothelial cells to promote the firm adhesion of the neutrophils to the endothelial wall.

For neutrophil activation and chemotaxis, CXC chemokines have a crucial (but not exclusive) role. Chemokines are positively charged molecules that can be immobilized in the endothelium forming intravascular chemotactic gradients. This immobilization is achieved by heparin sulphates which serve as anchors to prevent the shear forces to wash out these molecules away. In particular, the CXC chemokine family includes human CXCL8 (known as IL-8) and its mouse functional analogues, CXCL1, CXCL2 and CXCL5. These chemokines activate neutrophils via CXCR2 receptor, a G-protein-coupled receptor, and promote their adhesion to the endothelium.

The activation of this chemokine receptor on neutrophils induces changes in the conformation of cell surface-expressed integrins, namely, LFA1 (known as α1β2; β2 integrin CD11a complexed with CD18) and MAC1 (known as αMβ2; CD11b-CD18). Upon activation, these integrins bind to their ligands on endothelial cells, namely, the

immunoglobulin-like cell adhesion molecules (CAMs), ICAM1 and ICAM2. In particular, the binding of LFA1 to ICAM1 is essential to firm adhesion (14).

2.2.3 Transendothelial migration

After firm adhesion is achieved, neutrophils are prepared for transmigration. To leave the vessels, the neutrophils need to first cross the endothelium (which takes 2 to 5 minutes) and then the basement membrane (which take 5 to 15 minutes) (12). The passage across the endothelial cell layer occurs either (i) transcellularly, whereby neutrophils pass through an endothelial cell, or (ii) paracellularly, whereby neutrophils squeeze in between endothelial cells. Neutrophils preferentially choose the paracellular way (13). Transmigration requires again the action of integrins and CAMs (ICAM1, ICAM2 and vascular cell adhesion protein 1 (VCAM1)) (Figure 4), as well as, different junctional adhesion molecules (JAMs).

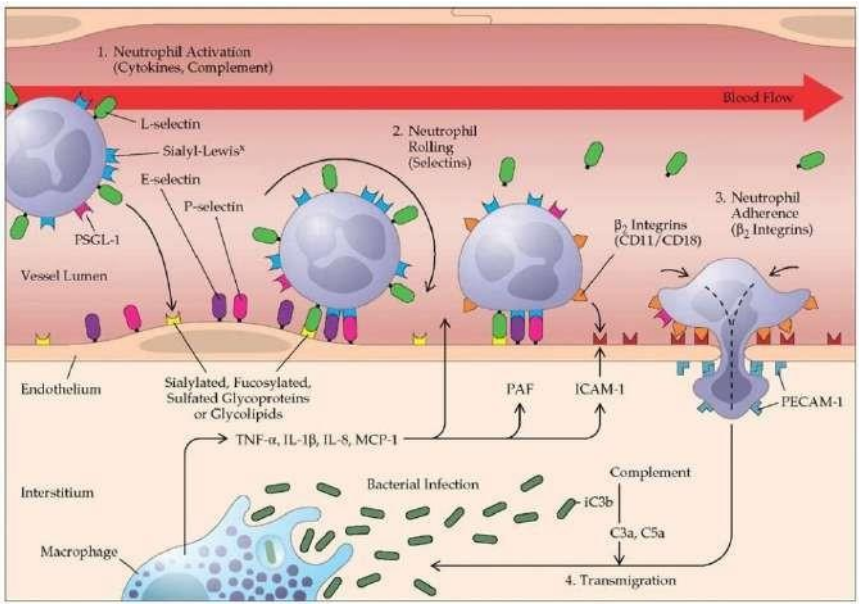

Figure 4 - Neutrophil-endothelial cell interactions in an inflammatory response (C—complement; ICAM-1—intercellular adhesion molecule-1; IL-1β— interleukin-1β; MCP-1—monocyte chemoattractant protein-1; PAF—platelet-activating factor; PECAM-1—platelet endothelial cell adhesion molecule-1; PSGL-1—P-selectin glycoprotein ligand-1; TNF-α—tumor necrosis factor-α). Adapted from (15).

2.3 The hemodynamic environment: leukocytes are deformable cells

The motility of leukocytes from the bloodstream to interstitial tissues is a fundamental host defense reaction (16). Although this process is, as explained before, largely initiated by PAMPs, released from invading microorganisms, or DAMPs, derived from damaged, dead, or environmentally stressed cells, the hemodynamic environment also has a role to play on the migration of leukocytes.

Under physiological conditions, the fluid shear stress (the tangential force per unit area; dyn/cm^2 and created by friction forces) maintains leukocytes in a spherical shape as well as minimizing cell stiffness, to ensure their passage through the microcirculation (17,18). In an inflammatory response in addition to the biochemical mediators, fluid shear stress resulting from blood flow also regulates leukocyte activity. When activated and recruited towards the endothelial wall the leukocytes change their rheological properties such as deformability which is consistent with their increased entrapment within the microcirculation (1,19–21).

The analysis of the leukocyte trajectories along the vessel wall reveal that a rolling cell does not flow continuously, but rather it moves in a “stop-and-go” manner due to the formation and breakage of bonds. Upon initial tethering, the cell/substrate contact area becomes flat allowing for the formation of newer microvilli tethers, which will further stabilize the rolling and allow the initiation of the adhesion process. Leukocytes deformability is, this way, an essential property of the leukocytes to allow rolling and adhesion (22,23).

In fact, both leukocyte rolling and adhesion result from a balanced formation and dissociation of selectin-ligand bonds in the presence of the hydrodynamic shear forces of the flow. It is known that leukocytes rolling at venular shear stress (>0.6 Pa) form long tethers and undergo cellular deformation. Recent studies, using dynamic footprinting (qDF) microscopy revealed that the footprinting of a neutrophil rolling at high shear stress (>0.6 Pa) is four times larger than that reported by the *in vivo* studies (23,24). This way, the hydrodynamic forces and torque acting on the rolling cell are thought to be synergistically balanced by the forces acting on the tethers and microvilli in order to promote an efficient slow rolling and the subsequent adhesion of the leukocytes.

2.4 Chronic inflammation

Chronic inflammation is commonly described as an inflammatory process of prolonged duration in which active inflammation, tissue destruction, and attempts at repair are proceeding simultaneously. Although it may follow acute inflammation, chronic inflammation frequently begins as a low-grade, often asymptomatic response. Distinct pathological conditions can lead to this scenario, such as, persistent infection by low toxicity organisms, prolonged exposure to potentially toxic agents and autoimmune diseases.

At the histological level, chronic inflammation is characterized by (i) the infiltration with mononuclear cells such as macrophages and lymphocytes, as a reflection of persistent reaction to injury; (ii) tissue destruction and necrosis, largely induced by the inflammatory cells and (iii) the attempt to heal the inflamed area, by the replacement of the damaged tissue by connective tissue which often requires the proliferation of small blood vessels (angiogenesis). As an example of this later histological marker, the original tissue can be replaced particularly by fibrotic tissue and thus evolve into fibrosis (11).

3. Inflammatory mediators

3.1 Platelet-activating factor (PAF)

PAF is a phospholipid that is released early in inflammation by a variety of cell types and is constitutively present in platelets, leukocytes and endothelial cells. PAF acts by binding to its receptor, PAF-R, a G-protein coupled receptor expressed by different cell types. PAF cooperates in the recruitment of leukocytes to the inflamed tissue by promoting leukocyte activation and thus, ensuing their adhesion to the endothelium and extravascular transmigration to the tissues.

In addition, PAF has been implicated in the physiological modulation of blood pressure, mainly by affecting the renal vascular circulation in a dose dependent manner. Moreover, Lang and others (25) disclosed the presence of PAF receptors in red blood cells and showed that PAF stimulates the breakdown of sphingomyelin and release of ceramide from RBCs at isotonic conditions. These effects may alter the structure of RBCs membrane thus modulating the deformability of those cells.

3.2 Lipopolysaccharide (LPS)

Lipopolysaccharide (LPS) is a bacterial component of the outer wall of most Gram-negative bacteria that acts as a PAMP. This way it is a potent inflammatory agent to induce leukocyte recruitment (12,26). LPS-induced cell activation depends on the

recognition of LPS by a multiprotein cell surface receptor complex - the LPS receptor complex. The first host protein involved in the recognition of LPS is the LPS-binding protein (LBP). LBP is an acute-phase protein, the role of which is to bring LPS to the cell surface by forming a ternary complex with the LPS receptor molecule CD14 (Figure 5).

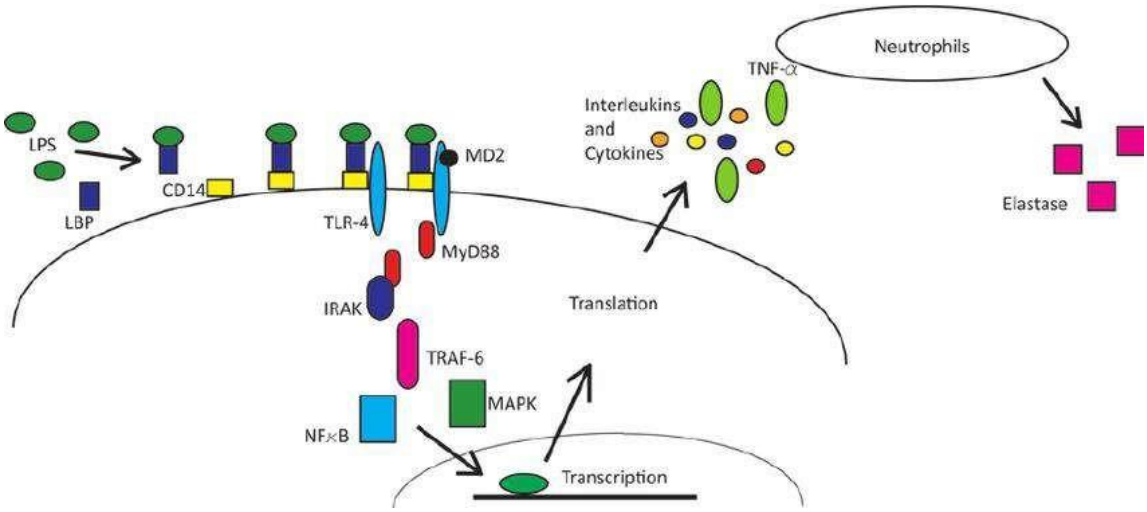

Figure 5 – LPS signaling cascade and inflammatory response. Adapted from reference (27).

CD14 is a 55-kDa glycoprotein present in either a soluble form (sCD14) in blood or as a membrane-bound form (mCD14) in myeloid lineage forms. CD14 principally acts by binding LPS but it does not participate in signaling directly. LPS is brought into close proximity to TLR4 (Toll-like receptor), the principal signaling receptor for LPS, only when it is present as an LPS-CD14 complex and when CD14 and TLR4 are co-expressed with MD-2 (26). In vivo, cytokines such as IL-1β and TNF-α are rapidly released in response to LPS, and both of these cytokines induce the expression of endothelial adhesion molecules (28).

4. Monitoring inflammation *in vivo* and *in silico*

Leukocyte recruitment is a hallmark feature of the inflammatory response, which involves a sequential series of molecular interaction between the leukocyte and endothelial cells. To study these fundamental interactions most experiments were done using simple leukocyte recruitment assays in which a stimulus is introduced into a tissue or body compartment, like the peritoneal cavity, where, at some delayed time, the number of cells is counted. Although this "black-box-type" experiment provides information regarding whether leukocytes can or not be recruited, it provides no meaningful insight as to the step at which leukocyte recruitment may be affected by a given experimental condition. In this respect, intravital microscopy appeared as a helpful technique to visualize the process of leukocyte recruitment: from the mainstream of blood to the vessel wall, out of the vasculature, and through the interstitial space.

4.1 Intravital microscopy

It is now well established that leukocytes play an important role in the development of an inflammatory response. Moreover, the identification of the tissue-specific factors that regulate leukocyte recruitment to sites of inflammation is crucial for the development of therapeutic strategies. Taken this, many are the studies that have investigated interactions between neutrophils and endothelial cells *in vitro* (29). However observations made *in vitro* do not reliably model the *in vivo* cellular interactions, which may at least in part be influenced by differences in shear forces (30,31) and blood properties. Taking this into

account, a major limitation to widen the knowledge of biological processes consists in the technical approach to perform in vivo studies. To overcome this, many techniques and analytical tools have been developed to image and study cellular and biological events in living animals. Among these techniques is the intravital microscopy. There are reports using this technique dating to the nineteenth century but with the constant improvement of the bioimaging techniques, namely of the fluorescent cell markers and the confocal and multi-photon microscopies, intravital microscopy can nowadays be performed as a non-invasive and non-labelling requiring technique (32,33). This technique allows the visualization of directed movement of the cells toward the inflammation area *in vivo*. Imaging always brings the opportunity to visualize more than previously expected, opening windows for other discoveries.

4.2 Mathematical models

Although the molecular mechanisms involved in leukocyte activation and recruitment towards the endothelial wall have been extensively studied, the precise dynamical mechanisms by which molecular mediators facilitate leukocyte arrest are still under investigation.

Many of the processes, which take place in living organisms, can be expressed as mathematical equations, meaning that mathematical models of many physiological, biochemical, pathological and toxicological events can be developed. In most cases, these models are produced and used on computers and as such, they are referred to as computer models or numerical simulations. So besides the experimental work, numerical simulations have the potential to be used to understand the dynamic mechanisms that govern leukocyte recruitment and rolling (34).

A large number of theoretical studies started to emerge since the late 1970s addressing the ligand–receptor interaction (35) and the receptor–mediated leukocyte adhesion where the leukocyte was considered as a three–dimensional rigid cell (36) or a two–dimensional deformable cell (37). The stochastic approach has been taken into account to model the mechanical contribution of an elastic cell membrane, the role of microvilli in the rolling to adhesion process, the shear threshold effect of velocity on a rolling neutro-

phil (38). In addition it has also been investigated the shear stress distribution on the leukocyte membrane surface (39).

Analysis of leukocyte rolling is an important tool for discovering potential novel anti-inflammatory treatments and for the evaluation of newly discovered drugs [8]. Due the multifactorial nature of leukocyte recruitment, in addition to the use of *in vivo* microscopy, numerical simulations can help on the understanding of the mechanisms of inflammation. Experimental data is always required to develop meaningful models of complex biological processes and will be necessary to validate the results obtained by mathematical models.

PART TWO

In this part of the work are presented the articles that contain all the experimental work concerning the development of the theme of this thesis. In the first article – *Effects of acetylcholine in an animal model of inflammation* – all the work was performed by Ana Santos Silva-Herdade and the results describe the animal model of inflammation that was further use for the second article. The second and third articles presented – *Localized hydrodynamics of clustering leukocytes* and *Leukocytes dynamics in microcirculation under shear-thining blood flow* – were in a side-by-side collaboration with a group of mathematicians of CEMAT (IST, UL, Lisbon) that, concerning our experimental data and knowledge, settled the necessary equations for the development of the numerical simulations. The experimental part of both of the articles was performed by Ana Santos Silva-Herdade as well as the interpretation of the numerical results from the physiological point of view. The fourth article - *Erythrocyte deformability – a partner of the inflammatory response* - comprises the experimental data of another animal model of inflammation and was completely developed by the author of this thesis. The fifth and last article - *Hydrodynamics of a free-flowing leukocyte toward the endothelial wall* – of this thesis was once again made in collaboration with mathematicians that wrote the equations of the numerical model. In this last article, the experimental data, the manipulation of the numerical model and interpretation of the obtained results was of Ana Santos Silva-Herdade responsibility.

II. Effects of acetylcholine in an animal model of inflammation

Ana Santos Silva-Herdade[1]

Carlota Saldanha[1]

Clinical Hemorheology and Microcirirculation (2013) 53(1-2):209–16

[1]*Unidade de Biologia Microvascular e Inflamação, Instituto de Medicina Molecular, Instituto de Bioquímica, Faculdade de Medicina, Universidade de Lisboa, Lisboa, Portugal*

Abstract

Acetylcholinesterase (AChE) is found both on the membranes of neuronal and non-neuronal cells. In this study we performed intravenous administrations of velnacrine (VLN) and acetylcholine (ACh), respectively, AChE inhibitor and substrate, in an animal model of lipopolysaccharide (LPS)-induced inflammation in Wistar rats. Using intravital microscopy the number of rolling and adherent leukocytes in post-capillary venules was monitorized and blood samples were collected for TNF-α plasma concentrations determination. Our results showed that in presence of LPS, ACh has an anti-inflammatory effect, seen by a decrease in TNF-α plasma levels and maintains the number of rolling and adherent leukocytes. The presence of VLN before LPS almost blocked the LPS-induced rolling and TNF-α releasing. Thereby VLN seems to have, like ACh, an anti-inflammatory effect by diminishing TNF-α concentrations.

Keywords

Inflammation, acetylcholine, TNF-α, velnacrine, rolling leukocytes, intravital microscopy

1. Introduction

Bacterial LPS, a component of the outer wall of most Gram-negative bacteria, is a potent inflammatory agent and plays a primary role in bacterial-induced leukocyte recruitment (1, 3, 4 and 5).

The four major steps in leukocyte recruitment are rolling, activation, firm adhesion, and migration across the endothelium and the basement membrane. Under normal, no inflammatory conditions many leukocytes come into brief contact with the endothelium and begin rolling, mainly via selectin interactions. In an inflammatory condition, chemokines produced by endothelial cells are believed to be presented to the slowing leukocytes, facilitating firm adhesion.

LPS-induced cell activation depends on the presence of three proteins comprising a multiprotein cell surface receptor complex - the LPS receptor complex. The first host

protein involved in the recognition of LPS is the LPS-binding protein (LBP). LBP is an acute-phase protein, the role of which is to bring LPS to the cell surface by binding to LPS and forming a ternary complex with the LPS receptor molecule CD14. CD14 is a 55-kDa glycoprotein present in soluble form (sCD14) in blood or as a membrane-bound form (mCD14) in myeloid lineage forms. CD14 principally acts to bind LPS and does not participate in signalling directly. LPS is brought into close proximity to TLR4 only when it is present as an LPS-CD14 complex and when CD14 and TLR4 are co-expressed with MD-2 (6, 7 and 8).

In vivo, cytokines such as IL-1 and TNF-α are rapidly released in response to LPS, and both of these cytokines induce endothelial adhesion molecules expression (9, 10 and 11). Recent studies have also demonstrated that the recruitment of monocytic cells and the expression of adhesion molecules is, besides TNF-α levels, influenced by the shear stress in the blood vessels 12 .

Intravital microscopy, a useful and established technique pioneered in the 1800s by Cohnheim 13, enhanced the study of inflammatory process by providing direct visual observation of living circulatory beds. Intravital microscopy is now used to evaluate leukocyte trafficking (rolling times and velocities, adhesion, and migration) after exposure to a variety of inflammatory stimuli and can be applied to different tissues as brain or the intestine 14–17.

It was recently found that electrical or pharmacological activation of the efferent vagus nerve inhibits TNF release and attenuate the endotoxin-induced shock in rodents and the stimulation of the efferent vagus activates the release of acetylcholine (ACh) (18, 19 and 20).

Concerning ACh release and the non-neuronal cholinergic system, other studies have demonstrated that both endothelial cells and T lymphocytes produce ACh (21, 22 and 23). ACh inhibits LPS-induced production of proinflammatory cytokines, inducing IL-1, from macrophages and microglia (24 and 25). ACh levels are continuously regulated by the hydrolytic enzyme acetylcholinesterase (AChE), that is found anchored to the membranes of various cellular types, such as erythrocytes, platelets, leukocytes and endothelial cells, by different kinds of tails (26, 27). However, the presence of acetylcholinesterase in blood

and in endothelial cells was identified without a description of is physiological function. Beyond the catalytic functions, other ones like intercellular adhesion were also described 28.

AChE inhibitors are found to be potent cholinergic agonists and are widely accepted as anti-AD (Alzheimer disease) drugs 29. Velnacrine (VLN) is known as an acetylcholinesterase inhibitor 30 that can modulate leukocyte activation. LPS is described as a potent inflammatory agent and plays a primary role in bacteria-induced leukocyte recruitment 31. Based on this, this work intends to evaluate the effect of the intravenous administration of an AChE inhibitor, velnacrine maleate and AChE substrate, acetylcholine, in the inflammatory response of LPS by the analysis of the leukocyte-endothelial cells interactions and quantification of TNF-α, as a pro-inflammatory cytokine.

2. Methods

2.1 Animal preparation

The animals used in this study received human care in accordance with the Directive of the European Community nº86/609/CEE that mentions the protection of animals used for economic ends and other scientific ends.

Wistar male rats (HsdBrlHan:Wist, Harlan Iberica), with an average weight of 270±16g, were kept in an animal facility with a 12h light/dark cycle and housed in cages in a temperature controlled room. All animals were kept on a diet standard rat food and water *ad libitum*. For the surgical procedures and microcirculatory measurements, the rats were anesthetized intraperitoneally with 1,5g/Kg body weight urethane (Sigma-Aldrich). Body temperature was maintained at 37ºC with a heating platform. A tracheostomy was performed to maintain the animal in spontaneous breath during all the experiment. For drug administration, the right jugular vein was cannulated with polyethylene tubing.

The preparation of cremaster for intravital microscopy is made in a Plexiglas support in accordance with 32. Using an electrocauter a small incision in scrotum is made and the right testicule is brought outside. Then the conjunctive tissue that surrounds the

cremaster is removed and an incision is made in the cremaster, fixing it to an appropriate support with silk sutures.

2.2 Intravital microscopy

The animal is then placed in an inverted microscope Leitz® FLUOVERT FU (Leica, Heerbrugg, Whisker) adapted for intravital microscopy, equipped with a 40X objective and a 10X ocular. The images are caught through a video camera CCD-IRIS DXC-107AP (Sony), visualised in a colour monitor PVM 1440QM (Sony) and recorded in a video SVHS AG-MD830 (Panasonic) for later analysis. After placing the support with the rat in the microscope, the venous catheter must be connected to a perfusion system with NaCl 0.9% pH 7.4, in a speed of 4ml/h and the cremaster must be placed in perfusion of NaCl 0.9% pH 7.4 being the excess of liquid removed with a vacuum system. The preparations were allowed a 30 min *post*-surgical equilibration period.

After the equilibration period the cremaster observation is started. *Post*-capillary venules with 20-35μm diameters were chosen for the quantification of the parameters previously defined. From the recorded images the interactions leukocytes/endothelial cells are quantified by the parameters already established 33: number of rolling and adherent leukocytes.

The leukocytes are considered in rolling on the endothelium if moving at a slower speed than erythrocytes in that vessel, and their number counted during 1 min. A leukocyte was considered adherent to the endothelium if it remained stationary for more than 30s in a 100μm length 33.

2.3 Experimental groups

A cross-study between LPS, ACh and VLN was established. All the experiments were made after a 30 min stabilization period. LPS (17.5 ng/g rat weight (*E.coli*, serotype 026:B6, Sigma) and ACh (200μg/Kg/ rat weight) or LPS and VLN (200μg/Kg/ rat weight) were administrated intravenous (i.v.) at times 0 and 5 minutes of the experiment. The

leukocyte counts and the blood determinations were performed after 0, 5 and 15 minutes as represented in Figure 1.

In the experimental groups in which an inflammatory state was previously induced (0 min) by LPS, ACh or VLN were administrated after 5 minutes of LPS administration – Group LPS+ACh and Group LPS+VLN. In the experimental groups in which a pre-conditioning with ACh or VLN was previously induced (0 min), LPS administration for inflammatory state induction was applied after 5 minutes – Group ACh+LPS and Group VLN+LPS. Blood collections were made in the different animal groups for TNF-α plasma determination (Calbiochem). All the experimental groups were performed for N=6 rats.

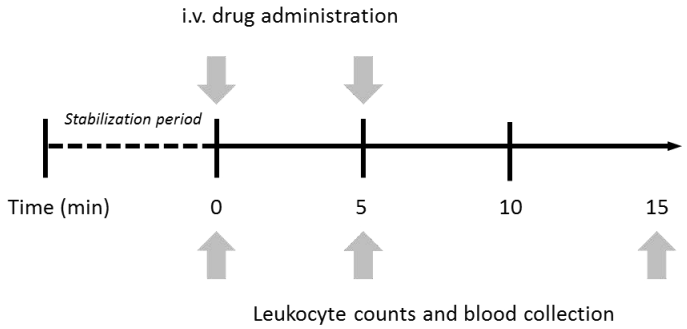

Figure 1 – Schematic representation (timeline) of the experiments performed.

2.4 Statistical analysis

Data are presented as means ± SD. The differences between the mean values were evaluated by using a one-way ANOVA statistical analysis with a Bonferroni's Multiple Comparison Test using GraphPrism Software. Values were considered statistically significant when *p* value was less than 0.05.

3. Results

Analysing the data obtain with the LPS administration on the number of rolling and adherent leukocytes (Fig. 2A and 2B) we observed an increase in both parameters. The administration of VLN after LPS increases ($p<0.001$) the number of rolling leukocytes, although the number of adherent leukocytes is not affected by the presence of VLN. The

administration of ACh alone doesn't show significant alterations in the number of rolling or adherent leukocytes after ACh administration (data not shown).

When ACh and VLN were administrated after the LPS-induced inflammatory state we observed that: (1) when ACh is administrated after LPS the number of rolling leukocytes is maintained, but adherent leukocytes decrease when compared with the effect obtained with LPS alone ($p<0.001$); (2) VLN administration after LPS-induced inflammation augments the rolling leukocytes but statistical significant variations are observed in the number of adherent leukocytes.

In the experimental groups where VLN and ACh were administrated before LPS addition (Fig. 1), the results show that: (1) with a preconditioning of ACh, LPS administration significantly increases the number of rolling leukocytes but decreases the number of leukocytes in adhesion when compared either with the NaCl or the LPS experiment; (2) the presence of VLN lowers the number of rolling and adherent leukocytes.

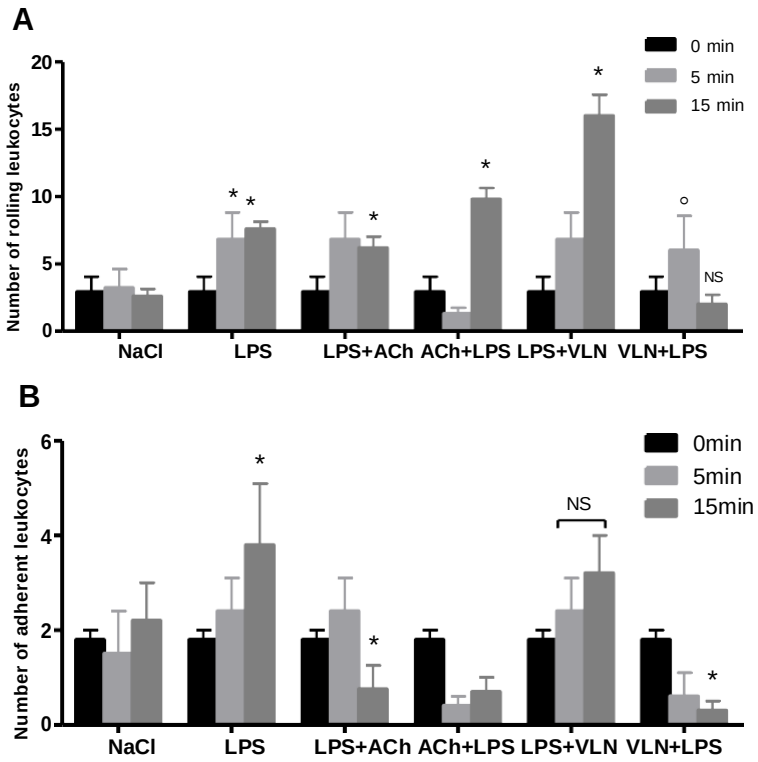

*Figure 2 - Mean and standard deviation of the number of rolling (A) and adhesion (B) leukocytes in the NaCl, LPS, LPS+ACh, ACh+LPS, LPS+VLN and VLN+LPS Wistar rat groups. Statistical significant results in relation to (0 min) are shown * $p<0.001$.*

TNF-α concentrations were determined at the same time of the leukocytes monitorization and the results show that when compared with NaCl administration, LPS increases TNF-α ($p<0.001$) plasma levels, as expected during an inflammatory state.

Regarding the results obtained for the TNF-α levels in presence of ACh and VLN both are capable of lowering this cytokine concentration after the LPS administration, when compared with its administration alone, although they are higher than the obtained with NaCl. TNF-α plasma levels show that LPS administration after VLN has no significant variation, when compared with NaCl administration, (Fig.3). When ACh is present before the LPS administration TNF-α ($p<0.01$) plasma concentrations are significantly increased.

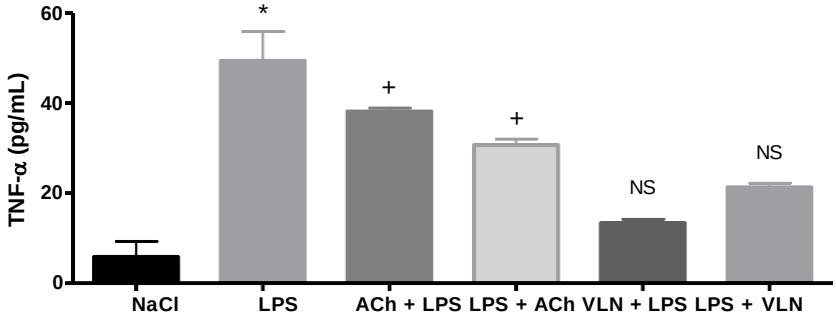

*Figure 3 – Mean and standard deviation of TNF-α plasma levels in the NaCl, LP", LP"+ACh, ACh+LPS, LPS+VLN and VLN+LPS Wistar rat groups after 15 min. Statistical significant results in relation to NaCl are shown * p<0.001, + p< 0.01*

4. Discussion

In our *in vivo* LPS-induced experimental model of inflammation the number of rolling leukocytes increased after LPS administration and are accompanied by an increase of the proinflammatory cytokines TNF-α ($p<0.001$), when compared with the initial levels. Administration of ACh and VLN, which correspond, respectively to substrate and inhibitor of AChE, after LPS induction results in the decrease of TNF-α plasma levels when compared with LPS group; concerning the number of rolling leukocytes, ACh seems to have an anti-inflammatory effect maintaining almost invariable the number of recruited leukocytes to roll; which not happen in presence of VLN besides its ability to maintain lower TNF-α plasma levels.

The presence of ACh and VLN without any preconditioning or induced inflammation doesn't induce any alterations on the number of rolling and adherent leukocytes and TNF-α plasma concentrations remained almost invariable (data not shown). With LPS-induced inflammation after the intravenous ACh administration, TNF-α concentrations increased significantly in response to LP", because of our observation that ACh alone doesn't produce any inflammatory effect this is consist with the increase of the rolling leukocytes after LPS administration even in presence of ACh. The presence of VLN before LPS almost blocked the LPS-induced rolling and TNF-α production. VLN and ACh act with different kinetic effects on AChE. Increase of ACh levels results from the inhibitory action of VLN on AChE enzyme activity with the generation of an inactive ACh-AChE complex. The binds of ACh to AChE produce an active enzyme complex ACh-AChE. Consequently we observe different effects for the VLN or ACh administration on leukocytes recruitment in post-capillary venules of Wistar rats.

Recent studies discovered the anti-inflammatory role of the efferent vagus nerve in inhibiting acute inflammation by ACh releasing, so for ACh it was already expected that its anti-inflammatory effect may inhibit the LPS-induced production of proinflammatory cytokines by endothelial cells, like TNF-α as was already demonstrated by others in macrophages 24 and microglia 25.

The anti-inflammatory capacity of ACh is already described (18, 19 and 20). VLN seems to have two effects namely an anti-inflammatory and a protective effect. The former probably resulting from the AChE inhibition and consequently with plasma ACh increase that was reflected on the impairment of the proinflammatory cytokines TNF-α levels results from LP" administration. Also VLN shows a "protective" effect by blocking, the proinflammatory cytokines production when administrated before LPS induction of inflammation.

Our data suggest that the modulation of AChE activation state can have in one hand, an anti-inflammatory effect during an inflammation state, but also a protective result before the inflammation development. This hypothesis is supported by our data, as described above, not only in the proinflammatory cytokines production, but also by leukocyte recruitment on endothelial cells.

It is known that cytokines, like TNF-α found in plasma may be produced by blood cells, endothelium or may originate from the brain. TNF-α can mediate the influx of leukocytes (both neutrophils and monocytes) to endothelial cells by stimulating the expression of adhesion molecules on the surface of leukocytes and vascular endothelial cells, process that is also mediated by the shear stress on the blood vessels 12. We have seen that the intravenous administration of VLN only influences the maintenance of TNF-α concentrations without affecting the leukocyte-endothelial cell interactions; others 37 have demonstrated that brain levels of IL-1β and TNF-α are decreased after intraperitoneally administration of AChE inhibitors. This suggests that the maintenance of low levels of cytokines influences their synthesis in the blood stream, by endothelium or blood cells, and, probably, block the activation of rolling and adhesion to the endothelial wall. This may explain the unchangeable number of rolling leukocytes by lacking of activation at the endothelial level in presence of VLN and after LPS-induced inflammation.

We can with our results raise the hypothesis that keeping the proinflammatory cytokines levels low has implications on endothelial cells at the level of the leukocytes recruitment preventing the development of an inflammation state.

Some studies mentioned the possible increased risk for the development of cytokine-mediated diseases in patients with decreased instantaneous heart rate variability 38. Our findings highlight the possibility of controlling the proinflammatory cytokines production with AChE inhibitors, like velnacrine, without alterations on the endothelial cells activation for leukocyte recruitment described by us, may be an important step for the control of cytokine-mediated diseases.

Acknowledgments

The authors would like to thank Serviço de Cirurgia Experimental of Hospital de Santa Maria, Portugal for the animals' husbandry and treatment during the experiments.

References

1. B. Newman and E.T. Liu, Perspective on BRCA1, Breast Disease 10 (1998), 3-10.
2. R.J. Ulevitch and P.S. Tobias, Receptor-dependent mechanisms of cell stimulation by bacterial endotoxin. Annu. Rev. Immunol. 14 (1995), 437.
3. M. Cybulsky, I.J. Cybulsky and H.Z. Movat. Neutropenic response to intradermal injections of *Eschericia coli*. Effects on the kinetics of polymorphonuclear leukocyte emigration. Am. J. Pathol. 124 (1996), 1.
4. M.I.Cybulsky, D.J. McComb and H.Z. Movat. Neutrophil leukocyte emigration induced by endotoxin: mediator roles of interleukin 1 and tumor necrosis factor α. J. Immunol.140 (1998), 3144.
5. K.L.Davenpeck,, J. Zagorski, R.P. Schleimer and B.S. Bochner. Lipopolysaccharide-induced leukocyte rolling and adhesion in the rat mesenteric microcirculation: regulation by glucocorticoids and role of cytokines. J. Immunol. 161 (1998), 6861-6870.
6. S.D. Wright, R.A., Ramos, P.S. Tobias, R.J. Ulevitch and J.C. Mathison. Science 249 (1990), 1431-1433.
7. J.S. Correia, K. Soldau, U. Christen, P.S. Tobias and R. Ulevitch. Lipopolysaccharide is in close proximity to each of the proteins in its membrane receptor complex. J. Biol. Chem. 276 (2001), 21129-21135.
8. S.M. Dauphinee and A. Karsan. Lipopolysaccharide signalling in endothelial cells. Laboratory Investigation 86 (2006), 9-22.
9. G.D. Martich, M.C. Danner and A.F. Suffredini. Detection of interleukin 8 and tumor necrosis factor in normal humans after intravenous endotoxin: the effect of anti-inflammatory agents. J. Exp. Med. 173 (1991), 1021.
10. D.G. Hesse, K.J. Tracey, Y. Fong, K.R. Manogue, M.A. Palladino, Jr.A. Cerami, G.T. Shires and S.F. Lowry. Cytokine appearance in human endotoxemia and primate bacterimia. Surg. Gynecol. Obstet. 166 (1998), 147.
11. S.W. Chensue, P.D. Terebuh, D.G. Remick, W.E. Scales and S.L. Kunkel. In vivo biological and immunohistochemical analysis of interleukin-1 β, and tumor necrosis factor-α during experimental endotoxemia: kinetics, kupffer cell expression and glucocorticoid. J. Clin. Invest. 81 (1991), 237.

12. K. Urschel, A. Wörner, W.G. Daniel, C.D. Garlichs, I. Cicha. Role of shear stress patterns in the TNF-alpha-induced atherogenic protein expression and monocytic cell adhesion to endothelium. Clin Hemorheol Microcirc. 46 (2010) 203-210.
13. J. Cohnheim, 1889. Inflammation Lectures in General Pathology 1. London: New Sydnham Society.
14. G. Andonegui, S.M. Goyert and P. Kubes. Lipopolysaccharide-induced leukocyte-endothelial cell interactions: a role for CD14 versus toll-like receptor 4 within microvessels. J. Immunol. 169 (2002) 2111-2119.
15. F. Jung, From hemorheology to microcirculation and regenerative medicine: Fahraeus Lecture 2009. Clin Hemorheol Microcirc. 45 (2010) 79-99.
16. M. Sitina, Z. Turek, R. Parizkova, C. Lehmann, V. Cerny, Preserved cerebral microcirculation in early stages of endotoxemia in mechanically-ventilated rabbits. Clin Hemorheol Microcirc. 47 (2011) 37-44.
17. J. Richter, J. Zhou, D. Pavlovic, R. Scheibe, V.H. Bac, J. Blumenthal, O. Hung, M.F. Murphy, S. Whynot, C. Lehmann. Vancomycin and to lesser extent tobramycin have vasomodulatory effects in experimental endotoxemia in the rat. Clin Hemorheol Microcirc. 46 (2010) 37-49.
18. V.A. Pavlov, M. Ochani, M. Gallowitsch-Puerta, K. Ochani, J.M. Huston, C.J. Czura, Y. Al-Abed and K.J. Tracey. Central muscarinic cholinergic regulation of the systemic inflammatory response during endotoxemia. PNAS 103 (2006), 5219-5223.
19. L.V. Borovikova, S. Ivanova, M. Zhang, H. Yang, G.I. Botchkina, L.R. Watkins, H. Wang, N. Abumrad, J.W. Eaton and K.J. Tracey. Vagus nerve stinulation attenuates systemic inflammatory response to endotoxin. Nature 405 (2000)m 458-461.
20. H. Wang, M. Yu, M. Ochani, C.A. Amella, M. Tanovic, S. Susarla, J.H. Li and Wang, H. Yang, L. Ulloa, Y. Al-Abed, C.J. Czura and K.J. Tracey.. Nicotinic acetylcholine receptor alpha7 subunit is an essential reguator of inflammation. Nature. 421 (2003), 384-8
21. K. Kawashima, K. Kajiyama, T. Suzuki and K. Fujimoto. Presence of acetylcholine in blood and its localization in circulating mononuclear leukocytes of humans. Biog. Amines. 9 (1993), 251-258.

22. K. Kawashima, T. Fujii, Y. Watanabe and H. Misawa. Acetylcholine synthesis and muscarinic receptor subtype mRNA expression in T-lymphocytes. Life Sci. 62 (1998), 198-206.

23. C. Kirkpatrick, F. Bitlinger, R. Unger, J. Kriesgsmann, H. Kilbinger and I. Wessler. The non-neuronal cholinergic system in the endothelium: evidence and possible patho-biological significance. Jpn. J. Pharmacol. 85 (2001), 24-28.

24. K.J. Tracey. The inflammatory reflex. Nature 420 (2002), 853-859.

25. R.D. Shytle, T. Mori, K. Townsend et al. Cholinergic modulation of microglial activation by a7 nicotinic receptors. J. Neurochem. 89 (2004), 337-343.

26. G. Cicco, M. Vetrugno, M.T. Rotelli, G. Sborgia, M. Pennetta, P.P. Vico, V. Menneo, L. Nitti, C. Sborgia. Red blood cell (RBC) surface acetylcholinesterase showing a hemorheological pattern during glaucoma treatment. Clin. Hemorheol. Microcirc. 35 (2006), 149-154.

27. X. Cousin, U. Strähle and A. Chatonnet. Are there non-catalytic functions of acetylcholinesteraes? Lessons from mutant animal models. BioEssays 27 (2005), 189-200.

28. A. Klegeris, T.C. Budd TC and S. A. Greenfield. Acethylcholinesterase-induced respiratory burst in macrophage: evidence for the involvement of the macrophage mannose-fucose receptor. Biochimica et Biophysica Acta 1289 (1996), 159-168.

29. A.M. Palmer. Cholinergic therapies for Alzheimer's disease: progress and propects. Curr. Opin. Investig. Drugs. 4 (2003), 820-825.

30. J. Wysocki, Z. Kalina and I. Owczarzy. Effect of organophospgoric pesticides on the behaviour of NBT-dye reduction and E rosette formation tests in human blood. Int. Arch. Occup. Environ. Health. 59 (1987), 63-71.

31. J.S. Correia, K. Soldan, U. Christen, P.S. Tobias and R.J. Ulvetich. Lipopolysaccharide is in close proximity to each of the proteins in its membrane receptor comples. J. Biol. Chem. 276 (2001), 21129-21135.

32. M. Hill, B. Simpson and G. Meininger. Altered cremaster muscles hemodynamics due to disruption of the deferential feed vessels. Microsvasc. Res. 39 (1990), 349-363.

33. K. Ley. Histamine can induce leukocyte rolling in rat mesenteric venules. Am. J. Physiol. 267 (1994), H1017-H1023.

34. L. Walch, C. Taisne, J.P. Gascard, N. Nashashibi, C. Brink and X. Norel. Cholinesterase activity in human pulmonary arteries and veins. Brist. J. Pharmacol. 121 (1997), 986-990.

35. H.P.A.Jersmann, C.S.T. Hii, G.L. Hodge and A. Ferrante. Synthesis and surface expression of CD14 by human endothelial cells. Infection and Immunity 69 (2001), 479-485.

36. S. Ebong, S.M. Goyert, J.A. Nemzek, G. Bolgos and D. Remick. Critical Role of CD14 for production of proinflammatory cytokines and cytokine inhibitors during sepsis with failure to alter morbidity or mortality. Infection and Immunity 69 (2001), 2099-2106.

37. Y. Pollak, A. Gilboa, O. Ben-Menachem, T. Ben-Hur, H. Soreq and R. Yirmiya. Acetylcholinesterase inhibitors reduce brain and blood interleukin-1 production. Ann. Neurol. 57 (2005), 741-745.

38. K. Tracey. Fat meets the cholinergic anti-inflammatory pathway. J. Exp. Med. 202 (2005), 1017-1021.

III. Localized hydrodynamics of clustering leukocytes

Abdel Monim Artoli[1]

Adélia Sequeira[1]

Ana Santos Silva-Herdade[2]

Carlota Saldanha[2]

Clin Hemorheol Microcirc 39 (2008) 375–380

[1] *CEMAT/IST and Department of Mathematics, Instituto Superior Técnico, Universidade Técnica de Lisboa, Portugal*

[2]*Unidade de Biologia Microvascular e Inflamação, Instituto de Medicina Molecular, Instituto de Bioquímica, Faculdade de Medicina, Universidade de Lisboa, Lisboa, Portugal*

The experimental part of this paper was performed by Ana Santos Silva-Herdade as well as the interpretation of the numerical results.

Abstract

The recruitment of leukocytes to the endothelial walls is intensively investigated both experimentally and through three dimensional computer simulations. The shear dependent viscosity has been obtained from measured values in post- capillary venules of Wistar rats' cremaster muscle. Localized velocity fields and shear stresses on the surface of leukocytes and near vessel wall attachment points have been computed and discussed for a cluster of recruited leukocytes under generalized Newtonian blood flow with shear thinning viscosity. We have observed one region of maximum shear stress and two regions of minimum shear stress on the surface of the leukocytes close to the endothelial wall. This suggests that the accumulation of selectins attains a minimum value in two regions, rather than in one region, on the surface of the leukocytes. We have also verified that the collective hemodynamic behavior of the cluster of recruited leukocytes establishes a strong motive for additional leukocyte recruitment. From this study we claim that the influence of the leukocytes rolling on the endothelial wall increases the shear stress on both the leukocyte and the endothelial wall which results in activating more signaling mediators during inflammation.

Keywords

Leukocytes dynamics, intravital microscopy, computational hemorheology, leukocyte wall shear stress

1. Introduction

Leukocyte arrest, recruitment and subsequent rolling, activation, adhesion and transmigration is a multistage process which is mainly triggered by hemorheologic forces and supported by shear-induced selectins, chemoattractants and adhesion molecules on the surface of the leukocytes and the endothelial wall [1–3]. A certain density of selectins and a high tensile strength of the selectin bond are required to confirm rolling. The mechanism of margination of leukocytes from the blood main stream is not well understood and deserves more focus on the causes and the force that initiate

margination. It is believed that rolling is mediated by adhesion molecules of the selectin family which are expressed on the leukocyte surface (L-selectin) on the endothelial wall (E-selectin) and in platelets (P-selectins). The forces applied by these mediators are not enough for marginating the leukocytes and therefore, it is necessary to study the hydrodynamic forces and their interaction with the molecular forces in detail. This is a multiscale process which requires more adequate sub-macroscopic models which are capable of computing localized hemodynamics such as on surface shear stress and velocity distribution. In this study we have performed experiments on Wistar male rats and recorded leukocytes dynamics in real time using intravital microscopy. We have used these experimental data to build a shear dependent viscosity model and plug it into a lattice Boltzmann numerical solver for shear thinning flows [4]. The lattice Boltzmann is a fully adaptive mesoscopic solver that has a number of benefits over the classical macroscopic fluid flow solvers. The most important feature of the lattice Boltzmann method is its capability to compute the shear stress independent of the velocity fields, from the non-equilibrium part of the distribution functions.

2. Materials and methods

2.1. Animal preparation

The animals used in this study received human care in accordance with the directive of the European community no. 86/609/CEE. The animals were prepared as explained in [1] with the right jugular vein and the left carotid artery catheterized. Pressure and cardiac frequencyweremonitored through thewhole time of experiment via a pressure transducer (TRANSPAC). The animals were prepared for intravital microscopy according to Hill [5]. Intravital images of the dynamics of leukocytes were recorded and analyzed. Blood samples were taken after the intravital microscopy observations to study the viscosity behavior in response to the shear rate using a Brookfield digital viscometer.

2.2. Numerical method

We have used a recently validated lattice Boltzmann model for shear thinning blood flow [4] to simulate individuals and clusters of moving leukocytes in three dimensions. The

method is mesosopic, based on the Boltzmann transport equation from physics, which is suitable for solving multiscale phenomena that commonly appear in complex fluid flows. For non-Newtonian flows, the shear rate is locally computed from the non-equilibrium parts of the distribution functions, without a need for calculating velocity gradients. The drag and lift forces and the torques are easily computed from momentum ex- change between the fluid and the structure [6]. Computed drags and torques were used to update the leukocyte positions. Translational and angular velocities were set on surface from the measured values.

3. Results

3.1. Experimental results

We have successfully tracked the dynamics of leukocytes from the in vivo experiment using the intravital microscopy and we were able to count the number of rolling leukocytes and measure the respective rolling speed as well as venule and leukocyte diameters. A snapshot of recorded video frames is shown in Fig. 1. An average leukocyte linear velocity of 8 rolling leukocytes was about 2.73 µm/s, with venule and leukocyte diameters being 23.7 and 6.8 µm, respectively.

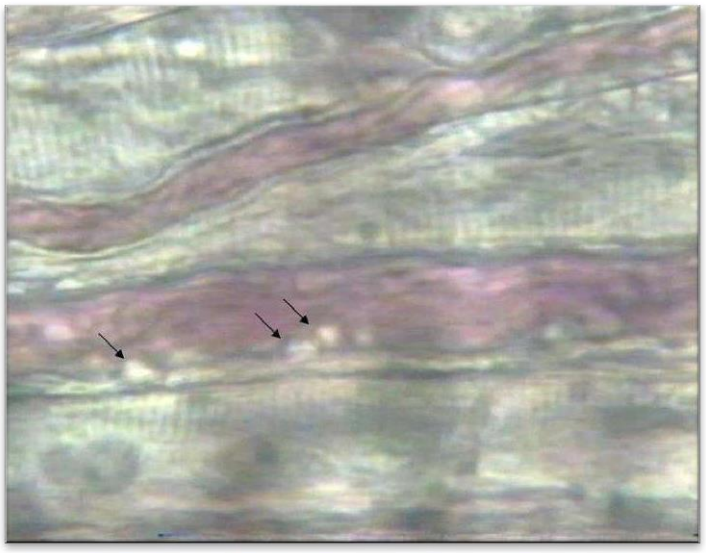

Figure 1. Intravital microscopy of recruited leukocytes (the white spots) in a post-capillary venule in aWistar rat cremaster muscle. Rolling leukocytes are indicated with arrows.

The hemodynamical parameters deter- mined by in vivo measurements have shown a systolic blood pressure of 131 mmHg, a diastolic blood pressure of 90 mmHg and a cardiac frequency of 394 BPM. Figure 2 shows individual tracking of some leukocytes as a function of time and relative distances from the nearest walls. (A) represents the path of a leukocyte from entrance until it rolls and (B) the relative position in time for the same leukocyte. Shown are also the time dependent components of velocity magnitudes (C) and accelerations (D). Blood samples were taken and analyzed by a viscometer to determine the shear thinning behavior of the rats' blood (see Fig. 3).

3.2. Numerical results

We have conducted a number of simulations for individual leukocytes, represented as irregular spheres, and for a cluster of moving leukocytes. From these simulations we have observed that the motion of leukocytes through a small enough venule results in disturbing the flow and increasing the endothelial wall shear stress at large distances. Shown in Fig. 4 is the influence of a not yet marginated leukocyte (moving through the centerline of the venule) on the endothelial wall shear stress.

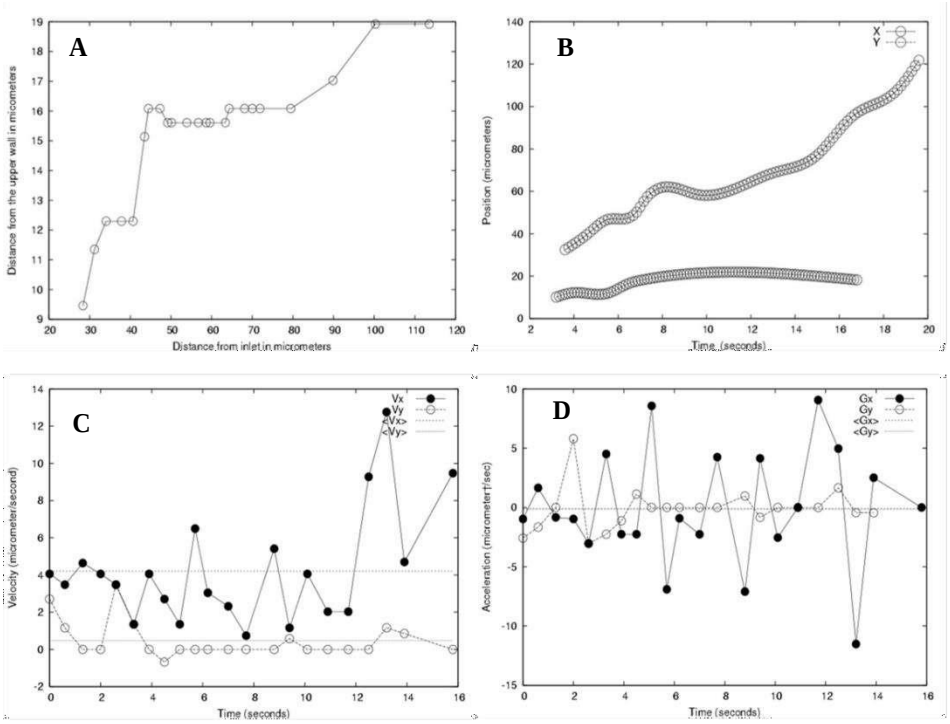

Figure. 2. Individual tracking of some leukocytes as a function of time (C and D) and relative distances from the nearest walls (A and B).

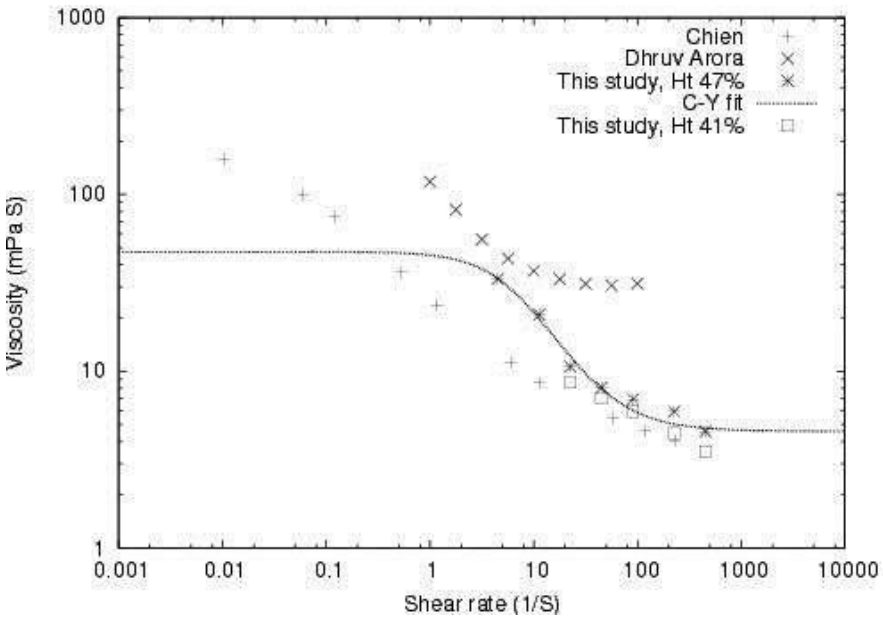

Figure 3. Shear rate dependent viscosity values (at different hematocrits) obtained from blood samples of Wistar rats. Shown is also the Carreau–Yasuda shear thinning fit

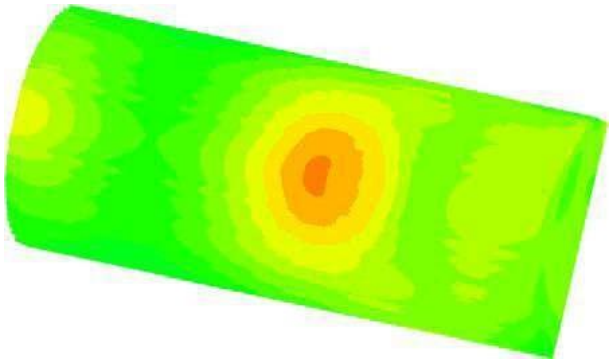

Figure. 4. Influence of a free flowing leukocyte on the endothelial wall shear stress.

We suggest that the endothelial wall shear stress will be high enough to activate the endothelial cell monolayer and the mediators of the selectin family, initiating the capture of the leukocytes from the blood mainstream. We have also observed four stagnation points on the endothelial wall: two upstream and two downstream with respect to the recruited leukocyte. These stagnant regions may help in the capture of leukocytes and decelerates their motion (see Fig. 5). For a cluster of recruited leukocytes, the traps and the vortexes form a helical stream, which also supports leukocytes margination toward and their rolling on the endothelial wall, as it is shown in Fig. 5.

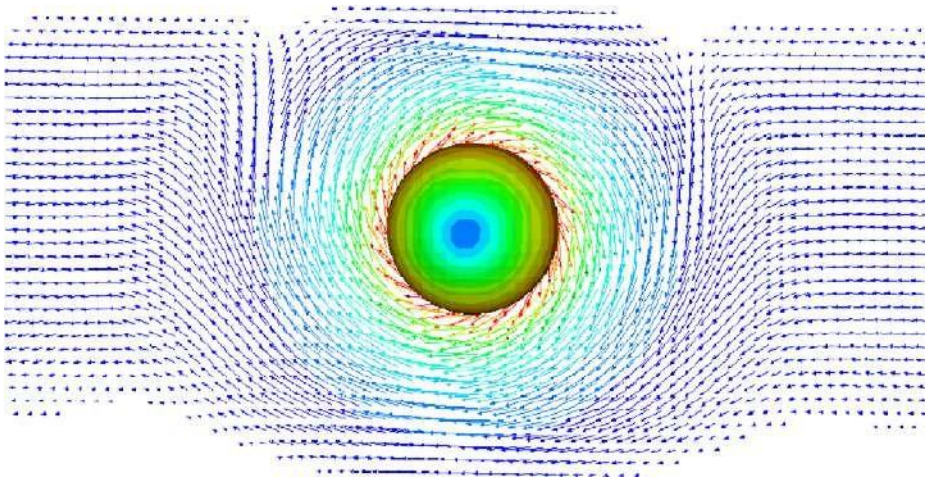

Figure. 5. Leukocytes are trapped by four stagnant regions close to the endothelial wall (with the flow motion directed to the right).

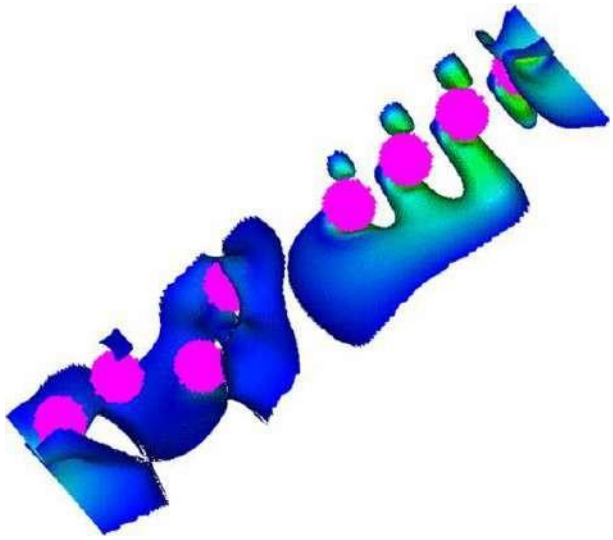

Figure. 6. Velocity isosurface around recruited leukocytes. The white jackets correspond to stagnant regions.

4. Discussion

During inflammation, the recruitment of leukocytes from the blood stream and their subsequent adhesion to the endothelial wall are essential stages to the immune response system. The interaction between the recruited leukocytes and the endothelial cells is a key parameter in some pathogenesis of vascular diseases. It is important to evaluate

leukocytes dynamics and quantify their localized velocities on surface shear stress and to capture the influence of the resulting hemodynamics on the endothelial wall at the inflammation regions.

Intravital microscopy is an adequate routine tool used for tracking the leukocyte dynamics but is restricted to two dimensions. In this study we were able to obtain more information by conducting three dimensional time dependent simulations for flow of leukocytes through a venule. Concerning the hemodynamical analysis of the results from the intravital microscopy, it is clearly observed that the velocity variations in the x-axis are higher than the ones observed in the y-axis, meaning that leukocytes move to the endothelial wall by modification of their position in the x-axis. Nevertheless, it was possible to obtain three-dimensional details on the flow field and the shear stress of marginated and rolling leukocytes. The data obtained from the experiments were used to set the initial and boundary conditions and to adopt a shear thinning viscosity model. It deserves noting that most of the studies reported in the literature (in vivo, in vitro or numerical) consider Newtonian flow dynamics of a 2Dsystem. In this study we have demonstrated the influence of shear thinning flow on the recruitment and rolling processes of leukocytes. The role of hemorheologic forces of a cluster of leukocytes was also demonstrated. Moreover we have observed that the surface shear stress on a recruited leukocyte shows two regions of minimum and one region of maximum shear stress. This may play a dominant role in directing the leukocyte toward the endothelial walls. Other studies refer to the leukocytes involvement in the signs and symptoms of chronic venous diseases [7–9] and it's also known that the properties of endothelial cells may be impaired in many diseases as atherosclerosis, hypertension, inflammation and metabolic diseases so, in this field, this work can be of great interest in the context of cardiovascular diseases. Ongoing research includes studies on adhesion and transmigration of rolling leukocytes.

5. Acknowledgements

This work has been partially supported by the grant SFRH/BPD/20823/2004 of FCT (A. Artoli) and by the project PTDC/MAT/68166/2006. FCT funds from the Centre for

Mathematics and its Applications – CEMAT and the Molecular Medicine Institute – Microvascular Biology and Inflammation Unit are highly appreciated.

References

1. A.S. Silva, C. Saldanha and J.Martins e Silva, Effects of velnacrine maleate in the leukocyte-endothelial cell interactions in rat cremaster microcirculatory network, Clin. Hemorheol. Microcirc. 36 (2007), 235–246.
2. A.M. Artoli, A. Sequeira, A.S. Silva-Herdade and C. Saldanha, Leukocytes rolling and recruitment by endothelial cells: Hemorheological experiments and numerical simulations, J. Biomech. 40(15) (2007), 3493–3502.
3. R. Alon, D.A. Hammer and T.A. Springer, Lifetime of the P-selectin-carbohydrate bond and its response to tensile force in hydrodynamic flow, Nature 374 (1995), 539–542.
4. A.M.Artoli and A. Sequeira, Mesoscopic simulations of unsteady shear thinning flows, Lecture Notes Computer Sci. 3992 (2006), 78–85.
5. M. Hill, B. Simpson and G. Meinninger, Altered cremaster muscles hemodynamics due to disruption of the deferential feed vessels, Microvasc. Res. 39 (1990), 349–363.
6. P. Lallemand and L.-S. Luo, Lattice Boltzmann method for moving boundaries, J. Comput. Phys. 184 (2003), 406–421.
7. M.R. Boisseau, Leukocyte involvement in the signs and symptoms of chronic venous disease. Perspectives for therapy, Clin. Hemorheol.Microcirc. 37 (2007), 277–290.
8. J.F. Stoltz, S. Muller, A. Kadi, V. Decot, P. Menu and D. Bensoussan, Introduction to endothelial cell biology, Clin. Hemorheol. Microcirc. 37 (2007), 5–8.
9. M.R.Boisseau, Fahraeus Lecture 2005: Hemorheology and vascular diseases: red cel should rub up to the wall, leucocytes should cope with it, Clin. Hemorheol.Microcirc. 35 (2006), 11–16

IV. Leukocytes dynamics in microcirculation under shear-thinning blood flow

Adélia Sequeira[1]

Abdel Monim Artoli[1]

Ana Santos Silva-Herdade[2]

Carlota Saldanha[2]

Computers and Mathematics with Applications 58 (2009) 1035-1044

[1] *CEMAT/IST and Department of Mathematics, Instituto Superior Técnico, Universidade Técnica de Lisboa, Portugal*

[2]*Unidade de Biologia Microvascular e Inflamação, Instituto de Medicina Molecular, Instituto de Bioquímica, Faculdade de Medicina, Universidade de Lisboa, Lisboa, Portugal*

The experimental part of this paper was performed by Ana Santos Silva-Herdade as well as the interpretation of the numerical results.

Abstract

We present detailed simulation results of localised hemodynamics for a cluster of rolling leukocytes under shear-thinning blood flow using a lattice Boltzmann model. Leukocytes were modelled as hard spheres moving through a venule of rigid walls. The used hemorheological parameters were obtained from in vivo measurements in blood samples of Wistar rats. Velocities, shear stresses and torques were computed and visualised for each individual cell, for the cluster and for the fluid. We have found that the flow is mainly three-dimensional due to the swirling and the asymmetry of the formed vortices during the recruitment process. The shear stress is maximum on a cap covering the cell and a cone with its base on the endothelial wall at the contact region. The leukocyte is recruited to the wall with the aid of trapping vortices and four stagnant regions surrounding the cell in addition to lateral motion towards the wall. We suggest that these phenomena are highly dependent on the angular velocity of the leukocyte and on the attractive force between the leukocyte and the endothelial wall. For a moving cluster of recruited leukocytes, velocities and shear stresses as well as torques are computed. It was found that the shear stress at the endothelium gets higher as the cluster moves in the main stream enabling early initialization of the rolling process.

Keywords

Leukocytes recruitment, blood rheology, flow in microvessels, inflammation

1. Introduction

Leukocyte arrest, recruitment and subsequent rolling, activation, adhesion and transmigration are essential stages in the immune response system to inflammation. Understanding this mechanism is of crucial importance in immunology and development of anti-inflammatory drugs such as modulators and blockers. The recruitment process is usually observed in post venules in the microcirculation. It is well accepted that the rolling process and the later adhesion cascade are mediated by a number of chemoattractants on the endothelial cell surface, selectins, integrins and other mediators on the surface of the

leukocytes, and in the tissue. The whole process is triggered by margination of free flowing leukocytes toward the endothelial wall. This process is believed to result from the interaction of leukocytes with surrounding erythrocytes which deform and support pushing the leukocytes to the wall [1-4].

The captured leukocyte starts to roll under the assistance of a number of selectin mediators (P-selectin, L-selectin and E-Selectin) or their ligands through a complex process of overlapping domination by these mediators. Most leukocytes adhere to the endothelium after their rolling speed is decelerated by the CD18 integrins. The adherence process is mediated by the E-selectins. Under the existence of exogenous chemoattractants the leukocyte changes shape and transmigrates through the endothelium. The main function of the process is to isolate or eradicate the irritants and repair the inflamed tissue. At the end of the process the leukocyte is extravated (e.g. [5]).

Despite the fact that numerous attempts of in vivo and in vitro experiments, as well as numerical simulations of leukocytes recruitment and adhesion have been reported, the phenomena is not yet well understood and is under intensive investigation due to the key role that the mechanism plays in different pathogenic and immunological activities such as cancer, kidney failure (e.g. [6]), drug delivery and allergies [7, 8]. The mechanism of margination of leukocytes from the blood main stream is not well understood and deserves more focus on the causes and the forces that initiate margination.

The main objective of this study is to probe the role of hemorheology in the margination process. Current experiments have focused on adhesion (e.g. [3,9,10]) from which the strength of signalling molecules, the rolling speeds and the transmigration scenario are well described. Theoretical studies are rare [11,12] and mainly couple the equations of motion and solve them numerically. Due to the multi-timescale nature of this cascade, it is necessary to combine a number of experimental techniques (see e.g. [13] for a review) or combined experiments and numerical simulations [9,14] when details of force interactions are acquired. It is to be noted that most of these studies, in vivo, in vitro or via numerical simulations are two dimensional and assume blood as a Newtonian fluid with constant viscosity. Commonly observed phenomena of spheres sedimenting near a wall,

such as anomalous rotation, tendency towards the wall and vortex formation are different in Newtonian and non-Newtonian fluids. For example, for shear-thinning flows, a sphere in the flow tends to move towards the wall and rotates more slowly than the Newtonian flow, causing anomalous rotation [15_17]. Formation of negative wakes have also been observed in shear-thinning fluids [18].

In this study, we made use of tracking of leukocytes via intravital microscopy [19] from an in vivo experiment in Wistar rats to track the leukocytes trajectories and measure their velocities and forces exerted on them. These results were then used to initialise a lattice Boltzmann shear-thinning solver. We have also studied viscosity dependence on the shear rate from obtained blood samples of the rats which was found to follow a shear-thinning behaviour. The results were then used in simulating three dimensional leukocyte dynamics in a model of the venule from which the observations were taken.

As the results obtained from experiments are usually two-dimensional, three-dimensional simulations will provide extra information on the localised hemodynamics such as the on-surface shear stress and the regions of stagnant flow. As the formation of vortices, their sizes and directions of rotation are largely affected by the relative cell positions, we also have studied the dynamics and highlighted the influence of clustering leukocytes on the endothelial wall shear stress which is the main activator for most endothelium activities.

2. Governing equations

We consider an incompressible shear-thinning blood flow model in a straight venule Ω with boundary $\partial\Omega$ and diameter d=17.5 μm. A group of leukocytes, represented as spheres Σ (t) with boundary $\partial\Sigma$ (t) and similar diameters D =9.5 μm are moving through the venule in the main stream where they are subjected to an attractive force towards the endothelial wall.

In rheology, the Deborah number is a dimensionless quantity relating the fluid relaxation and deformation time scales. Materials with a small Deborah number show only minor qualitative differences from a Newtonian fluid. More precisely, the Deborah number is

defined as $De = U\lambda/D$, where λ is the characteristic relaxation time of blood (time taken by deformed erythrocytes to return to their original non-deformed shape) and U is the magnitude of the downstream leukocyte velocity.

Moreover we also consider the dimensionless Reynolds number $Re = \rho UD/\eta$ and define the dimensionless distance from the wall as $h = H/D$ where H is the distance of the leukocytes from the endothelial wall and η is the zero shear rate viscosity. We assume similar densities for both leukocytes and the surrounding fluid. Typical simulation values are 0.01 for the Reynolds number and 0.03 for the Deborah number. The blockage ratio is $D/d = 0.54$, approximately.

The governing equations for the fluid-leukocyte system are the following: the momentum equation

(—) (1)

the continuity equation

(2)

And

( ) (3)

for the motion of the leukocyte. In these equations $\boldsymbol{u}$ is the instantaneous velocity, ω is the angular velocity appearing from the torque, $\boldsymbol{r}$ is the position vector from the centre of the cell and $\boldsymbol{U}$ is the downstream leukocyte velocity (averaged from experiments), as mentioned above. In addition, the leukocyte is subjected to an attraction force F_s towards the wall, computed from the experimental trajectories. The stress tensor is given by

(̇)(( )) (4)

where p is the pressure, $\boldsymbol{I}$ is the unit tensor and $\dot{\gamma}$ is the shear rate. The total viscosity η satisfies the Carreau-Yasuda model

( )((̇)) (5)

in which η_0 and η_∞ are the asymptotic low and high shear-rate viscosity values, respectively. Here λ is the characteristic time of the fluid which depends on the instantaneous state of the material, $\dot{\gamma}$ is the shear rate and the parameters *a* and *b* are determined from experimental data, with b < 0 for shear-thinning fluids. If *a* or *b* vanish, the fluid model behaves as Newtonian. The force on the leukocyte is given by

$$\int \qquad (6)$$

and the torque ***T*** at a distance ***r*** from the centre of leukocyte is

$$\int \qquad (7)$$

where **n** denotes the exterior unit normal vector to the leukocyte surface. The leukocyte velocity **U** and its angular velocity ω are expressed in the cell equations of motion

$$\ddot{} \qquad (8)$$

and

$$\ddot{} \qquad (9)$$

with **I** being the moment of inertia. The particle position is given by solving these equations.

3. Numerical method

The lattice Boltzmann method [20-22] is a special finite difference discretisation of the simplified Boltzmann equation which describes transport phenomena at the mesoscale level. The dynamics of the fluid is modelled by the transport of simple virtual particles on the nodes of a Cartesian grid. Simulations with this method involve two simple steps; streaming to the neighbouring nodes and colliding with local node populations represented by the probability f_i of a particle moving with a velocity $\mathbf{e}_i$ per unit time step δt. Populations are relaxed towards their equilibrium states during a collision process.

The equilibrium distribution function

$$() \left(\quad — \quad —() \quad — \quad \right) \qquad (10)$$

is a low Mach number approximation to the Maxwellian distribution. Here, ω_i is a weighting factor, $\upsilon = \delta x/\delta t$ is the lattice speed, and δx is the lattice spacing.

Studies on leukocytes and erythrocytes dynamics using lattice Boltzmann techniques have been reported (e.g. [23-25] in which blood was modelled as a Newtonian flow in 2D geometry. For non-Newtonian flow modelling, a number of lattice Boltzmann schemes were proposed for power law (e.g. [26, 27]), Bingham [28], shear-thinning Carreau-Yasuda [29] and viscoelastic (e.g. [30-32]) fluids. It is to be noted that most of the available viscosity models are empirical. Moreover, they rely on macroscopic observations. Kinetic theory based viscosity models for blood are still lacking in the literature. Following the trend of our experimental data obtained from Wistar rats, we have found that the Carreau-Yasuda shear-thinning model best fits these results within the range of 4.50 to 450,00 s^{-1} of shear rates [19]. Therefore, we have adopted the model proposed by Artoli and Sequeira [29] for the shear-thinning flow which will be explained subsequently.

3.1. A lattice Boltzmann model for shear-thinning fluids

The non-Newtonian behaviour of many fluids, including blood, may be studied using the shear-thinning Carreau-Yasuda viscosity model, given above in Eq. (5). In what follows we show that a shear-thinning fluid can be modelled by a simplified lattice Boltzmann scheme.

We start from the usually known lattice Boltzmann equation

( ) ( ) ⊢ ( ) ( ) (11)

which can be obtained by discretising the evolution equation of the distribution functions in the velocity space using a finite set of velocities $\boldsymbol{e}_i$. In this equation, τ is the dimensionless relaxation time which may be a constant, a discrete or a continuous variable. By Taylor expansion of the lattice Boltzmann equation up to $O(\delta t^2)$ and application of the multiscale Chapman-Enskog technique, the Navier-Stokes equations and the momentum flux tensor up to second order in the Knudsen number are obtained. The hydrodynamic densi-

ty, ρ, and the macroscopic velocity, u, are determined in terms of the particle distribution functions from the laws of conservation of mass

$$\sum \sum ( ) \qquad (12)$$

and momentum

$$\sum \sum ( ) \qquad (13)$$

The pressure is given from the equation of state $p=\rho c_s^2$ and the kinematic viscosity is defined by $\upsilon = c_s^2\ \delta t(\tau - 1/2)$, where c_s the lattice speed of sound. A number of lattice Boltzmann models have been introduced, being characterized by the choice distribution functions, the number of moving particles, the lattice speed of sound and the nature of the relaxation time. Expanding f_i about its equilibrium distribution f_i^{eq}.

$$( ) \qquad ( ) \qquad (14)$$

where $\in$ is of the order of the Knudsen number and in the limit of small $\in$, the momentum flux tensor is obtained from [33]

$$( ) \quad \sum \quad ( ) \qquad (\quad) \qquad (15)$$

In this equation C is a lattice-dependent constant (for the three-dimensional model with 19 particles (D3Q19), C = 1/3).

The momentum flux is therefore directly computed from the non-equilibrium part of the distribution functions. Hence, the strain rate tensor is

$$\qquad \sum ( ) \qquad (16)$$

and the stress tensor is [34]

$$(\quad) \sum \quad ( ) \qquad (17).$$

In constitutive equations of shear-thinning generalized Newtonian fluids, the viscosity depends on the magnitude of the second invariant of the strain rate tensor

$$| | \quad \cdot \quad \sqrt{\qquad\qquad} \qquad (18)$$

In detail, for the D3Q19 model, after making use of the symmetry of the strain rate tensor, we have

$$\cdot \quad \cdot \sqrt{\qquad\qquad (\qquad\qquad) \quad (\qquad\qquad)} \qquad (19)$$

where $\gamma_c = 3/2\rho\tau_c$ could be used as a characteristic shear rate. In this study we optionally $\tau_c = 1$ to benefit from the simplicity and the stability of the scheme at $\tau = 1$.

Now, since $\eta=\rho$ the Carreau_Yasuda model in its dimensionless form is [29]

$$(\qquad)(\quad (\quad \dot{})) \qquad (20)$$

where and correspond to and , respectively. The stability of the method is controlled by the difference ( ) which is normally large for shear-thinning fluids. However, shall be in the working stability region if is small. Another way to avoid instability is to tune the material relaxation time (in lattice units) by grid-refinement (or coarsening) in time. We note that the relaxation time here is a continuous function of six parameters, four of them are freely controllable during the simulations. Fig. 1 shows a possible range of LBM shear-thinning relaxation time profiles which could be obtained at different material characteristic times, and therefore, different materials may be simulated within the stable regime. Validation of this model against the finite elements was reported by Artoli et al. [35].

4. Results

4.1. Blood model

The viscosity of collected blood samples from the Wistar rats was found to fit the Carreau_Yasuda shear-thinning model, Eq. (5) with cP, cP, cP,

s, and with a maximum standard error of 6.0% and reduced of 1.05 at 45% hematocrit and a temperature of 37ºC. From these parameters we have build a lattice Boltzmann shear-thinning model using Eq. (20). The behaviour of the model in response to the simulated shear rate is shown in Fig. 1 for different values of the dimensionless material relaxation time (i.e. at different LBM material time scales).

The geometry was discretised as shown in Fig. 2 for an individual leukocyte (represented as a sphere of diameter equal to 9.5 mm) moving in a straight rigid venule of diameter 17.5 mm. The spatial resolution is 0.5 mm. Two time scales are represented by the choice of the material characteristic time and the regular updating time step.

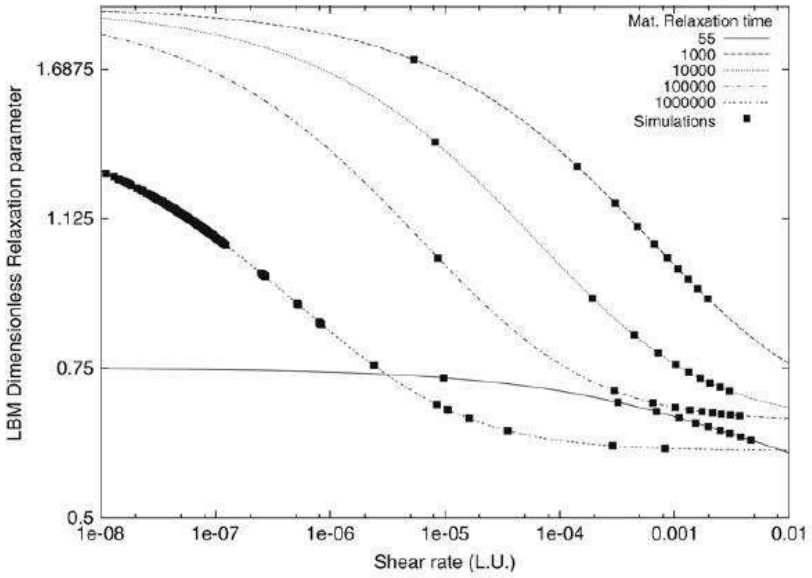

Figure 1. Possible range of LBM shear-thinning relaxation time profiles

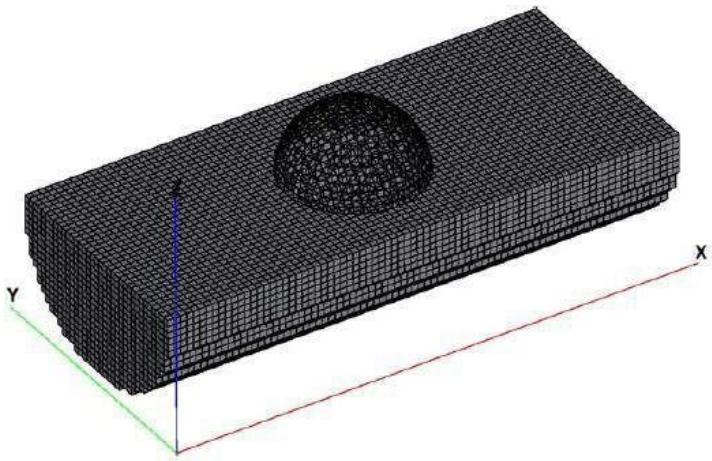

Figure 2. Discretisation of the model geometry for a single leukocyte in a straight venule.

Fig. 3 shows velocity vectors on a 2D projection of the leukocyte surface. We have used the Bouzidi et al. [36] boundary conditions for the moving boundaries and the wall. The inlet and the outlet conditions were implemented using an adaptation of the Zou and He [37] boundary conditions, with the pressure values obtained from the experiments [19]. The spherical leukocyte initially translates and rotates following the measured values obtained from the experiments. From these velocities, the pressure was computed and equilibrium distributions were computed and assigned to the relevant directions. The leukocyte moves downstream with a velocity 100 times less than the mainstream which flows at a Reynolds number of 0.017, based on the maximum axial velocity far from the leukocyte and on the centreline viscosity.

In addition, the drags and the lifts were computed from the momentum exchange between the fluid and the leukocyte [38]. The leukocyte rotates in response to the computed torque and is also subjected to a net attractive selectin force towards the wall proportional to the square of the distance between its surface and the sedimenting endothelium [12], estimated from the trajectory of the leukocytes. The cell position is updated using the relation ( ) . It is to be noted that the repulsive force was neglected due to its nanoscale nature. We highlight here the fact that the lattice Boltzmann method was found to be highly flexible when applied to the problem under investigation with a number of key features: (i) the mesoscopic multiscale nature of the lattice Boltzmann equation, (ii) the computation of local stresses from the non-equilibrium parts of the dis-

tribution functions and (iii) the straight forward implementation of fluid-structure interaction through momentum exchange.

4.2. Single leukocyte recruitment

We present here simulation results of flow around a spherical leukocyte sedimenting toward the endothelial wall of a straight cylindrical venule. Fig. 4 shows magnitudes and vectors for the velocity of the flow and the on-surface velocity of a rotating leukocyte. A trap of four stagnation regions, with two ahead and two behind the leukocyte close to the endothelial wall are formed, acting in support and possibly initiating the margination process. These stagnation regions have also been reported in previous experimental works [16,17].

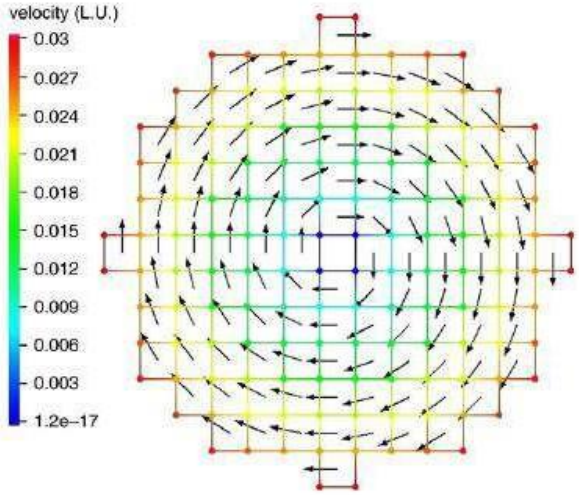

Figure 3. Boundary conditions on surface of a 2D projection of the leukocyte.

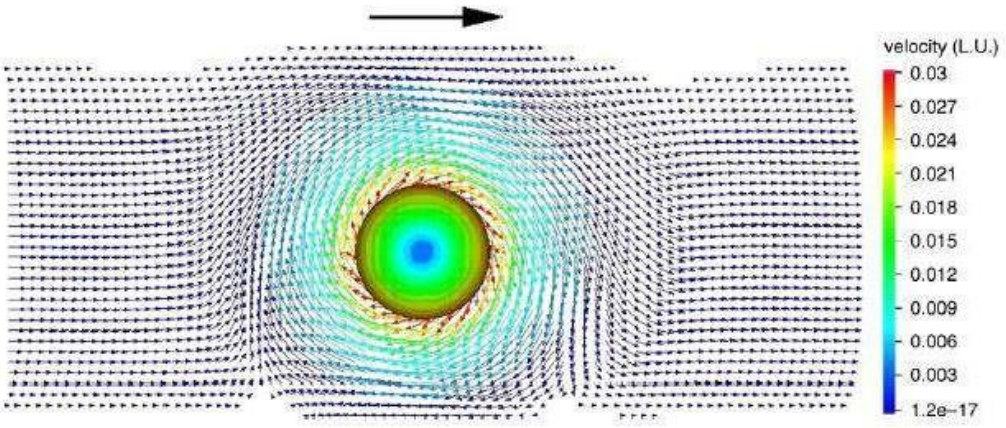

Figure 4. Velocity vector magnitudes around a recruited leukocyte. The arrow indicates the flow direction.

Upstream, the flow tends to go above the sedimenting cell and the situation is reversed downstream, creating a torque. This may be a reason for the anomalous rotation of the sphere sedimenting on a wall under shear-thinning flow. Fig. 5 represents a snapshot of the velocity contours for a fully developed flow around the recruited leukocyte under shear-thinning viscosity. The influence of the cell is clearly observed at large distances.

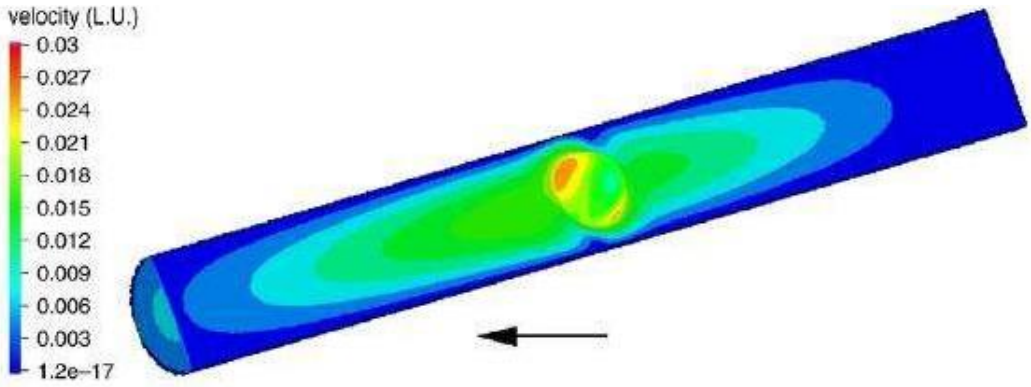

Figure 5. Fully developed velocity profile flow around a recruited leukocyte.

The shear stress in the sedimentation region gradually increases till it reaches a maximum value when the leukocyte is about half a micrometer from the endothelial wall (see Fig. 6).

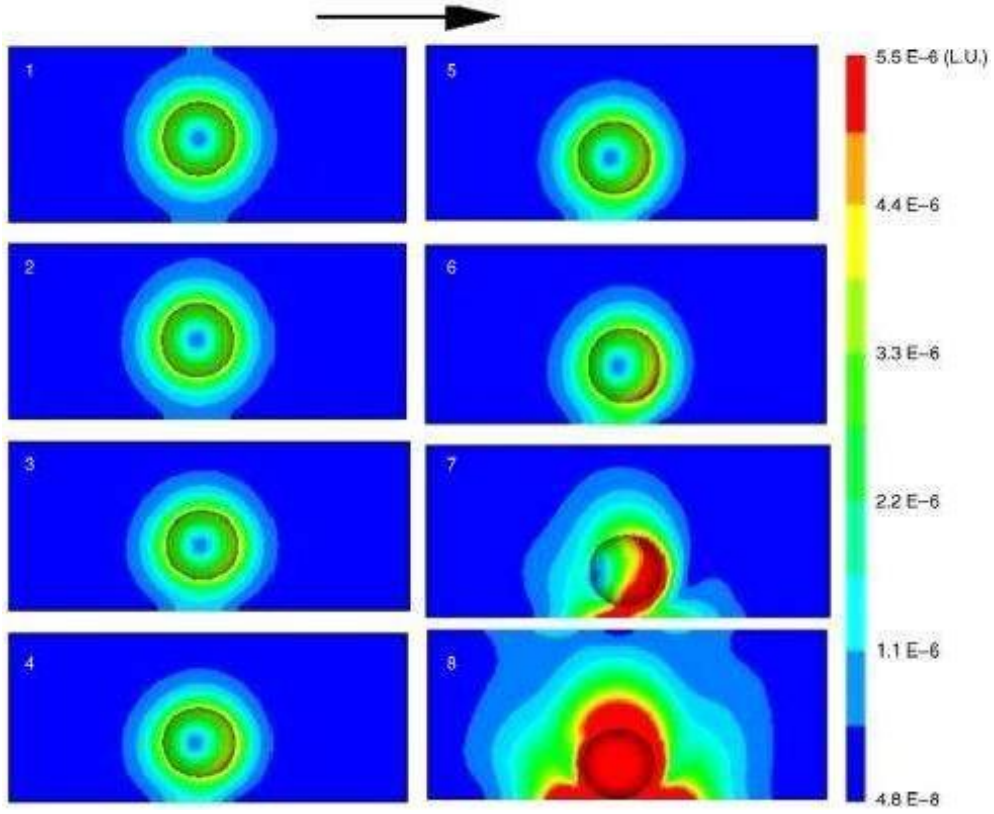

Figure 6. Changes in the shear stress as the cell approaches the endothelium

Increasing both the endothelium and the fluid shear stress near the contact region may result in releasing many chemoattractants known to be triggered by critical values for the shear stress (see e.g. [39]). In addition, we have found that the shear stress is maximum on a cap covering the leukocyte and a cone with base lying on the endothelium at the contact region (see Fig. 7) having maximum values on the endothelium wall downstream, directly ahead of the rolling leukocyte. We suggest that this shear stress value motivates the binding force that enables leukocytes to role on the endothelium wall downstream. Behind the rolling leukocyte the shear stress is smaller on the endothelium wall downstream and therefore, more bonds dissociate upstream while more appear downstream.

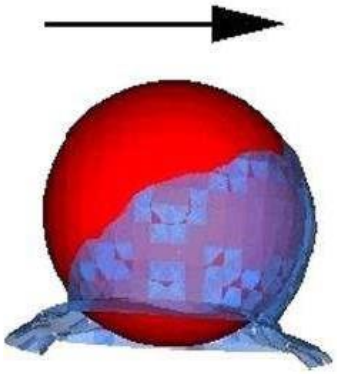

Figure 6. Regions of maximum shear stress as the leukocyte starts to roll.

4.3. Clustering leukocytes

We have also simulated the dynamics of a cluster of leukocytes moving from an initial random position through the microvessel. Fig. 8 shows velocity magnitudes on the surface of each cell from which we observe that the velocity of each leukocyte depends not only on its position in the mainstream but also on its relative positions to the other neighbouring leukocytes. The vortices and stagnation points observed in the case of a single leukocyte also appear here, but in a more complex pattern. The traps and the vortices form a helical stream which also supports leukocytes margination toward and their rolling on the endothelial wall (see Figs. 10 and 11).

The cluster of moving leukocytes largely disturbs the flow field on the endothelial wall, mainly increasing its shear stress, as shown in Fig. 11. However, a number of buffer zones of lower shear stress exist. From the intravital experiment we have observed that the rolling cells move in a series of non-smooth clusters and have attributed that to these buffer zones in the endothelial wall shear stress which results in non-synchronised bond creation and dissociation events. However, most rolling leukocytes tend to move with similar rolling speed (see Fig. 9).

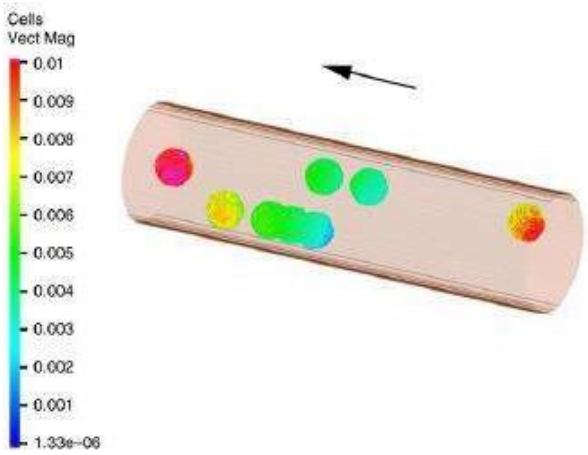

Figure 8. Velocity magnitudes for a cluster of moving leukocytes at different recruitment stages.

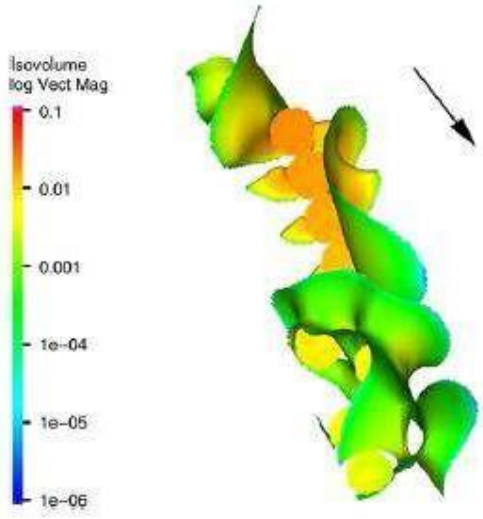

Figure 9. Velocity magnitudes and isosurfaces for a cluster of rolling leukocytes.

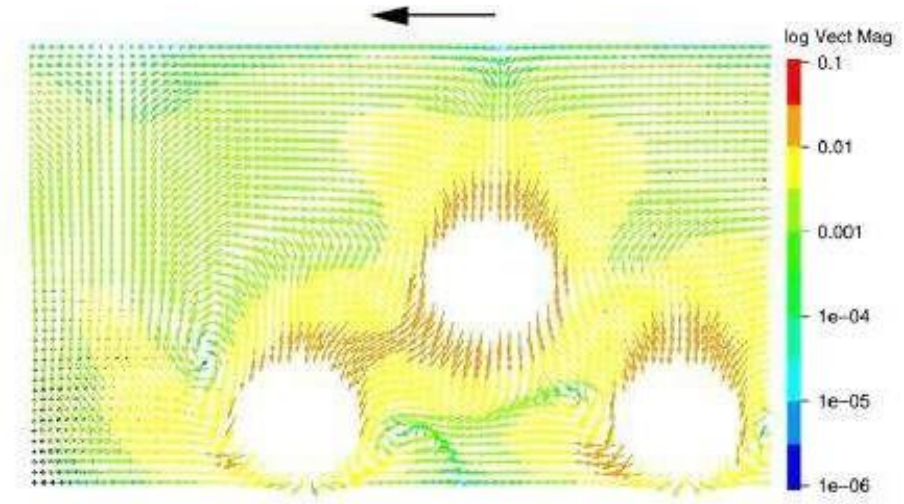

Fig. 10. Vortex formation during recruitment of leukocytes. The vortices act in support of the recruitment and rolling stages.

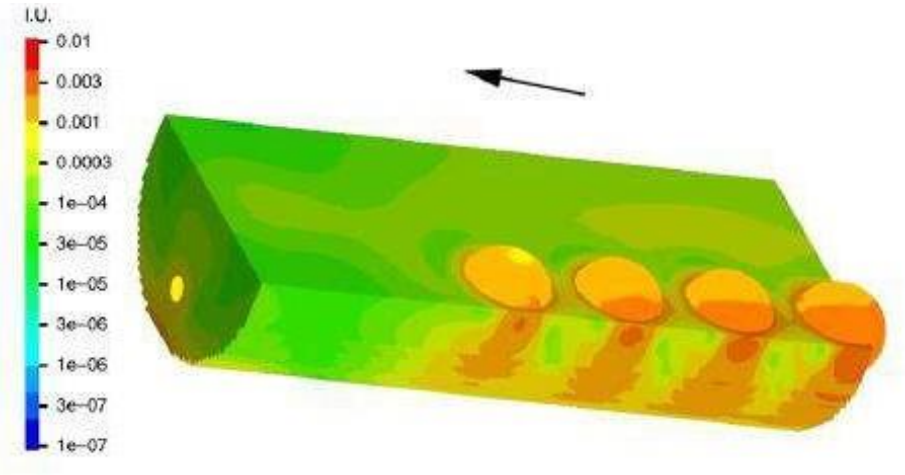

Figure 11. Effects of rolling leukocytes on the endothelial wall shear stress.

5. Conclusions

Our approach in this study was to use the parameters measured from intravital microscopy and rheometry to build a non-Newtonian shear-thinning model for blood and set the initial and boundary conditions for the mesoscopic lattice Boltzmann solver to probe the leukocyte recruitment to the endothelial wall in a straight venule of a Wistar rat.

We have intensively investigated the recruitment of leukocytes to the endothelial wall under shear-thinning blood flow based on intravital microscopy and rheometry from blood samples of Wistar rats. A lattice Boltzmann model for shear-thinning flow was used in three-dimensional computer simulations for individual and clustering leukocytes. Localised velocity field and shear stress on the surface of leukocytes under flow conditions similar to the experiments were presented and discussed. We were able to locate four stagnation regions close to the endothelial wall and have attributed the margination process mainly to their existence. However, it is not clear yet whether these stagnation points do always form, regardless of the fluid nature and the leukocytes rotational velocity. This issue deserves more investigation by conducting a number of experiments at different flow conditions. We also noticed two lateral wakes; one upstream directing the flow far from the sedimenting wall and another downstream directing the flow towards the wall, causing a torque on the sphere which acts in support of the rolling process.

From the computed shear stress near the point of contact we have noticed that the shear stress becomes high both on the leukocytes surface and around the point of contact. However, the maximum shear stress forms a conic cap with its base on the endothelium and most of it downstream. This indicates that the shear stress upstream of a rolling leukocyte is less than that downstream. The higher shear stress downstream ensures binding force formation while the relatively lower shear stress upstream suppresses the bonds behind the leukocytes and ease the bond dissociation. The cluster dynamics holds all the features observed in the single leukocytes, with the interfering caps of maximum shear stress and swirls of vortices and stagnation points which on average act in support of the rolling process. Ongoing research in our group involves firm adhesion and transmigration of the rolling leukocytes and also the influence of certain drug releases on the localized hemorheology.

Acknowledgements

This work has been partially supported by the grant SFRH/BPD/20823/2004 of Fundação para a Ciência e a Tecnologia (A. Artoli) and by the project PTDC/MAT/68166/2006. FCT funds from the Centre for Mathematics and its Applications CEMAT and the Molecular Medicine Institute Microvascular Biology and Inflammation Unit are highly appreciated.

References

1. S. Chien, White blood cell rheology, in: G.D.O. Lowe (Ed.), Clinical Blood Rheology, CRC Press, Taylor and Francis, 1988, pp. 87-109.
2. O.K. Baskurt, R.A. Farely, H.J. Meiselman, Erythrocyte aggregation tendency and cellular properties in horse, human, and rat: A comparative study. American Journal of Physiology-Hearth and Circulatory Physiology 273 (1997) 2604-2612.
3. K. Ley, Leukocyte recruitment as seen by intravital microscopy, in: K. Ley (Ed.), Physiology and Inflammation, Oxford University Press, New York,2001, pp. 301-337.

4. R.M. Rao, L. Yang, G. Garcia-Cardena, F.W. Luscinskas, Endothelial-dependent mechanisms of leukocyte recruitment to the vascular wall, Circulation Research 101 (2007) 234-247.
5. A. Evans, D.A. Calderwood, Forces and bond dynamics in cell adhesion, Science 316 (5828) (2007) 1148-1153.
6. K. Sigbartl, K. Ley, Leukocyte recruitment and acute renal failure, Journal of Molecular Medicine 82 (2004) 1432-1440.
7. R. Lever, C.R. Page, Novel drug development opportunities for heparin, Nature Review Drug Discovery 1 (2) (2002) 140-148.
8. Z. Szekanecz, A.E. Koch, Therapeutic inhibition of leukocyte recruitment in inflammatory diseases, Current Opinion in Pharmacology 4 (4) (2004) 423.
9. R. Alon, S. Chen, K.D. Puri, E.B. Finger, T.A. Springer, The kinetics of L-selectin tethers and the mechanics of selectin-mediated rolling, Journal of Cell Biology 138 (5) (1997) 1169-1180.
10. H.S. Rosário, C. Saldanha, J. Martins e Silva, The effect of velnacrine in lipopolysaccharide-induced leukocyte-endothelial interaction, in: B. Fragell (Ed.), 21st European Conference on Microcirculatin, Monduzzi Editore, Bologna, Italy, 2000, pp. 79-82.
11. G.I. Bell, Models for the specific adhesion of cells to cells: A theoretical framework for adhesion mediated by reversible bonds between cell surface molecules, Science 200 (1978) 618-627.
12. G.I. Bell, M. Dembo, P. Bongrand, Cell adhesion: Competition between non-specific repulsion and specific bonding, Biophysical Journal 45 (1984) 1051-1064.
13. E.A. Evans, D.A. Calderwood, Forces and bond dynamics in cell adhesion, Science 316 (2007) 1148-1153.
14. J. Lou, T. Yago, A.G. Klopocki, P. Mehta, W. Chen, V.I. Zarnitsyna, N.V. Bovin, C. Zhu, R.P. McEver, Flow-enhanced adhesion regulated by a selectin interdomain hinge, Journal of Cell Biology 174 (7) (2006) 1107-1117.
15. L.E. Becker, G.H. McKinley, H.A. Stone, Sedimentation of a sphere near a plane wall: Weak non-Newtonian and inertial effects, Journal of Non-Newtonian Fluid Mechanics 63 (1996) 201-233.

16. J.A. Tatum, M.V. Finnis, N.J. Lawson, G.M. Harrison, 3-D particle image velocimetry of the flow field around a sphere sedimenting near a wall: Part 2: Effects of distance from the wall, Journal of Non-Newtonian Fluid Mechanics 127 (2005) 95-106.
17. J.A. Tatum, M.V. Finnis, N.J. Lawson, G.M. Harrison, 3-D particle image velocimetry of the flow field around a sphere sedimenting near a wall: Part 1. Effects of Weissenberg number, Journal of Non-Newtonian Fluid Mechanics 141 (2007) 99-115.
18. M.T. Arigo, G.H. McKinley, An experimental investigation of negative wakes behind spheres settling in a shear-thinning viscoelastic fluid, Rheologica Acta 37 (1998) 307.
19. A.M. Artoli, A. Sequeira, A.S. Silva-Herdade, C. Saldanha, Leukocytes rolling and recruitment by endothelial cells: Hemorheological experiments and numerical simulations, Journal of Biomechanics 40 (15) (2007) 3493-3502.
20. D. d'Humiéres, P. Lallemand, U. Frisch, Lattice gas models for 3D hydrodynamics, Europhysics Letters 2 (1986) 291-297.
21. G.R. McNamara, G. Zanetti, Use of the Boltzmann equation to simulate Lattice-Gas Automata, Physical Review Letters 61 (1988) 2332-2335.
22. F.J. Higuera, S. Succi, R. Benzi, Lattice gas dynamics with enhanced collisions, Europhysics Letters 9 (1989) 345-349.
23. C. Migliorini, Y. Qian, H. Chen, E.B. Brown, R.K. Jain, L.L. Munn, Red blood cells augment leukocyte rolling in a virtual blood vessel, Biophysical Journal 83 (2002) 1834-1841.
24. C. Sun, C. Migliorini, L.L. Munn, Red blood cells initiate leukocyte rolling in postcapillary expansions: A lattice Boltzmann analysis, Biophysical Journal 85 (2003) 208_222.
25. C. Sun, L.L. Munn, Particulate nature of blood determines macroscopic rheology: A 2-D lattice Boltzmann analysis, Biophysical Journal 88 (2003) 1635-1645.
26. E.S. Boek, J. Chin, P.V. Coveney, Lattice Boltzmann simulation of the flow of non-Newtonian fluids in porous media, International Journal of Modern Physics B 17 (1-2) (2003) 99-102.
27. J. Boyd, J. Buick, S.A. Green, A second-order accurate lattice Boltzmann non-Newtonian flow model, Journal of Physics A: Mathematics and General 39 (2006) 14241-14247.

28. I. Ginzburg, K.A. Steiner, Free-surface lattice Boltzmann method for modelling the filling of expanding cavities by Bingham fluids, Philosophical Transactions of the Royal Society of London A (360) (2002) 453-466.
29. A.M. Artoli, A. Sequeira, Mesoscopic simulations of unsteady shear-thinning flows, Lecture Notes in Computer Science 3992 (2006b) 78-85.
30. Y.H. Qian, Y.F. Deng, A lattice BGK model for viscoelastic media, Physical Review Letters 79 (14) (1997) 2742-2745.
31. L. Giraud, D. d'Humiéres, P. Lallemand, A lattice Boltzmann model for Jeffreys viscoelastic fluid, Europhysics Letters 42 (1998) 625-630.
32. P. Lallemand, D. d'Humiéres, L.-S. Luo, R. Rubinstein, Theory of the lattice Boltzmann method: Three-dimensional model for linear viscoelastic fluids, Physical Review E 67 (2) (2003) 201-203.
33. B. Chopard, M. Droz, Cellular Automata Modeling of Physical Systems, Cambridge University Press, 1998.
34. A.M. Artoli, Mesoscopic computational haemodynamics, Ph.D. Thesis, University van Amsterdam, The Netherlands, 2003.
35. A.M. Artoli, J. Janela, A. Sequeira, A comparative numerical study of a non-Newtonian blood flow model, in: Proceedings of the 2006 IASME/WSEAS, International Conference on Continuum Mechanics, Chalkida, Greece, 11-13 May, 2006, 91-96.
36. M. Bouzidi, M. Firdaouss, P. Lallemand, Momentum transfer on a Boltzmann lattice fluid with boundaries, Physics of Fluids 13 (2001) 3452-3459.
37. Q. Zou, X. He, On pressure and velocity boundary conditions for the lattice Boltzmann BGK model, Physics of Fluids 9 (1997) 1591-1598.
38. P. Lallemand, L.-S. Luo, Lattice Boltzmann method for moving boundaries, Journal of Computational Physics 184 (2003) 406-421.
39. A. Dardik, A. Yamashita, F. Aziz, H. Asada, B. Sumpio, Shear stress-stimulated endothelial cells induce smooth muscle cell chemotaxis via platelet derived growth factor-BB and interleukin-1, Journal of Vascular Surgery 41 (2005) 321-331.

V. Erythrocyte deformability – a partner of the inflammatory response

Ana Santos Silva-Herdade[1]

Giulia Andolina[2]

Caterina Faggio[2]

Ângelo Calado[1]

Carlota Saldanha[1]

Microvascular Research 107 (2016) 34–38

[1]*Unidade de Biologia Microvascular e Inflamação, Instituto de Medicina Molecular, Instituto de Bioquímica, Faculdade de Medicina, Universidade de Lisboa, Lisboa, Portugal*

[2] *Department of Chemical, Biological, Pharmaceutical and Environmental Sciences, University of Messina, Sicily, Italy*

Abstract

We aim to establish an in vivo animal model of acute inflammation using PAF (platelet activating factor) as inflammatory agent and to study the erythrocyte deformability changes induced by the inflammatory response. Counting the number of rolling and adherent neutrophils to endothelium after 2, 4 and 6 h of intrascrotal injection of PAF we showed the induction of an inflammatory state. Blood samples are collected in order to measure the erythrocyte deformability and to quantify NO efflux from the red blood cells (RBCs). The results show an increased number of rolling and adherent neutrophils after 2 h and 4 h of inflammation as well as decreased values of erythrocyte deformability in the same time-points. This result is in line with the need of a low blood viscosity to the recruitment process that will improve leukocyte migration towards the endothelial wall. NO efflux from RBCs is also affected by the inflammatory response at the first hours of inflammation. This animal model demonstrates in vivo the association between an acute inflammatory response and the rheological properties of the blood, namely the RBCs deformability. For those reasons we consider this as an adequate model to study acute inflammatory responses as well as hemorheological parameters.

Keywords

Inflammation, erythrocyte deformability, nitric oxide, intravital microscopy

1. Introduction

Rolling of leukocytes in post-capillary venules and their subsequent adhesion to endothelial walls are crucial steps of the inflammation response. The migration of the leukocytes to the tissues is a multi-step process which includes, margination, rolling, adhesion and transmigration. During the approaching process, leukocytes exit the central bloostream, interacting with the erythrocytes and decelerate, initializing rolling. In this process, leukocytes tend to aggregate with the red blood cells, thus reducing its speed (1, 2). The whole process is believed to be triggered by the activation of the endothelial cell monolayer in

response to inflammation mediators and it is commonly accepted that the rolling of the leukocytes along the vascular wall is a result of intrinsic weak forces of adhesion between the leukocytes and the endothelial cells, on the one hand, and of the driving forces exerted by the blood flow, on the other (2). The rolling is mediated by adhesion molecules of the selectin family. The combined action of three families of selectins: L-selectins (associated with leukocytes), E- and P-selectins (associated with endothelial cells and platelets) is to promote leukocyte rolling, one key process for the inflammatory response (3 - 5). Besides those molecules that are essential for the leukocyte recruitment to occur, in vitro and in vivo experiments have shown that the margination of leukocytes may depend on rheological factors such as hematocrit, blood suspension medium and shear stress (6, 7) reinforcing that the hemodynamic properties of the blood also influence the migration process (2). Firm adhesion occurs when the cell stays still in the endothelial wall for a time equal to or greater than 30 s (1, 3, 8, 9). Once adhered to the endothelial wall, leukocytes can transmigrate to the tissue and initiate their anti-inflammatory action, phagocytosing pathogens or foreign bodies that have induced inflammation. To adhere the leukocytes do nothing but flatten out, emitting pseudopodia towards the leukocyte surface, by a process called chemotaxis the cells crawl along the endothelial to find a good place for the trans-endothelial migration (10, 11). This depends on a number of factors, including specific receptors, the type of inflammation and vascular architecture, and matrix proteins.

As is well known, erythrocytes are biconcave cells that change their shape according to the vessel lumen diameter and have a key role in the oxygen transport in the body (12). The deformability indicates a reversible change of erythrocytes aspect in response to a deforming force. It is an essential interfering property of blood flow and thus in oxygen delivery within the systemic microcirculation.

The low deformability of the erythrocytes can reduce the oxygen uptake or donation (13). The erythrocyte deformability largely influences the blood viscosity, the more the RBCs are deformed the lower the blood viscosity is. Over a deforming force, the erythrocytes may be submitted to chemical or physical stimulations and nitric oxide (NO) efflux occurs (14). NO is synthesized in endothelial cells by different isoforms of NO synthase and plays

a significant role in the control of the individual cell and organ functions (15). So the cells liberate a greater amount of NO which reduces platelet aggregation and leukocyte adhesion (antithrombin effect) and diffuses to the smooth muscle where relaxation occurs (16).

Using intravital microscopy as a qualitative and quantitative technique to observe and quantify epithelial cell–leukocyte interactions in vivo (17) we established an animal model of inflammation.

Using PAF (platelet activating factor) as inflammatory agent we studied the inflammatory response at different time point post inflammation by counting the number of rolling and adherent leukocytes and the changes induced in the erythrocyte deformability and erythrocyte efflux of NO concentration.

2. Materials and methods

2.1 Experimental design

The mice (BW: 23.0±2.3 g) used in this experiment were divided in four experimental groups according to time post-inflammation. An inflammatory response was induced using PAF (platelet-activating factor, Sigma, Germany) as an inflammatory agent. An intrascrotal (i.s.) injection of 300 µL of PAF 10−6 M in PB“ pH 7.4 was given to male mice and after 0, 2, 4 and 6 h of PAF administration the cremaster was prepared for intravital microscopy (N = 10 in each experimental group). At the end of the experiments, 500 µL blood was taken by cardiac puncture to heparinized tubes and the animals were euthanized with sodium pentobarbital (120 mg/kg BW).

2.2 Animal preparation

The animals used in this study received humane care in accordance with the Directive of the European Community 2010/63/EU that mentions the protection of animals used for economic and other scientific ends and also according to the Portuguese Legislation Law 113/2013.

Lys-EGFP-ki mice with 5 to 8 weeks (n = 40) (18) with an average weight of 23.0 ± 2.3 g, were kept in an animal facility with a 12 h light/dark cycle and housed in cages in a temperature controlled room. All animals were kept on a diet standard mouse food and water ad libitum. For the surgical procedures and microcirculatory measurements, the mice were anesthetized intraperitoneally (i.p.) with a cocktail of xylazine/ketamine (0.1 mL/10 g of BW). Body temperature was maintained between 35 and 37 °C with auto-regulated heating platform.

The preparation of cremaster for intravital microscopy was made in an appropriate support as described in (18). Using scissors a small incision in the scrotum was made and one of the testicles was exteriorized. Then the conjunctive tissue that surrounds the cremaster was removed, and an incision in the cremaster was made, fixing it to the appropriate support with silk sutures.

2.3 Intravital microscopy

After the cremaster preparation the support with the animal was placed in a confocal microscope Zeiss LSM 7 Live (Zeiss, Germany) adapted for intravital microscopy, equipped with a 20×water objective and a 10× ocular. All the images were recorded using the ZEN LSM2006 software. The cremaster was kept in perfusion of Krebs–Henseleit buffer with NaHCO3, warmed to 37 °C and bubbled with 95% N_2 and 5% CO_2 for the complete superfusion of the tissue throughout the experiment; the excess of liquid was removed with a vacuum system.

Post-capillary venules with 20–25 µm diameter were chosen for the quantification of the parameters previously defined. The duration which venules were registered was minimally 1min. From the recorded images the interactions between leukocytes and endothelial cells were quantified by the parameters already established (9): number of rolling leukocytes and their rolling speed, number of adherent leukocytes and venule diameters. The leukocytes were considered to be rolling on the endothelium if the leukocytes were moving at a slower speed than the erythrocytes in the same vessel over a 1 min duration. A

leukocyte was considered adherent to the endothelium if it remained stationary for more than 30 s in a 100 µm length (19).

2.4 Blood collection

At the end of the intravital microscopy observation 500 µL blood were taken by cardiac puncture to analyze erythrocyte deformability and NO concentrations according to the protocols described below. The blood was collected using heparin as an anticoagulant.

2.5 Erythrocytes deformability quantification

Erythrocyte deformability at different shear stress (0.30; 0.60; 1.20; 3.00; 12.00; 30.00; 60.00 Pa) was determined by using the Rheodyn SSD shear stress diffractometer from Myrenne GMBH (Roentgen, Germany) and erythrocyte deformability is expressed as the elongation index (EI) in percentage. Rheodyn SSD diffractometer determines RBC deformability by simulating shear forces exerted by blood flow and vascular walls on erythrocytes. Erythrocytes were suspended in a viscous medium and placed between a rotating optical disk and a stationary disk. A well-defined shear force was exerted upon the suspension which forces the erythrocytes to deform to ellipsoids and align with the fluid shear stresses. If a laser beam was allowed to pass through the erythrocyte suspension a diffraction pattern appears on the opposite end. That diffraction pattern will be circular with resting erythrocytes, but becomes elliptical when these ones were deformed by shear. Light intensity of the diffraction pattern was measured at two different points (A and B), equidistant from the center of the image. Erythrocyte elongation index (EEI), in percentage, was obtained according to the following equation: EEI (%) = A − B / A+B × 100.

2.6 Measurement of NO by an amperometric method

For NO determination the blood was centrifuged at 3000 rpm for 5 min in order to separate the red blood cells. Erythrocyte suspensions were centrifuged and sodium chloride 0.9% at pH 7.0 was added in order to reach a hematocrit of 0.05%. The suspension was mixed by gentle inversion of tubes. For amperometric NO quantification, we used the amino-IV sensor (Innovative Instruments Inc., FL, USA), as described in (20). Briefly, after

stabilization of the NO sensor immersed in erythrocyte suspensions, the erythrocytes were stimulated with 10mMof ACh and changes in the electric current registered, the change being proportional to the amount of NO mobilized by Ach stimulated erythrocytes. The NO concentration calculation was made based on the minimum peak and the maximum peaks obtain after the addition of ACh.

2.7 Statistical analysis

Data are expressed as mean values ± standard deviation (SD). Statistical analysis was conducted using the GraphPad Prism 5.0. Oneway ANOVA was applied to assess statistical significance between samples. Statistical significance was set at a $p < 0.05$ level.

3. Results and Discussion

The animal model of acute inflammation herein described uses PAF as an inflammatory agent. PAF is described as a phospholipid mediator of an inflammation that is released early in inflammation by a variety of cell types. It is also known that PAF cooperates in the recruitment of leukocytes in the inflamed tissue, promoting the activation of cells ensuing adhesion to the endothelium and extravascular transmigration of leukocytes (21) Therefore, after an intra-scrotal injection of PAF in mice, the numbers of rolling and adherent neutrophils were counted after 2, 4 and 6 h of inflammation. The rolling velocities and the vessel diameters were also determined. Fig. 1 shows a statistically significant increase in the number of rolling ($p < 0.001$) and adherent ($p < 0.05$) neutrophils after 2 and 4 h of inflammation and decrease at 6 h of inflammation. A control group of mice in which saline instead of PAF was injected with i.s. was used for similar measurements; no significant differences in the number of rolling and adherent neutrophils until 6 h after injection were observed (data not shown).

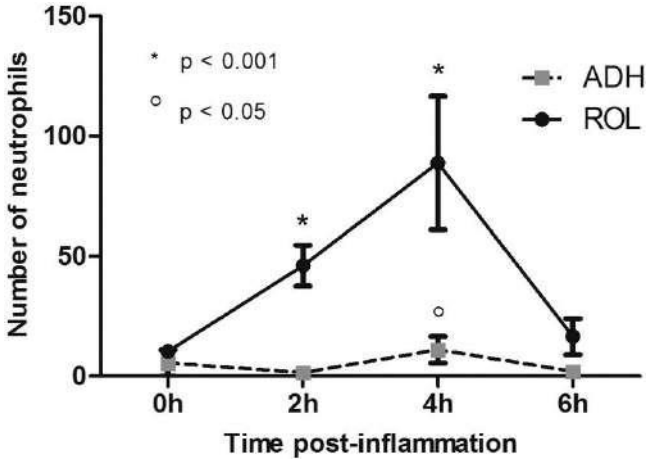

Figure 1. The number of rolling (ROL) and adherent (ADH) neutrophils after PAF-induced inflammation was determined at the beginning (0 h) and after 2, 4 and 6 h of PAF intrascrotal injection. After 4 h of PAF-induction of an acute inflammatory condition a statistically significant increase in the number of rolling ($p < 0.001$) and adherent ($p < 0.05$) leukocytes is observed. Representative results are mean values of the data obtained from a total of ten mice ($N = 10$) per experimental group. Error bars depict the associated standard deviations.

The rolling velocity decreases with time post-inflammation (Fig. 2A) which makes a part of a normal acute inflammatory response because the rolling velocity of neutrophils needs to become slower in order to facilitate the subsequent adhesion process.

This represents a typical acute inflammatory response, where there is a sequence of leukocyte recruitment in which we have an increase in the number of neutrophils in the first hours of the inflammatory response (22) that will be followed by an increase in the number of rolling monocytes. The increase of the vessel diameters Fig. 2B was also expected as vasodilation is also a main characteristic of the inflammatory response. Fig. 3 illustrates the deformability pattern of the erythrocytes. The cells are less deformable at 6 h of post-inflammation than after 2 h of inflammation.

The observed values are statistically significant ($p < 0.001$). The difference in the deformability in relation to the 0 h group is higher for high values of shear stress than for low values. The erythrocyte deformation index is an important physiological property of RBCs since those cells are the main cells in circulation and they are responsible for the oxygen transportation and delivery to the tissues.

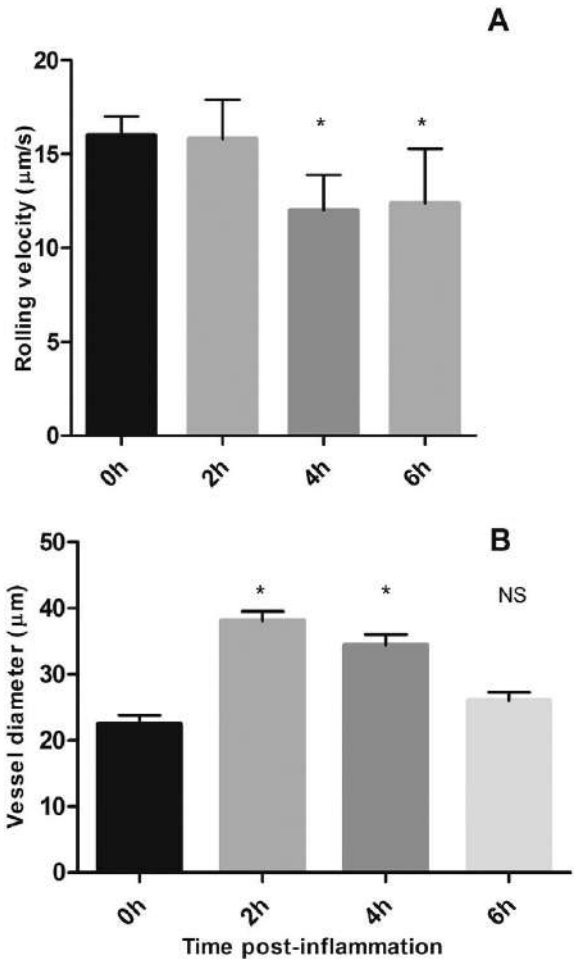

*Figure. 2. (A) Rolling velocities of the neutrophils with time post-inflammation and (B) diameters of the vessels visualized by intravital microscopy at the beginning (0 h) and after 2, 4, and 6 h post-inflammation. Four hours after PAF-induced inflammation, a decrease in the rolling velocity and an increase in the mean diameter of the vessels were observed. Representative results are mean values of the data obtained from a total of ten mice (N = 10) per experimental group. Statistical significance is presented in comparison to the initial time-point (0 h) and * p <0.05. Error bars depict the associated standard deviations.*

In order to pass through the capillary microcirculation the RBCs need to deform; the RBC membrane has the capacity to deform and maintain their integrity.

If the deformability of these cells is compromised the oxygen transportation to the tissues will also be impaired. In this study we observed a continuous decrease in the RBC deformability with the progression of the inflammatory response.

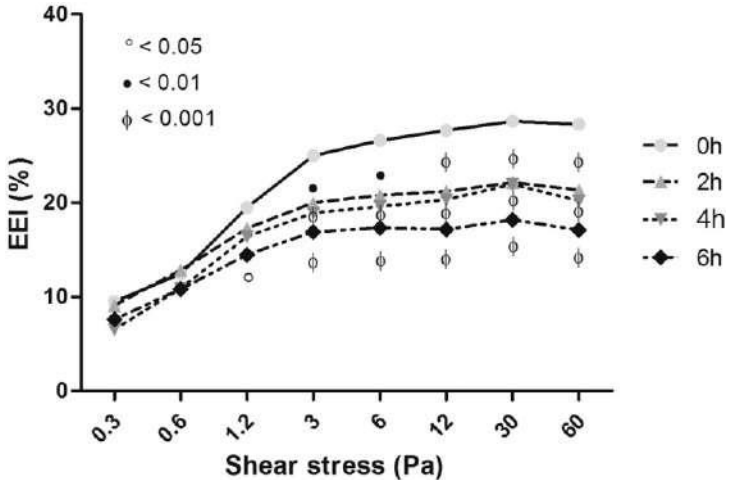

Figure. 3. Erythrocyte elongation index (EEI) expressed in percentage in the dependence of shear stress (Pa) at the beginning (0 h) and 2, 4, and 6 h post-inflammation. The deformability decreases significantly after 2, 4 and 6 h of PAF-induced acute inflammation. Statistical significance is presented in comparison to the control. Represented results are mean values of the data obtained from a total of ten mice (N=10) per experimental group.

PAF was used in the study as an inflammatory agent and although PAF-R (PAF receptor) is constitutively present on platelets, leukocytes and endothelial cells, Lang (22) disclosed the presence of PAF receptors in red blood cells but showed that PAF stimulates the breakdown of sphingomyelin on RBCs in isotonic conditions. Therefore, PAF may cause changes in the physicochemical structure of the erythrocyte membrane, which in turn may cause changes in RBC deformability. Taking this into account we entertain the possibility that the changes observed in RBC deformability at the first time-points may be independent of the inflammatory process but have a direct effect of the i.s. injected PAF on erythrocytes. Although, the subsequent decrease of the RBC deformability observed at the remaining time points cannot be disclosed from the inflammatory process, since no more PAF was injected and other mediators of inflammation, will be release as a result of the inflammatory response. Therefore, the hemorheological changes, observed in this animal model at the level of the RBCs deformability cannot be disclosed from the inflammatory component, besides an effect of PAF on the erythrocyte membrane may occur.

As published in (2) the rolling process is also mediated by the forces exerted by the blood flow and in order to adhere to the endothelial vessel wall the rolling velocity of the leukocyte decreases. Lower erythrocyte deformability will correspond to a higher blood viscosity which will contribute to the slower velocity of the rolling leukocytes. This will promote

the adhesion process which is essential for the inflammatory response and its resolution. Studies by Czepiel (24) reported that a decrease in RBCs deformability is correlated with the severity of inflammation in the case of an acute infection of the gastrointestinal tract by *Clostridium difficile*.

And also there is evidence that RBC deformability is impaired in chronic venous diseases (25). Other studies document that, in the course of an acute inflammatory response like in sepsis, pro-inflammatory cytokines activate inducible NOS (iNOS) resulting in large amounts of NO. NO has an effect on Ca2+-ATPase channels which leads to an increase in intracellular Ca2+, causing a decrease in RBC deformability (15).

In the acute inflammation model herein described Fig. 4 shows the concentration of NO efflux from RBC after 2, 4 and 6 h of PAF-induced inflammation. Although the values obtained are not statistically significant the mean value of NO efflux tend to decrease after 2 h of inflammation and to normalize to values similar to the control at 4 and 6 h of inflammatory response.

It seems that the return of NO efflux from erythrocytes precede the resolution of the inflammatory response observed after 6 h.

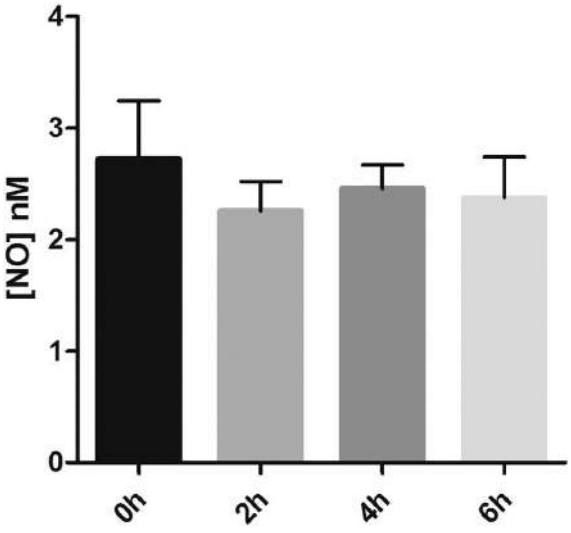

Figure 4. Nitric oxide (NO) efflux from mice erythrocytes at the beginning and after 2, 4 and 6 h of experimentally-induced inflammation following intra-scrotal PAF injection. Representative results are mean values of the data obtained from a total of ten mice (N= 10) per experimental group. Error bars depict the associated standard deviations.

NO is synthesized into and released from the endothelial cells by the help of nitric oxide synthases (NOs) that convert arginine into citrulline by a process that produces NO. NO produced in the endothelial cell diffuses, to the lumen where it is captured by RBCs or into muscle cells where it induces relaxation, eliciting vasodilation. This way, NO as an inflammatory mediator seems to have both pro- and anti-inflammatory effects depending on the mechanisms, on the NO concentration and levels of reactive oxygen species and also on the physiological environment.

High NO release from RBC samples was observed ex vivo from patients with hypoxia and inflammatory states, namely sickle cell disease, hypercholesterolemic, and hypertensive patients (26) associated with an impairment in the erythrocyte deformability. This inverse association could be a compensatory mechanism in low grade or chronic inflammation of those diseases.

4. Conclusions

The results herein presented describe an in vivo animal model of acute inflammation and demonstrate that there is a decrease in the deformability of the erythrocytes associated with the inflammatory response.

A decrease in the deformability of the red blood cells will create a higher blood viscosity and consequently will promote the formation of red blood cell aggregates. These conditions will in turn facilitate the margination of the neutrophils towards the vessel wall during the inflammatory response. After 6 h of inflammation we observe a decrease in the number of rolling neutrophils and lower values for the erythrocyte deformability. This means that the hemodynamic conditions of the blood flow are being maintained although the decrease in the number of rolling neutrophils indicates a pre-resolution state in which we could expect a return to normal values for RBC deformability. Besides further studies will be necessary to confirm the pre-resolution condition after 6 h of inflammation, it is well known that the recruitment of neutrophils is followed by the monocytes that will

need the same hemodynamic conditions to complete the migration process into the tissues.

This way, the continuous decrease observed in the RBC deformability after 6 h of inflammation is understandable. Therefore, the changes in the RBC deformability herein observed, in an in vivo animal model of inflammation, highlight the role of the hemodynamic properties of the blood in the development of the inflammatory response. In vitro studies (25) have already demonstrated that deformability can be ameliorated by the effect of carbenoxolone, a pannexin-1 inhibitor, so further studies will clarify if changes in the RBC deformability will affect (or not) the progression of an acute inflammatory response. The deformability of the red blood cells, as already described, is associated with the pathology of many diseases and could be used to evaluate disease status (27), therefore the determination of RBC deformability could be an important parameter in the study of any inflammatory response.

References

1. Zarbock, A., Ley, K., McEver, R.P., Hidalgo, A., 2011. Leukocyte ligands for endothelial selectins: specialized glycoconjugates that mediate rolling and signaling under flow. Blood 118, 6743–6751.
2. Sequeira, A., Artoli, A.M., Silva-Herdade, A.S., Saldanha, C., 2009. Leukocytes dynamics in microcirculation under shear-thinning blood flow. Comput. Math. Appl. 58, 1035–1044.
3. Artoli, A.M., Sequeira, A., Silva-Herdade, A.S., Saldanha, C., 2007. Leukocytes rolling and recruitment by endothelial cells: hemorheological experiments and numerical simulations. J. Biomech. 40, 3493–3502.
4. Huttenlocher, A., Poznansky, M.C., 2008. Reverse leukocyte migration can be attractive or repulsive. Trends Cell Biol. 18, 298–306.
5. Jung, U., Norman, K.E., Scharffetter-Kochanek, K., Beaudet, A.L., Ley, K., 1998. Transit time of leukocytes rolling through venules controls cytokine-induced inflammatory cell recruitment in vivo. J. Clin. Investig. 102, 1526–1533.

6. Jain, A., Munn, L.L., 2009. Determinants of leukocyte margination in rectangular microchannels. PLoS One 4, 1–8.
7. Vitorino de Almeida, V., Silva-Herdade, A.S., Calado, Â, Saldanha, C., 2015. Fibrinogen modulates leukocyte recruitment in vivo during the acute inflammatory response. Clin. Hemorheol. Microcirc. 59, 97–106.
8. Gavins, F.N.E., Chatterjee, B.E., 2004. Intravital microscopy for the study of mouse microcirculation in anti-inflammatory drug research: focus on the mesenter and cremaster preparations. J. Pharmacol. Toxicol. Methods 49, 1–14.
9. Kubes, P., Kerfoot, S.M., 2001. Leukocyte recruitment in the microcirculation: the rolling paradigm revisited. News Physiol. Sci. 16, 76–80.
10. McDonald, B., Kubes, P., 2011. Cellular and molecular choreography of neutrophil recruitment to sites of sterile inflammation. J. Mol. Med. 89, 1079–1088.
11. Phillipson, M., Kubes, P., 2011. The neutrophil in vascular inflammation. Nat. Med. 17, 1381–1390.
12. Pagano, M., Faggio, C., 2015. The use of erythrocyte fragility to assess xenobiotic cytotoxicity. Cell Biochem. Funct. 33, 351–355.
13. Tsukada, K., Sekizuka, E., Oshio, C., Minamitani, H., 2001. Direct measurement of erythrocyte deformability in diabetes mellitus with a transparent microchannel capillarymodel and high-speed video camera system. Microvasc. Res. 61, 231–239.
14. Barvitenko, N.N., Aslam, M., Filosa, J., Matteucci, E., Nikinmaa, M., Pantaleo, A., Saldanha, C., Baskurt, O.K., 2013. Tissue oxygen demand in regulation of the behavior of the cells in the vasculature. Microcirculation 20, 484–501.
15. Korhonen, R., Lahti, A., Kankaanranta, H., Moilanen, E., 2005. Nitric oxide production and signaling in inflammation. Curr. Drug Targets Inflamm. Allergy 4, 471–479.
16. Taha, Z.H., 2003. Nitric oxide measurements in biological samples. Talanta 61, 3–10.
17. Borregaard, N., 2010. Neutrophils, from marrow to microbes. Immunity 33, 657–670.
18. Faust, N., Varas, F., Kelly, L.M., Heck, S., Graf, T., 2000. Insertion of enhanced green fluorescent protein into the lysozyme gene creates mice with green fluorescent granulocytes and macrophages. Blood 96, 719–726.
19. Silva, A.S., Saldanha, C., Martins e Silva, J., 2007. Effects of velnacrine maleate in the leukocyte–endothelial cell interactions in rat cremaster microcirculatory network. Clin. Hemorheol. Microcirc. 36, 235–246.

20. Lopes de Almeida, J.P., Carvalho, F.A., Silva-Herdade, A.S., Santos-Freitas, T., Saldanha, C., 2009. Redox thiol status plays a central role in themobilization andmetabolism of nitric oxide in human red blood cells. Cell Biol. Int. 33, 268–275.
21. Montrucchio, G., Alloatti, G., Camussi, G., 2000. Role of platelet-activating factor in cardiovascular pathophysiology. Physiol. Rev. 80, 1669–1699.
22. Fukuda, S., Yasu, T., Predescu, D.N., Schmid-Schönbein, G.W., 2000. Mechanisms for regulation of fluid shear stress response in circulating leukocytes. Circ. Res. 86, E13–E18.
23. Lang, P.a., Kempe, D.S., Tanneur, V., Eisele, K., Klarl, B.a., Myssina, S., Jendrossek, V., Ishii, S., Shimizu, T.,Waidmann, M., Hessler, G., Huber, S.M., Lang, F.,Wieder, T., 2005. Stimulation of erythrocyte ceramide formation by platelet-activating factor. J. Cell Sci. 118, 1233–1243.
24. Czepiel, J., 2014. Rheological properties of erythrocytes in patients infected with Clostridium difficile. Postepy Hig. Med. Dosw. 68, 1397–1405.
25. Silva-Herdade, A.S., Freitas, T., Almeida, J.P., Saldanha, C., 2014. Erythrocyte deformability and nitric oxide mobilization under pannexin-1 and PKC dependence. Clin. Hemorheol. Microcirc. 59, 155–162.
26. Carvalho, F., Maria, A., 2006. The relation between the erythrocyte nitric oxide and hemorheological parameters. Clin. Hemorheol. Microcirc. 35, 341–347.
27. Santoso, A.T., Deng, X., Lee, J.-H., Matthews, K., Duffy, S.P., Islamzada, E., McFaul, S.M., Myrand-Lapierre, M.-E., Ma, H., 2015. Microfluidic cell-phoresis enabling highthroughput analysis of red blood cell deformability and biophysical screening of antimalarial drugs. Lab Chip 15, 4451–4460.

VI. Hydrodynamics of a free-flowing leukocyte towards the endothelial wall

Ana Santos Silva-Herdade[1]

Adélia Sequeira[2]

Ângelo Calado[1]

Carlota Saldanha[1]

Oualid Kafi[2]

Submited to publication in Microvascular Research

[1]*Unidade de Biologia Microvascular e Inflamação, Instituto de Medicina Molecular, Instituto de Bioquímica, Faculdade de Medicina, Universidade de Lisboa, Lisboa, Portugal*

[2] *CEMAT/IST and Department of Mathematics, Instituto Superior Técnico, Universidade de Lisboa, Lisboa, Portugal*

Abstract

Leukocyte recruitment is an essential stage of the inflammatory response and although the molecular mechanisms of this process are relatively well known, the influence of the hydrodynamic effects that govern the inflammatory response are still under study. In this paper we made use of the images and experimental parameters obtained by intravital microscopy in an *in vivo* animal model of inflammation to track the leukocytes trajectories and measure their velocities and diameters.

Using a recent validated mathematical model describing the coupled deformation-flow of an individual leukocyte in a microchannel, numerical simulations of an individual and of two leukocytes under flow were performed. The results showed that velocity plays an important role in the motion, deformation and attraction of the cells during an inflammatory response. In fact, for higher inlet velocities the cell movement along the endothelial wall is accelerated and the attraction forces break faster. These results highlight the role of the mechanical properties of the blood, namely the ones influenced by the velocity field, in the case of inflammation.

Keywords

Leukocyte; inflammatory response; intravital microscopy; mathematical model; coupled deformation-flow; numerical simulations

1. Introduction

Leukocyte recruitment and subsequent rolling, activation, adhesion and transmigration are essential stages of an inflammatory response. Understanding this mechanism is of crucial importance in immunology and in the development of anti-inflammatory drugs. In order to in vivo observe the recruitment process, post-capillary venules are usually observed by intravital microscopy. It is now well accepted that the rolling process and the later adhesion cascade are mediated by a number of chemoattractants on the endothelial cell surface, selectins, integrins and other mediators on the surface of the leukocytes and in the tissue. The whole process is triggered by margination of free flowing leukocytes

toward the endothelial wall. This process is believed to result fromthe interaction of leukocytes with surrounding erythrocytes which deform and support pushing the leukocytes to the wall [1,2]. Erythrocytes, leukocytes and platelets play an important role in the mechanical properties of blood, and are, to a certain degree, also responsible for different physiological phenomena and diseased states, such as inflammation, coagulation and blood diseases. Mathematical and numerical approaches have the potential to understand better the processes by which leukocytes interact with the endothelium under flow conditions. A large number of theoretical studies started to emerge since the late 1970s addressing the ligand–receptor interaction [3] and the receptor–mediated leukocyte adhesion where the leukocyte is a three–dimensional rigid cell [4] or a two–dimensional deformable cell [17]. The stochastic approach was taken into account in modelling the mechanical contribution of an elastic cell membrane, the role of microvilli in the rolling to adhesion process, the shear threshold effect of velocity on a rolling neutrophil [5]. Then, to simulate the receptor–mediated rolling of deformable cells, adhesive models have been used in [6–9]. Besides that, other models investigate the shear stress distribution on the cell membrane [10] or on both, the leukocyte and the endothelial wall under shear-thinning blood flow [15,16]. Another more complex framework is the modeling of cells that can be arranged into tissues of various topologies [19].

In this paper, we made use of the experimental parameters obtained in the recorded images of intravital microscopy experiments from an in vivo animal model of inflammation to track the leukocytes trajectories and measure their velocities and diameters which were applied to the mathematical model herein presented.

Using a mathematical model and finite element simulations we obtained numerical results, which allowed to derive some important conclusions on the hydrodynamic effects complementing the experimental observations.

The scientific relevance of this study is highlighted by the biological importance of blood physics and its successful simulation using numerical methods.

2. Materials and Methods

2.1 Experimental design

Using PAF (Platelet-activating factor, Sigma, Germany) as an inflammatory agent an animal model of inflammation as established in four experimental groups of mice (BW: 23.0 ± 2.34g) according to time post-inflammation (0, 2, 4 and 6h post-inflammation). PAF is a phospholipid mediator of inflammation that is released early in inflammation by a variety of cell types. To achieved the inflammatory state an intra-scrotal (i.s.) injection of 300µl of PAF 10^{-6}M in PBS pH7.4 was given to male mice and after 0, 2, 4 and 6h of PAF administration the cremaster was prepared for intravital microscopy (N=10 in each experimental group) in order to observe the interactions leukocyte-endothelial cells. At the end of the experiments the animals were euthanized with sodium pentobarbital (120mg/ kg BW).

2.2 Animal preparation

The animals used in this study received humane care in accordance with the Directive of the European Community 2010/63/EU that mentions the protection of animals used for economic and other scientific ends and also according to the Portuguese Legislation Law 113/2013.

Lys-EGFP-ki mice (40) with 5 to 8 weeks (n=40) [11] were kept in an animal facility with a 12h light/dark cycle, on a diet standard food ads water *ad libitum*. The animals were housed in cages in a temperature controlled room. The surgical procedures and microcirculatory measurements were performed under an intraperitoneally (i.p.) anesthesia of xylazine/ketamine (0.1mL/ 10g of BW). Using an auto-regulable heating platform the body temperature was maintained between 35-37ºC.

The preparation of the cremaster for intravital microscopy is made in a Plexiglas support in accordance with [12]. Using a scissor a small incision was made in the scrotum and one of the testicules was brought outside. After the removing of the conjunctive tissue that surrounds the cremaster a lengthwise incision is made on the ventral surface of the cremaster muscle. The muscle is then spread out over the appropriate support and fixed

with silk sutures. The exposed tissue cremaster must be kept in perfusion of Krebs-Henseleit buffer with $NaHCO_3$, warmed to 37°C and bubbled with 95% N_2 and 5% CO_2 for complete superfusion of the tissue throughout the experiment; the excess of liquid was removed with a vacuum system.

2.3 Intravital microscopy

After the cremaster preparation the support with the animal is placed in a confocal microscope Zeiss LSM 7 Live (Zeiss, Germany) adapted for intravital microscopy, equipped with a 20X water objective and a 10X ocular maintaining the superfusion at all time. All the images were recorded using the ZEN LSM 2006 software. *Post-capillary* venules with 20-25μm diameter were chosen for visualization and quantification of the parameters previously defined and the images were registered was made for at least 1min. The quantification of the interactions leukocytes/endothelial cells were made on the recorded images using the following parameters [13]: number of rolling leukocytes and the rolling speed, number of adherent leukocytes and venules diameters. The leukocytes were considered in rolling on the endothelium if moving at a slower speed than erythrocytes and their number was counted during 1 min. A leukocyte was considered adherent to the endothelium if it remained stationary for more than 30s in a 100μm length [12] .

2.4 Mathematical modelling

2.4.1 Flow configuration and model description

In this study, we have used a recently validated model describing the coupled deformation-flow of an individual cell in a microchannel [20]. The level set method was used to track the interface between two-phase immiscible flow, such as the computational domain contains two different immiscible incompressible phases (see Figure 1), the intracellular liquid composed of a viscoelastic fluid with density ρ_c and viscosity μ_c, immersed in the extracellular liquid which is a Newtonian fluid (e.g., plasma) with density ρ_{ec} and viscosity μ_{ec}. The computational domain is a geometry

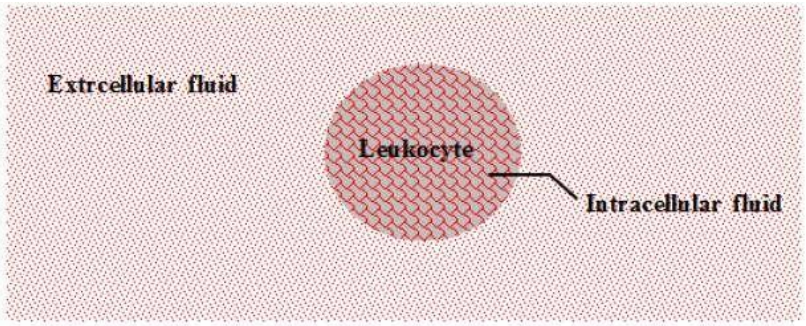

Figure 1 - Scheme of the flow configuration.

representing one branch of the bifurcation of a post-capillary venule showed in Figure 3, of height 35 µm and length L = 100 µm, bounded from the bottom and the top by two curved plates modelling the endothelial surface (Figure 2). The leukocyte initial shape is a circle of radius R = 3,75 µm.

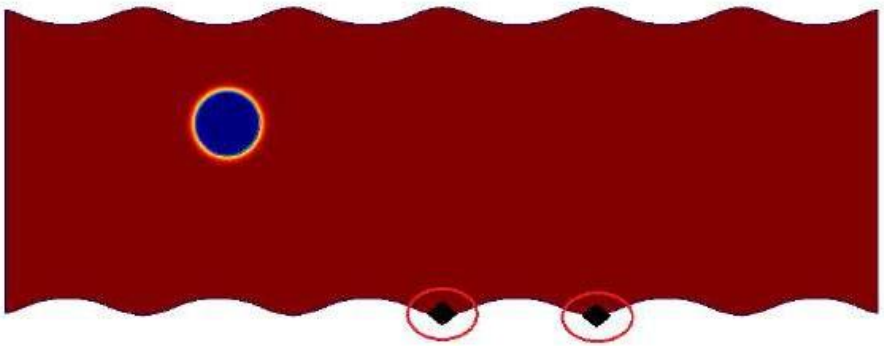

Figure 2 - Scheme of the computational domain. Two points are indicated, where attractive forces were applied

3.2. Governing equations

The velocity u and pressure γ of an incompressible fluid are governed by the momentum and continuity equations

— ( ) ( ) , (1)

, (2)

where ρ is the density, f is a force terme and τ denotes the extra stress tensor

[— ( ) ( ) ( )] ( ) (3)

where h is the relaxation time, (u) = ( ), the strain rate tensor and τ (u) denotes the matrix-matrix product between u and τ . Obviously, when τ = 0, the Oldroyd-B model reduces to the incompressible Navier-Stokes equations. The equations (1)-(3) coupled with level set function (4)

— (( )), (4)

are solved in Comsol Multiphysics [22], where v(m/s) is the velocity transporting the interface, çr(m/s) and ∠r(m) are reinitialization parameters, such that ∠r = hc/4, with hc the characteristic mesh size in the region passed by the interface and çr is the maximum velocity magnitude occurring in the model. The level set method [21], allows to simulate the flow of two immiscible fluids separated by a moving interface using the smooth continuous function ϕ. The value ϕ = 0.5 determines the position of the interface, which changes smoothly from 0 to 1 in the transition layer near the interface. The region where ϕ < 0.5 is filled with plasma and where ϕ > 0.5 is theintracellular region. The level set function is also used to determine the density and the dynamic viscosity as follows:

( )

( ) .

The coupled following model is solved using the CFD Module of Comsol Multiphysics [22]

(–) ,

where the surface tension force is [{ (}], I is the identity matrix, n is the interface unit normal, 6 is a Dirac delta function and σ denotes the total stress ten- sor such that:

( ) ( ) and | || ( )|.

The fluid enters the microchannel by the left hand side with the normal inflow velocity U0. The outlet is on the right hand side and it is the null pressure. At the top and the bottom curved plates the flow satisfies no-slip boundary conditions. At the interface between the cell and the plasma, the normal component of the boundary stress contribution from the polymer is equal to zero, ( ) .

3. Results

3.1 Experimental results

The animal model of acute inflammation used in this study uses PAF as an inflammatory agent. After an intra-scrotal injection of PAF in mice, the numbers of rolling and adherent neutrophils were counted after 2, 4 and 6h of inflammation. The rolling velocities and the vessels diameters were also determined. Table 1 shows a statically significant increase in the number of rolling ($p<0.001$) and adherent ($p<0.05$) neutrophils after 2 and 4h of inflammation and decrease at 6h of inflammation.

The rolling velocity decreases with time post-inflammation (Table 2) which makes part of a normal acute inflammatory response because the rolling needs to become slower in order to facilitate the subsequent adhesion process. Analyzing the recorded images at each of the time-points it is also easily seen how cells deform during the slow rolling and subsequent adhesion process.

A control group of mice in which saline instead of PAF was injected i.s. were used for similar measurements; no significant differences in the number of rolling and adherent neutrophils until 6h after injection were observed (data not shown).

Table 6 – Mean ± standard deviation of the number of rolling (ROL) and adherent (ADH) neutrophils after PAF-induced inflammation at the beginning (0h) and after 2, 4 and 6h of PAF i.s. injection. After 4h of PAF-induction of an acute inflammatory condition a statistically significant increase in the number of rolling ($p<0.001$) and adherent ($p<0.05$) leukocytes is observed. Representative results were obtained from a total of ten mice (N=10) per experimental group.

	Time *post*-inflammation			
NEUTROPHILS	0h	2h	4h	6h
Rolling (n/100μm)	10.3±1.7	46.0±8.5*	88.8±27.7*	16.5±7.4
Adherent (n/100μm)	0.5±0.5	2.2±1.0	11.0±5.5^{+}	2.0±1.3

*Statistical significance is presented in comparison to the initial time-point (0h) and * p< 0.05.*

The increase of the vessels diameters (Table 2) was also expected as vasodilation is also a main characteristic of the inflammatory response. The experimental data herein described will be applied to a numerical model in order to describe, using mathematical tools the recruitment of neutrophils inside the vessels towards the inflamed tissues. Concerning the inflammatory process described by Table 1 it is well noticed that the peak occurs at 4h post-inflammation. Since we are trying to numerically modulate the rolling and adhesion of the cells to the endothelial wall during inflammation, 4h was the time taken in account to acquire the experimental data.

Table II –Rolling velocities of the neutrophils with time post-inflammation and diameters of the vessels visualized by intravital microscopy at the beginning (0h) and after 2, 4, and 6h post-inflammation. Representative results are mean values of the data obtained from a total of ten mice (N=10) per experimental group.

	Time *post*-inflammation			
	0h	2h	4h	6h
Diameters (μm)	22.5±2.40	38.1±4.20*	34.5±5.53*	26.0±3.09
Rolling velocities (μm/s)	16.0±1.00	15.8±2.10	12.0±1.90*	12.38±2.89*

*Statistical significance is presented in comparison to the initial time-point (0h) and * p< 0.05.*

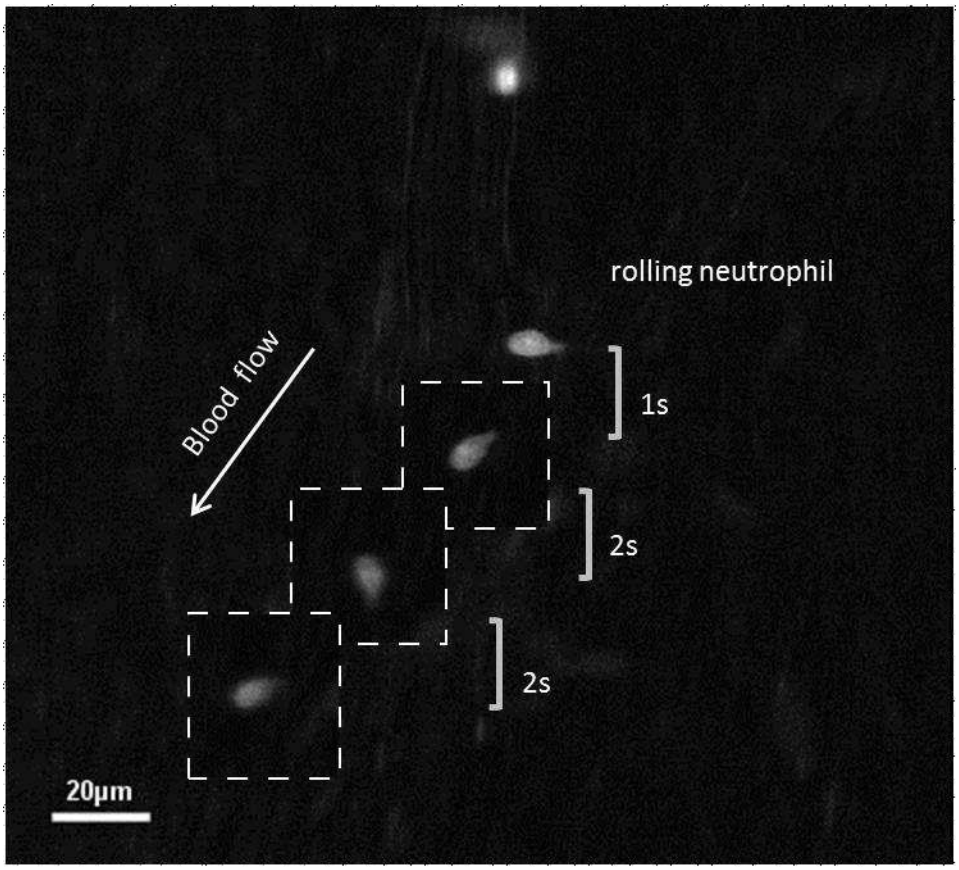

Figure 3 – Intravital microscopy image of a post-capillary venule of the cremaster muscle of Lys-EGFP-ki mice after 4h of PAF-induced inflammation. A neutrophil extending tethers is shown rolling along the endothelial wall.

Figure 3 shows the deformation of a neutrophil during rolling along the endothelial wall. The formation of tethers is well seen in the images. The tethers bind to endothelial, via P selectin/P selectin glycoprotein ligand 1 (PSGL1) at the endothelium, forming a temporary anchorage [14].

3.2 Numerical results

A number of simulations for the resulting coupled system were obtained using a finite element method solved in Comsol Multiphysics 4.3b [22], for an individual leukocyte and in the presence of another adherent cell. The computations and results were performed with the mesh shown in Figure 4, which corresponds to a total number of degrees of freedom (DOF) of 93 892. Additional simulations for the case of two cells were studied with a total number of 104 231 DOF. The simulations, in the case of an individual leukocyte, were carried out for three different inlet velocities. A force of attraction was applied

in two points shown in Figure 2. From these simulations we have observed that the fluid 2 modeling the cell travels down through the fluid 1 modeling the plasma, adheres to the curved plate representing the endothelial surface and starts rolling. Figures 5, 6 and 7 show the cell motion as well as its shapes and the resulting disturbed flow, represented by the arrows of the velocity vectors at different time instants and inlet velocities.

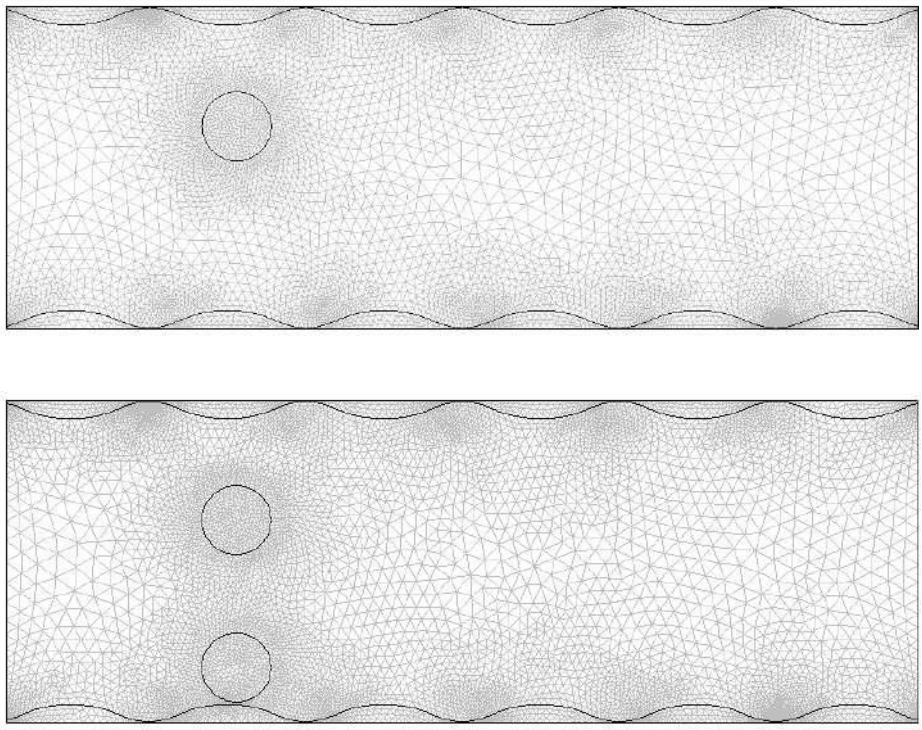

Figure 4 - The numerical meshes used for the one cell and two cells simulations

The velocity plays an important role in the motion, deformation and attraction of the cell to the endothelial wall. In fact, the results show that an increase of the inlet velocity accelerates the cell motion along the endothelial wall, and causes the bonds to break faster after reaching the regions of the attraction forces. We suggest that the hydrodynamic forces pushing the cell get higher as the inlet velocity is increasing.

The influence of another cell in the motion, deformation and attraction of a single leukocyte was also studied. We tested the case where U0 = 12µm/s and the second leukocyte was already adhering to the endothelial wall. In Figure 8 we have observed a reciprocal influence of one cell into the other.

Whereas the free cell is crawling towards the endothelial surface, the shape of the adherent cell is deforming. On the other hand, the presence of the adherent cell, slightly, slows

the motion at the begining (t =0.4 s) compared to the case of the individual leukocyte, then it's, practically, the same velocity of displacement. However, we note that the presence of the adherent cell may help in capturing the free leukocyte.

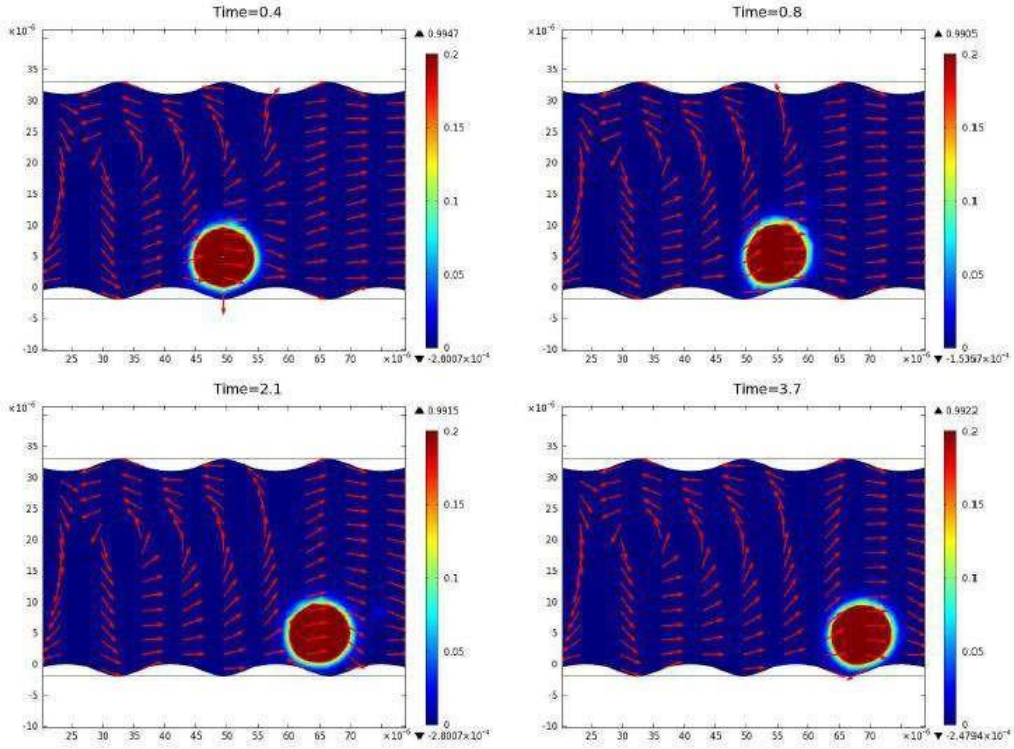

Figure 5. Snapshots showing the volume fraction of fluid 2 (cell) and the arrow velocity field at t =0.4s, 0.8s, 2.1s and 3.7s with U_0 = 12µm/s.

In fact, in Figure 9 the density of the recirculations, due to the perturbed flow, pushing the cell along the endothelial wall is less important in the case of the presence of the adherent cell, which could be explained by the promotion of the slow rolling that is needed and important to later promote the firm contact with the endothelial cells. In other words, the presence of an adherent cell can favor the slow rolling and consequent adhesion of another leukocyte.

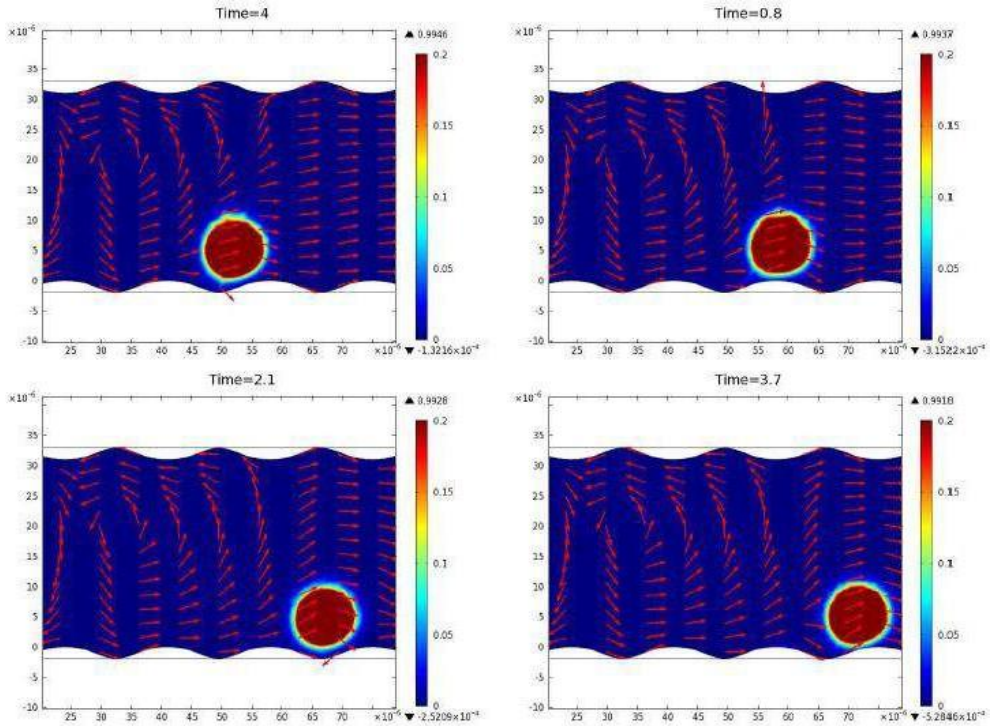

Figure 6 – Snapshots showing the volume fraction of fluid 2 (cell) and the arrow velocity field at t =0.4s, 0.8s, 2.1s and 3.7s with U_0 = 15µm/s.

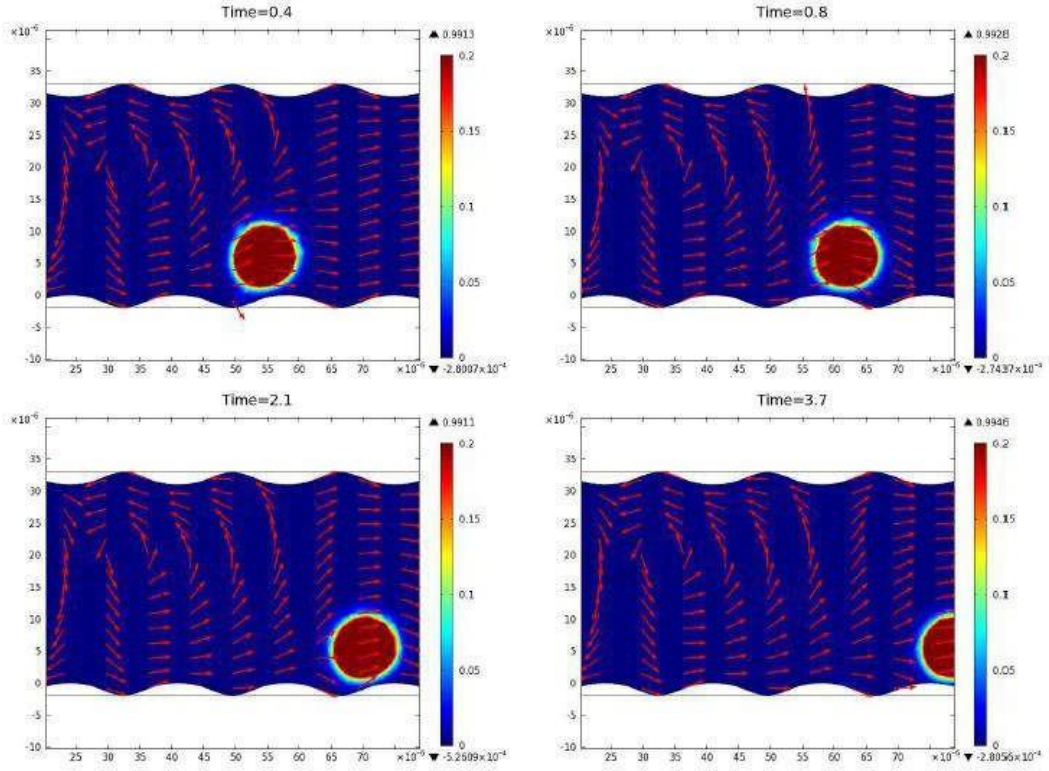

Figure 7. Snapshots showing the volume fraction of fluid 2 (cell) and the arrow velocity field at t =0.4s, 0.8s, 2.1s and 3.7s with U_0 = 18µm/s.

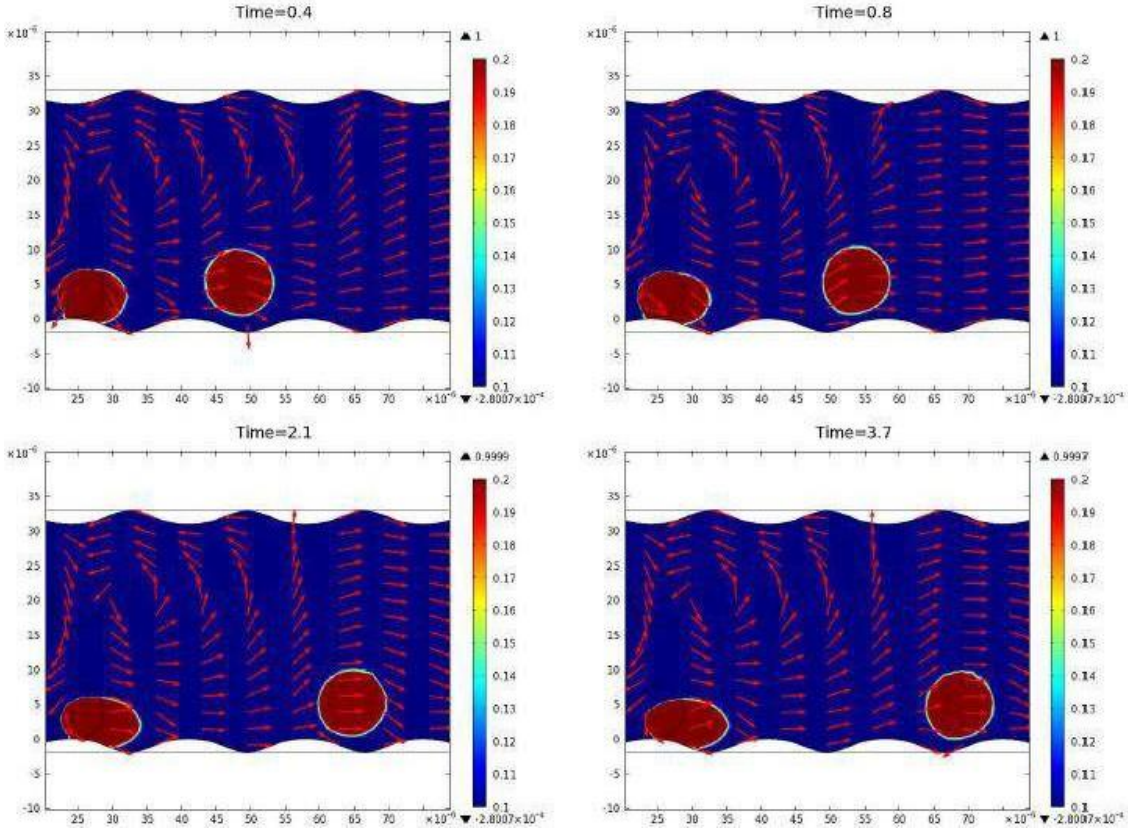

Figure 8. Snapshots showing the volume fraction of fluid 2 (in two cells) and the arrow velocity field at t =0.4s, 0.8s, 2.1s and 3.7s with U_0 = 12µm/s.

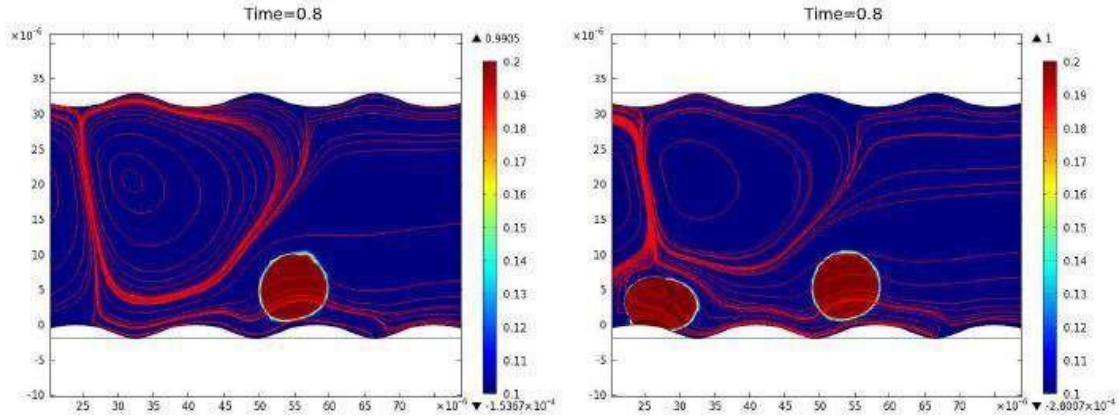

Figure 9. The volume fraction of fluid 2 (left: for one cell, right: for two cells) and the streamlines at t =0.8s with U_0 = 12µm

4. Conclusions

The paper shows the experimental results of an animal model of inflammation that uses PAF as an inflammatory agent. The results obtained with intravital microscopy show an

increase number of rolling neutrophils after 4h of inflammation which confirm the inflammatory state induced. After the analysis of the recorded images experimental parameters like vessel and neutrophil diameters, the rolling velocity and the time of adherence at the endothelium were applied in the numerical study, for which an attraction point at the endothelial wall and three different velocities were considered.

The numerical simulations performed took into account an individual cell and an adherent cell. These simulations have shown that the velocity plays an important role in the motion, deformation and attraction of the cell thus reinforcing the role of the hemodynamic conditions in the recruitment of the leukocytes to the inflamed area. Different inlet velocities result in different rolling patterns. In diseases where blood flow velocity is modified, this is particularly important because this will have a relevant effect on the inflammatory response. These numerical results strongly suggest that to ensure an efficient inflammatory response, the leukocyte velocity is required to decrease thus facilitating its slow rolling and its subsequent adhesion. On the other hand when simulating the presence of an adherent cell, our results showed that there is an initial slight deceleration of the rolling leukocyte, when compared with a situation where no adherent cell is present. As the observed deceleration will more rapidly promote the slow rolling of the leukocyte, we propose that the presence of adherent cells in the vicinity of rolling leukocytes will this way help the margination of the latter cells.

The numerical simulations obtained in this work can be used as first approaches to study and modulate the hemodynamic parameters involved in an inflammatory response. These numerical simulations will enable us to simulate and modulate at the same time a large number of parameters, which most of the times, is not possible in in vivo experiments, and to analyze how they will evolve over time.

Acknowledgments

FCT (Fundação para a Ciência e a Tecnologia, Portugal) the project EXCL/MAT-NAN/0114/2012 and the Research Center CEMAT-IST are gratefully acknowledged.

References

1. Acton, S.T., Wethmar, K., Ley, K., 2002. Automatic tracking of rolling leukocytes in vivo. Microvasc. Res. 63, 139148. doi:10.1006/mvre.2001.2373.
2. Rao, R.M., Yang, L., Garcia-Cardena, G., Luscinskas, F.W., 2007. Endothelial-dependent mechanisms of leukocyte recruitment to the vascular wall. Circ. Res. 101, 234247. doi:10.1161/CIRCRESAHA.107.151860b.
3. Bel, G., 1978. Models for the specific adhesion of cells to cells. Science. 200, 718727.
4. Hammer, D.A., Apte, S.M., 1992. Simulation of cell rolling and adhesion on surfaces in shear flow: General results and analysis of selectin-mediated neutrophil adhesion. Biophys. J. 63, 3557.
5. Caputo, K.E., Lee, D., King, M.R., Hammer, D.A., 2007. Adhesive dynamics simulations of the shear threshold effect for leukocytes. Biophys. J. 92, 787–797.
6. Jadhav, S., Eggleton, C.D., Konstantopoulos, K., 2005. A 3-D computational model predicts that cell deformation affects selectin–mediated leukocyte rolling. Biophys. J. 88, 96–104.
7. Pappu, V., Doddi, S.K., Bagchi, P., 2008. A computational study of leukocyte adhesion and its effect on flow pattern in microvessels. J. Theor. Biol. 254, 483–498.
8. Luo, Z.Y., Xu, F., Lu, T.J., Bai, B.F., 2011. Direct numerical simulation of detachment of single captured leukocyte under different flow conditions. J. Mech. Med. Biol. 11, 273–284.
9. Khismatullin, D.B., Truskey, G.A, 2012. Leukocyte rolling on P–selectin:a three– di-mensional numerical study of the effect of cytoplasmic viscosity. Biophys. J. 102, 1757–1766.
10. Su, S.S., Schmid-Schöbein, G.W, 2008. Fluid stresses on the membrane of migrating leukocytes. Ann. Biomed. Eng. 36, 298–307.
11. Faust, N., Varas, F., Kelly, L.M., Heck, S., Graf, T., 2000. Insertion of enhanced green fluorescent protein into the lysozyme gene creates mice with green fluorescent gran-ulocytes and macrophages. Blood 96, 719726.
12. Silva, A.S., Saldanha, C., Martins e Silva, J., 2007. Effects of velnacrine maleate in the leukocyte-endothelial cell interactions in rat cremaster microcirculatory network. Clin. Hemorheol. Microcirc. 36, 235246.

13. Kubes, P., Kerfoot, S.M., 2001. Leukocyte recruitment in the microcirculation: the rolling paradigm revisited. News Physiol. Sci. 16, 7680.
14. Kolaczkowska, E., Kubes, P., 2013. Neutrophil recruitment and function in health and inflammation. Nat. Rev. Immunol. 13, 159175. doi:10.1038/nri3399.
15. Sequeira, A., Artoli, A.M., Silva-Herdade, A.S., Saldanha, C., 2009. Leukocytes dynamics in microcirculation under shear-thinning blood flow. Comput. Math. Appl. 58, 1035–1044.
16. Artoli, A.M., Sequeira, A., Silva-Herdade, A. S., Saldanha, C., 2008. Localized hydrodynamics of clustering leukocytes. Clin. Hemorheol. Micro. 39, 375–380.
17. N'Dri, N.A., "hyy, W., Tran-Son-Tay, R., 2003. Computational modeling of cell adhesion and movement using a continuum-kinetics approach. Biophys. J. 85, 2273–2286.
18. Nava, M.M., Raimondi, M.T., Pietrabissa, R., 2014. Bio-chemo-mechanical models for nuclear deformation in adherent eukaryotic cells. Biomech. Model. Mechanobiol. 13, 929–943.
19. Rejniak, K.A., 2007.Modeling the development of complex tissues using individual viscoelastic cells, in: Anderson, A.R.A., Chaplain, M.A.J., Rejniak, K.A. (Eds.), Single-Cell-Based Models in Biology and Medicine. Birkhäser, Basel, 301–323.
20. Kafi, O., Sequeira, A., Boujena, S., 2016. On the mathematical modeling of monocytes transmigration. Lect. Notes Comput. Sci. Eng. 112, 107–115. http:dx.doi.org10.1007978-3-319-39929-4 49.
21. Osher, S., Sethian, J.A., 1988. Fronts propagating with curvature-dependent speed: algorithm based on Hamilton– Jacobi formations. J. Comput. Phys. 79, 12–49.
22. COM"OL Multiphysics, User's Guide 4.3b, Licence 17073661, 2012.

PART THREE

VI. Discussion and Conclusions

Microcirculation ensures the communication between blood and tissue and organs. Through it, the latter are supplied with oxygen and nutrients. The major cell types constituting microcirculation include the endothelial cells lining inside the microvessels, the smooth muscle cells present mostly in the arterioles, and the components of blood i.e., erythrocytes, leucocytes and plasma. The endothelial cell surface in the microcirculation is the largest cellular surface of the body - the largest 'organ' in the human body. It mediates and controls transendothelial exchanges between blood plasma and interstitial fluid, regulates the vasomotor tone by releasing vasodilating and vasoconstricting substances, maintains an anticoagulant state, and regulates the transmigration of leukocytes into surrounding tissues. It is at the microcirculation level, mostly within *post*-capillary venules, that the interactions between leukocytes and endothelial cells occur during an inflammatory response. Leukocyte recruitment is a hallmark feature of inflammation and involves a sequential series of molecular interactions between leukocytes and the endothelial cells. These interactions are controlled by a variety of factors, including expression of adhesion molecules on leukocytes and endothelial cells, products of leukocyte and endothelial cell activation, such as superoxide and nitric oxide, among others.

In addition to the molecular mechanisms that activate and guide the leukocytes towards the endothelial wall in the multi-step process of leukocyte recruitment, it is also important to consider the contribution of the physical forces generated by the movement of blood along the vessel wall. It is now known that normal fluid shear stress conditions maintain leukocytes in a rounded deformable and non-adhesive state, ensuring their efficient transit through the microvasculature. Importantly, it has been proposed that alterations in fluid shear stress resulting from changes in the blood flow also regulate leukocyte recruitment in inflammation (41). However, although the molecular mechanisms involved in leukocyte activation and recruitment have been identified and studied in detail, the mechanisms by which hemodynamics contribute to leukocyte

recruitment are still poorly defined and as such, are a current topic of intense research and debate.

The contribution of biomechanical forces to leukocyte recruitment, more specifically shear stress derived by the flow of blood and the vascular endothelium, has been scarcely addressed. This relates for instance to the existence of technical constraints in the determination of several hemodynamic parameters which makes it difficult to study hemodynamics in *in vivo* animal models. This can be circumvented using a combined experimental and numerical approach to develop numerical simulations to describe those processes.

Mathematical equations can be used to describe many of the processes that occur in living organisms, which means that mathematical models can be developed for many physiological events. Leukocyte recruitment is one of those cases, for which few numerical simulations had already been performed at the time this work was initiated (21,37,38) . Nevertheless, most of these are two-dimensional and simply consider blood flow as a Newtonian linear shear flow. In addition and despite considering other assumptions, such as the mechanical contribution of an elastic cell membrane and the role of microvilli in the rolling to the adhesion process or the shear threshold effect of velocity on a rolling neutrophil (38), those simulations did not consider simultaneously all the players enrolled in this process, namely, the vessel, the blood flow and the leukocytes.

To understand the contribution of hemodynamics to leukocyte recruitment in inflammation we aimed here at developing numerical simulations that could more adequately mimic this process. Our basic approach in this work was to focus first on the development of an animal model of inflammation which, at the microcirculation level, would mimic a physiological inflammatory response and that could further provide data to adequately develop a numerical simulation to describe leukocyte recruitment in inflammation.

For this purpose, our initial approach was to consider blood as a non-Newtonian fluid and, for the sake of simplicity, leukocytes as rigid spheres. To address this, we started by developing an animal model of inflammation in Wistar rats, using LPS as an inflammatory

agent. The onset of the inflammatory process was confirmed by evaluating the number of rolling and adherent leukocytes by intravital microscopy of the cremaster muscle, which were both increased under the inflammatory conditions employed. Accordingly, increased levels of TNF-α concentrations, a pro-inflammatory cytokine, were also detected in this model. This study was further complemented with the use of acetylcholine (ACh) and velnacrine maleate, respectively, the substrate and an inhibitor of acetylcholinesterase (AChE). ACh is a well-known neurotransmitter that has also been recognized to possess an anti-inflammatory function in the context of the cholinergic anti-inflammatory pathway, by suppressing the production of pro-inflammatory cytokines by macrophages via its interaction with α7 nACh' (41). Among other factors, ACh bioavailability is controlled by AChE, the enzyme responsible for its degradation. The results obtained *in vivo* in this animal model evidenced the anti-inflammatory effect of ACh as, in the presence of either ACh or velnacrine maleate, a decrease of the concentration of TNF-α in plasma and a decreased adhesion of the leukocytes to the endothelial wall were observed.

Based on the intravital microscopy recorded videos and parameters of the LPS-induced inflammation animal model, we next searched for a numerical tool to describe the motion of leukocytes and enable the simulation of blood flow. The experimental results obtained by our animal model were used to set the initial and boundary conditions for the mesoscopic lattice Boltzmann solver (3,42). Blood was considered as a non-Newtonian fluid and leukocytes as rigid spheres. The governing equations and the numerical model were established by the group of Adélia Sequeira from CEMAT (IST, UL) and the results produced by the numerical model were analyzed and discussed from the physiological point of view.

The obtained numerical simulations were further used to analyze two discrete situations *in silico*, namely, the recruitment of a single leukocyte and the recruitment of a cluster of leukocytes. In general, it was clearly observed that leukocyte velocity variations in the x-axis are higher than the ones observed in the y-axis, meaning that leukocytes move towards the endothelial wall mainly by modifying their position in the x-axis. Importantly, shear stress variations were also observed on the surface of both leukocytes and endothelial cells. When simulating the recruitment of a single rolling leukocyte, two

regions of minimum and one region of maximum shear stress were identified on its surface. On the endothelial wall, it was observed that the shear stress behind the rolling leukocyte is smaller. Surfaces with higher shear stress are likely to be correlated with areas of current strong interactions between the leukocyte and the vessel wall. Conversely, surfaces with lower shear stress may correspond to non-interacting areas or to areas of weaker interactions. These different areas of shear stress can thus correspond to regions where bonds are either being formed, downstream the leukocyte, or were previously dissociated, upstream the leukocyte, to support the rolling process along the endothelium. It is our belief that these distinct shear stress regions may correlate with areas of different distribution of adhesion molecules, such as selectins, that will promote the slow rolling and adhesion of the cells. Accordingly, it has been suggested that on the surface of leukocytes several signaling mediators are critically activated by changes of wall shear stress conditions (43). Moreover, it has been further proposed that selectins redistribute themselves dynamically on the surface of leukocytes in agreement to the endothelial wall shear stress profile (44). On the other hand, the numerical simulation for the movement of a cluster of leukocytes showed an increase in the endothelial wall shear stress. This observation suggests that the presence of rolling leukocytes potentiates the margination and recruitment of additional cells.

Overall with this first mathematical model, we were able to simulate the first full view of the shear stress profile on the surface of a leukocyte during recruitment and thus contribute to highlight the role of the shear stress in the inflammatory response. However, these first numerical simulations do not closely reproduce the *in vivo* scenario of leukocyte recruitment in inflammation. In this first simpler approach, rolling leukocytes were considered as spheres, which does not reflect reality. In fact, rolling leukocytes are deformable cells that do not present a rigid spherical shape as they move along the endothelium (45). The in vitro comparison of the rolling properties of ligand-coated microspheres and leukocytes suggested that the latter roll more smoothly with longer pauses when compared to the former (13). Moreover, upon the initial tethering step of leukocyte recruitment, the leukocyte needs to flatten on the endothelium so as to enable the formation of newer microvilli tethers to further stabilize its rolling movement and contribute for leukocyte adhesion. Taken this, it is clear that leukocyte deformability is

critical for its rolling and adhesion to the endothelium (17)(21)(46). Therefore, to obtain a numerical simulation that more closely reproduced leukocyte recruitment in inflammation, leukocyte deformability should also be accounted for, i.e., leukocytes should be considered as deformable cells.

To obtain *in vivo* images capable of capturing the deformability profile of recruited leukocytes under flow, we reasoned that intravital microscopy assays could be performed on the cremaster muscle of transgenic mice with fluorescent leukocytes. In fact, such strains enable the direct *in vivo* visualization of specific leukocytes by fluorescence live microscopy and, in our case, were expected to specifically allow the tracking of these leukocytes as individual cells under blood flow. Considering the available transgenic strains, we have decided to focus our study on the recruitment of neutrophils as these are the first leukocytes to reach the site of inflammation. For this purpose, we have employed the Lys-EGFP-ki transgenic mice strain in which the bright GFP (Green Fluorescence Protein) reporter is expressed under the control of the promoter of the gene encoding lysozyme, an enzyme which is specifically expressed in mouse neutrophils (40). In addition, we further used PAF as the inflammatory stimulus and confirmed the triggering of an inflammatory response by studying leukocyte recruitment by intravital microscopy. In this experimental setting, we monitored the elicited acute inflammatory responses for 6 hours upon PAF administration and, as expected, observed a peak of rolling and adherent neutrophils after 4 hours of inflammation.

In this acute inflammation model, we further addressed the variation of erythrocyte deformability throughout the 6-hour period upon eliciting the inflammatory response. It is well documented that red blood cell deformability strongly impacts the blood hemorheologic properties, as a decrease in erythrocyte deformability leads to an increase in the blood viscosity and a concomitant decrease in blood flow velocity (4). These hemodynamic conditions are expected to favor leukocyte recruitment and the progression of the inflammatory process. Consistently, we have observed a decrease in the deformability of the erythrocytes throughout the inflammatory response in our animal model, which further stresses the requirement for hemodynamic changes on the blood flow during the inflammatory response.

The experimental data collected from this second animal model of inflammation was then used for the development of a new numerical simulation that could more accurately describe leukocyte recruitment to the endothelial wall, by accounting for the deformability properties of leukocytes. As a first approach, a recently validated model describing the coupled deformation-flow of an individual monocyte in a microchannel (47) was used. The level set method was used to track the interface between two-phase immiscible flows (since the computational domain contains two different immiscible incompressible phases): (i) the intracellular liquid composed of a viscoelastic fluid, the leukocyte, and (ii) the extracellular liquid, the plasma/blood, which is a fluid. After the analysis of the recorded images, experimental parameters like vessel and neutrophil diameters, rolling velocity and time of adherence at the endothelium were applied to the numerical study, for which an attraction point at the endothelial wall and three different leukocyte velocities were considered. The results obtained with these numerical simulations reinforce the notion that leukocyte velocity plays an important role in its motion along the endothelium. Under conditions of increased velocity, the movement of a single leukocyte is accelerated along the endothelial layer and the contact time with the endothelial wall is smaller, which suggests that bonds are breaking off more easily at the attraction point. These results strongly suggest that leukocyte velocity is required to decrease so as to facilitate its slow rolling and subsequent adhesion and ensure an efficient inflammatory response. On the other hand, our results showed that there is an initial slight deceleration of a rolling leukocyte when simulating for the presence of an adherent cell in the vicinity as compared to the situation where no adherent cell is present. Because the observed deceleration will more rapidly promote the slow rolling of the leukocyte, we propose that the presence of adherent cells will contribute for the margination of nearby rolling leukocytes.

The use of numerical simulations allowed us to confirm the importance of the hemodynamic properties of the flow in the recruitment process of leukocytes. It was observed that the interaction of leukocytes with the endothelial cells depends not only on the biochemical interactions established between adhesion molecules expressed on their surfaces, but also on the physical forces that act on the leukocytes. From the shear stress profiles obtained for both leukocytes and the endothelium, we could understand that the

shear stress that leukocytes experience in the circulation depends on their position relative to the endothelium, which will, in turn, affect the recruitment process. In addition, we could confirm that changes in blood flow conditions, more precisely in flow velocities and consequently in shear stresses, strongly impact the recruitment process and possibly the success of an inflammatory response. We hence stress that the analysis of the blood mechanical properties is also important. For example, in diseases, like myocardial infarction or diabetes, where blood viscosity is affected, such evaluation can be particularly significant to understand a possible interference with the normal course of the inflammatory responses of those patients.

The numerical simulations obtained in this work can be used as first approaches to study and modulate the hemodynamic parameters involved in an inflammatory response. These numerical simulations will enable us to simulate and modulate many parameters simultaneously, which is rarely feasible in *in vivo* experiments, and to analyze how they will evolve over time. Nevertheless, although the results obtained support the important role of the hemodynamic conditions exerted by the flow in the inflammatory response, there is still a gap between the herein presented numerical simulations and reality, and further studies will be necessary to improve our mathematical models. Particularly, in the numerical simulation that considered the leukocyte as a deformable cell, a 3D analysis was not performed and the flow was merely considered to have a constant viscosity. To pursue our major goal in this work, we aim to develop in the near future a mathematical model amenable with a 3D analysis that accounts simultaneously for the non-Newtonian flow properties of blood and for the leukocyte deformability. In addition, it is important to emphasize that the *in vivo* validation of these and other numerical simulations will need to be performed. Moreover, despite the use of animals for developing and validating numerical simulations, it is highly expectable that the development of these will enable in the future the reduction of the number of animals necessary for addressing the contribution of hemodynamics to leukocyte recruitment.

In conclusion, the results herein obtained contributed to our knowledge of leukocyte recruitment through the improvement and development of numerical tools that can provide the medical and biological community with tools which, by closely describing the microcirculation and the inflammatory process, will be critical for a better understanding

of the inflammatory process and of the mechanisms underlying a multitude of inflammatory pathological conditions.

REFERENCES

1. Liu Z, Sniadecki NJ, Chen CS. Mechanical forces in endothelial cells during firm adhesion and early transmigration of human monocytes. Cell Mol Bioeng. 2010;3(1):50–9.

2. Gregory JL, Leech MT, David JR, Yang YH, Dacumos A, Hickey MJ. Reduced leukocyte-endothelial cell interactions in the inflamed microcirculation of macrophage migration inhibitory factor-deficient mice. Arthritis Rheum. 2004;50(9):3023–34.

3. Artoli AM, Sequeira A, Silva-Herdade AS, Saldanha C. Leukocytes rolling and recruitment by endothelial cells: Hemorheological experiments and numerical simulations. J Biomech. 2007;40(15):3493–502.

4. Robertson AM, Owens RG, Sequeira A. Rheological models for blood. Cardiovascular Mathematics Modeling and simulation of the circulatory system. Milano: Springer-Verlag Italia, Milano; 2009. p. 211–41.

5. Pagano M, Faggio C. The use of erythrocyte fragility to assess xenobiotic cytotoxicity. Cell Biochem Funct. 2015;33 (August):351–5.

6. Tsukada K, Sekizuka E, Oshio C, Minamitani H. Direct measurement of erythrocyte deformability in diabetes mellitus with a transparent microchannel capillary model and high-speed video camera system. Microvasc Res. 2001;61(3):231–9.

7. Bor-Kucukatay M, Wenby RB, Meiselman HJ, Baskurt OK. Effects of nitric oxide on red blood cell deformability. Am J Physiol Circ Physiol. 2003;284(5):1577–84.

8. Korhonen R, Lahti A, Kankaanranta H, Moilanen E. Nitric oxide production and signaling in inflammation. Curr Drug Targets Inflamm Allergy. 2005;4(4):471–9.

9. Taha ZH. Nitric oxide measurements in biological samples. Talanta. 2003;61(1):3–10.

10. The University of Waikato. Non-Newtonian fluids | Sciencelearn Hub [Internet]. 2010. Available from: http://www.sciencelearn.org.nz/Science-Stories/Strange-Liquids/Non-Newtonian-fluids

11. Robbins CKC. Robbins Pathologic Basis od Disease. 6th ed. 1999.

12. Ley K, Laudanna C, Cybulsky MI, Nourshargh S. Getting to the site of inflammation: the leukocyte adhesion cascade updated. Nat Rev Immunol. 2007;7(9):678–89.

13. Kolaczkowska E, Kubes P. Neutrophil recruitment and function in health and inflammation. Nat Rev Immunol. Nature Publishing Group; 2013;13(3):159–75.

14. Phillipson M, Heit B, Colarusso P, Liu L, Ballantyne CM, Kubes P. Intraluminal crawling of neutrophils to emigration sites: a molecularly distinct process from adhesion in the recruitment cascade. J Exp Med. 2006;203(12):2569–75.

15. Sepsis. [Internet] 2012. Available from: http://what-when-how.com/wp-content

16. Yadav R, Larbi KY, Young RE, Nourshargh S. Migration of leukocytes through the vessel wall and beyond. Thromb Haemost. 2003;90(4):598–606.

17. Moazzam F, DeLano F a, Zweifach BW, Schmid-Schönbein GW. The leukocyte response to fluid stress. Proc Natl Acad Sci U S A. 1997;94(10):5338–43.

18. Fukuda S, Yasu T, Predescu DN, Schmid-Schönbein GW. Mechanisms for regulation of fluid shear stress response in circulating leukocytes. Circ Res. 2000;86(1):E13–8.

19. Kalambur VS, Mahaseth H, Bischof JC, Kielbik MC, Welch TE, Vilbäck Å, et al. Microvascular blood flow and stasis in transgenic sickle mice: Utility of a dorsal skin fold chamber for intravital microscopy. Am J Hematol. 2004;77(2):117–25.

20. Izumi-Nagai K, Nagai N, Ozawa Y, Mihara M, Ohsugi Y, Kurihara T, et al. Interleukin-6 receptor-mediated activation of signal transducer and activator of transcription-3 (STAT3) promotes choroidal neovascularization. Am J Pathol. 2007;170(6):2149–58.

21. Shin HY, Simin SI, Schimid-Schönbein GW. Fluid Shear-Induced Activation and Cleavage of CD18 During Pseudopod Retraction by Human Neutrophils. J Cell Physiol. 2008;214:528–36.

22. Pappu V, Bagchi P. 3D computational modeling and simulation of leukocyte rolling adhesion and deformation. Comput Biol Med. 2008;38(6):738–53.

23. Sundd P, Pospieszalska MK, Ley K. Neutrophil rolling at high shear: Flattening, catch bond behavior, tethers and slings. Mol Immunol [Internet]. Elsevier Ltd; 2013;55(1):59–69.

24. Sundd P, Gutierrez E, Pospieszalska MK, Zhang H, Ley K. Quantitative dynamic footprinting microscopy reveals mechanisms of neutrophil rolling. Nat Methods. 2010;7(10):821–4.

25. Lang P a, Kempe DS, Tanneur V, Eisele K, Klarl B a, Myssina S, et al. Stimulation of erythrocyte ceramide formation by platelet-activating factor. J Cell Sci [Internet]. 2005;118(Pt 6):1233–43.

26. Dauphinee SM, Karsan A. Lipopolysaccharide signaling in endothelial cells. Lab Invest. 2006;86(1):9–22.

27. Astrakianakis G, Sample Organization. Conflicting Effects of Occupational Endotoxin Exposure on Lung Health - A Hypothesis- Generating Review of Cancer and COPD Risk. J Enviromental Immunol Toxicol [Internet]. 2014;2(1):24. Available from: http://www.stmconnect.com/jeit/content/2/1/19.abstract

28. Makó V, Czúcz J, Weiszhár Z, Herczenik E, Matkó J, Prohászka Z, et al. Proinflammatory activation pattern of human umbilical vein endothelial cells induced by IL-1β, TNF-α, and LPS. Cytom Part A. 2010;77(10):962–70.

29. Yang L, Froio RM, Sciuto TE, Dvorak AM, Alon R, Luscinskas FW. ICAM-1 regulates neutrophil adhesion and transcellular migration of TNF-α-activated vascular endothelium under flow. Blood. 2005;106(2):584–92.

30. Cinamon G, Shinder V, Alon R. Shear forces promote lymphocyte migration across vascular endothelium bearing apical chemokines. Nat Immunol. 2001;2:515–22.

31. Shulman Z, Shinder V, Klein E, Grabovsky V, Yeger O, Geron E, et al. Lymphocyte Crawling and Transendothelial Migration Require Chemokine Triggering of High-Affinity LFA-1 Integrin. Immunity. 2009;30:384–96.

32. TG P, A B. Practical intravital two-photon microscopy for immunological research: faster, brighter, deeper. Immunol Cell Biol. 2010;88:438–44.

33. Ishii T, Ishii M. Intravital two-photon imaging: a versatile tool for dissecting the immune system. Ann Rheum Dis. 2011;70(1):113–5.

34. King MR, Hammer D a. Multiparticle adhesive dynamics: hydrodynamic recruitment of rolling leukocytes. Proc Natl Acad Sci U S A. 2001;98(26):14919–24.

35. Bel G. Models for the specific adhesion of cells to cells. Science. 1978;200:718727.

36. Hammer DA, Apte SM. Simulation of cell rolling and adhesion on surfaces in shear flow: General results and analysis of selectin-mediated neutrophil adhesion. Biophys J. 1992;63:3557.

37. N'Dri NA, "hyy W, Tran-Son-Tay R. Computational modeling of cell adhesion and movement using a continuum-kinetics approach. Biophys J. 2003;85:2273–86.

38. Kelly E, Dooyoung L, King MR, Hammer DA. Adhesive- dynamics simulations of the shear threshold effect for leukocytes. Biophys J. 2007;92:787–97.

39. Su S., Schmid-Sch¨onbein G. Fluid stresses on the membrane of migrating leukocytes. Ann Biomed Eng. 2008;36:298–307.

40. Faust N, Varas F, Kelly LM, Heck S, Graf T. Insertion of enhanced green fluorescent protein into the lysozyme gene creates mice with green fluorescent granulocytes and macrophages. Blood. 2000;96(2):719–26.

41. Schmid-Schönbein GW. Analysis of inflammation. Annu Rev Biomed Eng. 2006;8:93–131.

42. Artoli AM, J J, Sequeira A. A comparative numerical study of a non-Newtonian blood flow model. Proceedings of the 2006 IASME/WSEAS, International Conference on Continuum Mechanics. 2006. p. 91–6.

43. Kubes P, Kerfoot SM. Leukocyte recruitment in the microcirculation: the rolling paradigm revisited. News Physiol Sci. 2001;16(April):76–80.

44. Dardik A, Yamashita A, Aziz F, Asada H, Sumpio BE. Shear stress-stimulated endothelial cells induce smooth muscle cell chemotaxis via platelet-derived growth factor-BB and interleukin-1α. J Vasc Surg. 2005;41(2):321–31.

45. Shirai A, Fujita R, Hayase T. Numerical simulation of flow for viscoelastic neutrophil models in a rectangular capillary network: effects of capillary shape and cell stiffness on transit time. Technol Health Care. 2007;15(2):131–46.

46. Fedosov D a., Fornleitner J, Gompper G. Margination of White blood cells in microcapillary flow. Phys Rev Lett. 2012;108(2):1–5.

47. Kafi O, Sequeira A, Boujena S. On the Mathematical Modeling of Monocytes Transmigration.pdf. Lect Notes Comput Sci Eng. 2016;112:107–15.

APPENDIXES

Articles concerned with this thesis:

- Silva-Herdade A. S, Saldanha C. Effects of acetylcholine on an animal model of inflammation. Clin Hemorheol Microcirc. 2013;53(1-2):209–16.

- Artoli AM, Sequeira, A, Silva-Herdade AS, Saldanha C. Localized hydrodynamics of clustering leukocytes. Clin Hemorheol Microcirc. 2008; 39 (2008) 375–380

- Sequeira, A, Artoli AM, Silva-Herdade, AS, Saldanha C. Leukocytes dynamics in microcirculation under shear-thinning blood flow. Computers and Mathematics with Applications 58 (2009) 1035–1044.

- Silva-Herdade AS, Andolina G, Faggio C, Calado A, Saldanha C. Erythrocyte deformability – a partner in the inflammatory response. Microvascular Research 2016; 107: 34-38.

Clinical Hemorheology and Microcirculation 53 (2013) 209–216
DOI 10.3233/CH-121646
IOS Press

Effects of acetylcholine on an animal mode of inflammation

A.S. Silva-Herdade* and C. Saldanha
Institute of Biochemistry, Institute of Molecular Medicine, University of Lisbon Medical School, Lisbon, Portugal

Abstract. Acetylcholinesterase (AChE) is found both on the membranes of neuronal and non-neuronal cells. In this study we performed intravenous administrations of velnacrine (VLN) and acetylcholine (ACh), respectively, AChE inhibitor and substrate, in an animal model of lipopolysaccharide (LPS)-induced inflammation in Wistar rats. Using intravital microscopy the number of rolling and adherent leukocytes in post-capillary venules was monitorized and blood samples were collected for TNF-a plasma concentrations determination. Our results showed that in presence of LPS, ACh has an anti-inflammatory effect, seen by a decrease in TNF-a plasma levels and maintains the number of rolling and adherent leukocytes. The presence of VLN before LPS almost blocked the LPS-induced rolling and TNF-a releasing. Thereby VLN seems to have, like ACh, an anti-inflammatory effect by diminishing TNF-a concentrations.

Keywords: Inflammation, acetylcholine, TNF-a, velnacrine, rolling leukocytes, intravital microscopy

1. Introduction

Bacterial LPS, a component of the outer wall of most Gram-negative bacteria, is a potent inflammatory agent and plays a primary role in bacterial-induced leukocyte recruitment [8, 9, 11, 30].

The four major steps in leukocyte recruitment are rolling, activation, firm adhesion, and migration across the endothelium and the basement membrane. Under normal, no inflammatory conditions many leukocytes come into brief contact with the endothelium and begin rolling, mainly via selectin interactions. In an inflammatory condition, chemokines produced by endothelial cells are believed to be presented to the slowing leukocytes, facilitating firm adhesion.

LPS-induced cell activation depends on the presence of three proteins comprising a multiprotein cell surface receptor complex - the LPS receptor complex. The first host protein involved in the recognition of LPS is the LPS-binding protein (LBP). LBP is an acute-phase protein, the role of which is to bring LPS to the cell surface by binding to LPS and forming a ternary complex with the LPS receptor molecule CD14. CD14 is a 55-kDa glycoprotein present in soluble form (sCD14) in blood or as a membrane-bound form (mCD14) in myeloid lineage forms. CD14 principally acts to bind LPS and does not participate in

*Corresponding author: A.S. Silva-Herdade, Institute of Biochemistry, Institute of Molecular Medicine, University of Lisbon Medical School, Av. Prof. Egas Moniz, 1649-028 Lisbon, Portugal. E-mail: anarmsilva@fm.ul.pt.

signalling directly. LPS is brought into close proximity to TLR4 only when it is present as an LPS-CD14 complex and when CD14 and TLR4 are co-expressed with MD-2 [6, 10, 34].

In vivo, cytokines such as IL-1 and TNF-a are rapidly released in response to LPS, and both of these cytokines induce endothelial adhesion molecules expression [3, 12, 20]. Recent studies have also demonstrated that the recruitment of monocytic cells and the expression of adhesion molecules is, besides TNF-a levels, influenced by the shear stress in the blood vessels [31].

Intravital microscopy, a useful and established technique pioneered in the 1800 s by Cohnheim [5], enhanced the study of inflammatory process by providing direct visual observation of living circulatory beds. Intravital microscopy is now used to evaluate leukocyte trafficking (rolling times and velocities, adhesion, and migration) after exposure to a variety of inflammatory stimuli and can be applied to different tissues as brain or the intestine [1, 14, 25, 27].

It was recently found that electrical or pharmacological activation of the efferent vagus nerve inhibits TNF release and attenuate the endotoxin-induced shock in rodents and the stimulation of the efferent vagus activates the release of acetylcholine (ACh) [2, 23, 33].

Concerning ACh release and the non-neuronal cholinergic system, other studies have demonstrated that both endothelial cells and T lymphocytes produce ACh [15–17]. ACh inhibits LPS-induced production of proinflammatory cytokines, inducing IL-1, from macrophages and microglia [26, 29]. ACh levels are continuously regulated by the hydrolytic enzyme acetylcholinesterase (AChE), that is found anchored to the membranes of various cellular types, such as erythrocytes, platelets, leukocytes and endothelial cells, by different kinds of tails [4, 7]. However, the presence of acetylcholinesterase in blood and in endothelial cells was identified without a description of is physiological function. Beyond the catalytic functions, other like intercellular adhesion were also described [18, 32].

AChE inhibitors are found to be potent cholinergic agonists and are widely accepted as anti-AD (Alzheimer disease) drugs [22]. Velnacrine (VLN) is known as an acetylcholinesterase inhibitor [35] that can modulate leukocyte activation. LPS is described as a potent inflammatory agent and plays a primary role in bacteria-induced leukocyte recruitment [6]. Based on this, this work intends to evaluate the effect of the intravenous administration of an AChE inhibitor, velnacrine maleate and AChE substrate, acetylcholine, in the inflammatory response of LPS by the analysis of the leukocyte-endothelial cells interactions and quantification of TNF-a, as a pro-inflammatory cytokine.

2. Methods

2.1. Animal preparation

The animals used in this study received human care in accordance with the Directive of the European Community n°86/609/CEE that mentions the protection of animals used for economic ends and other scientific ends.

Wistar male rats (HsdBrlHan:Wist, Harlan Iberica), with an average weight of 270 ± 16 g, were kept in an animal facility with a 12 h light/dark cycle and housed in cages in a temperature controlled room. All animals were kept on a diet standard rat food and water *ad libitum*. For the surgical procedures and microcirculatory measurements, the rats were anesthetized intraperitoneally with 1,5 g/Kg body weight urethane (Sigma-Aldrich). Body temperature was maintained at 37°C with a heating platform. A tracheostomy was performed to maintain the animal in spontaneous breath during all the experiment. For drug administration, the right jugular vein was cannulated with polyethylene tubing.

The preparation of cremaster for intravital microscopy is made in a Plexiglas support in accordance with [13]. Using an electrocauter a small incision in scrotum is made and the right testicule is brought outside. Then the conjunctive tissue that surrounds the cremaster is removed and an incision is made in the cremaster, fixing it to an appropriate support with silk sutures.

2.2. Intravital microscopy

The animal is then placed in an inverted microscope Leitz® FLUOVERT FU (Leica, Heerbrugg, Whisker) adapted for intravital microscopy, equipped with a 40X objective and a 10X ocular. The images are caught through a video camera CCD-IRIS DXC-107AP (Sony), visualised in a colour monitor PVM 1440QM (Sony) and recorded in a video SVHS AG-MD830 (Panasonic) for later analysis. After placing the support with the rat in the microscope, the venous catheter must be connected to a perfusion system with NaCl 0.9% pH 7.4, in a speed of 4 ml/h and the cremaster must be placed in perfusion of NaCl 0.9% pH 7.4 being the excess of liquid removed with a vacuum system. The preparations were allowed a 30 min *post*-surgical equilibration period.

After the equilibration period the cremaster observation is started. Post-capillary venules with 20–35 μm diameters were chosen for the quantification of the parameters previously defined. From the recorded images the interactions leukocytes/endothelial cells are quantified by the parameters already established [19]: number of rolling and adherent leukocytes.

The leukocytes are considered in rolling on the endothelium if moving at a slower speed than erythrocytes in that vessel, and their number counted during 1 min. A leukocyte was considered adherent to the endothelium if it remained stationary for more than 30 s in a 100 μm length [19].

2.3. Experimental groups

A cross-study between LPS, ACh and VLN was established. All the experiments were made after a 30 min stabilization period. LPS (17.5 ng/g rat weight (*E.coli*, serotype 026:B6, Sigma) and ACh (200 μg/Kg/rat weight) or LPS and VLN (200 μg/Kg/rat weight) were administrated intravenous (i.v) at times 0 and 5 minutes of the experiment. The leukocyte counts and the blood determinations were performed after 0, 5 and 15 minutes as represented in Fig. 1.

In the experimental groups in which an inflammatory state was previously induced (0 min) by LPS, ACh or VLN were administrated after 5 minutes of LPS administration – Group LPS+ACh and Group LPS+VLN. In the experimental groups in which a pre-conditioning with ACh or VLN was previously

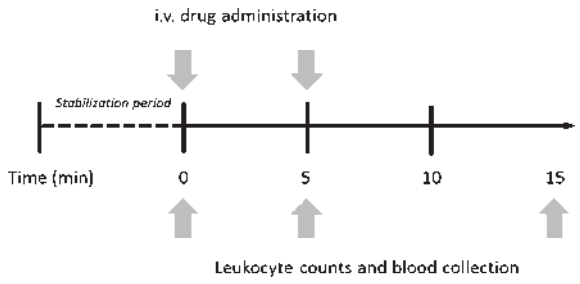

Fig. 1. Schematic representation (timeline) of the experiments performed.

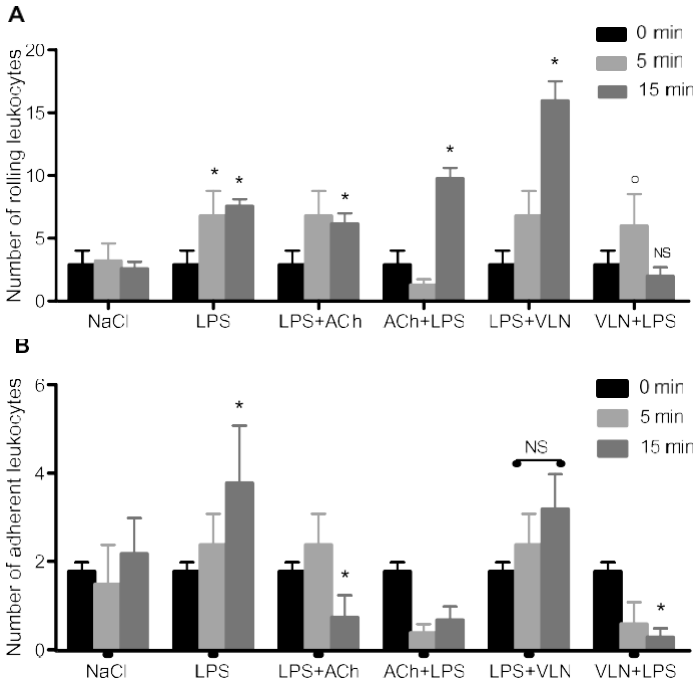

Fig. 2. Mean and standard deviation of the number of rolling (A) and adhesion (B) leukocytes in the NaCl, LPS, LPS+ACh, ACh+LPS, LPS+VLN and VLN+LPS Wistar rat groups. Statistical significant results in relation to the initial values (0 min) are shown $*p < 0.001$, $\circ p < 0.05$.

induced (0 min), LPS administration for inflammatory state induction was applied after 5 minutes – Group ACh+LPS and Group VLN+LPS. Blood collections were made in the different animal groups for TNF-a plasma determination (Calbiochem). All the experimental groups were performed for $N = 6$ rats.

2.4. Statistical analysis

Data are presented as means ± SD. The differences between the mean values were evaluated by using a one-way ANOVA statistical analysis with a Bonferroni's Multiple Comparison Test using GraphPrism Software. Values were considered statistically significant when p value was less than 0.05.

3. Results

Analysing the data obtain with the LPS administration on the number of rolling and adherent leukocytes (Fig. 2A and 2B) we observed an increase in both parameters. The administration of VLN after LPS increases ($p < 0.001$) the number of rolling leukocytes, although the number of adherent leukocytes is not affected by the presence of VLN. The administration of ACh alone doesn't show significant alterations in the number of rolling or adherent leukocytes after ACh administration (data not shown).

When ACh and VLN were administrated after the LPS-induced inflammatory state we observed that: (1) when ACh is administrated after LPS the number of rolling leukocytes is maintained, but adherent leukocytes decrease when compared with the effect obtained with LPS alone ($p < 0.001$); (2) VLN

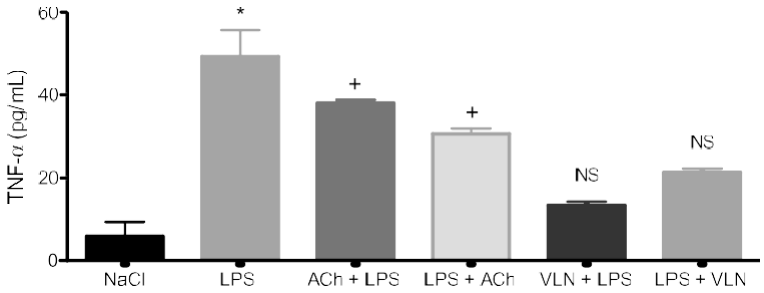

Fig. 3. Mean and standard deviation of TNF-a plasma levels in the NaCl, LPS, LPS+ACh, ACh+LPS, LPS+VLN and VLN+LPS Wistar rat groups after 15 min. Statistical significant results in relation to NaCL are shown $^{*}p < 0.001$, $^{+}p < 0.01$.

administration after LPS-induced inflammation augments the rolling leukocytes but statistical significant variations are observed in the number of adherent leukocytes.

In the experimental groups where VLN and ACh were administrated before LPS addition (Fig. 2), the results show that: (1) with a preconditioning of ACh, LPS administration significantly increases the number of rolling leukocytes but decreases the number of leukocytes in adhesion when compared either with the NaCl or the LPS experiment; (2) the presence of VLN lowers the number of rolling and adherent leukocytes.

TNF-a concentrations were determined at the same time of the leukocytes monitorization and the results show that when compared with NaCl administration, LPS increases TNF-a ($p < 0.001$) plasma levels, as expected during an inflammatory state (Fig. 3).

Regarding the results obtained for the TNF-a levels in presence of ACh and VLN both are capable of lowering this cytokine concentration after the LPS administration, when compared with its administration alone, although they are higher than the obtained with NaCl. TNF-a plasma levels show that LPS administration after VLN has no significant variation, when compared with NaCl administration, (Fig. 3). When ACh is present before the LPS administration TNF-a ($p < 0.01$) plasma concentrations are significantly increased.

4. Discussion

In our *in vivo* LPS-induced experimental model of inflammation the number of rolling leukocytes increased after LPS administration and are accompanied by an increase of the proinflammatory cytokines TNF-a ($p < 0.001$), when compared with the initial levels. Administration of ACh and VLN, which correspond, respectively to substrate and inhibitor of AChE, after LPS induction results in the decrease of TNF-a plasma levels when compared with LPS group; concerning the number of rolling leukocytes, ACh seems to have an anti-inflammatory effect maintaining almost invariable the number of recruited leukocytes to roll; which not happen in presence of VLN besides its ability to maintain lower TNF-a plasma levels.

The presence of ACh and VLN without any preconditioning or induced inflammation doesn't induce any alterations on the number of rolling and adherent leukocytes and TNF-a plasma concentrations remained almost invariable (data not shown). With LPS-induced inflammation after the intravenous ACh administration, TNF-a concentrations increased significantly in response to LPS, because of our observation that ACh alone doesn't produce any inflammatory effect this is consist with the increase of

the rolling leukocytes after LPS administration even in presence of ACh. The presence of VLN before LPS almost blocked the LPS-induced rolling and TNF-α production. VLN and ACh act with different kinetic effects on AChE. Increase of ACh levels results from the inhibitory action of VLN on AChE enzyme activity with the generation of an inactive ACh-AChE complex. The binds of ACh to AChE produce an active enzyme complex ACh-AChE. Consequently we observe different effects for the VLN or ACh administration on leukocytes recruitment in post-capillary venules of Wistar rats.

Recent studies discovered the anti-inflammatory role of the efferent vagus nerve in inhibiting acute inflammation by ACh releasing, so for ACh it was already expected that its anti-inflammatory effect may inhibit the LPS-induced production of proinflammatory cytokines by endothelial cells, like TNF-α as was already demonstrated by others in macrophages [29] and microglia [26].

The anti-inflammatory capacity of ACh is already described [2, 23, 33]. VLN seems to have two effects: an anti-inflammatory and a protective effect. The former probably resulting from the AChE inhibition and consequently with plasma ACh increase that was reflected on the impairment of the proinflammatory cytokines TNF-α levels results from LPS administration. Also VLN shows a "protective" effect by blocking, the proinflammatory cytokines production when administrated before LPS induction of inflammation.

Our data suggest that the modulation of AChE activation state can have in one hand, an anti-inflammatory effect during an inflammation state, but also a protective result before the inflammation development. This hypothesis is supported by our data, as described above, not only in the proinflammatory cytokines production, but also by leukocyte recruitment on endothelial cells.

It is known that cytokines, like TNF-α found in plasma may be produced by blood cells, endothelium or may originate from the brain. TNF-α can mediate the influx of leukocytes (both neutrophils and monocytes) to endothelial cells by stimulating the expression of adhesion molecules on the surface of leukocytes and vascular endothelial cells, process that is also mediated by the shear stress on the blood vessels [31]. We have seen that the intravenous administration of VLN only influences the maintenance of TNF-α concentrations without affecting the leukocyte-endothelial cell interactions; others [24] have demonstrated that brain levels of IL-1β and TNF-α are decreased after intraperitoneally administration of AChE inhibitors. This suggests that the maintenance of low levels of cytokines influences their synthesis in the blood stream, by endothelium or blood cells, and, probably, block the activation of rolling and adhesion to the endothelial wall. This may explain the unchangeable number of rolling leukocytes by lacking of activation at the endothelial level in presence of VLN and after LPS-induced inflammation.

We can with our results raise the hypothesis that keeping the proinflammatory cytokines levels low has implications on endothelial cells at the level of the leukocytes recruitment preventing the development of an inflammation state.

Some studies mentioned the possible increased risk for the development of cytokine-mediated diseases in patients with decreased instantaneous heart rate variability [28]. Our findings highlight the possibility of controlling the proinflammatory cytokines production with AChE inhibitors, like velnacrine, without alterations on the endothelial cells activation for leukocyte recruitment described by us, may be an important step for the control of cytokine-mediated diseases.

Acknowledgments

The authors would like to thank Serviço de Cirurgia Experimental of Hospital de Santa Maria, Portugal for the animals' husbandry and treatment during the experiments.

References

[1] G. Andonegui, S.M. Goyert and P. Kubes, Lipopolysaccharide-induced leukocyte-endothelial cell interactions: A role for CD14 versus toll-like receptor 4 within microvessels, *J Immunol* **169** (2002), 2111–2119.

[2] L.V. Borovikova, S. Ivanova, M. Zhang, H. Yang, G.I. Botchkina, L.R. Watkins, H. Wang, N. Abumrad, J.W. Eaton and K.J. Tracey, Vagus nerve stinulation attenuates systemic inflammatory response to endotoxin, *Nature* **405** (2000), 458–461.

[3] S.W. Chensue, P.D. Terebuh, D.G. Remick, W.E. Scales and S.L. Kunkel, *In vivo* biological and immunohistochemical analysis of interleukin-1 a, þ and tumor necrosis factor during experimental endotoxemia: Kinetics, kupffer cell expression and glucocorticoid, *J Clin Invest* **81** (1991), 237.

[4] G. Cicco, M. Vetrugno, M.T. Rotelli, G. Sborgia, M. Pennetta, P.P. Vico, V. Menneo, L. Nitti and C. Sborgia, Red blood cell (RBC) surface acetylcholinesterase showing a hemorheological pattern during glaucoma treatment, *Clin Hemorheol Microcirc* **35** (2006), 149–154.

[5] J. Cohnheim, Inflammation Lectures in General Pathology 1, New Sydnham Society, London, 1889.

[6] J.S. Correia, K. Soldan, U. Christen, P.S. Tobias and R.J. Ulvetich, Lipopolysaccharide is in close proximity to each of the proteins in its membrane receptor comples, *J Biol Chem* **276** (2001), 21129–21135.

[7] X. Cousin, U. Strähle and A. Chatonnet, Are there non-catalytic functions of acetylcholinesteraes? Lessons from mutant animal models, *BioEssays* **27** (2005), 189–200.

[8] M. Cybulsky, I.J. Cybulsky and H.Z. Movat, Neutropenic response to intradermal injections of *Eschericia coli*. Effects on the kinetics of polymorphonuclear leukocyte emigration, *Am J Pathol* **124** (1996), 1.

[9] M.I. Cybulsky, D.J. McComb and H.Z. Movat, Neutrophil leukocyte emigration induced by endotoxin: Mediator roles of interleukin 1 and tumor necrosis factor a, *J Immunol* **140** (1998), 3144.

[10] S.M. Dauphinee and A. Karsan, Lipopolysaccharide signalling in endothelial cells, *Laboratory Investigation* **86** (2006), 9–22.

[11] K.L. Davenpeck, J. Zagorski, R.P. Schleimer and B.S. Bochner, Lipopolysaccharide-induced leukocyte rolling and adhesion in the rat mesenteric microcirculation: Regulation by glucocorticoids and role of cytokines, *J Immunol* **161** (1998), 6861–6870.

[12] D.G. Hesse, K.J. Tracey, Y. Fong, K.R. Manogue, M.A. Palladino Jr., A. Cerami, G.T. Shires and S.F. Lowry, Cytokine appearance in human endotoxemia and primate bacterimia, *Surg Gynecol Obstet* **166** (1998), 147.

[13] M. Hill, B. Simpson and G. Meininger, Altered cremaster muscles hemodynamics due to disruption of the deferential feed vessels, *Microsvasc Res* **39** (1990), 349–363.

[14] F. Jung, From hemorheology to microcirculation and regenerative medicine: Fahraeus Lecture 2009, *Clin Hemorheol Microcirc* **45** (2010), 79–99.

[15] K. Kawashima, T. Fujii, Y. Watanabe and H. Misawa, Acetylcholine synthesis and muscarinic receptor subtype mRNA expression in T-lymphocytes, *Life Sci* **62** (1998), 198–206.

[16] K. Kawashima, K. Kajiyama, T. Suzuki and K. Fujimoto, Presence of acetylcholine in blood and its localization in circulating mononuclear leukocytes of humans, *Biog Amines* **9** (1993), 251–258.

[17] C. Kirkpatrick, F. Bitlinger, R. Unger, J. Kriesgsmann, H. Kilbinger and I. Wessler, The non-neuronal cholinergic system in the endothelium: Evidence and possible pathobiological significance, *Jpn J Pharmacol* **85** (2001), 24–28.

[18] A. Klegeris, T.C. Budd and S.A. Greenfield, Acethylcholinesterase-induced respiratory burst in macrophage: Evidence for the involvement of the macrophage mannose-fucose receptor, *Biochimica et Biophysica Acta* **1289** (1996), 159–168.

[19] K. Ley, Histamine can induce leukocyte rolling in rat mesenteric venules, *Am J Physiol* **267** (1994), H1017–H1023.

[20] G.D. Martich, M.C. Danner and A.F. Suffredini, Detection of interleukin 8 and tumor necrosis factor in normal humans after intravenous endotoxin: The effect of anti-inflammatory agents, *J Exp Med* **17** (1991), 1021.

[21] B. Newman and E.T. Liu, Perspective on BRCA1, *Breast Disease* **10** (1998), 3–10.

[22] A.M. Palmer, Cholinergic therapies for Alzheimer's disease: Progress and propects, *Curr Opin Investig Drugs* **4** (2003), 820–825.

[23] V.A. Pavlov, M. Ochani, M. Gallowitsch-Puerta, K. Ochani, J.M. Huston, C.J. Czura, Y. Al-Abed and K.J. Tracey, Central muscarinic cholinergic regulation of the systemic inflammatory response during endotoxemia, *PNAS* **103** (2006), 5219–5223.

[24] Y. Pollak, A. Gilboa, O. Ben-Menachem, T. Ben-Hur, H. Soreq and R. Yirmiya, Acetylcholinesterase inhibitors reduce brain and blood interleukin-1þ production, *Ann Neurol* **57** (2005), 741–745.

[25] J. Richter, J. Zhou, D. Pavlovic, R. Scheibe, V.H. Bac, J. Blumenthal, O. Hung, M.F. Murphy, S. Whynot and C. Lehmann, Vancomycin and to lesser extent tobramycin have vasomodulatory effects in experimental endotoxemia in the rat, *Clin Hemorheol Microcirc* **46** (2010), 37–49.
[26] R.D. Shytle, T. Mori, K. Townsend, et al., Cholinergic modulation of microglial activation by a7 nicotinic receptors, *J Neurochem* **89** (2004), 337–343.
[27] M. Sitina, Z. Turek, R. Parizkova, C. Lehmann and V. Cerny, Preserved cerebral microcirculation in early stages of endotoxemia in mechanically-ventilated rabbits, *Clin Hemorheol Microcirc* **47** (2011), 37–44.
[28] K. Tracey, Fat meets the cholinergic anti-inflammatory pathway, *J Exp Med* **202** (2005), 1017–1021.
[29] K.J. Tracey, The inflammatory reflex, *Nature* **420** (2002), 853–859.
[30] R.J. Ulevitch and P.S. Tobias, Receptor-dependent mechanisms of cell stimulation by bacterial endotoxin, *Annu Rev Immunol* **14** (1995), 437.
[31] K. Urschel, A. Wörner, W.G. Daniel, C.D. Garlichs and I. Cicha, Role of shear stress patterns in the TNF-alpha-induced atherogenic protein expression and monocytic cell adhesion to endothelium, *Clin Hemorheol Microcirc* **46** (2010), 203–210.
[32] L. Walch, C. Taisne, J.P. Gascard, N. Nashashibi, C. Brink and X. Norel, Cholinesterase activity in human pulmonary arteries, veins, *Brist J Pharmacol* **121** (1997), 986–990.
[33] H. Wang, M. Yu, M. Ochani, C.A. Amella, M. Tanovic, S. Susarla, J.H. Li, H. Wang, H. Yang, L. Ulloa, Y. Al-Abed, C.J. Czura and K.J. Tracey, Nicotinic acetylcholine receptor alpha7 subunit is an essential regulator of inflammation, *Nature* **421** (2003), 384–388.
[34] S.D. Wright, R.A. Ramos, P.S. Tobias, R.J. Ulevitch and J.C. Mathison, *Science* **249** (1990), 1431–1433.
[35] J. Wysocki, Z. Kalina and I. Owczarzy, Effect of organophospgoric pesticides on the behaviour of NBT-dye reduction and E rosette formation tests in human blood, *Int Arch Occup Environ Health* **59** (1987), 63–71.

Clinical Hemorheology and Microcirculation 39 (2008) 375–380
DOI 10.3233/CH-2008-1105
IOS Press

Localized hydrodynamics of clustering leukocytes

A.M. Artoli [a], A. Sequeira [a], A.S. Silva-Herdade [b,*] and C. Saldanha [b]
[a] *CEMAT/IST and Department of Mathematics, Instituto Superior Técnico, Lisbon, Portugal*
[b] *Instituto de Bioquímica/FML and Unidade de Biologia Microvascular e Inflamação/IMM, Lisbon, Portugal*

Abstract. The recruitment of leukocytes to the endothelial walls is intensively investigated both experimentally and through three dimensional computer simulations. The shear dependent viscosity has been obtained from measured values in post-capillary venules of Wistar rats' cremaster muscle. Localized velocity fields and shear stresses on the surface of leukocytes and near vessel wall attachment points have been computed and discussed for a cluster of recruited leukocytes under generalized Newtonian blood flow with shear thinning viscosity. We have observed one region of maximum shear stress and two regions of minimum shear stress on the surface of the leukocytes close to the endothelial wall. This suggests that the accumulation of selectins attains a minimum value in two regions, rather than in one region, on the surface of the leukocytes. We have also verified that the collective hemodynamic behavior of the cluster of recruited leukocytes establishes a strong motive for additional leukocyte recruitment. From this study we claim that the influence of the leukocytes rolling on the endothelial wall increases the shear stress on both the leukocyte and the endothelial wall which results in activating more signaling mediators during inflammation.

Keywords: Leukocytes dynamics, intravital microscopy, computational hemorheology, leukocyte wall shear stress

1. Introduction

Leukocyte arrest, recruitment and subsequent rolling, activation, adhesion and transmigration is a multistage process which is mainly triggered by hemorheologic forces and supported by shear-induced selectins, chemoattractants and adhesion molecules on the surface of the leukocytes and the endothelial wall [1–3]. A certain density of selectins and a high tensile strength of the selectin bond are required to confirm rolling. The mechanism of margination of leukocytes from the blood main stream is not well understood and deserves more focus on the causes and the force that initiate margination. It is believed that rolling is mediated by adhesion molecules of the selectin family which are expressed on the leukocyte surface (L-selectin) on the endothelial wall (E-selectin) and in platelets (P-selectins). The forces applied by these mediators are not enough for marginating the leukocytes and therefore, it is necessary to study the hydrodynamic forces and their interaction with the molecular forces in detail. This is a multiscale process which requires more adequate sub-macroscopic models which are capable of computing localized hemodynamics such as on surface shear stress and velocity distribution. In this study we have performed experiments on Wistar male rats and recorded leukocytes dynamics in real time using intravital microscopy. We have used these experimental data to build a shear dependent viscosity model and

*Corresponding author: A.S. Silva-Herdade, Instituto de Bioquímica/FML and Unidade de Biologia Microvascular e Inflamação/IMM, Av. Prof. Egas Moniz 1649-028, Lisbon, Portugal. E-mail: anarmsilva@fm.ul.pt.

plug it into a lattice Boltzmann numerical solver for shear thinning flows [4]. The lattice Boltzmann is a fully adaptive mesoscopic solver that has a number of benefits over the classical macroscopic fluid flow solvers. The most important feature of the lattice Boltzmann method is its capability to compute the shear stress independent of the velocity fields, from the non-equilibrium part of the distribution functions.

2. Materials and methods

2.1. Animal preparation

The animals used in this study received human care in accordance with the directive of the European community no. 86/609/CEE. The animals were prepared as explained in [1] with the right jugular vein and the left carotid artery catheterized. Pressure and cardiac frequency were monitored through the whole time of experiment via a pressure transducer (TRANSPAC). The animals were prepared for intravital microscopy according to Hill [5]. Intravital images of the dynamics of leukocytes were recorded and analyzed.

Blood samples were taken after the intravital microscopy observations to study the viscosity behavior in response to the shear rate using a Brookfield digital viscometer.

2.2. Numerical method

We have used a recently validated lattice Boltzmann model for shear thinning blood flow [4] to simulate individuals and clusters of moving leukocytes in three dimensions. The method is mesosopic, based on the Boltzmann transport equation from physics, which is suitable for solving multiscale phenomena that commonly appear in complex fluid flows. For non-Newtonian flows, the shear rate is locally computed from the non-equilibrium parts of the distribution functions, without a need for calculating velocity gradients. The drag and lift forces and the torques are easily computed from momentum exchange between the fluid and the structure [6].

Computed drags and torques were used to update the leukocyte positions. Translational and angular velocities were set on surface from the measured values.

3. Results

3.1. Experimental results

We have successfully tracked the dynamics of leukocytes from the *in vivo* experiment using the intravital microscopy and we were able to count the number of rolling leukocytes and measure the respective rolling speed as well as venule and leukocyte diameters. A snapshot of recorded video frames is shown in Fig. 1. An average leukocyte linear velocity of 8 rolling leukocytes was about 2.73 μm/s, with venule and leukocyte diameters being 23.7 and 6.8 μm, respectively. The hemodynamical parameters determined by *in vivo* measurements have shown a systolic blood pressure of 131 mmHg, a diastolic blood pressure of 90 mmHg and a cardiac frequency of 394 BPM.

Figure 2 shows individual tracking of some leukocytes as a function of time and relative distances from the nearest walls. (A) represents the path of a leukocyte from entrance until it rolls and (B) the relative position in time for the same leukocyte. Shown are also the time dependent components of

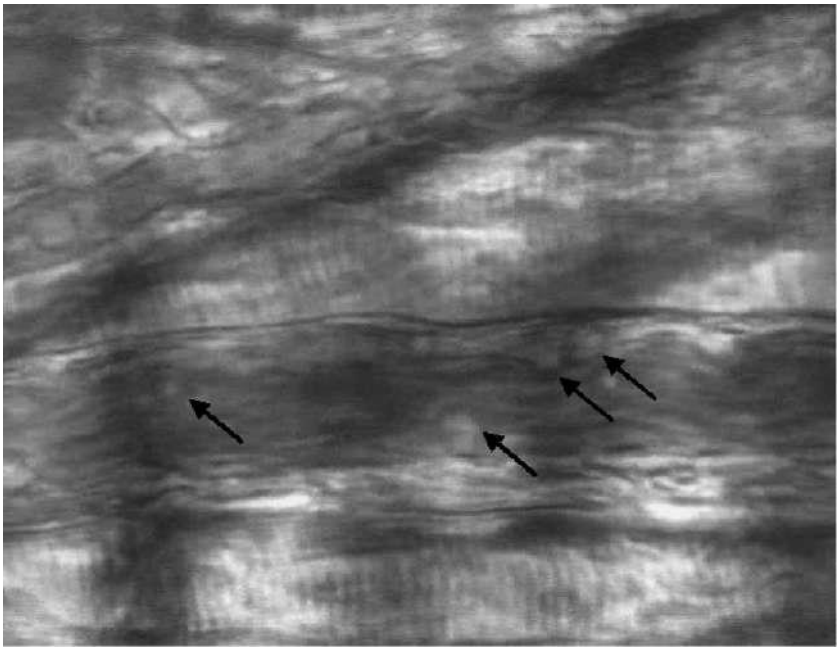

Fig. 1. Intravital microscopy of recruited leukocytes (the white spots) in a post-capillary venule in a Wistar rat cremaster muscle. Rolling leukocytes are indicated with arrows.

velocity magnitudes (C) and accelerations (D).

Blood samples were taken and analyzed by a viscometer to determine the shear thinning behavior of the rats' blood (see Fig. 3).

3.2. Numerical results

We have conducted a number of simulations for individual leukocytes, represented as irregular spheres, and for a cluster of moving leukocytes. From these simulations we have observed that the motion of leukocytes through a small enough venule results in disturbing the flow and increasing the endothelial wall shear stress at large distances. Shown in Fig. 4 is the influence of a not yet marginated leukocyte (moving through the centerline of the venule) on the endothelial wall shear stress. We suggest that the endothelial wall shear stress will be high enough to activate the endothelial cell monolayer and the mediators of the selectin family, initiating the capture of the leukocytes from the blood mainstream.

We have also observed four stagnation points on the endothelial wall: two upstream and two downstream with respect to the recruited leukocyte. These stagnant regions may help in the capture of leukocytes and decelerates their motion (see Fig. 5). For a cluster of recruited leukocytes, the traps and the vortexes form a helical stream, which also supports leukocytes margination toward and their rolling on the endothelial wall, as it is shown in Fig. 5.

4. Discussion

During inflammation, the recruitment of leukocytes from the blood stream and their subsequent adhesion to the endothelial wall are essential stages to the immune response system. The interaction between

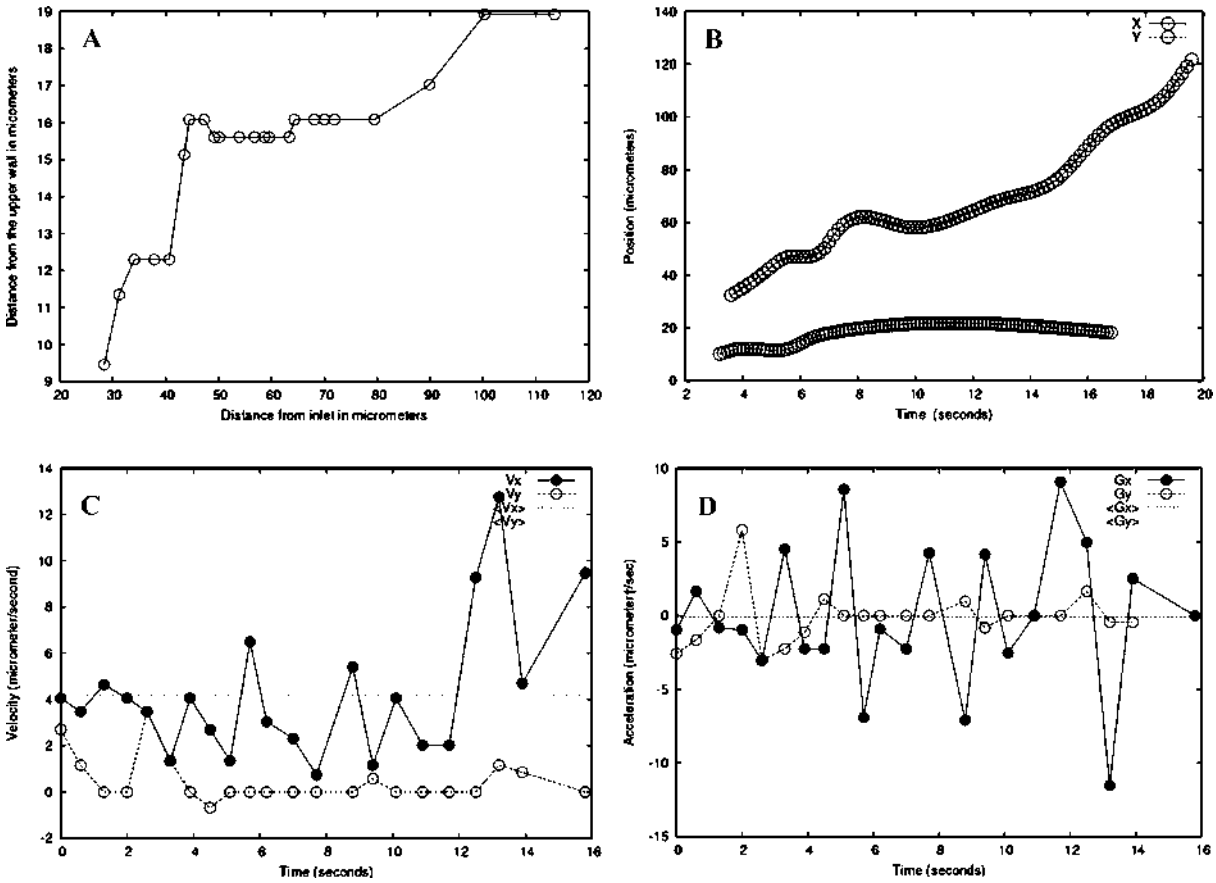

Fig. 2. Individual tracking of some leukocytes as a function of time (C and D) and relative distances from the nearest walls (A and B).

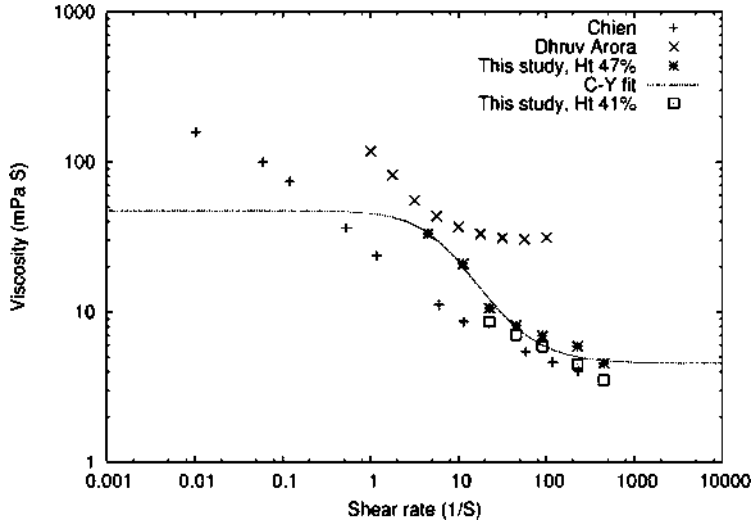

Fig. 3. Shear rate dependent viscosity values (at different hematocrits) obtained from blood samples of Wistar rats. Shown is also the Carreau–Yasuda shear thinning fit.

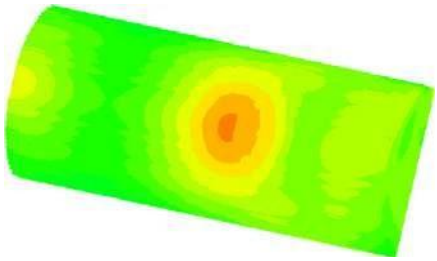

Fig. 4. Influence of a free flowing leukocyte on the endothelial wall shear stress.

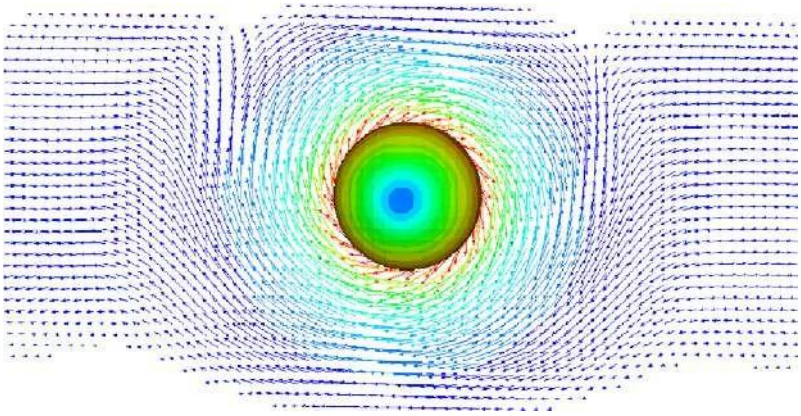

Fig. 5. Leukocytes are trapped by four stagnant regions close to the endothelial wall (with the flow motion directed to the right).

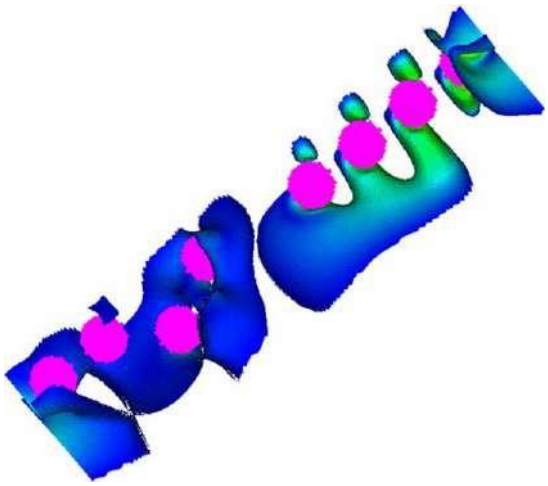

Fig. 6. Velocity isosurface around recruited leukocytes. The white jackets correspond to stagnant regions.

the recruited leukocytes and the endothelial cells is a key parameter in some pathogenesis of vascular diseases. It is important to evaluate leukocytes dynamics and quantify their localized velocities on surface shear stress and to capture the influence of the resulting hemodynamics on the endothelial wall at the inflammation regions.

Intravital microscopy is an adequate routine tool used for tracking the leukocyte dynamics but is restricted to two dimensions. In this study we were able to obtain more information by conducting three dimensional time dependent simulations for flow of leukocytes through a venule. Concerning the hemodynamical analysis of the results from the intravital microscopy, it is clearly observed that the velocity variations in the x-axis are higher than the ones observed in the y-axis, meaning that leukocytes move to the endothelial wall by modification of their position in the x-axis. Nevertheless, it was possible to obtain three-dimensional details on the flow filed and the shear stress of marginated and rolling leukocytes.

The data obtained from the experiments were used to set the initial and boundary conditions and to adopt a shear thinning viscosity model. It deserves noting that most of the studies reported in the literature (*in vivo*, *in vitro* or numerical) consider Newtonian flow dynamics of a 2D system. In this study we have demonstrated the influence of shear thinning flow on the recruitment and rolling processes of leukocytes. The role of hemorheologic forces of a cluster of leukocytes was also demonstrated. Moreover we have observed that the on surface shear stress on a recruited leukocyte shows two regions of minimum and one region of maximum shear stress. This may play a dominant role in directing the leukocyte toward the endothelial walls. Other studies refer to the leukocytes involvement in the signs and symptoms of chronic venous diseases [7–9] and it's also known that the properties of endothelial cells may be impaired in many diseases as atherosclerosis, hypertension, inflammation and metabolic diseases so, in this field, this work can be of great interest in the context of cardiovascular diseases. Ongoing research includes studies on adhesion and transmigration of rolling leukocytes.

Acknowledgements

This work has been partially supported by the grant SFRH/BPD/20823/2004 of FCT (A. Artoli) and by the project PTDC/MAT/68166/2006. FCT funds from the Centre for Mathematics and its Applications – CEMAT and the Molecular Medicine Institute – Microvascular Biology and Inflammation Unit are highly appreciated.

References

[1] A.S. Silva, C. Saldanha and J. Martins e Silva, Effects of velnacrine maleate in the leukocyte-endothelial cell interactions in rat cremaster microcirculatory network, *Clin. Hemorheol. Microcirc.* **36** (2007), 235–246.
[2] A.M. Artoli, A. Sequeira, A.S. Silva-Herdade and C. Saldanha, Leukocytes rolling and recruitment by endothelial cells: Hemorheological experiments and numerical simulations, *J. Biomech.* **40**(15) (2007), 3493–3502.
[3] R. Alon, D.A. Hammer and T.A. Springer, Lifetime of the P-selectin-carbohydrate bond and its response to tensile force in hydrodynamic flow, *Nature* **374** (1995), 539–542.
[4] A.M. Artoli and A. Sequeira, Mesoscopic simulations of unsteady shear thinning flows, *Lecture Notes Computer Sci.* **3992** (2006), 78–85.
[5] M. Hill, B. Simpson and G. Meinninger, Altered cremaster muscles hemodynamics due to disruption of the deferential feed vessels, *Microvasc. Res.* **39** (1990), 349–363.
[6] P. Lallemand and L.-S. Luo, Lattice Boltzmann method for moving boundaries, *J. Comput. Phys.* **184** (2003), 406–421.
[7] M.R. Boisseau, Leukocyte involvement in the signs and symptoms of chronic venous disease. Perspectives for therapy, *Clin. Hemorheol. Microcirc.* **37** (2007), 277–290.
[8] J.F. Stoltz, S. Muller, A. Kadi, V. Decot, P. Menu and D. Bensoussan, Introduction to endothelial cell biology, *Clin. Hemorheol. Microcirc.* **37** (2007), 5–8.
[9] M.R. Boisseau, Fahraeus Lecture 2005: Hemorheology and vascular diseases: red cell should rub up to the wall, leucocytes should cope with it, *Clin. Hemorheol. Microcirc.* **35** (2006), 11–16.

Computers and Mathematics with Applications 58 (2009) 1035 – 1044

Contents lists available at ScienceDirect

Computers and Mathematics with Applications

journal homepage: www.elsevier.com/locate/camwa

Leukocytes dynamics in microcirculation under shear-thinning blood flow

A. Sequeira[a], A.M. Artoli[a,*], A.S. Silva-Herdade[b], C. Saldanha[b]

[a] CEMAT/IST and Department of Mathematics, Instituto Superior Técnico, Av. Rovisco Pais 1, 1049-001 Lisboa, Portugal

[b] Biochemical Institute/FML and Microvascular Biology and Inflammation Unit/IMM, Av. Prof. Egas Moniz 1649-028, Lisboa, Portugal

article info

Keywords:
Leukocytes recruitment
Blood rheology
Flow in microvessels
Inflammation

abstract

We present detailed simulation results of localised hemodynamics for a cluster of rolling leukocytes under shear-thinning blood flow using a lattice Boltzmann model. Leukocytes were modelled as hard spheres moving through a venule of rigid walls. The used hemorheological parameters were obtained from in vivo measurements in blood samples of Wistar rats. Velocities, shear stresses and torques were computed and visualised for each individual cell, for the cluster and for the fluid. We have found that the flow is mainly three-dimensional due to the swirling and the asymmetry of the formed vortices during the recruitment process. The shear stress is maximum on a cap covering the cell and a cone with its base on the endothelial wall at the contact region. The leukocyte is recruited to the wall with the aid of trapping vortices and four stagnant regions surrounding the cell in addition to lateral motion towards the wall. We suggest that these phenomena are highly dependent on the angular velocity of the leukocyte and on the attractive force between the leukocyte and the endothelial wall. For a moving cluster of recruited leukocytes, velocities and shear stresses as well as torques are computed. It was found that the shear stress at the endothelium gets higher as the cluster moves in the main stream enabling early initialisation of the rolling process.

1. Introduction

Leukocyte arrest, recruitment and subsequent rolling, activation, adhesion and transmigration are essential stages in the immune response system to inflammation. Understanding this mechanism is of crucial importance in immunology and development of anti-inflammatory drugs such as modulators and blockers. The recruitment process is usually observed in post venules in the microcirculation. It is well accepted that the rolling process and the later adhesion cascade are mediated by a number of chemoattractants on the endothelial cell surface, selectins, integrins and other mediators on the surface of the leukocytes, and in the tissue. The whole process is triggered by margination of free flowing leukocytes toward the endothelial wall. This process is believed to result from the interaction of leukocytes with surrounding erythrocytes which deform and support pushing the leukocytes to the wall [1 – 4].

The captured leukocyte starts to roll under the assistance of a number of selectin mediators (P-selectin, L-selectin and E-Selectin) or their ligands through a complex process of overlapping domination by these mediators. Most leukocytes adhere to the endothelium after their rolling speed is decelerated by the CD18 integrins. The adherence process is mediated by the E-selectins. Under the existence of exogenous chemoattractants the leukocyte changes shape and transmigrates

* Corresponding author.
E-mail addresses: adelia.sequeira@math.ist.utl.pt (A. Sequeira), artoli@math.ist.utl.pt (A.M. Artoli).

0898-1221/$ – see front matter
doi:10.1016/j.camwa.2009.02.003

through the endothelium. The main function of the process is to isolate or eradicate the irritants and repair the inflamed tissue. At the end of the process the leukocyte is extravated (e.g. [5]).

Despite the fact that numerous attempts of *in vivo* and *in vitro* experiments, as well as numerical simulations of leukocytes recruitment and adhesion have been reported, the phenomena is not yet well understood and is under intensive investigation due to the key role that the mechanism plays in different pathogenic and immunological activities such as cancer, kidney failure (e.g. [6]), drug delivery and allergies [7,8]. The mechanism of margination of leukocytes from the blood main stream is not well understood and deserves more focus on the causes and the forces that initiate margination.

The main objective of this study is to probe the role of hemorheology in the margination process. Current experiments have focused on adhesion (e.g. [3,9,10]) from which the strength of signalling molecules, the rolling speeds and the transmigration scenario are well described. Theoretical studies are rare [11,12] and mainly couple the equations of motion and solve them numerically. Due to the multi-timescale nature of this cascade, it is necessary to combine a number of experimental techniques (see e.g. [13] for a review) or combined experiments and numerical simulations [9,14] when details of force interactions are acquired. It is to be noted that most of these studies, *in vivo*, *in vitro* or via numerical simulations are two dimensional and assume blood as a Newtonian fluid with constant viscosity. Commonly observed phenomena of spheres sedimenting near a wall, such as anomalous rotation, tendency towards the wall and vortex formation are different in Newtonian and non-Newtonian fluids. For example, for shear-thinning flows, a sphere in the flow tends to move towards the wall and rotates more slowly than the Newtonian flow, causing anomalous rotation [15 – 17]. Formation of negative wakes have also been observed in shear-thinning fluids [18].

In this study, we made use of tracking of leukocytes via intravital microscopy [19] from an in vivo experiment in Wistar rats to track the leukocytes trajectories and measure their velocities and forces exerted on them. These results were then used to initialise a lattice Boltzmann shear-thinning solver. We have also studied viscosity dependence on the shear rate from obtained blood samples of the rats which was found to follow a shear-thinning behaviour. The results were then used in simulating three dimensional leukocyte dynamics in a model of the venule from which the observations were taken. As the results obtained from experiments are usually two-dimensional, three-dimensional simulations will provide extra information on the localised hemodynamics such as the on-surface shear stress and the regions of stagnant flow. As the formation of vortices, their sizes and directions of rotation are largely affected by the relative cell positions, we also have studied the dynamics and highlighted the influence of clustering leukocytes on the endothelial wall shear stress which is the main activator for most endothelium activities.

2. Governing equations

We consider an incompressible shear-thinning blood flow model in a straight venule Ω with boundary $\partial\Omega$ and diameter $d = 17.5\ \mu$m. A group of leukocytes, represented as spheres $\Sigma(t)$ with boundary $\partial\Sigma(t)$ and similar diameters D of $9.5\ \mu$m are moving through the venule in the main stream where they are subjected to an attractive force towards the endothelial wall.

In rheology, the Deborah number is a dimensionless quantity relating the fluid relaxation and deformation time scales. Materials with a small Deborah number show only minor qualitative differences from a Newtonian fluid. More precisely, the Deborah number is defined as $De = U\lambda/D$, where λ is the characteristic relaxation time of blood (time taken by deformed erythrocytes to return to their original non-deformed shape) and U is the magnitude of the downstream leukocyte velocity. Moreover we also consider the dimensionless Reynolds number $Re = \rho UD/\eta$ and define the dimensionless distance from the wall as $h = H/D$ where H is the distance of the leukocytes from the endothelial wall and η is the zero shear rate viscosity. We assume similar densities for both leukocytes and the surrounding fluid. Typical simulation values are 0.01 for the Reynolds number and 0.03 for the Deborah number. The blockage ratio is $D/d = 0.54$, approximately.

The governing equations for the fluid-leukocyte system are the following: the momentum equation

$$\rho\left(\frac{\partial \mathbf{u}}{\partial t} + \mathbf{u}\cdot\nabla\boldsymbol{u}\right) = F_s - \nabla p + \nabla\cdot\mathbf{T} \quad \text{in } \Omega\setminus\overline{\Sigma} \tag{1}$$

the continuity equation

$$\nabla\cdot\mathbf{u} = 0 \quad \text{in } \Omega\setminus\overline{D} \tag{2}$$

and

$$\mathbf{u} = \mathbf{U} + \omega\times\mathbf{r} \text{ on } \partial\Sigma(t) \tag{3}$$

for the motion of the leukocyte. In theses equations $\mathbf{u}$ is the instantaneous velocity, ω is the angular velocity appearing from the torque, $\mathbf{r}$ is the position vector from the centre of the cell and $\mathbf{U}$ is the downstream leukocyte velocity (averaged from experiments), as mentioned above. In addition, the leukocyte is subjected to an attraction force F_s towards the wall, computed from the experimental trajectories. The stress tensor is given by

$$\sigma = -p\mathbf{I} + \eta(\dot{\gamma})(\nabla\mathbf{u} + (\nabla\mathbf{u})^{\mathrm{T}}) \tag{4}$$

where p is the pressure, $\mathbf{I}$ is the unit tensor and $\dot{\gamma}$ is the shear rate. The total viscosity η satisfies the Carreau – Yasuda model

$$\eta = \eta_\infty + (\eta_0 - \eta_\infty)(1 + (\lambda\dot{\gamma})^a)^b \tag{5}$$

in which η_0 and η_∞ are the asymptotic low and high shear-rate viscosity values, respectively. Here λ is the characteristic time of the fluid which depends on the instantaneous state of the material, $\dot{\gamma}$ is the shear rate and the parameters a and b are determined from experimental data, with $b < 0$ for shear-thinning fluids. If a or b vanish, the fluid model behaves as Newtonian. The force on the leukocyte is given by

$$\mathbf{F} = \int_\Sigma \sigma \cdot \mathbf{n} \mathrm{d}s \tag{6}$$

and the torque $\mathbf{T}$ at a distance r from the centre of leukocyte is

$$\mathbf{T} = \int_\Sigma r\sigma \cdot \mathbf{n} \mathrm{d}s \tag{7}$$

where $\mathbf{n}$ denotes the exterior unit normal vector to the leukocyte surface. The leukocyte velocity $\mathbf{U}$ and its angular velocity ω are expressed in the cell equations of motion

$$\ddot{\mathbf{U}} = \Delta p + \mathbf{F}, \tag{8}$$

and

$$I\ddot{\omega} = \sigma \tag{9}$$

with I being the moment of inertia. The particle position is given by solving these equations.

3. Numerical method

The lattice Boltzmann method [20 – 22] is a special finite difference discretisation of the simplified Boltzmann equation which describes transport phenomena at the mesoscale level. The dynamics of the fluid is modelled by the transport of simple virtual particles on the nodes of a Cartesian grid. Simulations with this method involve two simple steps; streaming to the neighbouring nodes and colliding with local node populations represented by the probability f_i of a particle moving with a velocity $\mathbf{e}_i$ per unit time step δt. Populations are relaxed towards their equilibrium states during a collision process. The equilibrium distribution function

$$f_i^{(eq)} = w_i\rho\left[1 + \frac{3}{v^2}\mathbf{e}_i \cdot \mathbf{u} + \frac{9}{2v^4}(\mathbf{e}_i \cdot \mathbf{u})^2 - \frac{3}{2v^2}\mathbf{u} \cdot \mathbf{u}\right] \tag{10}$$

is a low Mach number approximation to the Maxwellian distribution. Here, w_i is a weighting factor, $v = \delta x/\delta t$ is the lattice speed, and δx is the lattice spacing.

Studies on leukocytes and erythrocytes dynamics using lattice Boltzmann techniques have been reported (e.g. [23 – 25] in which blood was modelled as a Newtonian flow in 2D geometry. For non-Newtonian flow modelling, a number of lattice Boltzmann schemes were proposed for power law (e.g. [26,27], Bingham [28], shear-thinning Carreau – Yasuda [29] and viscoelastic (e.g. [30 – 32] fluids. It is to be noted that most of the available viscosity models are empirical. Moreover, they rely on macroscopic observations. Kinetic theory based viscosity models for blood are still lacking in the literature. Following the trend of our experimental data obtained from Wistar rats, we have found that the Carreau – Yasuda shear-thinning model best fits these results within the range of 4.50 to 450.00 s^{-1} of shear rates [19]. Therefore, we have adopted the model proposed by Artoli and Sequeira [29] for the shear-thinning flow which will be explained subsequently.

3.1. A lattice Boltzmann model for shear-thinning fluids

The non-Newtonian behaviour of many fluids, including blood, may be studied using the shear-thinning Carreau – Yasuda viscosity model, given above in Eq. (5). In what follows we show that a shear-thinning fluid can be modelled by a simplified lattice Boltzmann scheme.

We start from the usually known lattice Boltzmann equation

$$f_i(\mathbf{x} + \mathbf{e}_i\delta t, \mathbf{e}_i, t + \delta t) - f_i(\mathbf{x}, \mathbf{e}_i, t) = -\frac{1}{\tau}[f_i(\mathbf{x}, \mathbf{e}_i, t) - f_i^{(eq)}(\mathbf{x}, \mathbf{e}_i, t)] \tag{11}$$

which can be obtained by discretising the evolution equation of the distribution functions in the velocity space using a finite set of velocities $\mathbf{e}_i$. In this equation, τ is the dimensionless relaxation time which may be a constant, a discrete or a continuous variable. By Taylor expansion of the lattice Boltzmann equation up to $O(\delta t^2)$ and application of the multiscale Chapman – Enskog technique, the Navier – Stokes equations and the momentum flux tensor up to second order in the Knudsen number are obtained. The hydrodynamic density, ρ, and the macroscopic velocity, $\mathbf{u}$, are determined in terms of the particle distribution functions from the laws of conservation of mass

$$\rho = \sum_i f_i = \sum_i f_i^{(eq)} \tag{12}$$

and momentum

$$\rho \mathbf{u} = \sum_i \mathbf{e}_i f_i = \sum_i \mathbf{e}_i f^{(eq)}. \tag{13}$$

The pressure is given from the equation of state $p = \rho c_s^2$ and the kinematic viscosity is defined by $\nu = c_s^2 \delta t(\tau - \frac{1}{2})$, where c_s is the lattice speed of sound. A number of lattice Boltzmann models have been introduced, being characterised by the choice distribution functions, the number of moving particles, the lattice speed of sound and the nature of the relaxation time.

Expanding f_i about its equilibrium distribution f_i^{eq}

$$f_i = f_i^{eq} + \varepsilon f_i^{(1)} + \varepsilon^2 f_i^{(2)} + \cdots \tag{14}$$

where ε is of the order of the Knudsen number and in the limit of small ε, the momentum flux tensor is obtained from [33]

$$\Pi_{\alpha\beta}^{(1)} = \sum_i f_i^{(1)} \mathbf{e}_{i\alpha} \mathbf{e}_{i\beta} = -2\rho \delta_t \tau C(S_{\alpha\beta}). \tag{15}$$

In this equation C is a lattice-dependent constant (for the three-dimensional model with 19 particles (D3Q19), $C = 1/3$). The momentum flux is therefore directly computed from the non-equilibrium part of the distribution functions. Hence, the strain rate tensor is

$$S_{\alpha\beta} = -\frac{1}{2C\delta_t \tau \rho} \sum_i f_i^{(1)} \mathbf{e}_{i\alpha} \mathbf{e}_{i\beta} \tag{16}$$

and the stress tensor is [34]

$$\sigma_{\alpha\beta} = -\rho c_s^2 \delta_{\alpha\beta} - \left(1 - \frac{1}{2\tau_c}\right) \sum_{i=0} f_i^{(1)} e_{i\alpha} e_{i\beta}. \tag{17}$$

In constitutive equations of shear-thinning generalised Newtonian fluids, the viscosity depends on the magnitude of the second invariant of the strain rate tensor

$$|S| \equiv \dot{\gamma} = \sqrt{2 S_{\alpha\beta} : S_{\alpha\beta}}. \tag{18}$$

In detail, for the $D3Q$ 19 model, after making use of the symmetry of the strain rate tensor, we have

$$\dot{\gamma} = \dot{\gamma}_c \sqrt{0.5(S_{xx}^2 + S_{yy}^2 + S_{zz}^2) + (S_{xy}^2 + S_{xz}^2 + S_{yz}^2)} \tag{19}$$

where $\dot{\gamma}_c = \frac{3}{2\rho\tau_c}$ could be used as a characteristic shear rate. In this study we optionally set $\tau_c = 1$ to benefit from the simplicity and the stability of the scheme at $\tau = 1$.

Now, since $\eta = \rho\nu = \rho(2\tau - 1)/6$, the Carreau – Yasuda model in its dimensionless form is [29]

$$\tau = \tau_\infty + (\tau_0 - \tau_\infty)(1 + (\lambda\dot{\gamma})^a)^b \tag{20}$$

where τ_0 and τ_∞ correspond to η_0 and η_∞, respectively. The stability of the method is controlled by the difference $(\tau_0 - \tau_\infty)$ which is normally large for shear-thinning fluids. However, τ_∞ shall be in the working stability region if τ_0 is small. Another way to avoid instability is to tune the material relaxation time (in lattice units) by grid-refinement (or coarsening) in time. We note that the relaxation time here is a continuous function of six parameters, four of them are freely controllable during the simulations. Fig. 1 shows a possible range of LBM shear-thinning relaxation time profiles which could be obtained at different material characteristic times, and therefore, different materials may be simulated within the stable regime. Validation of this model against the finite elements was reported by Artoli et al. [35].

4. Results

4.1. Blood model

The viscosity of collected blood samples from the Wistar rats was found to fit the Carreau – Yasuda shear-thinning model, Eq. (5) with $\eta_0 = 42.77$ cP, $\eta_\infty = 4.56$ cP, $\lambda = 0.16$ s, $a = 1.52$ and $b = -0.83$ with a maximum standard error of 6.0% and reduced χ^2 of 1.05 at 45% hematocrit and a temperature of 37°C. From these parameters we have build a lattice Boltzmann shear-thinning model using Eq. (20). The behaviour of the model in response to the simulated shear rate is shown in Fig. 1 for different values of the dimensionless material relaxation time (i.e. at different LBM material time scales).

The geometry was discretised as shown in Fig. 2 for an individual leukocyte (represented as a sphere of diameter equal to 9.5 μm) moving in a straight rigid venule of diameter 17.5 μm. The spatial resolution is 0.5 μm. Two time scales are

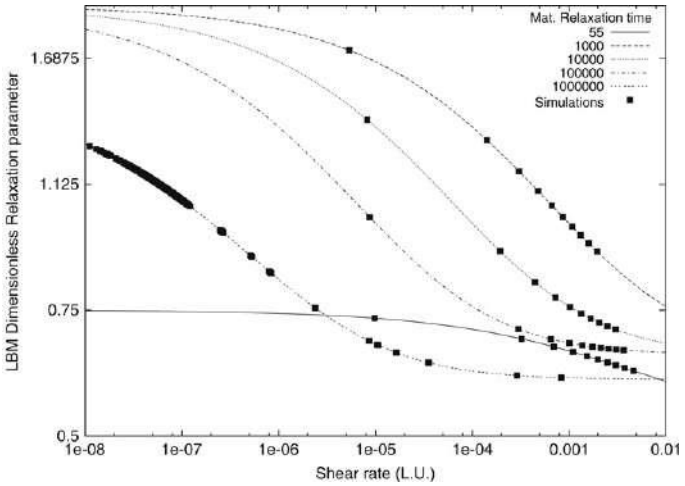

Fig. 1. Discretisation of the model geometry for a single leukocyte in a straight venule.

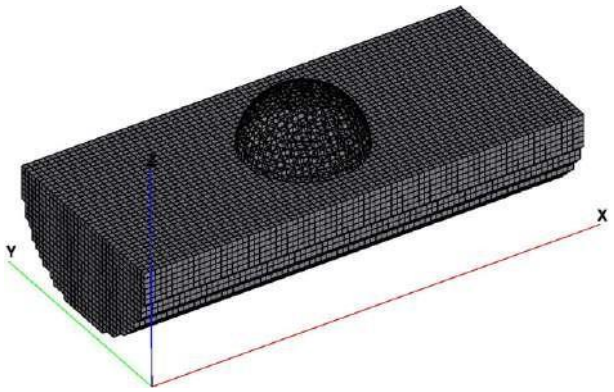

Fig. 2. Discretisation of the model geometry for a single leukocyte in a straight venule.

represented by the choice of the material characteristic time λ and the regular updating time step. Fig. 3 shows velocity vectors on a 2D projection of the leukocyte surface. We have used the Bouzidi et al. [36] boundary conditions for the moving boundaries and the wall. The inlet and the outlet conditions were implemented using an adaptation of the Zou and He [37] boundary conditions, with the pressure values obtained from the experiments [19]. The spherical leukocyte initially translates and rotates following the measured values obtained from the experiments. From these velocities, the pressure was computed and equilibrium distributions were computed and assigned to the relevant directions. The leukocyte moves downstream with a velocity 100 times less than the mainstream which flows at a Reynolds number of 0.017, based on the maximum axial velocity far from the leukocyte and on the centreline viscosity.

In addition, the drags and the lifts were computed from the momentum exchange between the fluid and the leukocyte [38]. The leukocyte rotates in response to the computed torque and is also subjected to a net attractive selectin force F_s towards the wall proportional to the square of the distance between its surface and the sedimenting endothelium [12], estimated from the trajectory of the leukocytes. The cell position is updated using the relation $\Delta r = \frac{1}{2}F_s(\delta t)^2$. It is to be noted that the repulsive force was neglected due to its nanoscale nature. We highlight here the fact that the lattice Boltzmann method was found to be highly flexible when applied to the problem under investigation with a number of key features: (i) the mesoscopic multiscale nature of the lattice Boltzmann equation, (ii) the computation of local stresses from the non-equilibrium parts of the distribution functions and (iii) the straightforward implementation of fluid-structure interaction through momentum exchange.

4.2. *Single leukocyte recruitment*

We present here simulation results of flow around a spherical leukocyte sedimenting toward the endothelial wall of a straight cylindrical venule. Fig. 4 shows magnitudes and vectors for the velocity of the flow and the on-surface velocity of a rotating leukocyte. A trap of four stagnation regions, with two ahead and two behind the leukocyte close to the endothelial wall are formed, acting in support and possibly initiating the margination process. These stagnation regions have also been

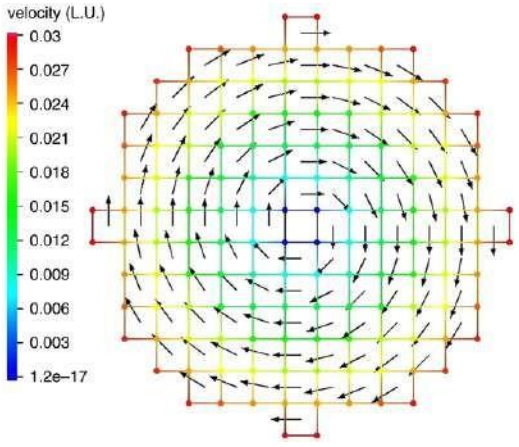

Fig. 3. Boundary conditions on surface of a 2D projection of the leukocyte.

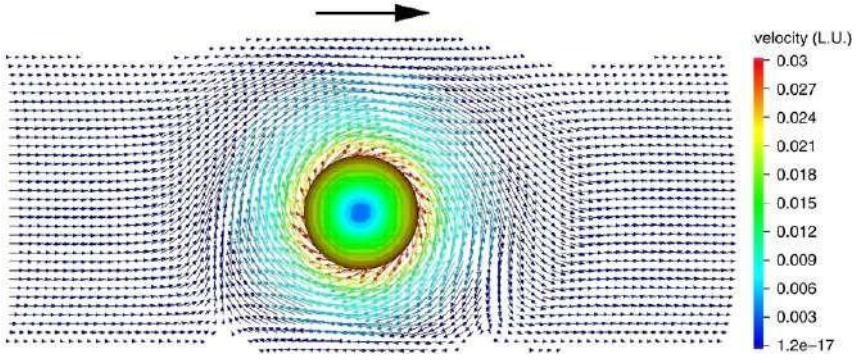

Fig. 4. Velocity vector magnitudes around a recruited leukocyte. The arrow indicates the flow direction.

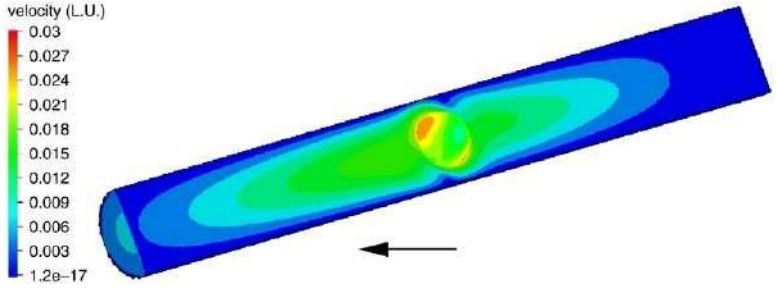

Fig. 5. Fully developed velocity profile flow around a recruited leukocyte.

reported in previous experimental works [16,17]. Upstream, the flow tends to go above the sedimenting cell and the situation is reversed downstream, creating a torque. This may be a reason for the anomalous rotation of the sphere sedimenting on a wall under shear-thinning flow. Fig. 5 represents a snapshot of the velocity contours for a fully developed flow around the recruited leukocyte under shear-thinning viscosity. The influence of the cell is clearly observed at large distances.

The shear stress in the sedimentation region gradually increases till it reaches a maximum value when the leukocyte is about half a micrometer from the endothelial wall (see Fig. 6). Increasing both the endothelium and the fluid shear stress near the contact region may result in releasing many chemoattractants known to be triggered by critical values for the shear stress (see e.g. [39]). In addition, we have found that the shear stress is maximum on a cap covering the leukocyte and a cone with base lying on the endothelium at the contact region (see Fig. 7) having maximum values on the endothelium wall downstream, directly ahead of the rolling leukocyte. We suggest that this shear stress value motivates the binding force that enables leukocytes to role on the endothelium wall downstream. Behind the rolling leukocyte the shear stress is smaller on the endothelium wall downstream and therefore, more bonds dissociate upstream while more appear downstream.

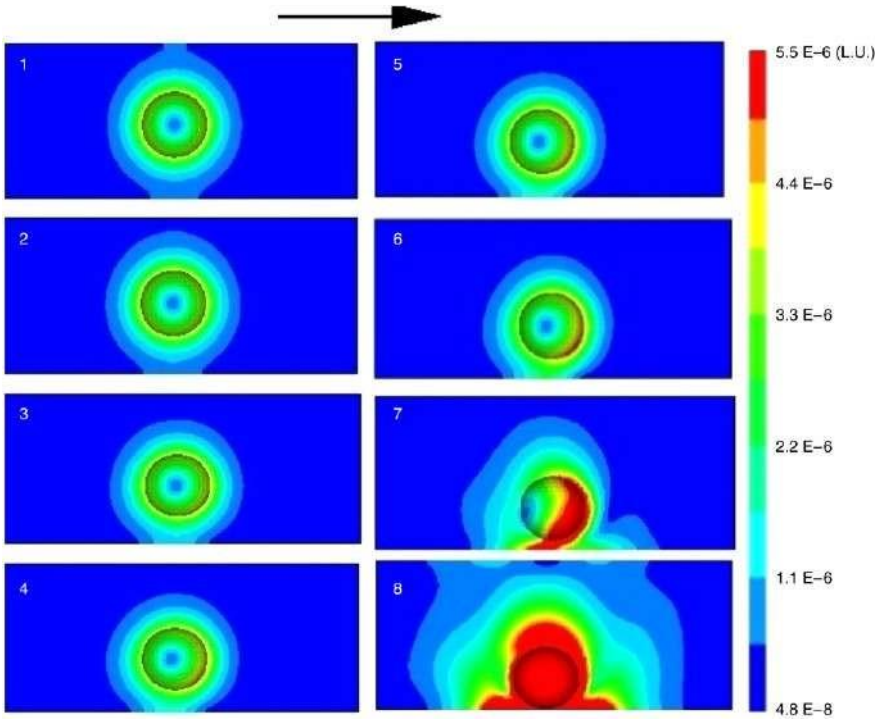

Fig. 6. Changes in the shear stress as the cell approaches the endothelium.

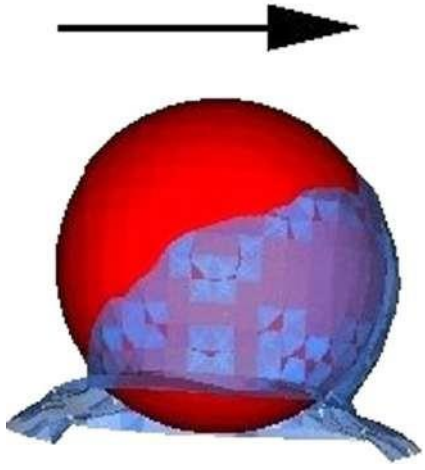

Fig. 7. Regions of maximum shear stress as the leukocyte starts to roll.

4.3. *Clustering leukocytes*

We have also simulated the dynamics of a cluster of leukocytes moving from an initial random position through the microvessel. Fig. 8 shows velocity magnitudes on the surface of each cell from which we observe that the velocity of each leukocyte depends not only on its position in the mainstream but also on its relative positions to the other neighbouring leukocytes. The vortices and stagnation points observed in the case of a single leukocyte also appear here, but in a more complex pattern. The traps and the vortices form a helical stream which also supports leukocytes margination toward and their rolling on the endothelial wall (see Figs. 10 and 11).

The cluster of moving leukocytes largely disturbs the flow field on the endothelial wall, mainly increasing its shear stress, as shown in Fig. 11. However, a number of buffer zones of lower shear stress exist. From the intravital experiment we have observed that the rolling cells move in a series of non-smooth clusters and have attributed that to these buffer zones in the endothelial wall shear stress which results in non-synchronised bond creation and dissociation events. However, most rolling leukocytes tend to move with similar rolling speed (see Fig. 9).

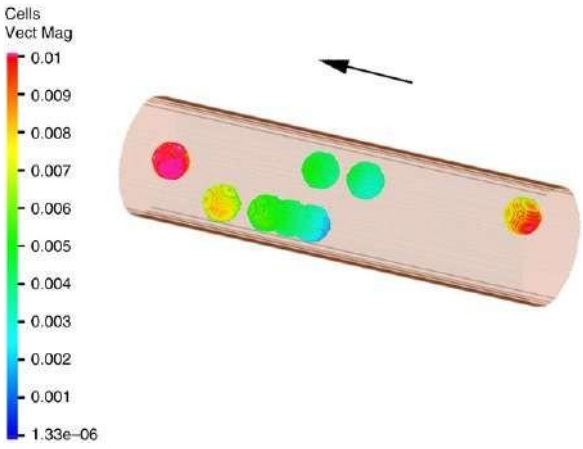

Fig. 8. Velocity magnitudes for a cluster of moving leukocytes at different recruitment stages.

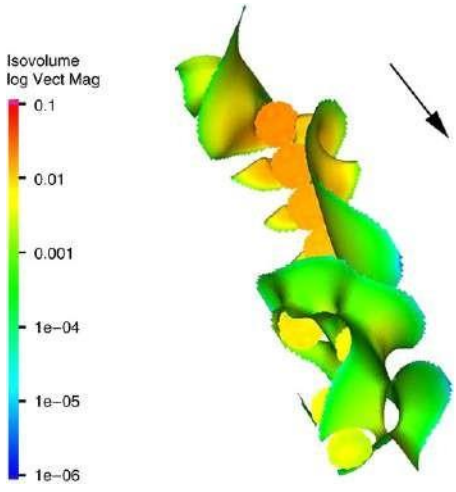

Fig. 9. Velocity magnitudes and isosurfaces for a cluster of rolling leukocytes.

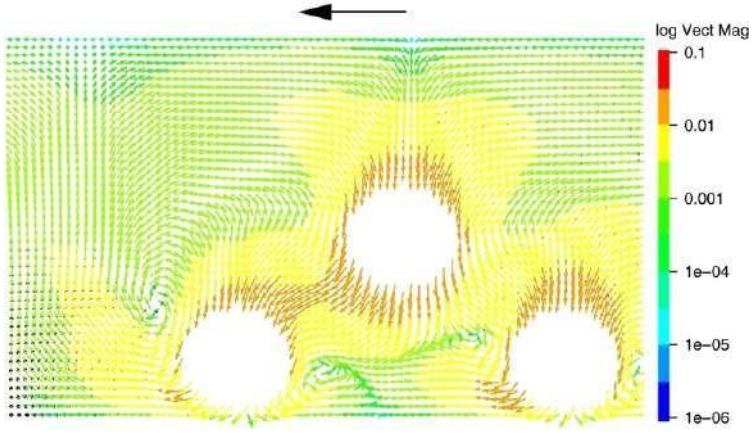

Fig. 10. Vortex formation during recruitment of leukocytes. The vortices act in support of the recruitment and rolling stages.

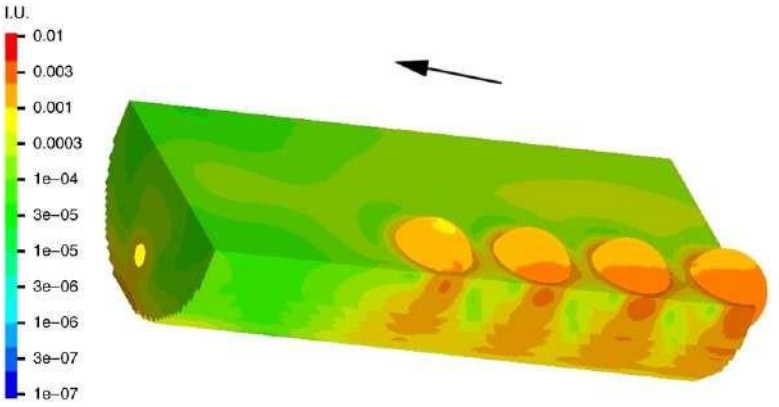

Fig. 11. Effects of rolling leukocytes on the endothelial wall shear stress.

5. Conclusions

Our approach in this study was to use the parameters measured from intravital microscopy and rheometry to build a non-Newtonian shear-thinning model for blood and set the initial and boundary conditions for the mesoscopic lattice Boltzmann solver to probe the leukocyte recruitment to the endothelial wall in a straight venule of a Wistar rat.

We have intensively investigated the recruitment of leukocytes to the endothelial wall under shear-thinning blood flow based on intravital microscopy and rheometry from blood samples of Wistar rats. A lattice Boltzmann model for shear-thinning flow was used in three-dimensional computer simulations for individual and clustering leukocytes. Localised velocity field and shear stress on the surface of leukocytes under flow conditions similar to the experiments were presented and discussed. We were able to locate four stagnation regions close to the endothelial wall and have attributed the margination process mainly to their existence. However, it is not clear yet whether these stagnation points do always form, regardless of the fluid nature and the leukocytes rotational velocity. This issue deserves more investigation by conducting a number of experiments at different flow conditions. We also noticed two lateral wakes; one upstream directing the flow far from the sedimenting wall and another downstream directing the flow towards the wall, causing a torque on the sphere which acts in support of the rolling process.

From the computed shear stress near the point of contact we have noticed that the shear stress becomes high both on the leukocytes surface and around the point of contact. However, the maximum shear stress forms a conic cap with its base on the endothelium and most of it downstream. This indicates that the shear stress upstream of a rolling leukocyte is less than that downstream. The higher shear stress downstream ensures binding force formation while the relatively lower shear stress upstream suppresses the bonds behind the leukocytes and ease the bond dissociation. The cluster dynamics holds all the features observed in the single leukocytes, with the interfering caps of maximum shear stress and swirls of vortices and stagnation points which on average act in support of the rolling process. Ongoing research in our group involves firm adhesion and transmigration of the rolling leukocytes and also the influence of certain drug releases on the localised hemorheology.

Acknowledgements

This work has been partially supported by the grant SFRH/BPD/20823/2004 of Fundação para a Ciência e a Tecnologia (A. Artoli) and by the project PTDC/MAT/68166/2006. FCT funds from the Centre for Mathematics and its Applications – CEMAT and the Molecular Medicine Institute – Microvascular Biology and Inflammation Unit are highly appreciated.

References

[1] S. Chien, White blood cell rheology, in: G.D.O. Lowe (Ed.), Clinical Blood Rheology, CRC Press, Taylor and Francis, 1988, pp. 87 – 109.
[2] O.K. Baskurt, R.A. Farely, H.J. Meiselman, Erythrocyte aggregation tendency and cellular properties in horse, human, and rat: A comparative study, American Journal of Physiology-Hearth and Circulatory Physiology 273 (1997) 2604 – 2612.
[3] K. Ley, Leukocyte recruitment as seen by intravital microscopy, in: K. Ley (Ed.), Physiology and Inflammation, Oxford University Press, New York, 2001, pp. 301 – 337.
[4] R.M. Rao, L. Yang, G. Garcia-Cardena, F.W. Luscinskas, Endothelial-dependent mechanisms of leukocyte recruitment to the vascular wall, Circulation Research 101 (2007) 234 – 247.
[5] A. Evans, D.A. Calderwood, Forces and bond dynamics in cell adhesion, Science 316 (5828) (2007) 1148 – 1153.
[6] K. Sigbartl, K. Ley, Leukocyte recruitment and acute renal failure, Journal of Molecular Medicine 82 (2004) 1432 – 1440.
[7] R. Lever, C.R. Page, Novel drug development opportunities for heparin, Nature Review Drug Discovery 1 (2) (2002) 140 – 148.
[8] Z. Szekanecz, A.E. Koch, Therapeutic inhibition of leukocyte recruitment in inflammatory diseases, Current Opinion in Pharmacology 4 (4) (2004) 423.
[9] R. Alon, S. Chen, K.D. Puri, E.B. Finger, T.A. Springer, The kinetics of L-selectin tethers and the mechanics of selectin-mediated rolling, Journal of Cell Biology 138 (5) (1997) 1169 – 1180.

[10] H.S. Rosário, C. Saldanha, J. Martins e Silva, The effect of velnacrine in lipopolysaccharide-induced leukocyte-endothelial interaction, in: B. Fragell (Ed.), 21st European Conference on Microcirculatin, Monduzzi Editore, Bologna, Italy, 2000, pp. 79 – 82.
[11] G.I. Bell, Models for the specific adhesion of cells to cells: A theoretical framework for adhesion mediated by reversible bonds between cell surface molecules, Science 200 (1978) 618 – 627.
[12] G.I. Bell, M. Dembo, P. Bongrand, Cell adhesion: Competition between non-specific repulsion and specific bonding, Biophysical Journal 45 (1984) 1051 – 1064.
[13] E.A. Evans, D.A. Calderwood, Forces and bond dynamics in cell adhesion, Science 316 (2007) 1148 – 1153.
[14] J. Lou, T. Yago, A.G. Klopocki, P. Mehta, W. Chen, V.I. Zarnitsyna, N.V. Bovin, C. Zhu, R.P. McEver, Flow-enhanced adhesion regulated by a selectin interdomain hinge, Journal of Cell Biology 174 (7) (2006) 1107 – 1117.
[15] L.E. Becker, G.H. McKinley, H.A. Stone, Sedimentation of a sphere near a plane wall: Weak non-Newtonian and inertial effects, Journal of Non-Newtonian Fluid Mechanics 63 (1996) 201 – 233.
[16] J.A. Tatum, M.V. Finnis, N.J. Lawson, G.M. Harrison, 3-D particle image velocimetry of the flow field around a sphere sedimenting near a wall: Part 2: Effects of distance from the wall, Journal of Non-Newtonian Fluid Mechanics 127 (2005) 95 – 106.
[17] J.A. Tatum, M.V. Finnis, N.J. Lawson, G.M. Harrison, 3-D particle image velocimetry of the flow field around a sphere sedimenting near a wall: Part 1. Effects of Weissenberg number, Journal of Non-Newtonian Fluid Mechanics 141 (2007) 99 – 115.
[18] M.T. Arigo, G.H. McKinley, An experimental investigation of negative wakes behind spheres settling in a shear-thinning viscoelastic fluid, Rheologica Acta 37 (1998) 307.
[19] A.M. Artoli, A. Sequeira, A.S. Silva-Herdade, C. Saldanha, Leukocytes rolling and recruitment by endothelial cells: Hemorheological experiments and numerical simulations, Journal of Biomechanics 40 (15) (2007) 3493 – 3502.
[20] D. d' Humiéres, P. Lallemand, U. Frisch, Lattice gas models for 3D hydrodynamics, Europhysics Letters 2 (1986) 291 – 297.
[21] G.R. McNamara, G. Zanetti, Use of the Boltzmann equation to simulate Lattice-Gas Automata, Physical Review Letters 61 (1988) 2332 – 2335.
[22] F.J. Higuera, S. Succi, R. Benzi, Lattice gas dynamics with enhanced collisions, Europhysics Letters 9 (1989) 345 – 349.
[23] C. Migliorini, Y. Qian, H. Chen, E.B. Brown, R.K. Jain, L.L. Munn, Red blood cells augment leukocyte rolling in a virtual blood vessel, Biophysical Journal 83 (2002) 1834 – 1841.
[24] C. Sun, C. Migliorini, L.L. Munn, Red blood cells initiate leukocyte rolling in postcapillary expansions: A lattice Boltzmann analysis, Biophysical Journal 85 (2003) 208 – 222.
[25] C. Sun, L.L. Munn, Particulate nature of blood determines macroscopic rheology: A 2-D lattice Boltzmann analysis, Biophysical Journal 88 (2003) 1635 – 1645.
[26] E.S. Boek, J. Chin, P.V. Coveney, Lattice Boltzmann simulation of the flow of non-Newtonian fluids in porous media, International Journal of Modern Physics B 17 (1 – 2) (2003) 99 – 102.
[27] J. Boyd, J. Buick, S.A. Green, A second-order accurate lattice Boltzmann non-Newtonian flow model, Journal of Physics A: Mathematics and General 39 (2006) 14241 – 14247.
[28] I. Ginzburg, K.A. Steiner, Free-surface lattice Boltzmann method for modelling the filling of expanding cavities by Bingham fluids, Philosophical Transactions of the Royal Society of London A (360) (2002) 453 – 466.
[29] A.M. Artoli, A. Sequeira, Mesoscopic simulations of unsteady shear-thinning flows, Lecture Notes in Computer Science 3992 (2006b) 78 – 85.
[30] Y.H. Qian, Y.F. Deng, A lattice BGK model for viscoelastic media, Physical Review Letters 79 (14) (1997) 2742 – 2745.
[31] L. Giraud, D. d' Humiéres, P. Lallemand, A lattice Boltzmann model for Jeffreys viscoelastic fluid, Europhysics Letters 42 (1998) 625 – 630.
[32] P. Lallemand, D. d' Humiéres, L.-S. Luo, R. Rubinstein, Theory of the lattice Boltzmann method: Three-dimensional model for linear viscoelastic fluids, Physical Review E 67 (2) (2003) 021203.
[33] B. Chopard, M. Droz, Cellular Automata Modeling of Physical Systems, Cambridge University Press, 1998.
[34] A.M. Artoli, Mesoscopic computational haemodynamics, Ph.D. Thesis, University van Amsterdam, The Netherlands, 2003.
[35] A.M. Artoli, J. Janela, A. Sequeira, A comparative numerical study of a non-Newtonian blood flow model, in: Proceedings of the 2006 IASME/WSEAS, International Conference on Continuum Mechanics, Chalkida, Greece, 11 – 13 May, 2006, pp. 91 – 96.
[36] M. Bouzidi, M. Firdaouss, P. Lallemand, Momentum transfer on a Boltzmann lattice fluid with boundaries, Physics of Fluids 13 (2001) 3452 – 3459.
[37] Q. Zou, X. He, On pressure and velocity boundary conditions for the lattice Boltzmann BGK model, Physics of Fluids 9 (1997) 1591 – 1598.
[38] P. Lallemand, L.-S. Luo, Lattice Boltzmann method for moving boundaries, Journal of Computational Physics 184 (2003) 406 – 421.
[39] A. Dardik, A. Yamashita, F. Aziz, H. Asada, B. Sumpio, Shear stress-stimulated endothelial cells induce smooth muscle cell chemotaxis via platelet-derived growth factor-BB and interleukin-1α, Journal of Vascular Surgery 41 (2005) 321 – 331.

Microvascular Research 107 (2016) 34-38

Contents lists available at ScienceDirect

Microvascular Research

j our nal homepage: www.elsevier. com/l ocate/ ymvre

Erythrocyte deformability – A partner of the inflammatory response

Ana Santos Silva-Herdade [a,*], Giulia Andolina [b], Caterina Faggio [b], Ângelo Calado [a], Carlota Saldanha [a]

[a] CSaldanha Lab, Instituto de Medicina Molecular, Faculdade de Medicina, Universidade de Lisboa, Av. Professor Egas Moniz, 1649-028 Lisbon, Portugal
[b] Department of Chemical, Biological, Pharmaceutical and Environmental Sciences, University of Messina, Sicily, Italy

article info

Article history:
Received 17 March 2016
Revised 27 April 2016
Accepted 27 April 2016
Available online 01 May 2016

Keywords:
Inflammation
Erythrocyte deformability
Nitric oxide
Intravital microscopy

abstract

We aim to establish an *in vivo* animal model of acute inflammation using PAF (platelet activating factor) as inflammatory agent and to study the erythrocyte deformability changes induced by the inflammatory response. Counting the number of rolling and adherent neutrophils to endothelium after 2, 4 and 6 h of intrascrotal injection of PAF we showed the induction of an inflammatory state. Blood samples are collected in order to measure the erythrocyte deformability and to quantify NO efflux from the red blood cells (RBCs). The results show an increased number of rolling and adherent neutrophils after 2 h and 4 h of inflammation as well as decreased values of erythrocyte deformability in the same time-points. This result is in line with the need of a low blood viscosity to the recruitment process that will improve leukocyte migration towards the endothelial wall. NO efflux from RBCs is also affected by the inflammatory response at the first hours of inflammation. This animal model demonstrates *in vivo* the association between an acute inflammatory response and the rheological properties of the blood, namely the RBCs deformability. For those reasons we consider this as an adequate model to study acute inflammatory responses as well as hemorheological parameters.

Introduction

Rolling of leukocytes in post-capillary venules and their subsequent adhesion to endothelial walls are crucial steps of the inflammation response. The migration of the leukocytes to the tissues is a multi-step process which includes, margination, rolling, adhesion and transmigration. During the approaching process, leukocytes exit the central blood stream, interacting with the erythrocytes and decelerate, initializing rolling. In this process, leukocytes tend to aggregate with the red blood cells, thus reducing its speed (Zarbock et al., 2011; Sequeira et al., 2009). The whole process is believed to be triggered by the activation of the endothelial cell monolayer in response to inflammation mediators and it is commonly accepted that the rolling of the leukocytes along the vascular wall is a result of intrinsic weak forces of adhesion between the leukocytes and the endothelial cells, on the one hand, and of the driving forces exerted by the blood flow, on the other (Sequeira et al., 2009). The rolling is mediated by adhesion molecules of the selectin family. The combined action of three families of selectins : L-selectins (associated with leukocytes), E- and P-selectins (associated with endothelial cells and platelets) is to promote leukocyte rolling, one key process for the inflammatory response (Artoli et al., 2007; Huttenlocher and Poznansky, 2008; Jung et al., 1998). Besides those molecules that are essential for the leukocyte recruitment to occur, *in vitro* and *in vivo* experiments have shown that the margination of leukocytes may depend on rheological factors such as hematocrit, blood suspension medium and shear stress (Jain and Munn, 2009; Vitorino de Almeida et al., 2015) reinforcing that the hemodynamic properties of the blood also influence the migration process (Sequeira et al., 2009).

Firm adhesion occurs when the cell stays still in the endothelial wall for a time equal to or greater than 30 s (Artoli et al., 2007; Gavins and Chatterjee, 2004; Kubes and Kerfoot, 2001; Zarbock et al., 2011). Once adhered to the endothelial wall, leukocytes can transmigrate to the tissue and initiate their anti-inflammatory action, phagocytosing pathogens or foreign bodies that have induced inflammation. To adhere the leukocytes do nothing but flatten out, emitting pseudopodia towards the leukocyte surface, by a process called chemotaxis the cells crawl along the endothelial to find a good place for the trans-endothelial migration (McDonald and Kubes, 2011; Phillipson and Kubes, 2011). This depends on a number of factors, including specific receptors, the type of inflammation and vascular architecture, and matrix proteins.

As is well known, erythrocytes are biconcave cells that change their shape according to the vessel lumen diameter and have a key role in the oxygen transport in the body (Pagano and Faggio, 2015). The deformability indicates a reversible change of erythrocytes aspect in response to a deforming force. It is an essential interfering property of blood flow and thus in oxygen delivery within the systemic microcirculation. The low deformability of the erythrocytes can reduce the oxygen uptake or donation (Tsukada et al., 2001). The erythrocyte deformability largely influences the blood viscosity, the more the RBCs are deformed the lower the blood viscosity is. Over a deforming force, the erythrocytes may be submitted to chemical or physical stimulations and nitric oxide (NO) efflux occurs (Barvitenko et al., 2013). NO is synthesized in endothelial cells by different isoforms of NO synthase and

* Corresponding author.
E-mail address: anarmsilva@medicina.ulisboa.pt (A.S. Silva-Herdade).

http://dx.doi.org/10.1016/j.mvr.2016.04.011
0026-2862/

plays a significant role in the control of the individual cell and organ functions (Korhonen et al., 2005). So the cells liberate a greater amount of NO which reduces platelet aggregation and leukocyte adhesion (antithrombin effect) and diffuses to the smooth muscle where relaxation occurs (Taha, 2003).

Using intravital microscopy as a qualitative and quantitative technique to observe and quantify epithelial cell–leukocyte interactions *in vivo* (Borregaard, 2010) we established an animal model of inflammation. Using PAF (platelet activating factor) as inflammatory agent we studied the inflammatory response at different time point post-inflammations by counting the number of rolling and adherent leukocytes and the changes induced in the erythrocyte deformability and erythrocyte efflux of NO concentration.

Materials and methods

Experimental design

The mice (BW: 23.0 ± 2.3 g) used in this experiment were divided in four experimental groups according to time post-inflammation. An inflammatory response was induced using PAF (platelet-activating factor, Sigma, Germany) as an inflammatory agent. An intra-scrotal (i.s.) injection of 300 μL of PAF $1O^{-6}$ M in PBS pH 7.4 was given to male mice and after 0, 2, 4 and 6 h of PAF administration the cremaster was prepared for intravital microscopy (N = 10 in each experimental group). At the end of the experiments, 500 μL blood was taken by cardiac puncture to heparinized tubes and the animals were euthanized with sodium pentobarbital (120 mg/kg BW).

Animal preparation

The animals used in this study received humane care in accordance with the Directive of the European Community 2010/63/EU that mentions the protection of animals used for economic and other scientific ends and also according to the Portuguese Legislation Law 113/2013.

Lys-EGFP-ki mice with 5 to 8 weeks (n = 40) (Faust et al., 2000) with an average weight of 23.0 ± 2.3 g, were kept in an animal facility with a 12 h light/dark cycle and housed in cages in a temperature controlled room. All animals were kept on a diet standard mouse food and water *ad libitum*. For the surgical procedures and microcirculatory measurements, the mice were anesthetized intraperitoneally (i.p.) with a cocktail of xylazine/ketamine (0.1 mL/10 g of BW). Body temperature was maintained between 35 and 37 °C with auto-regulated heating platform.

The preparation of cremaster for intravital microscopy was made in an appropriate support as described in (Silva et al., 2007). Using scissors a small incision in the scrotum was made and one of the testicles was exteriorized. Then the conjunctive tissue that surrounds the cremaster was removed, and an incision in the cremaster was made, fixing it to the appropriate support with silk sutures.

Intravital microscopy

After the cremaster preparation the support with the animal was placed in a confocal microscope Zeiss LSM 7 Live (Zeiss, Germany) adapted for intravital microscopy, equipped with a 20× water objective and a 10× ocular. All the images were recorded using the ZEN LSM 2006 software. The cremaster was kept in perfusion of Krebs–Henseleit buffer with $NaHCO_3$, warmed to 37 °C and bubbled with 95% N_2 and 5% CO_2 for the complete superfusion of the tissue throughout the experiment; the excess of liquid was removed with a vacuum system.

Post-capillary venules with 20-25 μm diameter were chosen for the quantification of the parameters previously defined. The duration which venules were registered was minimally 1 min. From the recorded images the interactions between leukocytes and endothelial cells were quantified by the parameters already established (Kubes and Kerfoot, 2001): number of rolling leukocytes and their rolling speed, number of adherent leukocytes and venule diameters. The leukocytes were considered to be rolling on the endothelium if the leukocytes were moving at a slower speed than the erythrocytes in the same vessel over a 1 min duration. A leukocyte was considered adherent to the endothelium if it remained stationary for more than 30 s in a 100 μm length (Silva et al., 2007).

Blood collection

At the end of the intravital microscopy observation 500 μL blood were taken by cardiac puncture to analyze erythrocyte deformability and NO concentrations according to the protocols described below. The blood was collected using heparin as an anticoagulant.

Erythrocytes deformability quantification

Erythrocyte deformability at different shear stress (0.30; 0.60; 1.20; 3.00; 12.00; 30.00; 60.00 Pa) was determined by using the Rheodyn SSD shear stress diffractometer from Myrenne GMBH (Roentgen, Germany) and erythrocyte deformability is expressed as the elongation index (EI) in percentage. Rheodyn SSD diffractometer determines RBC deformability by simulating shear forces exerted by blood flow and vascular walls on erythrocytes. Erythrocytes were suspended in a viscous medium and placed between a rotating optical disk and a stationary disk. A well-defined shear force was exerted upon the suspension which forces the erythrocytes to deform to ellipsoids and align with the fluid shear stresses. If a laser beam was allowed to passthrough the erythrocyte suspension a diffraction pattern appears on the opposite end. That diffraction pattern will be circular with resting erythrocytes, but becomes elliptical when these ones were deformed by shear. Light intensity of the diffraction pattern was measured at two different points (A and B), equidistant from the center of the image. Erythrocyte elongation index (EEI), in percentage, was obtained according to the following equation: $EEI\ (\%) = A - B \cdot A + B \times 100$.

Measurement of NO by an amperometric method

For NO determination the blood was centrifuged at 3000 rpm for 5 min in order to separate the red blood cells. Erythrocyte suspensions were centrifuged and sodium chloride 0.9% at pH 7.0 was added in order to reach a hematocrit of 0.05%. The suspension was mixed by gentle inversion of tubes. For amperometric NO quantification, we used the amino-IV sensor (Innovative Instruments Inc., FL, USA), as described in (Lopes de Almeida et al., 2009). Briefly, after stabilization of the NO sensor immersed in erythrocyte suspensions, the erythrocytes were stimulated with 10 mM of ACh and changes in the electric current registered, the change being proportional to the amount of NO mobilized by ACh-stimulated erythrocytes. The NO concentration calculation was made based on the minimum peak and the maximum peaks obtain after the addition of ACh.

Statistical analysis

Data are expressed as mean values ± standard deviation (SD). Statistical analysis was conducted using the GraphPad Prism 5.0. One-way ANOVA was applied to assess statistical significance between samples. Statistical significance was set at a $p < 0.05$ level.

Results and discussion

The animal model of acute inflammation herein described uses PAF as an inflammatory agent. PAF is described as a phospholipid mediator of an inflammation that is released early in inflammation by a variety of cell types. It is also known that PAF cooperates in the recruitment of leukocytes in the inflamed tissue, promoting the activation of cells

ensuing adhesion to the endothelium and extravascular transmigration of leukocytes (Montrucchio et al., 2000) Therefore, after an intra-scrotal injection of PAF in mice, the numbers of rolling and adherent neutrophils were counted after 2, 4 and 6 h of inflammation. The rolling velocities and the vessel diameters were also determined. Fig. 1 shows a statistically significant increase in the number of rolling ($p < 0.001$) and adherent ($p < 0.05$) neutrophils after 2 and 4 h of inflammation and decrease at 6 h of inflammation. A control group of mice in which saline instead of PAF was injected with i.s. was used for similar measurements; no significant differences in the number of rolling and adherent neutrophils until 6 h after injection were observed (data not shown). The rolling velocity decreases with time *post*-inflammation (Fig. 2A) which makes a part of a normal acute inflammatory response because the rolling velocity of neutrophil s needs to become slower in order to facilitate the subsequent adhesion process.

This represents a typical acute inflammatory response, where there is a sequence of leukocyte recruitment in which we have an increase in the number of neutrophils in the first hours of the inflammatory response (Fukuda et al., 2000) that will be followed by an increase in the number of rolling monocytes. The increase of the vessel diameters Fig. 2B was also expected as vasodilation is also a main characteristic of the inflammatory response.

Fig. 3 illustrates the deformability pattern of the erythrocytes. The cells are less deformable at 6 h of post-inflammation than after 2 h of inflammation. The observed values are statistically significant ($p < 0.001$). The difference in the deformability in relation to the 0 h group is higher for high values of shear stress than for low values. The erythrocyte deformation index is an important physiological property of RBCs since those cells are the main cells in circulation and they are responsible for the oxygen transportation and delivery to the tissues. In order to pass through the capillary microcirculation the RBCs need to deform; the RBC membrane has the capacity to deform and maintain their integrity. If the deformability of these cells is compromised the oxygen transportation to the tissues will also be impaired. In this study we observed a continuous decrease in the RBC deformability with the progression of the inflammatory response.

PAF was used in the study as an inflammatory agent and although PAF-R (PAF receptor) is constitutively present on platelets, leukocytes and endothelial cells, Lang (Lang et al., 2005) disclosed the presence of PAF receptors in red blood cells but showed that PAF stimulates the breakdown of sphingomyelin on RBCs in isotonic conditions. Therefore, PAF may cause changes in the physico-chemical structure of the erythrocyte membrane, which in turn may cause changes in RBC deformability. Taking this into account we entertain the possibility

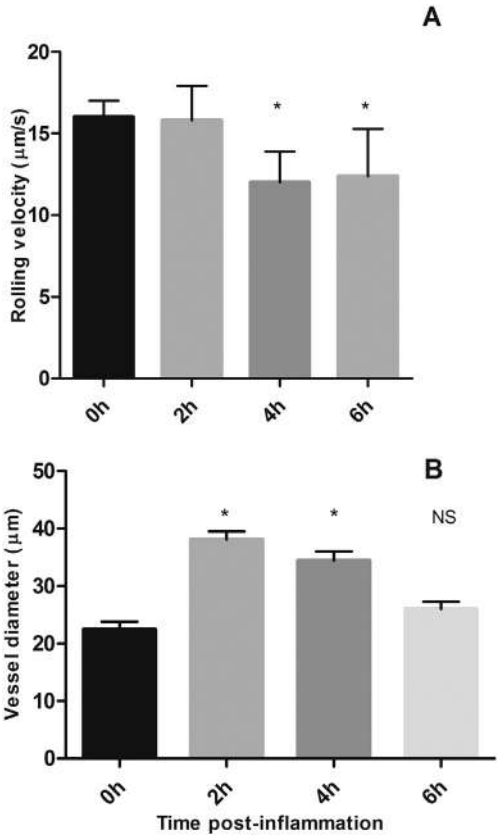

Fig. 2. (A) Rolling velocities of the neutrophils with time post-inflammation and (B) diameters of the vessels visualized by intravital microscopy at the beginning (0 h) and after 2, 4, and 6 h post-inflammation. Four hours after PAF-induced inflammation, a decrease in the rolling velocity and an increase in the mean diameter of the vessels were observed. Representative results are mean values of the data obtained from a total of ten mice (N = 10) per experimental group. Statistical significance is presented in comparison to the initial time-point (0 h) and * $p < 0.05$. Error bars depict the associated standard deviations.

that the changes observed in RBC deformability at the first time-points may be independent of the inflammatory process but have a direct effect of the i.s. injected PAF on erythrocytes. Although, the subsequent decrease of the RBC deformability observed at the remaining time-points cannot be disclosed from the inflammatory process, since

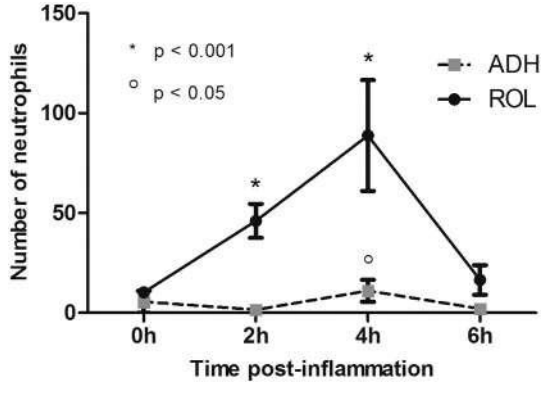

Fig. 1. The number of rolling (ROL) and adherent (ADH) neutrophils after PAF-induced inflammation was determined at the beginning (0 h) and after 2, 4 and 6 h of PAF intra-scrotal injection. After 4 h of PAF-induction of an acute inflammatory condition a statistically significant increase in the number of rolling ($p < 0.001$) and adherent ($p < 0.05$) leukocytes is observed. Representative results are mean values of the data obtained from a total of ten mice (N = 10) per experimental group. Error bars depict the associated standard deviations.

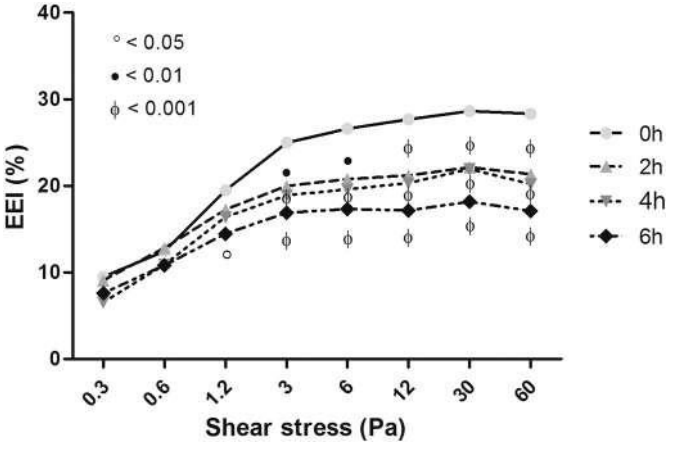

Fig. 3. Erythrocyte elongation index (EEI) expressed in percentage in the dependence of shear stress (Pa) at the beginning (0 h) and 2, 4, and 6 h post-inflammation. The deformability decreases significantly after 2, 4 and 6 h of PAF-induced acute inflammation. Statistical significance is presented in comparison to the control. Represented results are mean values of the data obtained from a total of ten mice (N = 10) per experimental group.

no more PAF was injected and other mediators of inflammation, will be release as a result of the inflammatory response. Therefore, the hemorheological changes, observed in this animal model at the level of the RBCs deformability cannot be disclosed from the inflammatory component, besides an effect of PAF on the erythrocyte membrane may occur.

As published in (Sequeira et al., 2009) the rolling process is also mediated by the forces exerted by the blood flow and in order to adhere to the endothelial vessel wall the rolling velocity of the leukocyte decreases. Lower erythrocyte deformability will correspond to a higher blood viscosity which will contribute to the slower velocity of the rolling leukocytes. This will promote the adhesion process which is essential for the inflammatory response and its resolution.

Studies by Czepiel (2014) reported that a decrease in RBCs deformability is correlated with the severity of inflammation in the case of an acute infection of the gastrointestinal tract by *Clostridium difficile*. And also there is evidence that RBC deformability is impaired in chronic venous diseases (Silva-Herdade et al., 2014). Other studies document that, in the course of an acute inflammatory response like in sepsis, pro-inflammatory cytokines activate inducible NOS (iNOS) resulting in large amounts of NO. NO has an effect on Ca^{2+}-ATPase channels which leads to an increase in intracellular Ca^{2+}, causing a decrease in RBC deformability (Korhonen et al., 2005).

In the acute inflammation model herein described Fig. 4 shows the concentration of NO efflux from RBC after 2, 4 and 6 h of PAF-induced inflammation. Although the values obtained are not statistically significant the mean value of NO efflux tend to decrease after 2 h of inflammation and to normalize to values similar to the control at 4 and 6 h of inflammatory response.

It seems that the return of NO efflux from erythrocytes precede the resolution of the inflammatory response observed after 6 h.

NO is synthesized into and released from the endothelial cells by the help of nitric oxide synthases (NOs) that convert arginine into citrulline by a process that produces NO. NO produced in the endothelial cell diffuses, to the lumen where it is captured by RBCs or into muscle cells where it induces relaxation, eliciting vasodilation. This way, NO as an inflammatory mediator seems to have both pro- and anti-inflammatory effects depending on the mechanisms, on the NO concentration and levels of reactive oxygen species and also on the physiological environment. High NO release from RBC samples was observed *ex vivo* from patients with hypoxia and inflammatory states, namely sickle cell disease, hypercholesterolemic, and hypertensive patients (Carvalho and Maria, 2006) associated with an impairment in the erythrocyte deformability.

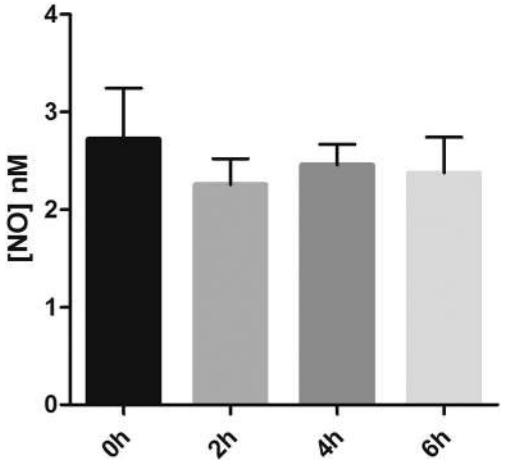

Fig. 4. Nitric oxide (NO) efflux from mice erythrocytes at the beginning and after 2, 4 and 6 h of experimentally-induced inflammation following intra-scrotal PAF injection. Representative results are mean values of the data obtained from a total of ten mice (N = 10) per experimental group. Error bars depict the associated standard deviations.

This inverse association could be a compensatory mechanism in low grade or chronic inflammation of those diseases.

Conclusions

The results herein presented describe an *in vivo* animal model of acute inflammation and demonstrate that there is a decrease in the deformability of the erythrocytes associated with the inflammatory response. A decrease in the deformability of the red blood cells will create a higher blood viscosity and consequently will promote the formation of red blood cell aggregates. These conditions will in turn facilitate the margination of the neutrophils towards the vessel wall during the inflammatory response. After 6 h of inflammation we observe a decrease in the number of rolling neutrophils and lower values for the erythrocyte deformability. This means that the hemodynamic conditions of the blood flow are being maintained although the decrease in the number of rolling neutrophils indicates a pre-resolution state in which we could expect a return to normal values for RBC deformability. Besides further studies will be necessary to confirm the pre-resolution condition after 6 h of inflammation, it is well known that the recruitment of neutrophils is followed by the monocytes that will need the same hemodynamic conditions to complete the migration process into the tissues. This way, the continuous decrease observed in the RBC deformability after 6 h of inflammation is understandable.

Therefore, the changes in the RBC deformability herein observed, in an *in vivo* animal model of inflammation, highlight the role of the hemodynamic properties of the blood in the development of the inflammatory response. *In vitro* studies (Silva-Herdade et al., 2014) have already demonstrated that deformability can be ameliorated by the effect of carbenoxolone, a pannexin-1 inhibitor, so further studies will clarify if changes in the RBC deformability will affect (or not) the progression of an acute inflammatory response. The deformability of the red blood cells, as already described, is associated with the pathology of many diseases and could be used to evaluate disease status (Santoso et al., 2015), therefore the determination of RBC deformability could be an important parameter in the study of any inflammatory response.

References

Artoli, A.M., Sequeira, A., Silva-Herdade, A.S., Saldanha, C., 2007. Leukocytes rolling and recruitment by endothelial cells: hemorheological experiments and numerical simulations. J. Biomech. 40, 3493–3502. http://dx.doi.org/10.1016/j.jbiomech.2007.05.031.

Barvitenko, N.N., Aslam, M., Filosa, J., Matteucci, E., Nikinmaa, M., Pantaleo, A., Saldanha, C., Baskurt, O.K., 2013. Tissue oxygen demand in regulation of the behavior of the cells in the vasculature. Microcirculation 20, 484–501. http://dx.doi.org/10.1111/micc.12052.

Borregaard, N., 2010. Neutrophils, from marrow to microbes. Immunity 33, 657-670. http://dx.doi.org/10.1016/j.immuni.2010.11.011.

Carvalho, F., Maria, A., 2006. The relation between the erythrocyte nitric oxide and hemorheological parameters. Clin. Hemorheol. Microcirc. 35, 341–347.

Czepiel, J., 2014. Rheological properties of erythrocytes in patients infected with *Clostridium difficile*. Postepy Hig. Med. Dosw. 68, 1397–1405.

Faust, N., Varas, F., Kelly, L.M., Heck, S., Graf, T., 2000. Insertion of enhanced green fluorescent protein into the lysozyme gene creates mice with green fluorescent granulocytes and macrophages. Blood 96, 719–726.

Fukuda, S., Yasu, T., Predescu, D.N., Schmid-Schönbein, G.W., 2000. Mechanisms for regulation of fluid shear stress response in circulating leukocytes. Circ. Res. 86, E13–E18.

Gavins, F.N.E., Chatterjee, B.E., 2004. Intravital microscopy for the study of mouse microcirculation in anti-inflammatory drug research: focus on the mesentery and cremaster preparations. J. Pharmacol. Toxicol. Methods 49, 1-14. http://dx.doi.org/10.1016/S1056-8719(03)00057-1.

Huttenlocher, A., Poznansky, M.C., 2008. Reverse leukocyte migration can be attractive or repulsive. Trends Cell Biol. 18, 298–306. http://dx.doi.org/10.1016/j.tcb.2008.04.001.

Jain, A., Munn, L.L., 2009. Determinants of leukocyte margination in rectangular microchannels. PLoS One 4, 1–8. http://dx.doi.org/10.1371/journal.pone.0007104.

Jung, U., Norman, K.E., Scharffetter-Kochanek, K., Beaudet, A.L., Ley, K., 1998. Transit time of leukocytes rolling through venules controls cytokine-induced inflammatory cell recruitment in vivo. J. Clin. Investig. 102, 1526–1533. http://dx.doi.org/10.1172/JCI119893.

Korhonen, R., Lahti, A., Kankaanranta, H., Moilanen, E., 2005. Nitric oxide production and signaling in inflammation. Curr. Drug Targets Inflamm. Allergy 4, 471–479. http://dx.doi.org/10.2174/1568010054526359.

Kubes, P., Kerfoot, S.M., 2001. Leukocyte recruitment in the microcirculation: the rolling paradigm revisited. News Physiol. Sci. 16, 76–80.

Lang, P.a., Kempe, D.S., Tanneur, V., Eisele, K., Klarl, B.a., Myssina, S., Jendrossek, V., Ishii, S., Shimizu, T., Waidmann, M., Hessler, G., Huber, S.M., Lang, F., Wieder, T., 2005. Stimulation of erythrocyte ceramide formation by platelet-activating factor. J. Cell Sci. 118, 1233–1243. http://dx.doi.org/10.1242/jcs.01730.

Lopes de Almeida, J.P., Carvalho, F.A., Silva-Herdade, A.S., Santos-Freitas, T., Saldanha, C., 2009. Redox thiol status plays a central role in the mobilization and metabolism of nitric oxide in human red blood cells. Cell Biol. Int. 33, 268–275. http://dx.doi.org/10.1016/j.cellbi.2008.11.012.

McDonald, B., Kubes, P., 2011. Cellular and molecular choreography of neutrophil recruitment to sites of sterile inflammation. J. Mol. Med. 89, 1079–1088. http://dx.doi.org/10.1007/s00109-011-0784-9.

Montrucchio, G., Alloatti, G., Camussi, G., 2000. Role of platelet-activating factor in cardiovascular pathophysiology. Physiol. Rev. 80, 1669–1699.

Pagano, M., Faggio, C., 2015. The use of erythrocyte fragility to assess xenobiotic cytotoxicity. Cell Biochem. Funct. 33, 351–355. http://dx.doi.org/10.1002/cbf.3135.

Phillipson, M., Kubes, P., 2011. The neutrophil in vascular inflammation. Nat. Med. 17, 1381–1390. http://dx.doi.org/10.1038/nm.2514.

Santoso, A.T., Deng, X., Lee, J.-H., Matthews, K., Duffy, S.P., Islamzada, E., McFaul, S.M., Myrand-Lapierre, M.-E., Ma, H., 2015. Microfluidic cell-phoresis enabling high-throughput analysis of red blood cell deformability and biophysical screening of antimalarial drugs. Lab Chip 15, 4451–4460. http://dx.doi.org/10.1039/C5LC00945F.

Sequeira, A., Artoli, A.M., Silva-Herdade, A.S., Saldanha, C., 2009. Leukocytes dynamics in microcirculation under shear-thinning blood flow. Comput. Math. Appl. 58, 1035–1044. http://dx.doi.org/10.1016/j.camwa.2009.02.003.

Silva, A.S., Saldanha, C., Martins e Silva, J., 2007. Effects of velnacrine maleate in the leukocyte-endothelial cell interactions in rat cremaster microcirculatory network. Clin. Hemorheol. Microcirc. 36, 235–246.

Silva-Herdade, A.S., Freitas, T., Almeida, J.P., Saldanha, C., 2014. Erythrocyte deformability and nitric oxide mobilization under pannexin-1 and PKC dependence. Clin. Hemorheol. Microcirc. 59, 155–162. http://dx.doi.org/10.3233/ch-141833.

Taha, Z.H., 2003. Nitric oxide measurements in biological samples. Talanta 61, 3–10. http://dx.doi.org/10.1016/S0039-9140(03)00354-0.

Tsukada, K., Sekizuka, E., Oshio, C., Minamitani, H., 2001. Direct measurement of erythrocyte deformability in diabetes mellitus with a transparent microchannel capillary model and high-speed video camera system. Microvasc. Res. 61, 231–239. http://dx.doi.org/10.1006/mvre.2001.2307.

Vitorino de Almeida, V., Silva-Herdade, A.S., Calado, Â, Saldanha, C., 2015. Fibrinogen modulates leukocyte recruitment in vivo during the acute inflammatory response. Clin. Hemorheol. Microcirc. 59, 97–106. http://dx.doi.org/10.3233/CH-121660.

Zarbock, A., Ley, K., McEver, R.P., Hidalgo, A., 2011. Leukocyte ligands for endothelial selectins: specialized glycoconjugates that mediate rolling and signaling under flow. Blood 118, 6743–6751. http://dx.doi.org/10.1182/blood-2011-07-343566.

Articles not concerned with this thesis:

- Silva-Herdade, AS, Freitas, T, Almeida, JP and Saldanha, C. (2016) Fibrinogen Signalling in Erythrocyte Nitric Oxide Mobilization in Presence of PI3-K and Adenylyl Cyclase Inhibitors, European Journal of Biomedical and Pharmaceutical Sciences 3, 28-34.

- de Almeida VV, Silva-Herdade A, Calado A, Rosário HS, Saldanha C. (2015) Fibrinogen modulates leukocyte recruitment in vivo during the acute inflammatory response. Clin Hemorheol Microcirc. 59(2): 97-106

- Silva-Herdade AS, Freitas T, Almeida JP, Saldanha C. (2015) Erythrocyte deformability and nitric oxide mobilization under pannexin-1 and PKC dependence. Clin Hemorheol Microcirc. 59(2):155-162.

- Saldanha, Carlota; Freitas, T.; Lopez de Almeida, J. P.; Silva-Herdade, AS. (2014) Korea-Australia Rheology Journal 26(2): 217-223

- Saldanha C, Silva-Herdade A (2014) The Ubiquity Nature of Acetylcholine. Clin Exp Pharmacol 4:159. doi:10.4172/2161-1459.1000159

- Saldanha C, Lopes de Almeida JP, Silva-Herdade AS. (2014) Application of a nitric oxide sensor in biomedicine. Biosensor 4(1):1-17

- de Almeida VV, Calado A, Silva-Herdade AS, Rosário HS, Saldanha C. (2014) An in vitro study on the modulation of the neutrophil adhesive behavior by soluble fibrinogen. Clin Hemorheol Microcirc. 56(1):47-56.

- Silva-Herdade, AS., Saldanha, C. (2011) Hemorheological Effects of Valsartan in L-NAME Induced Hypertension in Rats. The Open Circulation and Vascular Journal 4, 1-5.

- Saldanha, C, Lopes de Almeida, JP, Freitas, T, Oliveira, S, Silva-Herdade, AS. (2010) Erythrocyte deformability responses to shear stress under external and internal stimuli influences. Series on Biomechanics 25, 1-2, 54-60.

EUROPEAN JOURNAL OF BIOMEDICAL AND PHARMACEUTICAL SCIENCES
http://www.ejbps.com

ISSN 2349-8870
Volume: 3
Issue: 4
28-34
Year: 2016

FIBRINOGEN SIGNALLING IN ERYTHROCYTE NITRIC OXIDE MOBILIZATION IN PRESENCE OF PI3-K AND ADENYLYL CYCLASE INHIBITORS

Ana S. Silva-Herdade, Teresa Freitas, José P. Almeida and Carlota Saldanha*

Instituto de Bioquímica, Instituto de Medicina Molecular, Faculdade de Medicina da Universidade de Lisboa. Av. Prof Egas Moniz Lisboa,1649-028. Portugal.

***Author for Correspondence: Carlota Saldanha**
Instituto de Bioquímica, Instituto de Medicina Molecular, Faculdade de Medicina da Universidade de Lisboa. Av. Prof Egas Moniz Lisboa,1649-028. Portugal.

Article Received on 24/01/2016 **Article Revised on 15/02/2016** **Article Accepted on 07/03/2016**

ABSTRACT
Soluble form of fibrinogen (Fib) and the peptide 4N1K are ligands of erythrocyte membrane CD47. Fibrinogen reinforces the ability of erythrocyte to scavenger nitric oxide (NO). Hiperfibrinogenemia increased NO efflux from erythrocyte in dependence of band 3 phosphorylation which is abolished by the presence of 4N1K. Herein we study *in vitro* the effect of high fibrinogen levels, on the NO efflux from erythrocytes and on its mobilization under influence of phosphoinositide-3 kinase (PI3-K) and adenylyl cyclase (AC) inhibitors in presence of 4N1K. Erythrocyte NO efflux, peroxynitrite, nitrite, nitrate and S-nitrosoglutathione (GSNO) were determined in blood samples in presence of 4N1K, wortmannin (WORT, PI3-K inhibitor) and MDL (AC inhibitor) under high fibrinogen concentrations. 4N1K with WORT and high fibrinogen levels induce, in relation to Fib plus WORT samples no variations on the erythrocyte NO efflux, decreased peroxynitrite, increased of nitrite, nitrate and GSNO concentrations. When 4N1K is present with MDL and high fibrinogen levels show, in relation to fibrinogen plus MDL samples increased erythrocyte NO efflux and nitrite, nitrate and GSNO concentrations. In conclusion, under high Fib levels and 4N1K the erythrocytes show: preservation of NO and impaired peroxynitrite in presence of PI3K inhibition; increased efflux of NO at lower levels of cAMP resulting from adenylyl cyclase inhibition.

KEYWORDS: Nitric oxide; S-nitrosoglutathione; human erythrocyte; phosphoinositide -3 kinase; adenylyl cyclase; fibrinogen; wortmannin ; peroxynitrite.

1. INTRODUCTION
The endothelial nitric oxide (NO) liberated to the lumen of the vessel passes through the erythrocyte membrane band 3 protein and is fixed by hemoglobin molecules with generation of S-nitrosohemoglobin (SNO-Hb) (Stamler et al.1997; Huang et al. 2001). Inside erythrocytes the glutathione reacts with NO originating S-nitrosoglutathione (GSNO) (Gali et al. 2002). Also NO can react with superoxide anion forming peroxynitrite that decomposes in nitrites and nitrates (Murphy and Sies 1991; Huie and Padmaja 1993; May et al. 2000). The efflux of NO from erythrocytes occurs through a trans-nitrosylation process involving the thiol group of the band 3 protein that receives NO from SNO-Hb (Gross, 2001; Pawloski et al. 2005). We have documented that band 3 is directly involved in NO efflux and mobilization, by modulation of its phosphorylation degree (Carvalho et al 2008). Band 3 phosphorylation is promoted by tyrosine-kinases (PTK) and dephosphorylation by tyrosine-phosphatases (PTP) (Bordin et al. 2005; Brunati et al. 2005; Brunati et al. 1996). The enzymes PTP and PTK when are phosphorylated in serine/threonine residues by protein kinase C (PKC) become, respectively, into inactive and active forms (Zipser et al. 2012). The PKC enzyme activity increases in presence of adenylyl cyclase inhibitor (MDL) (Almeida et al. 2008). The cell amount of cyclic adenosine monophosphate (cAMP) decreases by the action of phospodiesterase-3 (PDE3) (Hanson et al. 2008). PDE3 enzyme activity is activated by phosphoinositide-3 kinase (PI3-K) in a directly dependent way or indirectly via protein kinase B (PKB) (Shakur et al. 2001). There is a need to clarify the participation of AC and PI3-K in the erythrocyte NO signaling pathway.

Tissues present lower partial oxygen pressure (PaO2) are prone to receive NO from erythrocytes while the opposite is observed it tissues with higher PaO2 where NO is scavenged by erythrocytes (Sonveaux et al.2007). The erythrocyte bioavailability in NO is perturbed by endogenous and exogenous stimuli (Gross 2001; Lopes de Almeida et al 2009a , b; Saldanha et al. 2013). Present in plasma there is acetylcholine that signaling the NO pathway in erythrocytes through the formation of an enzyme complex with the membrane

acetylcholinesterase, associated to Gi protein and band 3 protein (Gross 2001) Fibrinogen (Fib) is known as an acute phase protein due to its high plasma levels in inflammatory response and mediate erythrocyte aggregation (Rampling 1998; Saldanha 2013). At physiological concentrations fibrinogen modulates erythrocyte NO mobilization by decreasing NO efflux and enhancing the formation of GSNO, nitrites and nitrates (Lopes de Almeida et al 2009a). When hyperfibrinogenemia was simulated *in vitro* erythrocyte NO efflux was reinforced when band 3 was phosphorylated (Lopes de Almeida et al 2011). However both high Fib levels and acetylcholine rescue NO inside erythrocyte (Saldanha et al. 2012). Soluble Fib binds erythrocyte membrane CD47 (de Oliveira et al. 2012). Erythrocyte membrane CD47 in the complex Rh establishes contact with protein 4.2 which in turn interacts with band 3 (Dahl et al. 2004). The agonist peptide 4N1K binds to CD47 and induced mobilization of NO in the erythrocyte in dependence of the status of phosphorylation of band 3 protein in an *in vitro* model of hiperfibrinogenemia (Saldanha et al. 2014). The manipulation of human blood samples by adding fibrinogen has done before and mimics the pathological condition of hyperfibrinogenemia (Lopes de Almeida eta al. 2011; Saldanha et al. 2012). Using this same model herein, we reported the study of its effect on the erythrocyte NO efflux and mobilization under influence of PI3-K and adenylyl cyclase inhibitors in absence and presence of CD47 agonist peptide, 4N1K

2. Experimental Section

2.1 Materials and Reagents

General reagents were purchased by Sigma- Aldrich Co., Wortmannin (WORT), a PI3-K inhibitor and MDL hydrochloride (MDL) an adenylyl cyclase inhibitor were purchased from Sigma-Aldrich Co. Inhibitors were prepared as recommended in the information sheet of the products: WORT is prepared in a DMSO solution at 10−3 M concentration; MDL was prepared in distilled water at the same concentration; nitrate reductase from Aspergillus Niger, NADPH (tetra sodium salt), sodium nitrate, sodium nitrite and atropine were all from Sigma Chemical Co., St Louis, MO, USA. The Griess Reagent kit was purchased from Molecular Probes, Eugene, USA. Sodium chloride was purchased from AnalaR (UK) and chloroform and ethanol 95% from MERCK, Darmstadt, Germany.Blood samples were collected into tubes BD VacuntainerTM with Lithium heparin (17UI/mL) as an anticoagulant. This ‒in vitro‖ study was performed under the protocol established with the Portuguese Institute of Blood in Lisbon. All males donors (N=10; aged between 30 and 40 years old) were duly informed and signed their agreement. The chosen concentrations for fibrinogen were based on its physiological levels and previous studies (Sargento et al. 2005).The human fibrinogen was purchased from Sigma (Poole, UK).

2.2 Experimental model

The experimental model that we here describe was done for each blood sample taken from ten donors. So, each blood sample was divided into six aliquots of 1 mL centrifuged at 11,000rpm (Biofuge 15 Centrifuge, Heraus) during 1 min at room temperature. In 3 aliquots 60µL of plasma was replaced with the 50 µL of fibrinogen NaCL isotonic solutions pH 7.4 (30 mg/dL) plus 10 µ L of MDL or 10 µL of WORT or 10 µL of 4N1K to achieve the 10µM final concentration. The same procedure for the control sample has been performed with the difference that, 50 µL of plasma was replaced with the same volume of isotonic NaCl. From the others 2 samples, 70 µL of plasma was taken and replaced by 50 µL of Fib solution plus 10 µL of MDL plus 10 µL of 4N1K or 50 µL of Fib solution plus 10 µL of WORT plus 10 µ L of 4N1K to achieve the 10µM final concentration. Blood samples were then incubated during 15 min with slight agitation. To avoid changes on blood samples due to possible temperature fluctuations during incubation all measurements of the NO and its derivatives molecules were performed at room temperature. At the end of incubation samples were centrifuged and plasma removed for fibrinogen concentration assessment. Plasma fibrinogen concentrations were evaluated using the Fibritimer BFT* Analyser (Dade Behring, Marburg GmbH, Germany) based on the Clot technology.

2.3 Measurement of erythrocyte NO efflux, nitrite, nitrate, GSNO and peroxynitrite

Following incubation, blood samples were centrifuged and sodium chloride 0.9 % at pH 7.0 was added on to compose a hematocrit of 0.05%. The suspension was mixed by gently inversion of tubes. For amperometric NO quantification we used the amino-IV sensor (Innovative Instruments Inc. FL, USA), according to the method described previously (Carvalho et al. 2004). NO diffuses through the gas-permeable membrane tripleCOAT of the sensor probe and it is then oxidized at the working platinum electrode, resulting on an electric current. The redox current is proportional to the NO concentration outside the membrane and it was continuously monitored with a computerized inNOTM system (with a software version 1.9, Innovative Instruments Inc., Tampa, FL, USA) and connected to a computer. Calibration of the NO sensor was performed daily. For each experiment, the NO sensor was immersed vertically in the erythrocyte suspension vials and allowed to stabilize for 30 min to achieve NO basal levels. 30 µl of acetylcholine (ACh) was added to erythrocyte suspension samples in order to achieve the final concentrations of 10µM of ACh and NO. Data were recorded from constantly stirred suspensions at room temperature. The measurement of nitrite/nitrate concentration was done using the spectrophotometric Griess method as described previously (Guevara et al. 1998), after submitting the pellet of each centrifuged blood sample to haemolysis and haemoglobin precipitation. Haemolysis was induced with distilled

water and hemoglobin precipitation with a mixture of ethanol and chloroform (5v/3v).The nitrite concentrations were measured with the spectrophotometric Griess reaction, at 548 nm. For nitrate measurement, this compound was first reduced to nitrites in presence of nitrate reductase (Cook et al. 1996). For measurement of S-nitrosoglutathione (GSNO) colorimetric solutions containing a mixture of sulfanilic acid (B component of Griess reagent) and NEDD (A component of Griess reagent), consisting of 57.7 mM of sulfanilic acid and 1 mg/mL of NEDD, were dissolved in phosphate-buffered solution (PBS; pH 7.4). To constitute the 10 mM HgCl2 (Aldrich) mercury ion stock solutions were prepared in 0.136g/50mL of dimethyl sulfoxide (DMSO) (Aldrich). GSNO was diluted to the following desired concentrations :7,5 µ M; 15 µM; 30 µM; 45 µM; 60 µM; 120 µM; 240 µM; 300 µM in the colorimetric analysis solutions. Various concentrations of mercury were then added to a final concentration of 100 µM. Following gentile shaking the solution was let to stand for twenty minutes. A control spectrum was measured by spectrophotometry at 496 nm against a solution without mercury ion. 300 µl of erythrocyte suspensions were added to the reaction mixture and GSNO concentrations were obtained as described [39]. For determinations of peroxinitrite levels the erythrocyte suspensions (1mL) were incubated with 2,7-dichlorofluorescein diacetate (DCFC-DA) 15µM, in 3mL buffer (Pi 155mM, pH 7.4) during 30 min, at room temperature. Suspensions were rinsed several times and diluted in the working solution with 1.8mL of the same buffer. The pellets were rinsed and used for fluorescence measurement with a Hitachi F-300 fluorospectrophotometer (Hitachi, Japan) with excitation and emission wavelengths at 503 and 523nm, respectively. The concentration of peroxynitrite was finally calculated through a calibration graph (Possel et al. 1997).

2.4 Statistical analysis

Data are expressed as mean values ± SD. Student's paired t-tests were used to compare values between different samples of erythrocyte suspensions. Statistical analysis was conducted using the Statistical Package from the Social Sciences (SPSS; version 16.0). One-way analysis of variance and paired t-tests were applied to assess statistical significance between samples. Bonferroni post-hoc tests were conducted when appropriate. Statistical significance was set at a $p<0.05$ level.

3. RESULTS

3.1. In vitro hyperfibrinogenemia effects on erythrocyte nitric oxide efflux, S-nitrosoglutathione, peroxynitrite, nitrite and nitrate levels in presence of 4N1K and PI3-K inhibitor (WORT), Table 1.

Our results showed that in high fibrinogen concentration (510 mg/dL), the efflux of NO from erythrocyte is not changed significantly by the presence of wortmannin (WORT, PI3-K inhibitor), neither by 4N1K nor by the presence of both effectors, Table 1. Significant increased levels of GSNO were obtained in samples with Fib plus WORT plus 4N1K in relation to Fib plus WORT ($p< 0.0001$) and the control ($p< 0.001$). Regarding the sample Fib plus WORT plus 4N1K and comparing them with Fib plus WORT and with control samples significantly decreased values of peroxinitrite were verified respectively $p<0.05$ and $p< 0.001$, Table 1. In Fib plus WORT plus 4N1K samples significantly augmented values of nitrite ($p<0.001$; $p<0.0001$) and nitrate ($p<0.001$; $p<0.001$) were obtained when compared with Fib plus WORT samples and control samples, Table 1.

Table 1. Values (Mean±SD) of erythrocyte nitric oxide (NO) efflux, GSNO, peroxynitrite, nitrite and nitrate

Blood samples	NO	GSNO	Peroxinitrite	Nitrite	Nitrate
Control	1.50±0.89	8.05±0.34	199.10±46.77	7.95±0.75	8.85±0.68
Fib+MDL	1.26±0.18	8.81±0.76	196.04±55.21	9.65±0.86*	9.95±0.97 $^{\#}$
Fib+WORT	1.47±0.13	9.56±0.72*	184.71±60.67	9.40±0.71**	10.15±0.76 $^{\#}$
Fib+4N1K	1.33±0.26	10.52±0.86*	193.18±27.07	10.40±0.59*	10.70±0.74**
Fib+MDL+4NIK	1.64±0.36 $^{\partial}$	12.28±0.70$^{*, \&}$	187.71±34.45	10.90±1.06$^{*,\&}$	11.55±0.69$^{*, \&}$
Fib+WORT+4N1K	1.40±0.361	11.73±1.17$^{**, \times}$	145.30±42.99$^{\#, @}$	11.35±0.35$^{*,+}$	11.75±0.47$^{**, +}$

In relation to the control *p<0.0001; **p<0.001; # < 0.05
In relation to Fib+MDL $^{\&}$ p<0.0001; ∂ p<0.05
In relation to Fib+Wort $^{\times}$ p<0.0001; $^{@}$ p<0.05; + p<0.001

3.2 Effects of *in vitro* hyperfibrinogenemia, on erythrocyte nitric oxide efflux, S-nitrosoglutathione, peroxynitrite, nitrite and nitrate levels in presence of 4N1K and adenylyl cyclase inhibithor. Table 1.

We observed that in high fibrinogen concentration (510 mg/dL) the erythrocyte efflux of NO is increased significantly by the presence of MDL (adenylyl cyclase inhibitor) plus 4N1K ($p< 0.05$) in relation to the sample of Fib plus MDL, Table 1. However there is no variation in NO efflux when compared to the control or with Fib plus 4N1K samples.

Significantly increased values of NO derivatives molecules namely GSNO ($p< 0.0001$; $p<0.0001$), nitrite ($p< 0.0001$; $p<0.0001$), and nitrate ($p< 0.0001$; $p<0.0001$), were obtained in presence of MDL plus 4N1K under high Fib levels in relation to control or to

high Fib plus MDL blood samples, Table 1. However no variations on peroxynitrite concentrations were observed in all manipulated blood samples, Table 1.

DISCUSSION

Previously was verified that in high Fib levels and presence of 4N1K, the equilibrium existing between the phosphorylated and dephosphorylated state of band 3 inside the erythrocyte of healthy humans is maintained (Carvalho et al. 2008). Under high Fib concentrations with and without 4N1K similar profile of the NO derivatives molecules content inside the erythrocytes has been obtained in dependence of band 3 protein phosphorylation (Lopes de Almeida et al. 2011). It was observed that WORT plus 4N1K are unable to increase the band 3 protein phosphorylation that mediates the NO efflux from erythrocytes under high fibrinogen levels (Lopes de Almeida et al. 2011). In the present work we confirm that the NO efflux from erythrocyte do not change in samples under high Fib plus WORT plus 4N1K in relation to control or to Fib plus WORT, Table 1.

Peroxynitrite is a reactive nitrogen species (RNS) and an index of auto-oxidation of oxyhemoglobin (Balagopalakrishna et al.1996). In the present work the samples containing WORT plus 4N1K with high Fib concentration are able to decrease the levels of erythrocyte peroxynitrite in relation to control and to Fib plus WORT samples, Table 1. The inhibition of PI3-K by WORT prevents the activation of phosphodiesterase 3 (PDE3) and consequently there is no decrease in the levels of cAMP allowing the activation of the cAMP-dependent kinase (Jindal et al. 1996). Pyruvate kinase (PK) turns to an inactive form after phosphorylation by cAMP- protein kinase dependent (Jindal, 1980). It is expected inhibition of glycolysis and promotion of the pentose phosphate pathway with decreases of oxidative stress environment in erythrocytes. This means less expected peroxinitrite formation which is confirmed in those samples referred above namely Fib plus WORT plus 4N1K, in comparison with Fib plus WORT and with control samples (Table 1). It is known that decomposition of peroxynitrite leads to nitrite and nitrate molecules and contributes to decrease oxidation in glutathione leaving it prone to become a reservoir of NO inside erythrocytes in the form of GSNO (May 2000; Pfeiffer and Mayer 1998; Soszynski and Bartosz 1996). So, we have observed increase of nitrite and nitrate concentrations inside the erythrocyte under high Fib plus WORT plus 4N1K Table 1. We cannot exclude the possible reaction of peroxynitrite with haemoglobin generating SNOHb, which could in a reductive erythrocyte environment liberate NO to thiol group of glutathione generating GSNO and nitrate (Gladwin et al. 2002). These could explain the increased levels of GSNO and nitrate found in those samples, Table 1. Another possible explanation for GSNO levels could come from the remaining NO inside erythrocyte resulting from the slight not significantly decrease of NO efflux observed in the blood samples with high Fib, WORT and 4N1K. The NO may reduce oxyhaemoglobin to methaemoglobin (MetHb) along with the formation of nitrate instead to combine with superoxide anion (Mesquita et al 2001). This will be another explanation for the lower peroxynitrite level inside erythrocyte of samples under high Fib plus WORT plus 4N1K.

Beyond the contribution of PI3-K inhibition by WORT when associated to 4N1K and high Fib levels in erythrocytes protection from RNS effects, it was published that when WORT is present in blood samples induce decreased erythrocyte aggregation without modification on erythrocyte deformability (Saldanha et al 2007). The inhibitor of adenylyl cyclase MDL do not induces variations in the erythrocyte deformability (Saldanha et al 2007) and promotes decrease in cAMP levels which impair the enzyme activity of the cAMP kinase dependent (Almeida et al. 2008). Consequently pyruvate kinase it will be in the dephosphorylated active state allowing glycolysis to function. For that the glycolytic enzymes are release from band 3 protein which becomes able to be phosphorylated. MDL activates PKC which will inhibit PTK and activate PTP by phosphorylation (Carvalho et al. 2008; Almeida et al. 2008). Probably the band 3 phosphorylation do not result only from the enzymatic action of PTK (p72 ^{syk}) but either by p59/61 ^{hck} or by casein kinase I (Carvalho et al. 2008; Wang et al. 1997). Another possibility is through PKC itself that when activated moves from cytoplasm to membrane coupled receptor protein G promoting phosphorylation of band 3 (Escribá et al.2003). So, the presence of 4N1K and Fib (both ligands of CD47 in erythrocyte of membrane) stimulate NO efflux from erythrocytes under MDL (or lower levels of cAMP) may be through the band 3 phosphorylation. All together, these stimuli contribute to the active conformation state of AChE necessary to the signaling pathway coupled with band 3 protein phosphorylation (Carvalho et al. 2009; Teixeira et al. 2015). SNOHb is a reservoir of NO inside erythrocyte and responsible for the NO mobilization inside the erythrocyte, as well as, for its efflux (Carvalho et al 2008; Carvalho et al 2004). The NO could be transferred from SNOHb to glutathione originate GSNO and nitrate or react with anion superoxide forming peroxynitrite (Carvalho et al 2004). In the present study the first reaction seems to occur and originate higher GSNO concentrations as obtained in samples with high Fib plus MDL plus 4 N1K in relation to control and also to Fib plus MDL. Any significant changes of peroxynitrite levels were observed in all samples in relation to the control or between each other, beside their lower levels. Otherwise, NO could also reduce oxyhaemoglobin to methaemoglobin along with the formation of nitrate (Mesquita et al. 2001). Increased nitrate concentrations were obtained. Besides the absence of measurement of MetHb in this work, it was expect no variation in MetHb concentration due the presence of haemoglobin reductase coupled with the NADH produced in the glycolytic pathway (Inal and

Egüz 2004). In the previous work no changes in MetHb concentrations were obtained in presence of each enzyme inhibitors WORT and MDL respectively of PI3K and AC (Saldanha et al 2007).

4. CONCLUSIONS

In conclusion the inhibition of PI3-K enzyme activity (by WORT) when associated to 4N1K and high Fib levels, in erythrocytes, unchanged the NO efflux and contribute to lower the peroxynitrite concentration which protect the erythrocytes from the RNS effects avoiding oxidation of glutathione and promoting inactivation of AChE (Soszynski and Bartosz 1996). The inactive state of the enzyme contributes to the unchanged normal values of NO efflux from erythrocytes (Carvalho et al 2008; Teixeira et al 2015). Also the inhibition of PI3-K became unable to activate PDE3 leaving the cAMP levels dependent of PKB. However the lower levels of cAMP provoked by AC inhibition in presence of the 4N1K and Fib (in high concentration) generates proper band 3 protein conditions to transfer to outside increased levels of NO. Three major messages were taken from the present work under high Fib concentration and 4N1K associated with the erythrocyte NO availability based on signaling pathway: dependence on PI3-K and adenylyl cyclase enzymes activity; lower values of cAMP promote increased efflux of NO from erythrocytes and left unchanged peroxynitrite levels; direct inhibition of PD3 by PI3K induce unchanged efflux of NO from erythrocytes and decreased peroxynitrite concentration lowering RNS.

ACKNOWLEDGMENTS

This study was supported by grants from the FCT—Fundação para a Ciência e a Tecnologia (project reference PTDC/SAU-OSM/73449/2006). The authors also thank Emília Alves for all the help with the typewriting.

Author Contributions

CS conceived, designed and managed the project; MTS performed the assays; ASH leads the experimental work and performed statistical analysis : JPA performed assays.

Conflicts of Interest

The authors declare no conflict of interest.

REFERENCES

1. Stamler, J.; Jia, L.; Eu ,J,:P.; McMahon ,T,J.; Demchenko ,J.; Bonaventura, C.; Gernert, K.; Piantadosi, C.;A. Blood flow regulation by S-nitrosohemoglobin in the physiological oxygen gradient. *Science.*, 1997; *276:* 2034- 47.
2. Huang, K.T., Han, T.H. Hyduke, D.R.; Vaughn, M.W,.;Van Herle ,H.; Hein, T.W.; Zhang, C.; Kuo, L.; Liao, J.;C. Modulation of nitric oxide bioavailability by erythrocytes. *Proc Natl Acad Sci U S A.*, 2001; *98*: 11771-11776.
3. Galli, F., R.; Rossi, P.;D.; Simplicio, A.; Floridi, Canestrari, F. Protein thiols and glutathione influence the nitric oxide-dependent regulation of the red blood cell metabolism. *Nitric Oxide.*, 2002; *6*: 186-199.
4. Murphy, M.: Sies, H. Reversible conversion of nitroxyl anion to nitric oxide by superoxide dismutase. *Proc. Natl. Acad. Sci.* USA., 1991; *88*: 10860-10864.
5. Huie, R.; Padmaja S. The reaction of NO with superoxide. *Free Radic. Res. Commun*. 1993, *18*, 195 -199.
6. May, J.M., Qu Z.; C.; Xia L.; Cobb, C.;E. Nitrite uptake and metabolism and oxidant stress in human erythrocytes. *Am. J. Physiol.Cell Physiol*., 2000; *279*: C1946-C1954.
7. Gross, S.;S. Target delivery of nitric oxide. *Nature.*, 2001; *409*: 577-588.
8. Pawloski, R.; Hess, D.;T.; Stamler, J.;S. Impaired vasodilation by red blood cells in sickle cell disease. *Proc. Natl. Acad.Sci.USA.*, 2005; *102*: 2531-2536.
9. Carvalho, F.;A.; Almeida, J.P.; Fernandes, I.;O.; Freitas-Santos, T.; Saldanha ,C. Non-neuronal cholinergic system and signal transduction pathways mediated by band 3 in red blood cells. *Clin Hemorheol Microcirc*., 2008; *40*: 207-227.
10. Bordin, L.; Ion-Popa F.; Brunati, A.;M.; Clari G.; Low, P.;S. Effector-induced Syk-mediated phosphorylation in human erythrocytes. *Biochim. Biophys. Acta.*, 2005; *1745*: 20-28.
11. Brunati, A.;M.; Bordin L.; Clari, G.; James, P.; Quadroni, M.; Baritono, E.;Pinna L.;A.; Donella-Deana, A. Sequential phosphorylation of protein band 3 by Syk and Lyn tyrosine kinases in intact human erythrocytes: identification of primary and secondary phosphorylation sites, *Blood.*, 2000; *96*: 1550-1557.
12. Brunati, A.;M.; Bordin L.; Clari, G.; Moret, V. The Lyn-catalyzed Tyr phosphorylation of the transmembrane band-3 protein of human erythrocytes. *Eur. J. Biochem.*, 1996; *240*: 394-399.
13. Zipser, Y.; Piedade, A.; Barbul, A.; Korenstein, R.; Kosower, N.; S. Ca+ promotes erythrocyte band 3 tyrosine phosphorylation via dissociation of phosphotyrosine phosphatase from band 3. *Biochem J.*, 2002; *368*: 137-144.
14. Almeida, J.P.; Carvalho, F.A.; Martins-Silva, J.; Saldanha, C. The modulation of cyclic nucleotide levels and PKC activity by acetylcholinesterase effectors in human erythrocytes. *Actas Bioquímica.*, 2008; *9*: 111-114.
15. Hanson ,M.S.; Stephenson, A.H.; Bowles, E.A.; Sridharan. M.; Adderley, S.; Sprague, R.; S. Phosphodiesterase 3 is present in rabbit and human erythrocytes and its inhibition potentiates iloprost-induced increases in cAMP. *Am J Physiol Heart Circ Physiol*., 2008; *295*: H786–H793.
16. Shakur, Y.; Holst, L.; S.; Landstrom, T. R.; Movsesian, M.; Degerman, E.; Manganiello ,V. Regulation and function of the cyclic nucleotide

phosphodiesterase (PDE3) gene family. *Prog Nucleic Acid Res Mol Biol.,* 2001; *66*: 241–277.
17. Sonveaux, P.; Lobysheva, I.;I.; Feron O.; McMahon, T.;J. Transport and peripheral bioactivities of nitrogen oxides carried by red blood cell hemoglobin: role in oxygen delivery. *Physiology.*, 2007; *22:* 97-112.
18. Lopes de Almeida, J.;P.; Freitas-Santos, T.; Saldanha C. Fibrinogen-dependent signalling in microvascular erythrocyte function: Implications on nitric oxide efflux. *J Memb Biol*., 2009; *231*: 47-53.
19. Lopes de Almeida, J.;P.; Carvalho, F.;A.; Silva-Herdade, A.;S.; Santos-Freitas, T.; Saldanha C. Redox thiol status plays a central role in the mobilization and metabolism of nitric oxide in human red blood cells. *Cell Biol Int.,* 2009; *33*: 268-275.
20. Saldanha, C.; Teixeira, P.; Santos-Freitas, T.; Napoleão, P. Timolol modulates erythrocyte nitric oxide bioavailability. *J Clin Exp Opthalmol* . 2013; *4*: 285.
21. Rampling, M.;W. *Clin. Hemorheol. Microcirc*., 1998; 19: 129-32.
22. Saldanha C. Fibrinogen interaction with the red blood cell membrane. *Clin Hemorheol Microcirc*., 2013; *53*: 39-44.
23. Lopes de Almeida, J.;P.; Freitas-Santos, T.; Saldanha C. Evidence that the degree of band 3 phosphorylation modulates human nitric oxide efflux-in vitro model of hyperfibrinogenemia. *Clin Hemorheol Microc*., 2011; *49*: 407-416.
24. Saldanha, C.; Freitas, T.; Almeida J.; P. Fibrinogen effects on erythrocyte nitric oxide mobilization in presence of acetylcholine. *Life Sci*., 2012; *91*: 1017-1022.
25. de Oliveira, S.; Vitorino de Almeida, V.; Calado, A.; Rosário, H.;S.; Saldanha, C. Integrin-associated protein (CD47) is a putative mediator for soluble fibrinogen interaction with human red blood cells membrane. *Biochim Biophys Acta.* 2012; *1818*: 481-490.
26. Dahl, K.; Parthasarathy, N.; R,; Westhoff, M.; Layton, D.;M.; Discher, D.;E. 2004, *Blood 1*03, 1131-1136.
27. Saldanha, C.; Freitas, T.; Lopes de Almeida J.;P.; Silva-Herdade A. Signal transduction pathways in erythrocyte nitric oxide metabolism under high fibrinogen levels. *KARJ*., 2014; *26*: 217-223.
28. Pfeiffer, S., Mayer, B. Lack of tyrosine nitration by peroxynitrite generated at physiological pH. *J. Biol. Chem*., 1998; *273*: 27280–27285.
29. Soszynski, M,; Bartosz .G. Effect of peroxynitrite on erythrocytes. *Bioch Bioph Acta.* 1996; *1291*: 107-114.
30. Balagopalakrishna, C.; Manoharan, P.;T.; Abugo, O.;O.; Rifkind, J,;M. Production of superoxide from hemoglobin-bound oxygen under hypoxic conditions. Biochemestry., 1996; *35*: 6393-6398.
31. Jindal, H.; K.; Ai, Z.; Gascard P.; Horton, C.; Cohen, C.; M. Specific Loss of Protein Kinase Activities in Senescent Erythrocytes. Blood., 1996; *88*: 1479-1487.
32. Kiener, P.;A.; Westhead, E.;W. Dephosphorylation and reactivation of phosphorylated pyruvate kinase by a cytosolic phosphoprotein phosphatases from human erythrocytes. *Biochem Biophys Res Comm.*, 1980; *96*: 551-557.
33. Gladwin, M.; T.; Wang, X.; Reiter, C.; D. SNitrosohemoglobin is unstable in the reductive erythrocyte environment and lacks O2/NO-linked allosteric function. *J. Biol. Chem*., 2002; *277*: 27818–27828.
34. Mesquita, R.; Pires, I.; Saldanha, C. Martins-Silva, J. Effects of acetylcholine and spermineNONOate on erythrocyte hemorheologic and oxygen carrying properties. *Clin.Hemorheol. Microcirc.,* 2001; *25*: 153–163.
35. Saldanha, C.; Silva, A.;S.; Gonçalves, S.; Martins-Silva, J. Modulation of erythrocyte hemorheological properties by band 3 phosphorylation and dephosphorylation. *Clin Hemorheol Microcir*., 2007; *36*: 183-194.
36. Wang, C., C; Tao, M.; Wei, T.; Low, P.; S. Identification of the major casein kinase I phosphorylation sites on erythrocyte band 3. *Blood* ., 1999; *89:* 3019-3024.
37. Escribá, P.; V.; Sanchez-Dominguez, J.; M.; Alemany, R.; Perona, J.; S.; Ruiz- Gutiérrz, V.Alterations of lipids. G protein, and PKC in Cell membranes of elderly hypertensives. Hypertension, 2003; *41*: 176-182.
38. Carvalho, F.; A.; Almeida, J.; P.; Fernandes, I.;O.; Freitas-Santos, T.; Saldanha C. Modulation of erythrocyte acetylcholinesterase activity and its association with G Protein Band 3 interactions. *J Membr Biol*., 2009; *228*: 89-97
39. Teixeira, P.; Duro, N.; Napoleão, P.; Saldanha C. Acetylcholinesterase Conformational States Influence Nitric Oxide Mobilization in the Erythrocyte. *J Membr Biol*. 2015; *248*: 349-354.
40. Carvalho, F.;A.; Mesquita R.; Martins-Silva J.; Saldanha, C. Acetylcholine and choline effects on erythrocyte nitrite and nitrate levels, J. Appl. Toxicol., 2004; *24*: 419–427.
41. Inal, M.;E.; Egüz, A.;M. The effects of isosorbide dinitrate on methemoglobin reductase enzyme activity and antioxidant states. Cell Biochem. Funct., 2004; *22*: 129–133.
42. Sargento, L.; Saldanha, C.; Monteiro, J.; Perdigão, C.; Silva, J.M. Long-term prognostic value of protein C activity, erythrocyte aggregation and membrane fluidity in transmural myocardial infarction. Thromb. Haemost . 2005, *94*, 380-388.
43. Carvalho, F.A.; Martins-Silva, J.; Saldanha, C. Amperometric measurements of nitric oxide in erythrocytes. Biosens Bioelectron., 2004; *20:* 505-508.
44. Guevara, I.; Iwanejko, J.; Dembińska-Kieć, A.; Pankiewicz, J.; Wanat, A.; Anna, P.; Gołabek, I.; Bartuś, S.; Malczewska-Malec, M.; Szczudlik, A.

Determination of nitrite/nitrate in human biological material by the simple Griess reaction. Clin Chim Acta., 1998; *274:* 177-188.

45. Cook, J.; A.; Kim, S.;Y.; Teague, D.; Krishna, M. C.; Pacelli, R.; Mitchell, J.B.; Vodovotz, Y.; Nims, R.; W.; Christodoulou, D.; Miles, A.M.; Grisham, M.B.; Wink, D.A. Convenient colorimetric and fluorometric assays for S-nitrosothiols. *Anal Biochem.*, 1996; *238*: 150-158.
46. Possel, H.; Noack, H.; Augustin, W.; Keilhoff, G.; Wolf, G. 2,7-dichlorofluorescein diacetate as a fluorescent marker for peroxinitrite formation. FEBS Letters., 1997; *416:* 175-178.

Clinical Hemorheology and Microcirculation 59 (2015) 97–106
DOI 10.3233/CH-121660
IOS Press

Fibrinogen modulates leukocyte recruitment *in vivo* during the acute inflammatory response

V. Vitorino de Almeida*, A. Silva-Herdade, A. Calado, H.S. Rosário and C. Saldanha
Unidade de Biologia Microvascular e Inflamação, Instituto de Medicina Molecular, Instituto de Bioqu´ımica, Faculdade de Medicina, Universidade de Lisboa, Portugal

Abstract. Besides playing an important role in blood hemostases, fibrinogen also regulates leukocyte function in inflammation. Our previous *in vitro* studies showed that the adhesive behaviour of the neutrophil is modulated by soluble fibrinogen when present at a physiological concentration. This led us to propose that this plasma glycoprotein might further influence leukocyte recruitment *in vivo* and thus contribute to the inflammatory response.

To address this *in vivo*, leukocyte recruitment was here investigated under acute inflammatory conditions in the absence of soluble fibrinogen in the blood circulation. For such, intravital microscopy on mesentery post-capillary venules was performed on homozygous fibrinogen a chain-deficient mice (($a^{-/-}$) mice). Acute inflammatory states were induced by perfusing platelet activating factor (PAF) over the exposed tissue. As control animals, two groups of mice expressing soluble fibrinogen in circulation were used, namely, C57BL/6 wild type animals and heterozygous fibrinogen a chain-deficient mice (($a^{+/-}$) mice).

Under acute inflammatory conditions, an abnormal pattern of recruitment was observed for leukocytes in homozygous ($a^{-/-}$) mice in comparison to both control groups. In fact, the former exhibited a significantly decreased number of rolling leukocytes that nevertheless, migrated with increased rolling velocities when compared to leukocytes from control animals. Consistently, homozygous mice further displayed a diminished number of adherent leukocytes than the other groups. Altogether our observations led us to conclude that leukocyte recruitment in homozygous ($a^{-/-}$) mice is compromised what strongly suggests a role for soluble fibrinogen in leukocyte recruitment in inflammation.

Keywords: Neutrophil recruitment, fibrinogen, intravital microscopy, Inflammation

1. Introduction

Acute inflammation constitutes an essential part of the host response to eradicate the agent of lesion or infection. This response importantly requires the migration of specific leukocyte populations from the blood circulation towards the inflamed area. Leukocyte recruitment constitutes a complex cellular process by which leukocytes are first recruited to the endothelial vascular wall of postcapillary venules across which they further extravasate into the interstitial tissue. It is mediated via cell-cell interactions between the leukocyte and the endothelium and occurs through a cascade of multiple step, namely: “tethering”, rolling, slow rolling, arrest, post-adhesion strengthening, crawling, and paracellular or transcellular transmigration [2, 9].

*Corresponding author: V. Vitorino de Almeida, Unidade de Biologia Microvascular e Inflamação, Instituto de Medicina Molecular, Instituto de Bioqu´ımica, Faculdade de Medicina, Universidade de Lisboa, Portugal. Tel.: +351 217 999 479; Fax: +351 217 999 477; E-mail: vandaalmeida@fm.ul.pt.

Throughout these distinct steps, a myriad of specific factors is sequentially involved. Among these, several adhesion molecules expressed on the cell surface of leukocytes and endothelial cells, such as integrins and selectins, have been shown to be central for leukocyte recruitment. This is the case of members of the β2 integrin family, such as $\alpha_L\beta_2$ and $\alpha_M\beta_2$ (also known as Mac-1 or CD11b/CD18), that have been shown to cooperatively contribute for the firm adhesion of leukocytes to the vessel wall [5]. For such, β2 integrins are required to bind to members of the immunoglobulin superfamily expressed on the surface of endothelial cells, such as endothelial intercellular adhesion molecule-1 (ICAM-1) and vascular cell adhesion molecule-1 (VCAM-1) [1]. In order to control for their function in leukocyte recruitment, circulating leukocytes maintain their integrin receptors in a low affinity and non-adhesive state under steady state conditions. But in response to local inflammatory stimuli, integrins are rapidly activated to bind specific ligands [6, 13–15, 18]. Besides ICAM-1, the $\alpha_M\beta_2$ integrin is further capable of binding a remarkable assortment of seemingly unrelated ligands, including the complement C3 derivative, platelet membrane glycoprotein GP1bα and importantly, immobilized fibrinogen [18].

Fibrinogen is a large multidomain plasma glycoprotein that is normally expressed as a dimer of α, β and μ polypeptide chains. This protein is a major player in the coagulation process by polymerizing into the major protein component of blood clots, fibrin [15]. As an acute phase protein, fibrinogen is also involved in other biological responses, such as in inflammation [13]. For this, it requires its recognition by a variety of integrin and non-integrin receptors on multiple cell types. Via these interactions, it can even serve as an intercellular bridging molecule. In inflammation, fibrinogen has been shown to target cellular mediators central to this response, such as neutrophils and endothelial cells [18]. In particular and as a ligand for neutrophil Mac-1, fibrinogen has been shown to play a role in neutrophil signalling by modulating: the generation of second messengers, the production of oxygen free radicals and cell adhesion under inflammatory conditions. Overall, these findings clearly illustrate that leukocyte-fibrinogen interaction can alter leukocyte function and thus can lead to changes in cell migration [5].

Accordingly, our previous studies showed that soluble fibrinogen when present at a physiological concentration (300 mg/dL) modulated the adhesive behaviour of neutrophils *in vitro* [6, 19]. In flow chamber assays, fibrinogen significantly increased the velocity of neutrophils rolling on activated endothelial monolayers without interfering with their total number. Consistently, the capacity of fibrinogen-treated neutrophils to adhere to this endothelial bedding was significantly diminished. These data importantly suggest to us that soluble fibrinogen may modulate leukocyte recruitment towards the vascular wall and thus further influence the inflammatory response [14, 20]. In this respect, fibrinogen may actually act as a non-diffusible cue for leukocyte targeting, for instance through its deposition in the form of a provisional fibrin matrix, an event due to occur at virtually any site of overt tissue damage.

To address the role of fibrinogen in leukocyte recruitment, we decided here to investigate what effects may be imposed onto the recruitment of leukocytes in inflammation by the absolute absence of fibrinogen in the blood circulation. For such, we employed a mice model bearing a disrupted fibrinogen α chain gene. In both neonatal and adult homozygous fibrinogen α chain-deficient mice (referred throughout this study as homozygous ($\alpha^{-/-}$) mice), all the three distinct fibrinogen chain components (α, β and y) are immunologically undetectable in the circulation. Accordingly, their blood samples fail either to clot or support platelet aggregation *in vitro* [4, 16]. With these mice, we made here use of an intravital microscopy approach to inspect the mesentery microcirculation. Such approach has been used extensively in the past to evaluate leukocyte trafficking (rolling velocities, leukocyte flux, adhesion, and transmigration) after exposure to an inflammatory stimuli, as it provides a direct visual observation of leukocytes moving, tether to and roll along the vessel wall before adhering at the site of inflammation [3, 7]. In this study, we

were able to show that the lack of circulating soluble fibrinogen interferes with the pattern of leukocyte recruitment in inflammation.

2. Materials and methods

2.1. Mice and reagents

Fibrinogen a chain-deficient mice were kindly provided by Stephen Smiley (Trudeau Institute). In order to screen for homozygous and heterozygous fibrinogen a chain-deficient mice, all animals were genotyped by PCR prior to their use in this study. For PCR genotyping, we made use of the following oligonucleotide primers presented from the 5′ to the 3′ ends: mFGAx1F: GCTTCAGCTCCAGTTCTC-CTCATGAGCCAT; mFGAiIR: TGCTGGATCAATCCCCAGCAACCGTGAGAG and HPRTx1R: TATTACCAGTGAATCTTTGTCAGCAG. The experimental control group of wild-type (WT) mice referred below were age-matched C57BL/6 mice purchased from Charles River.

All animal were housed in specific pathogen-free (SPF) animal facilities, according to the FELASA recommendation, at Instituto de Medicina Molecular (IMM). They were maintained on a low-fat chow pellet diet with tap water ad libitum using a 12 h light/dark cycle. All animals used were euthanized with an intraperitoneal injection of an overdose of sodium pentobarbital (Eutasil 20%, Ceva, Sante Animale) at the end of the experiment or when any signs of pain or distress were observed. The experimental protocol was previously analysed and approved by the competent governmental institution (DGV-Direcção Geral de Veterinaria).

Where not referred, chemicals were purchased from Sigma-Aldrich.

2.2. Animal preparation and surgery

Mice were anesthetized with an intraperitoneal (i.p.) injection of a cocktail containing ketamine hydrochloride 50 mg/mL (Ketalar, Pfizer), Xylazine hydrochloride 20 mg/mL (Rompun 2%, Bayer) and a saline solution of 0,9% sodium chloride. In order to maintain body temperature, mice were laid on a heating pad kept at 37◦C during surgery. This consisted in performing an abdominal midline incision and subsequently exposing the mesentery into the observation platform.

2.3. Intravital microscopy

After surgery, the mesentery was prepared for intravital microscopy for which a schematic representation is depicted in Fig. 1. Throughout tissue exteriorization and the remainder of the experiment, the mesentery was superfused with a thermocontrolled (37◦C) Krebs-Henseleit buffered saline solution (132,0 mM NaCl; 2,2 mM $NaHCO_3$; 4,7 mM KCl; 2,0 mM $CaCl_2$ and 1,2 mM $MgCl_2$) equilibrated with 5% CO_2 in N_2 (Air Liquide). Upon exteriorization of the mesentery, the mouse was transferred to the stage of a Zeiss LSM 5 Live *confocal line-scanning microscope* (Carl Zeiss MicroImaging). Microscopic observations were performed with a saline immersion objective (Objective W Plan-Apochromat 20x/1,0) [11].

Under normal conditions, tissue observation immediately following exteriorization of the mesentery revealed an initial increase of the numbers of rolling and adherent leukocytes that declined to new steady state levels after 10 minutes of stabilization. These levels were further considered as our experimental baselines as thereafter, leukocyte adhesion, rolling and rolling velocities in each individual were constant

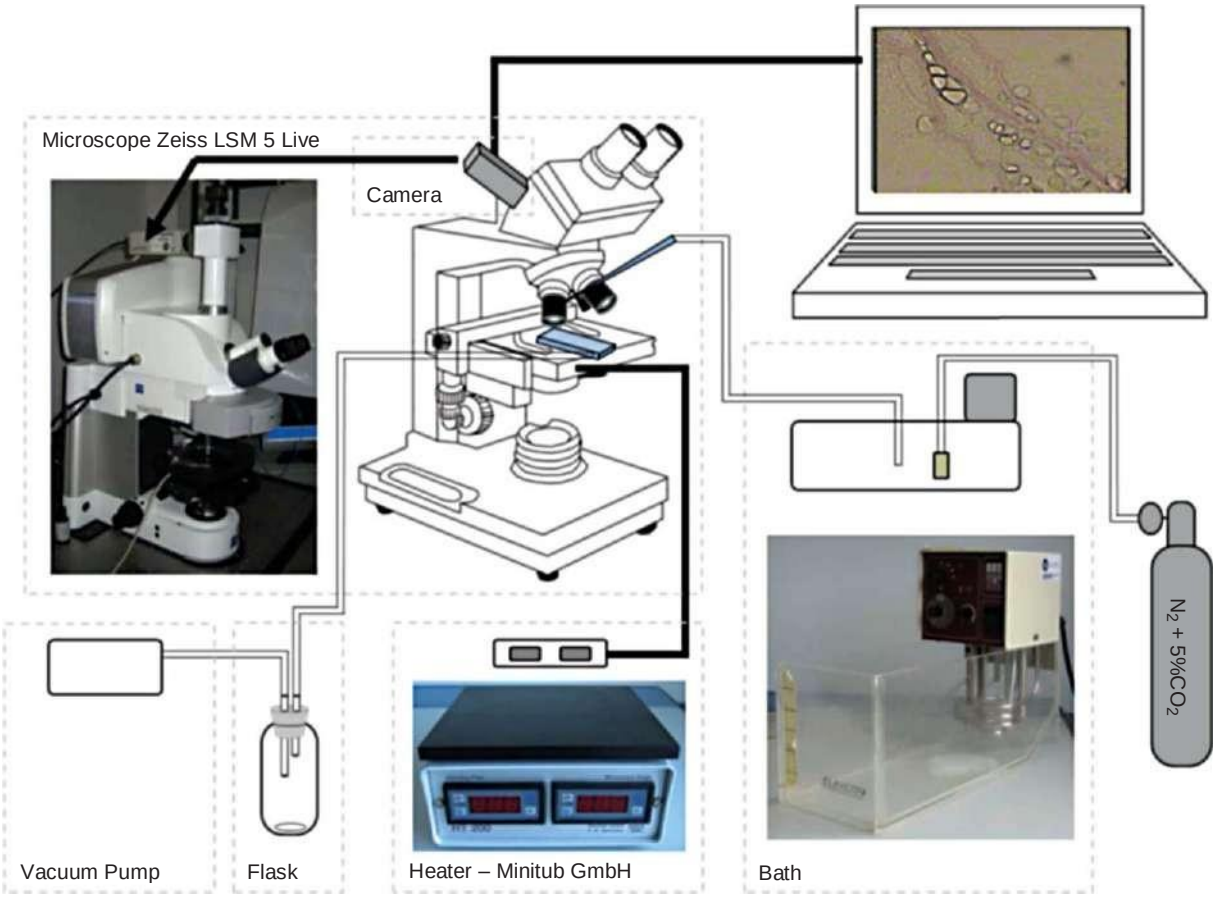

Fig. 1. Schematic representation of the assembly of the intravital microscopy experiment.

through all the time of acquisition under normal conditions. As such, video acquisition was routinely initiated 10 minutes after exteriorization of the mesentery and performed for a total time of acquisition of 30 minutes for all animals assayed.

Three distinct experimental groups of mice were employed: wild-type C57BL/6 mice (thereafter referred as WT or wild-type); heterozygous fibrinogen a chain-deficient mice (referred throughout this study as heterozygous ($a^{+/-}$) mice) and homozygous fibrinogen a chain-deficient mice (homozygous ($a^{-/-}$) mice). On the other hand, for each group two experimental conditions were assayed: a normal condition and acute inflammatory condition, locally elicited by supplemeting the superfusion saline solution with 10^{-2}M PAF (CalBiochem) 10 min after exteriorization. In each group in each experimental condition, a total of six mice were assayed ($n = 6$).

Acquired video sequences were further analysed with ImagePro-Plus software (Media Cybernetics) to quantify: (i) the number of rolling leukocytes (defined as the number of leukocytes moving at a low-velocity with a high-variance translation of 100μm) as well as their rolling velocities (calculated by $v = d/t$, where d stands for the displacement of the leukocyte over a period of time, t) and (ii) the number of adherent leukocytes (defined as the total number of leukocytes bound to the vascular wall per unit area for at least 30 sec) [8, 17]. These leukocyte recruitment parameters were determined at 15 min after

image acquisition started. For this analysis, leukocytes were manually tagged and their movements on the post-capillary venules monitored.

2.4. Statistical analysis

For each experimental group in a given experimental condition, data were obtained from six independent experiments and expressed as mean values ± standard error deviation (SD). Student´s *t* test was used to determine the significance of differences between samples means. Statistical analysis was performed using Origin Pro8.

3. Results

To further investigate this *in vivo*, we addressed here whether the absence of soluble fibrinogen in the blood circulation could interfere with the normal leukocyte recruitment pattern observed under acute inflammatory processes.

For such, leukocyte recruitment was analysed by using an intravital microscopy approach for the visualization of the mesenteric microcirculation. Here, we made use of a mouse model harbouring a disrupted fibrinogen α chain gene, for which homozygous animals have been shown to express no fibrinogen in the blood circulation [4]. Homozygous mice ($\alpha^{-/-}$) were here assayed in parallel with two groups of animals possessing soluble fibrinogen in their blood circulation, namely wild-type animals as well as in heterozygous ($\alpha^{+/-}$) mice. All these three experimental groups were studied under both normal and acute inflammatory conditions. In order to simulate locally an acute inflammatory environment, the mesentery tissue perfusion was performed in the presence of the platelet activating factor (PAF), a known promoter of neutrophil activation and adhesion [10, 12]. Image acquisition was initiated 10 minutes after the exteriorization of the mesentery from the animal body and performed for a total time of 30 minutes for all animals assayed. The acquired data was further analyzed so as to determine three distinct recruitment parameters, namely: the number of leukocytes rolling on the vascular endothelium for which results are presented in Table 1 and Fig. 2; their rolling velocities presented in Table 1 and graphically depicted in Fig. 3 and the number of leukocytes adhering to vascular wall, for which results are shown in table 1 and Fig. 4. These leukocyte recruitment parameters were determined at 15 min after image acquisition started and 25 min after mesentery exteriorization.

Our first aim in this study was to establish whether heterozygous ($\alpha^{+/-}$) mice would show a similar leukocyte recruitment pattern to that observed in wild type animals. The obtained results depicted in Figs. 2 to 4 showed that under both experimental conditions, there was no significant difference for the several leukocyte recruitment parameters determined between these two experimental groups. In both groups by comparing acute inflammatory conditions to normal conditions, we observed as expected, an increase in the number of rolling leukocytes and in the number of adherent leukocytes and a reduction of leukocyte rolling. This led us to conclude that leukocytes from both animal groups displayed identical recruitment behaviour.

Leukocyte recruitment was further addressed in the absence of any circulating fibrinogen in the homozygous ($\alpha^{-/-}$) mice. Under inflammatory conditions, these mice displayed a slightly reduced number of rolling leukocytes when compared to normal as depicted in Fig. 2 and Table 1. Despite the fact that the observed difference is not significant, this result is unexpected taking into account the data collected for the other two experimental groups. In comparison to these control groups, we further observed that

Table 1

Leukocyte recruitment parameters determined under normal conditions as well as under acute inflammatory conditions. Three experimental groups were used namely, wild-type mice (referred here as wild-type); heterozygous $a^{+/-}$ mice (referred here as Heterozygous) and homozygous $a^{-/-}$ animals (referred here as Homozygous). Acute inflammatory conditions were elicited via mesentery perfusion with a saline solution supplemented with PAF (this conditions is here designated as PAF) and under normal conditions for which tissue perfusion was performed in the absence of PAF (condition used when no PAF treatment is stated). For each condition in each experimental group, six assays were performed ($N = 6$). Results are presented as mean values with the associated standard error deviations

	Number of rolling neutrophils	Number of adherent neutrophils	Rolling Velocities (μm/s)
Wild-type	7 ± 1,6	2 ± 0,4	16 ± 1,2
Wild-type + PAF	22 ± 2,8	8 ± 0,6	6,8 ± 2,4
Heterozygous	7 ± 1,2	2 ± 0,3	13 ± 1,1
Heterozygous + PAF	19 ± 3,4	9 ± 0,2	8,6 ± 0,9
Heterozygous	10 ± 1,3	3 ± 0,4	18 ± 0,6
Heterozygous + PAF	8 ± 1,6	4 ± 0,3	14 ± 1,1

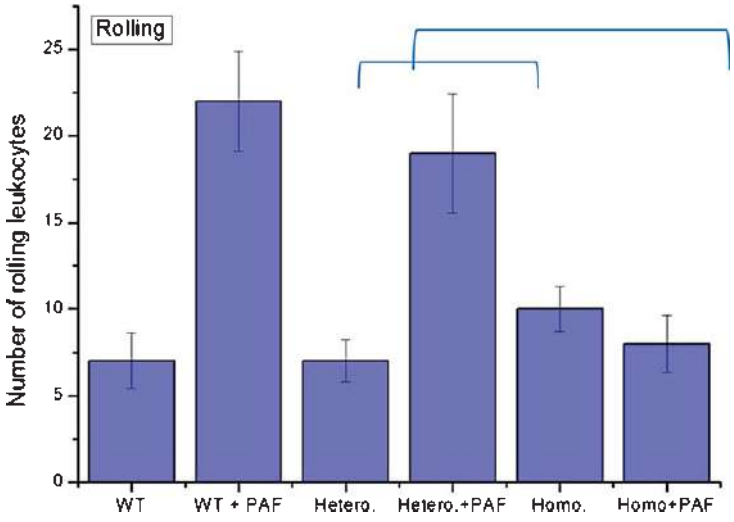

Fig. 2. These leukocyte recruitment parameters were determined at 15 min after image acquisition started. Homozygous ($a^{-/-}$) mice displayed a reduced number of rolling leukocytes under acute inflammatory conditions when compared to either wild-type animals and heterozygous ($a^{+/-}$) mice. This differences were statistically significant ($p < 0,05$). In both control groups, acute inflammatory conditions induced an increase of the number of rolling leukocytes when compared to normal conditions. Paradoxically, an inverse behaviour was observed for homozygous ($a^{-/-}$) mice. This figure displays graphically the number of rolling leukocytes determined for each of experimental groups under each experimental condition. Three experimental groups were assayed: wild-type mice (referred here as WT); heterozygous ($a^{+/-}$) mice (referred here as Hetero) and homozygous ($a^{-/-}$) mice (referred here as Homo). On the other hand, two distinct experimental conditions were used here: normal conditions (used when no treatment is stated) and acute inflammatory conditions stimulated by tissue perfusion with PAF (this condition is here designated as PAF). Represented results are mean values of the data obtained from a total of six mice ($N = 6$) per experimental group per experimental condition. Error bars depict the associated standard error deviations.

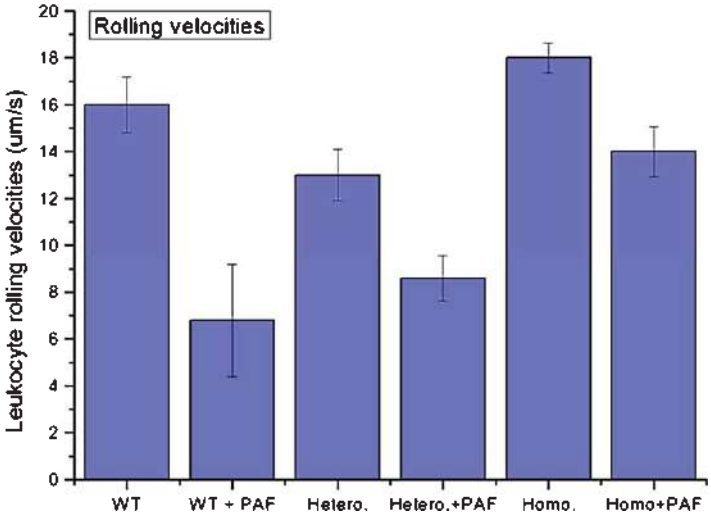

Fig. 3. These leukocyte recruitment parameters were determined at 15 min after image acquisition started. The leukocyte rolling velocity in homozygous ($a^{-/-}$) mice is significantly ($p < 0.05$) higher than that determined for heterozygous ($a^{+/-}$) mice as well as for wild-type mice both in the basal state and in an inflammatory environment induced by PAF tissue perfusion. In all experimental groups, leukocyte rolling velocities measured under PAF treatment were lower in comparison to those determined for the normal conditions. This figure displays graphically the leukocyte rolling velocities determined for each of experimental groups under each experimental condition. Three experimental groups were assayed: wild-type mice (referred here as WT); heterozygous ($a^{+/-}$) mice (referred here as Hetero) and homozygous ($a^{-/-}$) mice (referred here as Homo). On the other hand, two distinct experimental conditions were used here: normal conditions (used when no treatment is stated) and acute inflammatory conditions stimulated by tissue perfusion with PAF (this condition is here designated as PAF). Results are here represented as mean values of the data obtained from a total of six mice ($N = 6$) per experimental group per experimental condition. Error bars depict the associated standard error deviations.

homozygous ($a^{-/-}$) mice exhibited increased and decreased counts of rolling leukocytes, respectively at normal and acute inflammatory conditions.

As obtained for the control groups, we also observed in homozygous ($a^{-/-}$) mice that leukocyte rolling velocities were decreased in the presence of PAF when comparing to the normal conditions, as depicted in Fig. 3 and Table 1. Additionally, these results were higher than those determined for the other two experimental groups both under normal conditions and acute inflammatory.

Finally in what concerns specifically to leukocyte adhesion, our results showed that in homozygous ($a^{-/-}$) mice as for the other animal groups, the induction of an acute inflammatory process resulted in an increased count of adherent leukocytes in comparison to normal conditions as depicted in Fig. 4 and Table 1. When comparing these results to those obtained for both control groups, we further observed that similarly as for leukocyte rolling, homozygous ($a^{-/-}$) mice exhibited increased and decreased counts of adherent leukocytes, respectively at normal and acute inflammatory conditions.

4. Discussion

Previously, the use of flow chamber assays have enabled us to demonstrate *in vitro* that the presence of soluble fibrinogen at a physiological concentration modulated the adhesive behaviour of human neutrophils [14, 20]. The evaluation of these data led us to suggest that apart from other contributions to

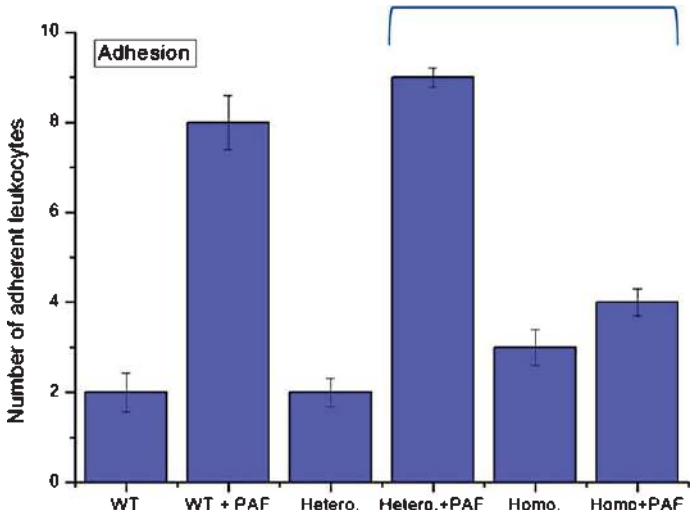

Fig. 4. These leukocyte recruitment parameters were determined at 15 min after image acquisition started. The number of adherent leukocytes observed in homozygous ($a^{-/-}$) mice was significantly lower than that measured in either wild-type animals or heterozygous ($a^{+/-}$) mice under acute inflammatory conditions ($p < 0{,}01$). Wild type animals and heterozygous ($a^{+/-}$) mice displayed a similar number of adherent leukocytes in presence of PAF. This figure displays graphically the number of adherent leukocytes determined for each of experimental groups under each experimental condition. Three experimental groups were assayed: wild-type mice (referred here as WT); heterozygous ($a^{+/-}$) mice (referred here as Hetero) and homozygous ($a^{-/-}$) mice (referred here as Homo). On the other hand, two distinct experimental conditions were used here: normal conditions (used when no treatment is stated) and acute inflammatory conditions stimulated by tissue perfusion with PAF (this condition is here designated as PAF). Represented results are mean values of the data obtained from a total of six mice ($N = 6$) per experimental group per experimental condition. Error bars depict the associated standard error deviations.

the inflammatory process, fibrinogen could as well modulate specifically the recruitment of leukocytes towards the vascular wall in inflammation. This was precisely the main goal of the present study.

To address this, leukocyte recruitment was assayed by intravital microscopy of the post-capillary venules of mouse mesentery under acute inflammatory conditions in the absence or presence of soluble fibrinogen in the blood circulation. For such, we made use of a mouse model bearing a disrupted fibrinogen a chain gene for which homozygous mice do not express any experimentally detected plasmatic soluble fibrinogen. As control mice, we made use of two groups of animals namely, wild-type mice and heterozygous mice, which express soluble fibrinogen in the blood circulation.

Leukocyte recruitment is initiated with the capture of free-flowing leukocytes to the vessel wall which is then followed by the rolling of leukocytes along the endothelial surface layer. This movement is further slowed down so as to favour the subsequent adhesion of leukocytes to and their transmigration through the vascular wall. Our experimental setting allowed us here to observe directly the contribution of this plasmatic protein for the two major steps of this recruitment process namely, leukocyte rolling and leukocyte adhesion. For such, the detailed analysis of the acquired videos enabled us to determine three important leukocyte recruitment parameters: the number of rolling leukocytes; the rolling velocities of these leukocytes and finally, the number of leukocytes adhering to the vascular wall of the imaged post-capillary venules.

Through this approach, we were initially able to understand that although possessing different levels of plasmatic soluble fibrinogen, leukocytes from the two control groups in use exhibited a normal and

identical recruitment behaviour. These results suggest that the levels of soluble fibrinogen expressed in heterozygous ($a^{+/-}$) mice should be enough to support its putative contribution to leukocyte recruitment.

In addition, we were able to further conclude that leukocyte recruitment is negatively affected by the absence of soluble fibrinogen in the blood circulation. In fact, we observed that in the mesentery of homozygous ($a^{-/-}$) mice subjected locally to PAF, leukocytes in the microcirculation presented an abnormal pattern of rolling and adhesion along the endothelial wall of postcapillary venules. These *in vivo* results came in support to our previous *in vitro* observations obtained in a flow chamber model [14, 20]. In this first study, we have shown that neutrophil rolling velocities were substantially augmented when these cells were pre-incubated in the presence of a physiological concentration of soluble fibrinogen in comparison to an untreated condition. Consistently, the number of neutrophils adhering to the endothelial monolayer was diminished upon pre-treatment with soluble fibrinogen. In the present study that information was further complemented with the fact that in comparison to the control animals, the homozygous (-/-) mice, displayed consistently under inflammatory conditions: a substantially reduced number of rolling leukocytes that were actually migrating at higher rolling velocities and consistently, a diminished number of adherent leukocytes.

Overall these results are consistent as higher rolling velocities can logically be converted in a reduced number of slow rolling events and consequently into a reduced number of adherent leukocytes. In fact, for a successful leukocyte adhesion, the rolling velocities must gradually decrease as a function of their contact time with the inflamed endothelium.

Altogether these studies further lead us to propose that soluble fibrinogen constitutes an important factor for the capture of the leukocytes by the activated endothelium. The mechanisms behind this effect are still not fully understood. Notwithstanding, they most probably, relate to the fact that soluble fibrinogen is not only able of individually binding either to the neutrophil membrane or to the endothelial cell, but is moreover able to bridge these two cellular entities thus leading to a more stable and effective recruitment process.

Importantly, these results have profound implications for the inflammatory response. Leukocyte recruitment from the blood is a central event in the innate immune responses to invading pathogens. In these pathological situations, leukocytes need to cross rapidly the vascular wall to reach the site where the inflammatory is taking place. If this ability is somehow compromised as observed here in homozygous ($a^{-/-}$) mice due to the absence of proper levels of soluble fibrinogen in the blood circulation, the normal progression of the elicited inflammatory process will be as well severely affected and a deficient inflammatory response will be mounted. Such a situation may ultimately evolve towards extreme consequences such as sepsis among others that will further put the organism's health at risk.

Acknowledgments

We would like to acknowledge FCT (Fundação para a Ciência e Tecnologia, Portugal) for funding this scientific project (PTDC/SAU-OSM/73449/2006) and for the Ph.D. Grant (SFRH/BD/30145/2006).

References

[1] R. Alon and K. Ley, Cells on the run: Shear-regulated integrin activation in leukocyte rolling and arrest on endothelial cells, *Current Opinion in Cell Biology* **20** (2008), 525–532.

[2] A. Atherton and G. Born, Quantitative investigations of the adhesiveness of circulating polymorphonuclear leucocytes to blood vessel walls, *JPhysiol* **222** (1972), 447–474.
[3] J.L. Dunne, A.P. Goobic, S.T. Acton and K. Ley, A novel method to analyze leukocyte rolling behavior *in vivo*, *Biol Proced Online* **1**(6) (2004), 173–179.
[4] M.J. Flick, X. Du, D.P. Witte, M. Jirousková, D.A. Soloviev, S.J. Busuttil, E.F. Plow and J.L. Degen, Leukocyte engagement of fibrin(ogen) via the integrin receptor aMb2/Mac-1 is critical for host inflammatory respose *in vivo*, *The Journal of Clinical Investigation* **113**(11) (2004), 1596–1606.
[5] M.J. Flick, D. Xinli and J.L. Degen, Fibrin(ogen)-alphaMbeta2 Interactions Regulate Leukocyte Function and Innate Immunity *In Vivo*, *Exp Biol Med* **229** (2004), 1105–1110.
[6] K.R.G.T. Fornal M, Relevance of erythrocyte deformability to the concentration of soluble cell adhesion molecules and glomerular filtration rate in patients with untreated essential hypertension, *Clin Hemorheol Microcirc* **49**(1-4) (2011), 323–329.
[7] S. Herrick, O. Blanc-Brude, A. Gray and G. Laurent, Fibrinogen, *The International Journal of Biochemistry and Cell Biology* **31** (1999), 741–746.
[8] F. Jung, From hemorheology to microcirculation and regenerative medicine: Fåhraeus Lecture 2009, *Clin Hemorheol Microcirc* **45**(2-4) (2010), 79–99.
[9] P. Kubes and S.M. Kerfoot, Leukocyte Recruitment in the Microcirculation: The rolling paradigm revisited, *News Physiol Sci* **16** (2001), 76–80.
[10] P. Kubes, M. Suzuki and D.N. Granger, Modulation of PAF-induced leukocyte adherence and increased microvascular permeability, *Am J Physiol* **259**(5) (1990), 859–864.
[11] C. Lehmann, V. Cerny, I. Abdo, H. Kern and M. Sander, Microcirculation diagnostics and applied studies in circulatory shock - research from the bench to the bedside, *Clin Hemorheol Microcirc* **52**(2) (2012), 131–139.
[12] M. Mosesson, Fibrinogen and fibrin structure and functions, *Journal of Thrombosis and Haemostasis* **3**(8) (2005), 1894–1904.
[13] S. Ramos, J. Brun, B. Gray, S. Rogerson, R. Weatherby, L. Tajouri and S. Marshall-Gradisnik, The effects of short term recombinant human growth hormone (rhGH) on blood rheology in healthy young males, *Clin Hemorheol Microcirc* **47**(2) (2011), 121–129.
[14] M. Rampling, Haemorheology and the inflammatory process, *Clin Hemorheol Microcirc* **19**(2) (1998), 129–132.
[15] M. Spengler, M. Svetaz, M. Leroux, S. Bertoluzzo, P. Carrara, F. Van Isseldyk, D. Petrelli, F. Parente and P. Bosch, Erythrocyte aggregation in patients with systemic lupus erythematosus, *Clin Hemorheol Microcirc* **47**(4) (2011), 279–285.
[16] T.T. Suh, K. Holmbäck, N.J. Jensen, C.C. Daugherty, K. Small, D.I. Simon, S. Potter and J.L. Degen, Resolution of spontaneous bleeding events but failure of pregnancy in fibrinogen-deficient mice, *Genes and Development* **9**(16) (1995), 2020–2033.
[17] S.C. Tromp, *In vivo* Modulation of Leukocyte-Endothelium Interactions, S.C. Tromp, 1999.
[18] A. Vayá, A. Hernández-Mijares, M. Suescun, E. Solá, R. Cámara, M. Romagnoli, D. Bautista and B. Laiz, Metabolic alterations in morbid obesity. Influence on the haemorheological profile, *Clin Hemorheol Microcirc* **48**(4) (2011), 247–255.
[19] V. Vitorino de Almeida, Â. Calado, H.S. Rosário and C. Saldanha, Differential effect of soluble fibrinogen as a neutrophil activator, *Microvasc Res* **83**(3) (2012), 332–336.
[20] V. Vitorino de Almeida, Â. Calado, A. Silva-Herdade, H. Rosário and C. Saldanha, An *in vitro* study on the modulation of the neutrophil adhesive behavior by soluble fibrinogen, in submission.

Erythrocyte deformability and nitric oxide mobilization under pannexin-1 and PKC dependence

A.S. Silva-Herdade, T. Freitas, J. Pedro Almeida and C. Saldanha*
Unidade de Biologia Microvascular e Inflamação, Instituto de Medicina Molecular, Instituto de Bioqu´ımica, Faculdade de Medicina, Universidade de Lisboa, Lisboa, Portugal

Abstract. The erythrocyte adenosine triphosphate (ATP) is utilised for protein phosphorylation and exported through the pannexin 1 hemichannel (Px1) in the microcirculation. The physiological stimuli for ATP release are dependent of blood shear rate level and of the tissue oxygen content. The deoxygenated and oxygenated states of haemoglobin are respectively bound and unbound to N terminal domain of the protein band 3 of the erythrocyte membrane in dependence of its degree of phosphorylation. The protein tyrosine kinase (PTK) and protein tyrosine phosphatase (PTP) contribute to the phosphorylation degree of band 3 and are modulated by protein kinase C (PKC). Chelerythrine (Che) is a competitive inhibitor of ATP for PKC and a negative modulator of erythrocyte deformability.

The aim of this study was to assess the mobilization of nitric oxide (NO) in erythrocyte in absence and presence of Che and Px1 inhibitor (carbenoxolone). Erythrocyte deformability was evaluated in presence of carbenoxolone (Carb). Regarding the effects observed in the erythrocyte by presence of Che or Carb, the values of efflux of NO and the concentration of nitrosogluthatione are similar and with no changes in relation to their absence. Px1inhibition by Carb 10 μM ameliorates the erythrocyte deformability at a shear force of 0.6 and 1.2 Pa. The PKC inhibitor shows similar effects to the Carb on the mobilization of nitric oxide in erythrocyte. The blockage of ATP release by Carb from erythrocytes suggests a possible benefit to develop in ischemia reperfusion or in inflammatory response where will be needed to rescue the excess of NO present and ameliorate the red blood cell deformability at low shear rates.

Keywords: Erythrocyte, protein kinase C, pannexin 1, carbenoxolone nitric oxide

1. Introduction

Erythrocyte adenosine triphosphate (ATP) molecules are produced in the glycolytic pathway and are utilised for example in membrane active transport process, in protein phosphorylation reactions, and are exported into microcirculation through pannexin 1 hemichannel (Px1) [12, 29, 34]. Among several physiological stimuli for ATP release through erythrocyte we can consider the magnitude and the duration of the local blood shear rate, the oxygen tissue partial pressure, the erythrocyte deformability and the donors of nitric oxide (NO) [12, 29]. In endothelial cells, NO is synthesised from L-arginine in the

*Corresponding author: C. Saldanha, Unidade de Biologia Microvascular e Inflamação, Instituto de Medicina Molecular, Instituto de Bioqu´ımica, Faculdade de Medicina, Universidade de Lisboa, 1649-028 Lisboa, Portugal. E-mail: carlotasaldanha@fm.ul.pt.

presence of molecular oxygen by the nitric oxide synthase (eNOS) isoform type III and liberated to the vascular lumen and into the smooth muscle cells (SMC) induces vasodilation [18, 19].

The endothelial NO liberated by the vessel passes through erythrocyte membrane protein band 3 and is fixed by haemoglobin molecules with generation of nitrosohemoglobin [17, 35]. Inside erythrocytes the glutathione is an abundant molecule that reacts with nitric oxide originating S-nitrosoglutathione (GSNO) [13]. The metabolism of NO inside erythrocyte generates several derivatives molecules such as nitrite and nitrate [26]. The efflux of NO in erythrocyte occurs through a trans-nitrosylation process between the thiol group of protein band 3 that receives NO from S-nitrosohemoglobin (SNO-Hb) molecules [15, 30]. Furthermore the efflux of NO in erythrocyte mediated by the protein band 3 is blocked when methemoglobin or deoxygenated hemoglobin bind to the cytoskeleton proteins [17]. The Band 3 protein is found in the erythrocyte membranes either as dimers or a tetramer, and its functional role on NO efflux is in dependence of its degree of phosphorylation [17].

The phosphorylation status of the band 3 protein results from the balance between the action of protein tyrosine kinase (PTK) and of the protein tyrosine phosphatase (PTP) [4, 5]. We have evidenced higher erythrocyte NO efflux when PTP is inhibited than when PTK is inhibited in blood samples of healthy humans [6]. The protein Band 3 dephosphorylated is associated with oxyhemoglobin and glycolytic enzymes which upon phosphorylation of the protein band 3 the oxyhemoglobin, the glyceraldehyde dehydrogenase, the aldolase and the phosphofructokinase are displaced to the cytosol [5]. The enzymes PTP and PTK when are phosphorylated in serine/threonine residues by protein kinase C (PKC) become, respectively, into inactivate and activate forms [36].

Besides its role in erythrocyte metabolism the band 3 protein establishes great number of interaction points with the proteins of the cytoskeleton that are targets of PKC enzyme activity [1, 21]. Consequently the band 3 protein plays a role in maintenance of erythrocyte stability and shape [14, 28]. Decreased erythrocyte deformability by inhibition of PKC in absence and presence of PTP inhibitor was verified [10]. However, the presence of inhibitors of PTP or PTK does not induce modifications in the erythrocyte elongation index (EEI) or deformability [32]. Regarding all the connections between the status of phosphorylation of protein band 3 and the erythrocyte metabolism, the deformability and of the nitric oxide efflux the objective of this work was to study the effects of inhibitor of PKC and of the Px1 inhibitor on efflux and mobilization of nitric oxide and the influence of the inhibitor of Px1 in erythrocyte deformability.

2. Experimental

2.1. Materials

PKC inhibitor, chelerythrine (Che) and carbenoxolone, a pannexin-1 inhibitor were purchased by Sigma- Aldrich Co. Acetylcholine iodide, choline chloride, nitrate reductase from *Aspergillus Niger*, NADPH (tetra sodium salt), sodium nitrate, sodium nitrite and atropine were all from Sigma Chemical Co. (St Louis, MO, USA). The Griess Reagent kit was purchased from Molecular Probes (Eugene, USA). Sodium chloride was purchased from AnalaR (UK) and chloroform and ethanol 95% from MERCK (Darmstadt, Germany).

Blood samples were collected into tubes BD VacuntainerTM with Lithium heparin (17UI/mL) as an anticoagulant. The study was performed in accordance with the guidelines for hemorheological laboratory techniques and under the protocol established with the Portuguese Institute of Blood in Lisbon, Portugal. All donors were males and duly informed and signed their agreement.

2.2. Experimental model

Each blood sample was divided into tree aliquots of 1 mL centrifuged at 11,000 rpm (Biofuge 15 Centrifuge, Heraus) during 1 min at room temperature. One aliquot is used as control and in the others were removed 10 μL of plasma in order to achieve respectively Che 10 μM, and carbenoxolone (Carb) 10 μM.

Nitric oxide efflux, nitrite, nitrate and Snitrosoglutathione levels were determined in all treated blood samples. Erythrocyte deformability was evaluated in control and Carb 10 μM blood samples

2.3. Measurement of NO by amperometric method

Following incubation, blood samples were centrifuged and sodium chloride 0.9% at pH 7.0 was added on to compose a hematocrit of 0.05%. The suspension was mixed by gently inversion of tubes.

For amperometric NO quantification we used the *amino-IV* sensor (Innovative Instruments Inc. FL, USA), according to the method described previously [7]. NO diffuses through the gas-permeable membrane *tripleCOAT* of the sensor probe and it is then oxidized at the working platinum electrode, resulting on an electric current. The redox current is proportional to the NO concentration outside the membrane and it was continuously monitored with a computerized inNO^{TM} system (with a software version 1.9, Innovative Instruments Inc., Tampa, FL, USA) and connected to a computer. Calibration of the NO sensor was performed daily. For each experiment, the NO sensor was immersed vertically in the erythrocyte suspension vials and allowed to stabilize for 30 min to achieve NO basal levels. 30 μl of acetylcholine (ACh) was added to erythrocyte suspension samples in order to achieve the final concentrations of 10 μM of ACh and NO. Data were recorded from constantly stirred suspensions at room temperature.

2.4. Measurement of nitrite/nitrate concentration using the spectrophotometric Griess method

After incubation for 30 min (as described above) blood samples were centrifuged at 9600 g for 1 minute using the Biofuge 15 Heraeus centrifuge. The supernatants were then separated from the pellet (packed erythrocytes).

Nitrite and nitrate levels in the intra-erythrocyte compartment were determined as described previously [8] after submitting the pellet of each centrifuged blood sample to haemolysis and haemoglobin precipitation (erythrocyte cytoplasm values registered). Haemolysis was induced with distilled water and hemoglobin precipitation with a mixture of ethanol and chloroform (5v/3v).

The nitrite concentrations were measured with the spectrophotometric *Griess* reaction, at 548 nm. For nitrate measurement, this compound was first reduced to nitrites in presence of nitrate reductase [16].

2.5. Measurement of S-nitrosoglutathione (GSNO)

Colorimetric solutions containing a mixture of sulfanilic acid (B component of Griess reagent) and NEDD (A component of Griess reagent), consisting of 57.7 mM of sulfanilic acid and 1 mg/mL of NEDD, were dissolved in phosphate-buffered solution (PBS; pH 7.4). To constitute the 10 mM $HgCl_2$ (Aldrich) mercury ion stock solutions were prepared in 0.136 g/50 mL of dimethyl sulfoxide (DMSO) (Aldrich). GSNO was diluted to the following desired concentrations: 7,5 μM; 15 μM; 30 μM; 45 μM; 60 μM; 120 μM; 240 μM; 300 μM in the colorimetric analysis solutions. Various concentrations of mercury were then added to a final concentration of 100 μM. Following gentile shaking the solution was let to stand for twenty minutes. A control spectrum was measured by spectrophotometry at 496 nm against a

solution without mercury ion. 300 μl of erythrocyte suspensions were added to the reaction mixture and GSNO concentrations were obtained as described [9].

2.6. Erythrocyte deformability determination by laser diffractometry

Erythrocyte deformability was assayed by using a Rheodyn SSD laser diffractometer (Myrenne, Roetgen, Germany) Twenty μL of whole blood samples were diluted in 2 mL dextran solution (Pharmacia; osmolality 0.300, and pH 7.4; viscosity 0.24 mPa.s). This suspension was introduced into a measuring chamber formed by two glass disks, one static and other connected through a rotational arm to a synchronised step motor. A 1 mV helium-neon laser beam is passed through the blood suspension, and the diffraction pattern analyzed at following shear stress forces values: 0.3, 0.6, 1.2, 3.0, 6.0, 12.0, 30.0, 60.0 Pa. In the static position at rest, the laser diffraction pattern is circular, becoming elliptic as the erythrocyte were deformed by application of increasing shear stress. Light intensity and the diffraction pattern were measured in two orthogonal axes and the erythrocyte elongation index (EEI) calculated from the length (L) and width (W) by the following formula $EEI = 100 \times (L-W)/(L+W)$. EEI values are expressed as percentage.

3. Statistical analysis

Data are presented as mean ± SD. Differences between the mean values were evaluated by using software GraphPad Prism 4version and analysis test used ANOVA followed the test of multiple comparison of Dunnet. Values were considered statistically significant for $p < 0.05$.

4. Results

4.1. Effects of Px1 inhibitor (carbenoxolone 10 μM) on erythrocyte deformability

The results of erythrocyte elongation index (EEI) obtained for the different shear stress applied to control and Carb 10 μM blood samples are present in Table 1. Significantly increased levels of erythrocyte deformability were verified at 0.6 Pa and 1.2 Pa for Carb 10 μM ($p < 0.05$) samples when compared with the control sample.

No statistically significant values were found in the other shear stress conditions for the erythrocyte deformability Table 1.

4.2. Effects of PKC and Px1, inhibitors on erythrocyte nitric oxide efflux

The erythrocyte nitric oxide values obtained in treated blood samples with Che (PKC inhibitor) or Carb 10 μM (Px1 inhibitor) were not statistically different from the control (Che 10 μM 1.99 ± 0.31 nM and Carb 10 μM 1.99 ± 0.33 nM both versus control 1.63 ± 0.49 nM).

4.3. Effects of PKC and Px1 inhibitors on erythrocyte S-nitrosoglutathione

No statistically significant values of GSNO concentrations were obtained in the blood samples treated with Che 10 μM (9.45 ± 0.67 μM) or Carb 10 μM (10.10 ± 1.33 μM) when compared with the control samples 8.91 ± 1.44 μM.

Table 1
Values (Mean ± SD) of erythrocyte nitric oxide efflux (nM) GSNO (μM), peroxinitrite (μM), nitrite (μM) and nitrate (μM)

Shear Stress (Pa)	Control EEI (%)	Carb EEI (%)
0.3	0.92 ± 0.72	1.73 ± 1.1
0.6	3.38 ± 1.56	4.64 ± 1.66
1.2	13.23 ± 3.0	15.26 ± 3.18
3.0	29.58 ± 3.55	30.84 ± 3.03
6.0	39.99 ± 3.58	40.86 ± 3.35
12.0	46.66 ± 3.98	47.46 ± 4.12
30.0	49.34 ± 4.72	50.06 ± 5.12
60.0	48.84 ± 4.85	49.72 ± 5.02

Mean ± SD values of erythrocyte elongation index (EEI) expressed in percentage obtained at shear stress values varied from 0.3 and 60.0 Pa. Blood samples were incubated with or without Carb10 μM. a − $p < 0.05$ versus Control.

4.4. Effects of PKC and Px1, inhibitors on erythrocyte nitrite and nitrate levels

Statistically significant higher values ($p < 0.001$) of nitrite concentrations were obtained in the blood samples treated with Che 10 μM (10.30 ± 0.89 μM) and Carb 10 μM (9.96 ± 0.74 μM) when compared with the control samples 8.05 ± 0.88 μM. Concerning the values obtained for the nitrate determination all were statistically significant ($p < 0.001$) higher namely for Che 10 μM (11.00 ± 0.88 μM) and for Carb 10 μM (10.19 ± 0.74 μM when compared with the control samples 8.05 ± 0.88 μM.

5. Discussion

In treated blood samples with carbenoxolone we verified that the values of erythrocyte deformability for all shear stress increased significantly at 0.6 Pa and 1.2 Pa in relation with the untreated blood samples. The enhanced values of deformability obtained in treated blood samples with pannexin-1 inhibitor may result from reinforced contribution of ATP inside the cell to the phosphorylation status of the cytoskeleton proteins. This phosphorylation status in turn induces lost of bridges formation between proteins and decreases their interconnections and consequently allows more membrane ability to freely deform [23]. The flippase enzyme activity is ATP-dependent and assures the normal erythrocyte deformability [24] what in the present study the ATP was maintained inside the erythrocyte by inhibition of pannexin-1. The inhibition of pannexin-1 acts differently than PKC inhibition in the erythrocyte deformability. The inhibition of PKC eliminates the phosphorylation of the erythrocyte membrane protein 4.1 increases the interaction of membrane proteins with those of cytoskeleton and consequently decreases the erythrocyte deformability [25]. The association between the protein 4.1 and the protein Glycophorin C originates a junction complex that associates with the protein band 3, known as the anion exchanger [1]. The significant improvement of erythrocyte deformability under the influence of carbenoxolone, was detectable only at low shear forces between 0.6 and 1.2 Pa which may be relevant *in vivo* mainly in the venous vessels that have shear rates in the same range of values [22]. It was evidenced that erythrocyte deformability is impaired in chronic venous disease [20]. Further studies in animal models with insufficient venous diseases are needed in order to verify the benefit effect of carbenoxolone in the erythrocyte deformability.

The results obtained in the present study done in blood samples of healthy humans demonstrated no changes in the efflux of NO through the erythrocyte or in the levels of GSNO under presence of carbenoxolone or Che in relation to untreated sample. In contrast the nitrite and nitrate levels were higher than the control in all treated blood samples which means it enhances production inside the erythrocyte. The efflux of NO through the erythrocyte is favoured when the protein band 3 is phosphorylated by the protein tyrosine kinase which in turn is activated by PKC [36]. Once in presence of Che (PKC inhibitor) the protein band 3 will be in the dephosphorylated state by the action of protein tyrosine phosphatase [4, 5]. The NO levels are unchanged in presence of the pannexin-1 blocker. The maintenance of ATP inside the erythrocyte activates the enzyme phosphofructokinase 2 decreasing the amount of fructose-6-phosphate decreasing the lactic fermentation. This can interfere with binding of the glycolitic enzymes into the protein band 3 with absence of repercussions in the efflux of nitric oxide during the time of the experimental model. The GSNO concentration didn't changed in treated blood samples by Che or by Carb suggesting absence of participation in the irreversible reaction of the GSNO molecules with deoxygenated haemoglobin generating glutathione, methahemoglobin and NO [33]. The values of GSNO are in normal concentration range that does not inhibit the haemoglobin reductase responsible to normalise the levels of metahemoglobin [3]. In a same way the values of the efflux of nitric oxide show no alteration in both blood samples treated with Che or carbenoxolone and for this we did not expect its reaction with oxyhemoglobin for generation of nitrate and methahemoglobin [3]. The SNOHb biomolecules are a great reservoir of NO inside the erythrocyte that can transfer it to the glutathione molecule generating nitrate and GSNO or release it for combining with anion superoxide (when auto-oxidation of haemoglobin occur) for formation of peroxinitrite [2, 27]. The decomposition of peroxynitrite generates molecules of nitrite and nitrate [31]. So in blood samples treated with Che or Carb the higher levels of nitrite and nitrate obtained may result from the decomposition of peroxynitrite molecules. It was attributed to carbenoxolone the capacity for scavenger superoxide anion of the erythrocyte when present at high concentrations that was not the case of our samples where was used small concentration of 10μM [11].

In conclusion the efflux of nitric oxide through erythrocytes is unchanged by inhibition of PKC or pannexin-1 which may constitute therapeutic targets for vascular pathologies. The inhibition of the channel of pannexin-1 increased the erythrocyte deformability under lower shear stress what *in vivo* may have benefit in the passage of the erythrocyte through the microcirculation network especially in venous side facilitating the oxygen and nitrogen exchange with tissues.

Acknowledgments

This study was supported by grants from the FCT - Fundação para a Ciência e a Tecnologia (project reference PTDC/SAU-OSM/73449/2006).

References

[1] X.L. An, Y. Takakuwa, W. Nunomura, S. Manno and N. Mohandas, Modulation of Band 3-Ankyrin Interaction by Protein 4.1, Functional implications in regulation of erythrocyte membrane mechanical properties, *J Biol Chem* **271** (1996), 33187–33191.

[2] C. Balagopalakrishna, P.T. Manoharan, O.O. Abugo and J.M. Rifkind, Production of superoxide from hemoglobin-bound oxygen under hypoxic conditions, *Biochemistry* **35** (1996), 6393–6398.

[3] K. Becker, M. Gui and R.H. Schirmer, Inhibition of human glutathione reductase by S-nitrosoglutathione, *Eur J Biochem* **234** (1995), 472–478.
[4] L. Bordin, A.M. Brunati, A. Donella-Deana, B. Baggio, A. Toninello and G. Clari, Band 3 is an anchor protein and a target for SHP-2 tyrosine phosphatase in human erythrocytes, *Blood* **100** (2002), 276–278.
[5] M.E. Campanella, H. Chu and P.S. Low, Assembly and regulation of a glycolytic enzyme complex on the human erythrocyte membrane, *Proc Natl Acad Sci USA* **102** (2005), 2402–2407.
[6] F.A. Carvalho, J.P. Almeida, I.O. Fernandes, T. Freitas-Santos and C. Saldanha, Non-neuronal cholinergic system and signal transduction pathways mediated by band 3 in red blood cells, *Clin Hemorh Microc* **40** (2008), 207–227.
[7] F.A. Carvalho, J. Martins-Silva and C. Saldanha, Amperometric measurements of nitric oxide in erythrocytes, *Biosens Bioelectron* **20** (2004), 505–508.
[8] F.A. Carvalho, R. Mesquita, J. Martins-Silva and C. Saldanha, Acetylcholine and choline effects on erythrocyte nitrite and nitrate levels, *J Appl Toxicol* **24** (2004), 419–427.
[9] J.A. Cook, S.Y. Kim, D. Teague, M.C. Krishna, R. Pacelli, J.B. Mitchell, Y. Vodovotz, R.W. Nims, D. Christodoulou, A.M. Miles, M.B. Grisham and D.A. Wink, Convenient colorimetric and fluorometric assays for S-nitrosothiols, *Anal Biochem* **238** (1996), 150–158.
[10] S. de Oliveira, A.S. Silva-Herdade and C. Saldanha, Modulation of erythrocytes deformability by PKC activity, *Clin hemorheol Microc* **39** (2008), 363–373.
[11] A. Dembinska-Kiec, D. Pallapies, T.H. Simmet, B.M. Peskar and B.A. Peskar, Effect of carbenoxolone on the biological activity of nitric oxide: Relation to gastroprotection, *Br J Pharmacol* **104** (1991), 811–816.
[12] A.M. Forsyth, J. Wan, P.D. Owrutsky, M. Abkarian and H.A. Stone, Multiscale approach to link red blood cell dynamics shear viscosity, and ATP release, *Proc Natl Acad Sci USA* **108** (2011), 10986–10991.
[13] F. Galli, R. Rossi, P. Di Simplicio, A. Floridi and F. Canestrari, Protein thiols and glutathione influence the nitric oxide-dependent regulation of the red blood cell metabolism, *Nitric Oxide* **6** (2002), 186–199.
[14] D.M. Gilligan and V. Bennett, The junctional complex of the membrane skeleton, *Seminars in Haematology* **30** (1993), 74–83.
[15] S.S. Gross, Target delivery of nitric oxide, *Nature* **409** (2001), 577–588.
[16] I. Guevara, J. Iwanejko, A. Dembińska-Kieć, J. Pankiewicz, A. Wanat, P. Anna, I. Gołabek, S. Bartuś, M. Malczewska-Malec and A. Szczudlik, Determination of nitrite/nitrate in human biological material by the simple Griess reaction, *Clin Chim Acta* **274** (1998), 177–188.
[17] K.T. Huang, T.H. Han, D.R. Hyduke, M.W. Vaughn, H. Van Herle, T.W. Hein, C. Zhang, L. Kuo and J.C. Liao, Modulation of nitric oxide bioavailability by erythrocytes, *Proc Natl Acad Sci USA* **98** (2001), 11771–11776.
[18] L.J. Ignarro, G.M. Buga, K.S. Wood, R.E. Byrns and G. Chaudhuri, Endothelium-derived relaxing factor produced and released from artery and vein is nitric oxide, *Proc Natl Acad Sci, USA* **84** (1987), 9265–9269.
[19] P. Lane and S. Gross, Hemoglobin as a chariot for NO bioactivity, *Nature Medicine* **8** (2002), 657–658.
[20] C. Le Dévéhat, M. Vimeux and T. Khodabandehlou, Hemorheology of venous insufficiency, *J Mal Vasc* **15** (1990), 360–363.
[21] E. Ling, Y.N. Danilov and C.M. Cohens, Modulation of red cell 4.1 function by cAMP-dependent kinase and protein kinase C phosphorylation, *J Biol Chem* **263** (1988), 2209–2216.
[22] H. Lipowski, Microvascular Rheology and Hemodynamics, *Microcirculation* **12** (2005), 5–15.
[23] P.S. Low, P.S. Willardson, N. Mohandas, M. Rossi and S. Shohet, Contribution of band 3-ankyrin interaction to erythrocyte membrane mechanical stability, *Blood* **77** (1991), 1581–1586.
[24] S. Manno, N. Mohandas and Y. Takakuwa, ATP-dependent mechanism protects spectrin against glycation in human eythrocytes, *J Biol Chem* **205** (2010), 33923–33929.
[25] S. Mannot, Y. Takakuwa and N. Mohandas, Modulation of erythrocyte membrane mechanical function by protein 4.1 phosphorylation, *J Biol Chem* **280** (2005), 7581–7587.
[26] J.M. May, Z.-C. Qu, L. Xia and C.E. Cobb, Nitrite uptake and metabolism and oxidant stress in human erythrocytes, *Am J Physiol Cell Physiol* **279** (2000), C1946–C1954.
[27] T.J. McMahon, A.E. Stone, J. Bonaventura and J.S. Stamler, Functional coupling of oxygen binding and vasoactivity S-nitrosohemoglobin, *J Biol Chem* **275** (2000), 16738–16745.
[28] R. Moryayama, C.R. Lombardo, R.F. Workman and P.S. Low, Regulation of linkages between the erythrocyte membrane and its cekeleton by 2,3 DPG, *J Biol Chem* **268** (1993), 10990–10996.
[29] J.J. Olearczyk, M.L. Ellsworth, A.H. Stephenson, A.J. Lonigro and R.S. Sprague, Nitric oxide inhibits ATP release from erythrocytes, *J Pharmacol Experimental Therapeutics* **309** (2004), 1079–1084.

[30] R. Pawloski, D.T. Hess and J.S. Stamler, Impaired vasodilation by red blood cells in sickle cell disease, *Proc Nat Acad Sci USA* **102** (2005), 2531–2536.
[31] S. Pfeiffer and B. Mayer, Lack of tyrosine nitration by peroxynitrite generated at physiological pH, *J Biol Chem* **273** (1998), 27280–27285.
[32] C. Saldanha, A.S. Silva, S. Gonçalves and J. Martins Silva, Modulation of erythrocyte hemorheological properties by band 3 phosphorylation and dephosphorylation, *Clin Hemorheol Microc* **36** (2007), 183–194.
[33] N.Y. Spencer, H. Zeng, R.P. Patel and N. Hogg, Reaction of S-nitrosoglutathione with the heme group of deoxyhemoglobin, *J Biol Chem* **275** (2000), 36562–36567.
[34] R.S. Sprague and M.L. Ellsworth, Erythrocyte–derived ATP and perfusion distribution role of intracellular and intercellular communication, *Microcirculation* **19** (2012), 430–439.
[35] J.S. Stamler, L. Jia, J.P. Eu, T.J. McMahon, I.T. Demchenko, J. Bonaventura, K. Gernert and C.A. Piantadosi, Blood flow regulation by S-nitrosohemoglobin in the physiological oxygen gradient, *Science* **276** (1997), 2034–2037.
[36] Y. Zipser, A. Piedade, A. Barbul, R. Korenstein and N.S. Kosower, Ca+ promotes erythrocyte band 3 tyrosine phosphorylation via dissociation of phosphotyrosine phosphatase from band 3, *Biochem J* **368** (2002), 137–144.

Korea-Australia Rheology Journal, Vol.26, No.2, pp.1-7 (May 2014) www.springer.com/13367
DOI: 10.1007/s13367-014-0024-2

Signal transduction pathways in erythrocyte nitric oxide metabolism under high fibrinogen levels

Carlota Saldanha[1,*], T. Freitas[1], J.P. Lopez de Almeida[2] and A. Silva-Herdade[1]
[1]*Instituto de Medicina Molecular, Faculdade de Medicina da Universidade de Lisboa, Lisboa 1649-028, Portugal*
[2]*Serviço de Imunoalergologia, Hospital de Santa Maria, Lisboa 1649-035, Portugal*

(Received January 28, 2014; final revision March 26, 2014; accepted April 12, 2014)

Previous studies show that the fibrinogen molecule modulates the metabolism of nitric oxide (NO) in erythrocyte. The *in vitro* induced hiperfibrinogenemia interferes in the metabolism of the NO in the erythrocyte in dependence of the phosphorylation degree of the band 3. The soluble form of fibrinogen binds into CD47 protein present in the erythrocyte membrane. The soluble thrombomodulin is an inflammatory marker that binds to the erythrocyte CD47 in a site with a sequence peptide known as 4N1K. A study done in vitro shows that when hiperfibrinogenemia was induced in the presence of the peptide 4N1K agonist of CD47 it were observed variations in the efflux of NO from erythrocyte and an increase in the concentrations of GSNO, peroxinitrite, nitrite and nitrate of the erythrocytes. The aim of this work was to study the influence of the peptide 4N1K, on the metabolism of NO in the erythrocyte under high fibrinogen concentration and in the presence of inhibitors of the status of phosphorylation of protein band 3. In this *in vitro* study, whole blood samples were harvested from healthy subjects and NO, peroxynitrite, nitrite, nitrate and S-nitroglutathione (GSNO) were determined in presence of 4N1K, calpeptine, Syk inhibitor and under high fibrinogen concentrations. The results obtained in erythrocytes under high fibrinogen levels when 4N1K is present with the Syk inhibitor or with calpeptine, showed in relation to the control samples increased significant concentrations of efflux of NO and of peroxynitrite, nitrite, nitrate and GSNO. In conclusion it was verified that in the *in vitro* model of hiperfibrinogenemia the peptide 4N1K, agonist of CD47, induces mobilization of NO in the erythrocyte in dependence of the status of phosphorylation of protein band 3.

Keywords: nitric oxide, erythrocyte, fibrinogen, CD47, 4N1K

1. Introduction

In endothelial cells, NO is synthesised from L-arginine in presence of molecular oxygen by the nitric oxide synthase (eNOS) isoform type III and liberated to the vascular lumen and into the smooth muscle cells (SMC) where induces vasodilation as described by Ignarro *et al.* (1987). The endothelial NO liberated to the vessel passes through the erythrocyte membrane protein band 3 and is fixed by haemoglobin molecules with generation of nitrosohemoglobin demonstrated by Stamler *et al.* (1997) and Huang *et al.* (2001). Inside erythrocytes the glutathione is an abundant molecule that reacts with nitric oxide originating S-nitrosoglutathione (GSNO) as showed by Galli *et al.* (2002). Also NO can react with superoxide anion forming peroxynitrite that subsequently forms nitrites and nitrates (Murphy and Sies, 1991; Huie and Padmaja, 1993; May *et al.*, 2000). The efflux of NO from erythrocyte occurs through a trans-nitrosylation process involving the thiol group of the protein band3 that receives NO from S-nitrosohemoglobin (SNO-Hb) molecules as previous showed by Gross (2001) and after by Pawloski *et al.* (2005). The protein Band 3 is present in the erythrocyte membranes, and its functional role on NO efflux is dependent of its degree of associations in dimmers or tetramers well documented by Huang *et al.* (2001). The (also called "Anion Exchanger 1") is the most abundant protein in the erythrocyte membrane and has an important role *e.g.* in gas exchange, senescence and removal of cells from the circulation, as anchoring motifs for the glycolytic enzymes (GE) and functions as a point of attachment for the cytoskeleton maintaining the mechanical and osmotic properties of the erythrocyte (Anong *et al.*, 2009; Jiang *et al.*, 2013). The phosphorylation status of the protein band 3 results from the balance between the action of protein tyrosine kinase (PTK) and of the protein tyrosine phosphatase (PTP) showed by Bordin *et al.* (2002) and by Campanella *et al.* (2005). Carvalho *et al.* (2008) evidenced higher erythrocyte NO efflux when PTP is inhibited than when PTK is inhibited in blood samples of healthy humans in presence of acetylcholine. This signalling mechanism involves the acetylcholinesterase which forms an active complex state with acetylcholine and the Gi protein Carvalho *et al.* (2008). Erythrocyte protein band 3 when present as tetramers binds to protein 4.2 and ankyrin that associate with

This article was presented at the 17th Conference of the European Society for Clinical Hemorheology & Microcirculation (ESCHM), held on 6-9 July, 2013, Hungary.
*Corresponding author: carlotasaldanha@fm.ul.pt

Rh complex (De Oliveira *et al.*, 2010).

Erythrocyte membrane CD47 in the complex Rh establishes contact with protein 4.2 which in turn interacts with band 3 (Dahl *et al.*, 2004). Fibrinogen is a plasma protein that beyond its hemostatic function behaves as an acute phase protein and as a hemorheological factor and a revision of its properties and effects on erythrocyte has performed recently by Saldanha (2013). Rampling *et al.* (1998) have performed a revision about the fibrinogen and inflammation highlighting the participation of fibrinogen in the inflammatory response. Soluble form of fibrinogen binds to erythrocyte membrane in the integrin associated protein CD47 as evidenced by De Oliveira *et al.* (2012). Soluble thrombospondin is an inflammatory marker that binds its C terminal domain to CD47 in a sequence peptide known as 4N1K as described by Wang and Frazier (1998). *In vitro* induced hiperfibrinogenemia modulates erythrocyte nitric oxide (NO) metabolism in dependence of membrane protein band 3 phosphorylation degree according Lopes de Almeida (2011). When in presence of the CD47 agonist peptide, 4N1K and in hiperfibrinogenemia it was verified by Saldanha *et al.* (2012) increased GSNO, peroxinitrite, nitrite and nitrate concentrations. It remains to be clarified in terms of the nitric oxide mobilization if there is crosstalk between the transduction mechanism resulting from the binding of the peptide 4N1K to CD47 and the status of phosphorylation of the protein band 3. So, the aim of this work was to study the influence of the CD47 agonist peptide, 4N1K, under high fibrinogen concentration on the erythrocyte NO metabolism in the presence of inhibitors of membrane protein band 3 phosphorylation degree.

2. Experimental

2.1. Materials

General reagents were purchased by Sigma- Aldrich (Madrid, Spain). For protein tyrosine kinase (PTK) inhibition Syk, a PTK p72syk inhibitor and calpeptin used as a PTP inhibition PTK and PTP inhibitors were provide by Clabiochem, Merk, (Darmstad, Germany). Acetylcholine iodide, choline chloride, nitrate reductase from *Aspergillus Niger*, NADPH (tetra sodium salt), sodium nitrate, sodium nitrite and atropine were all from Sigma-Aldrich (Madrid, Spain). The Griess Reagent kit was purchased from Molecular Probes, Eugene, USA. Sodium chloride was purchased from AnalaR (UK) and chloroform and ethanol 95% from Merck (Darmstadt, Germany).

Blood samples were collected into tubes BD VacuntainerTM with Lithium heparin (17 UI/mL) as an anticoagulant.

The study was performed under the protocol established with the Portuguese Institute of Blood in Lisbon. All donors (N = 10) were males, duly informed, and signed an appropriate agreement.

The chosen concentrations for fibrinogen were based on its physiological levels and previous studies (Sargento *et al.*, 2005). The human fibrinogen was purchased from Sigma-Aldrich (Madrid, Spain).

2.2. Experimental model

The experimental method that we here describe was done in each blood sample (3 tubes of 5 ml) taken from the ten donors. So, each blood sample was divided into ten aliquots of 1 mL centrifuged at 11,000 rpm (Biofuge 15 Centrifuge, Heraus) during 1 min at room temperature.

In two samples 50 µL of plasma was replaced with the same volume of fibrinogen NaCL isotonic solutions pH 7.4 (30 mg/dL). The same procedure for the control sample has been performed with the difference that, 50 µL of plasma was replaced with the same volume of isotonic NaCl. From the others 3 samples, 10 µL of plasma was taken and replaced by same volume in order to achieve 10 µM final concentration of syk inhibitor, calpeptine (PTP inhibitor) and 4N1K.

To the 3 others blood samples 50 µL of each fibrinogen solutions was added as well as the Syk, Calpeptine and 4N1K to achieve the 10 µM final concentration. To the remaining 3 blood samples 50 µL of each fibrinogen solutions was added as well the syk, Calpeptine and 4N1K to achieve the 10 µM final concentration Blood samples were then incubated during 15 min with slight agitation. To avoid changes on blood samples due to possible temperature fluctuations during incubation all measurements of the NO and its derivatives molecules were performed at room temperature.

2.3. Determination of fibrinogen concentration by clot-based technology

At the end of incubation samples were centrifuged and plasma removed for fibrinogen concentration assessment. Plasma fibrinogen concentrations were evaluated using the Fibritimer BFT* Analyser (Dade Behring, Marburg GmbH, Germany) based on the Clot technology.

2.4. Measurement of NO by amperometric method

Following incubation, blood samples were centrifuged and sodium chloride 0.9% at pH 7.0 was added on to compose a hematocrit of 0.05%. The suspension was mixed by gently inversion of tubes.

For amperometric NO quantification we used the *amino-IV* sensor (Innovative Instruments Inc. FL, USA), according to the method described previously by Carvalho *et al.* (2004a). NO diffuses through the gas-permeable membrane *tripleCOAT* of the sensor probe and it is then oxidized at the working platinum electrode, resulting on an electric current. The redox current is proportional to the NO concentration outside the membrane and it was continuously monitored with a computerized inNO system™

(with a software version 1.9, Innovative Instruments Inc., Tampa, FL, USA) and connected to a computer. Calibration of the NO sensor was performed daily. For each experiment, the NO sensor was immersed vertically in the erythrocyte suspension vials and allowed to stabilize for 30 min to achieve NO basal levels. 30 µl of acetylcholine (ACh) was added to erythrocyte suspension samples in order to achieve the final concentrations of 10 µM of ACh and NO. Data were recorded from constantly stirred suspensions at room temperature.

2.5. Measurement of nitrite/nitrate concentration using the spectrophotometric Griess method

After incubation for 30 min (as described above) blood samples were centrifuged at 9600 g for 1 minute using the Biofuge 15 Heraeus centrifuge. The supernatants were then separated from the pellet (packed erythrocytes).

Nitrite and nitrate levels in the intra-erythrocyte compartment were determined as described previously Carvalho *et al.* (2004b) after submitting the pellet of each centrifuged blood sample to haemolysis and haemoglobin precipitation (erythrocyte cytoplasm values registered). Haemolysis was induced with distilled water and hemoglobin precipitation with a mixture of ethanol and chloroform (5v/3v).

The nitrite concentrations were measured with the spectrophotometric *Griess* reaction, at 548 nm. For nitrate measurement, this compound was first reduced to nitrites in presence of nitrate reductase *Guevara et al.* (1998).

2.6. Measurement of S-nitrosoglutathione (GSNO)

Colorimetric solutions containing a mixture of sulfanilic acid (B component of Griess reagent) and NEDD (A component of Griess reagent), consisting of 57.7 mM of sulfanilic acid and 1 mg/mL of NEDD, were dissolved in phosphate-buffered solution (PBS; pH 7.4). To constitute the 10 mM $HgCl_2$ (Sigma-Adrich, Madrid, Spain) mercury ion stock solutions were prepared in 0.136 g / 50 mL of dimethyl sulfoxide (DMSO) from Sigma-Aldrich (Madrid, Spain). GSNO was diluted to the following desired concentrations :7,5 µM; 15 µM; 30 µM; 45 µM; 60 µM; 120 µM; 240 µM; 300 µM in the colorimetric analysis solutions. Various concentrations of mercury were then added to a final concentration of 100 µM. Following gentile shaking the solution was let to stand for twenty minutes. A control spectrum was measured by spectrophotometry at 496 nm against a solution without mercury ion. 300 µl of erythrocyte suspensions were added to the reaction mixture and GSNO concentrations were obtained as described Cook *et al.* (1996).

2.7. Determinations of peroxinitrite levels

The erythrocyte suspensions (1 mL) were incubated with 2,7-dichlorofluorescein diacetate (DCFC-DA) 15 µM, in 3 mL buffer (Pi 155 mM, pH 7.4) during 30 min, at room temperature. Suspensions were rinsed several times and diluted in the working solution with 1.8 mL of the same buffer. The pellets were rinsed and used for fluorescence measurement with a Hitachi F-300 fluorospectrophotometer (Hitachi, Japan) with excitation and emission wavelengths at 503 and 523 nm, respectively. The concentration of peroxynitrite was finally calculated through a calibration graph Possel *et al.* (1997).

2.8. Statistical analysis

Data are expressed as mean values ± SD. Student's paired t-tests were used to compare values between different samples of erythrocyte suspensions. Statistical significance was set at a $p < 0.05$ level. Statistical analysis was conducted using the Statistical Package from the Social Sciences (SPSS; version 21.0).

3. Results

The manipulation of human blood samples by adding fibrinogen mimics the experimental model of hyperfibrinogenemia. A better physiological similarity was attained by using blood samples instead of erythrocytes suspension.

3.1. Effects of in vitro hyperfibrinogenemia and 4N1K on nitric oxide levels in absence and presence of syk inhibitor and calpeptine in erythrocytes

In the presence of high fibrinogen levels, 510±10 mg/dL the concentrations for erythrocyte NO efflux obtained is (1.19 ±0.14 nM) not significant when compared with the value obtained in the control sample (1.08 ±0.11 nM).

The values of erythrocyte NO efflux obtained in presence of 4N1K 10 µM (1.15 ±0.14 nM) is not significant but in variance in presence of Syk 10 µM (1.32 ±0.15 nM, $p < 0.05$) or calpeptine (1.28 ±0.20 nM, $p = 0.05$) they are.

In the presence of high fibrinogen levels, 510 ±10 mgdL the following NO levels were obtained with 4N1K (1.40 ±0.19 nM, $p < 0.05$); with Syk inhibitor (1.36±0.17 nM, N.S); and with calpeptine (1.49 ±0.25 nM, $p < 0.001$). In the presence of high fibrinogen levels, 510±10 mg/dL and 4N1K, the following NO levels were observed: in presence of Syk inhibitor (1.49±0.23 nM, N.S); in presence of calpeptine (1.37 ±0.23 nM, $p < 0.05$).

3.2. Effects of in vitro hyperfibrinogenemia and 4N1K on the levels of nitrite in absence and presence of syk inhibitor and calpeptine in erythrocytes

In the presence of high fibrinogen levels, 510±10 mg/dL the concentrations obtained for erythrocyte nitrite is significant higher (9.40 ±1.37 µM, $p < 0.001$) than the value

Table 1. Values (Mean±SD) of erythrocyte nitric oxide efflux GSNO, peroxinitrite, mitrite and nitrate.

Blood samples	Nitric oxide	GSNO	Peroxinitrite	Nitrite	Nitrate
Control	1.08 ± 0.11	7.51 ± 0.56	8.80 ± 0.74	7.70 ± 1.37	8.30 ± 1.23
Fibrinogen	1.19 ± 0.14	8.81 ± 0.56*	10.56 ± 0.79*	9.40 ± 1.21*	9.55 ± 1.07***
4N1K	1,15 ± 0.14	10.09 ± 0.45*	10.98 ± 1.59*	9.65 ± 1.62**	10.25 ± 1.58**
Syk inhib	1.32 ± 0.15**	9.88 ± 1.27**	10.50 ± 1.75*	10.65 ± 0.60	11.35 ± 0.82*
Calp	1.28 ± 0.20#	9.45 ± 1.11*	12.61 ± 1.09*	10.10 ± 0.71	10.80 ± 0.89*
Fib+ 4N1K	1.40 ± 0.19***	10.86 ± 1.28*	12.67 ± 2.26*	11.00 ± 0.88*	11.40 ± 0.75*
Fib+ Syk inhib	1.36 ± 0.17***	11.90 ± 0.93*	12.31 ± 1.39*	12.25 ± 0.78***	12.45 ± 0.53*
Fib+ Calp	1.49 ± 0.25*	11.73 ± 0.91*	13.21 ± 1.58**	11.65 ± 1.17**	12.45 ± 0.94**
Fib+ 4N1K + Syk inhib	1.49 ± 0.23**	13.16 ± 0.93^{*a,b}	14.74 ± 0.78^{*a,c}	12.45 ± 0.94^{*d}	12.90 ± 0.59^{*a}
Fib+ 4N1K + Calp	1.37 ± 0.23**	11.84 ± 0.93*	14.20 ± 1.97**	12.25 ± 0.78^{*e}	12.55 ± 0.96^{***e}

In relation to control sample: *p < 0.001; **p < 0.05; ***p < 0.005: # = 0.05 ; (a) p < 0.001 Fib+4N1K+Syk in relation to Fib+4N1K; (b) p < 0.05 Fib+4N1K+Syk in relation to Fib+Syk ; (c) p < 0.005 Fib+4N1K+Syk in relation to Fib+Syk ; (d) p < 0.05 Fib+4N1K+Syk in relation to Fib+4N1K; (e) p < 0.001 Fib+4N1K+Calp in relation to Fib+4N1K

obtained in the control sample (7.70 ±1.37 μM).

The values of erythrocyte nitrite obtained in presence of 4N1K 10 μM (9.65 ±1.62 μM, p < 0.05) or in presence of Syk 10 μM (10.65 ±0.60 μM, p < 0.001) or calpeptine (10.10 ±0.70 μM, p < 0.001) are significant higher than in control sample (7.70 ±1.37 μM). In the presence of high fibrinogen levels, 510 ±10 mg/dL the following significant values of nitrite levels were obtained with 4N1K (11.00 ± 0.88 μM, p < 0.001); with Syk inhibitor (12.25 ±0.78 mM, p < 0.005) and with calpeptine (11.65 ±1.17 μM, p < 0.05) in relation to the control sample (7.70 ±1.37 μM).

In the presence of high fibrinogen levels, 510±10 mg/dL and 4N1K, the following significant values of nitrite levels were observed: in presence of Syk inhibitor (12.45 ±0.94 μM, p < 0.001) or in presence of calpeptine (12.25 ±0.78 μM, p < 0.001) in relation to the control sample (7.70 ±1.37 μM).

Under high fibrinogen levels when 4N1K is present with syk inhibitor the value of nitrite increased (12.45 ±0.94 mM, p < 0.05) in relation to the samples without Syk (11.00 ±0.88 mM).

Under high fibrinogen levels when 4N1K is present with calpeptine the value of nitrite increased (12.25 ±0.78 mM, p < 0.001) in relation to the samples without calpeptine (11.00 ±0.88 mM).

3.3. Effects of in vitro hyperfibrinogenemia and 4N1K on the levels of nitrate in absence and presence of syk inhibitor and calpeptin in erythrocytes

In the presence of high fibrinogen levels, 510±10 mg/dL the concentrations obtained for erythrocyte nitrate is significant higher (9.55 ±1.07 μM, p < 0.005) than the value obtained in the control sample (8.30 ±1.23 μM).

The values of erythrocyte nitrate obtained in presence of 4N1K 10 μM (10.25 ±1.58 μM, p < 0.005) or in presence of Syk 10 μM (11.35 ±0.82 μM, p < 0.001) or calpeptine (10.80 ±0.89 μM, p < 0.001) are significant higher than in control sample (8.30 ±1.23 μM). In the presence of high fibrinogen levels, 510 ±10 mg/dL the following significant values of nitrate levels were obtained with 4N1K (11.40 ± 0.75 μM, p < 0.001) with Syk inhibitor (12.45 ±0.53 μM, p < 0.001) and with calpeptine (12.45 ±0.94 μM, p < 0.05) in relation to the control sample (8.30 ±1.23 μM).

In the presence of high fibrinogen levels, 510±10mg/dL and 4N1K, the following significant values of nitrate levels were observed: in presence of Syk inhibitor (12.90 ± 0.59 μM, p < 0.001) or in presence of calpeptine (12.55 ± 0.96 μM, p < 0.005) in relation to the control sample (8.30 ±1.23 μM).

Under high fibrinogen levels when 4N1K is present with syk inhibitor the value of nitrate increased (12.90±0.59 μM, p < 0.001) in relation to the samples without Syk (11.40 ±0.75 μM).

Under high fibrinogen levels when 4N1K is present with calpeptine the value of nitrate increased (12.55±0.96 μM, p < 0.001) in relation to the samples without calpeptine (11.40 ±0.75 μM).

3.4. Effects of in vitro hyperfibrinogenemia and 4N1K on S-nitrosoglutathione (GSNO) levels in absence and presence of syk inhibitor and calpeptine in erythrocytes

In the presence of high fibrinogen levels, 510±10 mg/dL the concentrations obtained for erythrocyte *GSNO* is significant higher (8.81 ±1.07 μM, p < 0.001) than the value obtained in the control sample (7.51 ±0.56 μM).

The values of erythrocyte *GSNO* obtained in presence of

4N1K 10 μM (10.09 ±0.45 μM, $p < 0.005$) or in presence of Syk 10 μM (9.88 ±1.27 μM, $p < 0.05$) or calpeptine (9.45 ±1.11 μM, $p < 0.001$) are significant higher than in control sample (7.51 ±0.56 μM). In the presence of high fibrinogen levels, 510 ±10 mg/dL the following significant values of *GSNO* levels were obtained with 4N1K (11.86 ± 1.28 μM, $p < 0.001$); with Syk inhibitor (11.90 ±0.93 μM, $p < 0.001$) and with calpeptine (11.73 ±0.91 μM, $p < 0.001$) in relation to the control sample (7.51 ±0.56 μM).

In the presence of high fibrinogen levels, 510±10 mg/dL and 4N1K, the following significant values of *GSNO* levels were observed: in presence of Syk inhibitor (13.16 ± 0.93 μM, $p<0.001$) or in presence of calpeptine (11.84 ± 0.93 μM, $p < 0.005$) in relation to the control sample (7.51 ±0.56 μM).

Under high fibrinogen levels when 4N1K is present with syk inhibitor the value of GSNO increased (13.16 ±0.93 μM, $p < 0.001$) in relation to the samples without Syk (10.86 ±1.28 μM).

Under high fibrinogen levels when 4N1K is present with syk inhibitor the value of GSNO increased (13.16 ±0.93 μM, $p < 0.005$) in relation to the samples without 4N1K (11.90 μM±0.93).

3.5. Effects of in vitro hyperfibrinogenemia and 4N1K on levels of peroxinitrite in absence and presence of syk inhibitor and calpeptine in erythrocytes

In the presence of high fibrinogen levels, 510±10 mg/dL the concentrations obtained for erythrocyte peroxinitrite is significant higher (10.56 ±0.79 μM, N.S.) than the value obtained in the control sample (8.80 ±0.74 μM).

The values of erythrocyte peroxinitrite obtained in presence of 4N1K 10 μM (10.98 ±1.59 μM, $p < 0.001$) or in presence of Syk 10 μM (10.50 ±1.75 μM, N.S) or calpeptine (12.61 ±1.09 μM, $p < 0.001$) are significant higher than in control sample (8.80±0.74 μM). In the presence of high fibrinogen levels, 510 ±10 mg/dL the following significant values of peroxinitrite levels were obtained with 4N1K (12.67 ±2.26 μM, $p < 0.001$); with Syk inhibitor (12.31 ±1.39 μM, $p < 0.001$) and with calpeptine (13.21 ± 1.58 μM, $p < 0.05$) in relation to the control sample (8.80 ±0.74 μM).

High levels of fibrinogen, 510 ±10 mg/dL, and 4N1K resulted in the following significant values of peroxinitrite: in presence of Syk inhibitor (14.74 ±0.78 μM, $p < 0.001$) and in presence of calpeptine (14.20±1.97 μM, $p < 0.05$) in relation to the control sample (8.80 ±0.74 μM).

Under high fibrinogen levels when 4N1K is present with syk inhibitor the value of peroxinitrite increased (14.74± 0.78 μM, $p < 0.001$) in relation to the samples without Syk (12.67 ±2.26 μM). In the same conditions but in relation to the samples without 4N1K (12.31 ±1.39 μM) the value of peroxinitrite increased (14.74 ±0.78 μM, $p < 0.005$).

4. Discussions

It was demonstrated by Huang *et al.* (2001) that erythrocyte membrane protein band 3 is responsible for the influx and efflux of nitric oxide. CD47 in the erythrocyte membrane was identified by De Oliveira *et al.* (2012) as the binding site for the soluble form of fibrinogen. The CD47 exist in the Rh complex that binds protein 4.2 which in turn establish interaction with protein band 3. From our results we can assume that any conformational change resulting from the CD47 binding to fibrinogen affects the nitric oxide metabolism increasing the concentration of nitrite, nitrate, GSNO and peroxinitrite remaining unchanged the NO efflux in relation to the control sample. The same profile of results has been previously observed by Lopes de Almeida *et al.* (2009).

We showed that the presence of high fibrinogen concentrations increase the erythrocyte NO efflux obtained in presence of phosphorylated band 3 (in presence of calpeptine) or dephosphorylated (presence of Syk inhibitor). So we confirmed the previous results obtained by Lopes de Almeida *et al.* (2011) that evidenced the phosphorylation status of protein band 3 as an influent factor in human nitric oxide efflux and mobilization, in an *in vitro* model of fibrinogenemia.

So, a modification done in one erythrocyte membrane leaf such as fibrinogen binding in the outer site or a modification in band 3 phosphorylation status induced in the inner site is communicated to the opposite side interfering in the nitric oxide signal transduction pathway. Adding the CD47 agonist peptide 4N1K to erythrocytes in presence of high fibrinogen levels it has been reported by Saldanha *et al.* (2012) increased concentrations of GSNO, peroxinitrite, nitrite and nitrate concentrations. Here in the present work we also observed the same tendency. The 4N1K stimulate the phosphorylation of non-SRC kinase Syk and SRC kinase Lyn that became activated (Brow and Frasier, 2001) and consequently phosphorylate the band 3 protein. It will be expected an increased of NO efflux but this was not observed. Until now it is not proved the effect of 4N1K on the enzyme activity of PTP that could favour or not the balance status of protein band 3 phosphorylation. Instead there was an increased in peroxinitrite (index of erythrocyte oxidation and presence of peroxide anion) concentration that can modulate the enzyme activity of Syk as stated by Mallosi *et al.* (2001). However this hypothesis needs to be clarified in order to contribute to a better understanding of the erythrocyte hemorheological properties. It was verified by Saldanha *et al.* (2007) a decreased tendency of the erythrocyte to aggregate when the balance between protein band 3 phosphorylation/ dephosphorylation is changed.

As mentioned above we are interested in studying the influence of the status of protein band 3 phosphorylation

in the NO metabolism when both fibrinogen and 4N1K are present. The results obtained in erythrocytes under high fibrinogen levels when 4N1K is present with syk inhibitor or with calpeptine, show increased significant concentrations of NO efflux, peroxynitrite, nitrite, nitrate and GSNO in relation to the samples control. We can say that the CD47 ligands fibrinogen and 4N1K and the modulators of the protein band 3 phosphorylation status interfere in the NO efflux and NO derivatives molecules.

In high fibrinogen levels the concentrations of erythrocyte nitrite and nitrate obtained in presence of Syk inhibitor and 4N1K or calpeptine and 4N1K are higher than those obtained in the presence of high fibrinogen levels and 4N1K. The protein band 3 phosphorylation status increases the levels of erythrocyte nitrite and nitrates when both CD47 ligands fibrinogen and 4N1K are present.

The values of GSNO and peroxinitrites obtained in erythrocytes under the presence of high fibrinogen levels plus Syk inhibitor and 4N1K are higher than those obtained in presence of high fibrinogen levels plus Syk inhibitor and also with those observed in samples with high fibrinogen levels plus 4N1K. At variance there are no significant differences in the values of GSNO, peroxinitrite, concentrations obtained in presence of high fibrinogen levels, 4N1K and calpeptine in relation to those obtained in higher fibrinogen levels plus 4N1K or in those with higher fibrinogen levels plus calpeptine.

So, the levels of erythrocyte GSNO and peroxinitrite under high fibrinogen levels and 4N1K are increased by the presence of Syk inhibitor but not by calpeptine. These results evidenced the overcome effect of the Syk inhibitor face to 4N1K maintaining less protein band 3 phosphorylated with consequences in the erythrocyte NO metabolism under fibrinogen high concentration. Recalling the phosphorylation process of band 3, tyrosine kinase Syk precedes the catalytic action of Lyn, as documented by Brunatti *et al.* (2000). Other apart kinase namely p59/61 ^{hck} (hck) belonging to the Src-family could also underlie protein band 3 phosphorylation as evidenced by Mallozzi *et al*. (2001). The increased levels of peroxinitrite are an indicator of the augmented peroxide anion concentration inside the erythrocyte resulting from the autoxidation of oxyhemoglin (Balagopalakrishna *et al.*, 1996). Our results raise the hypothesis that the binding of 4N1K peptide to CD47 is not able to stimulate the tyrosine kinase Syk and overcome the inhibition effect of Syk inhibitor. If the opposite will be verified, an increase of glycolysis with NADH formation will occur and consequently with activation of metahemoglobin redutase with decrease of metahemoglobin (index of autoxidation of haemoglobin) and lower peroxide anion generation (Weber *et al.* 2004). This mechanism needs to be verified as well as the identification of others molecules implicated in the 4N1K signal transduction mechanism underlying the NO efflux and mobilization inside the erythrocyte in this model in vitro of hyperfibrinogenemia. Also we planned to evaluate if the same behaviour will be verified with blood samples obtained from patients with hiperfibrinogenemia. After this study we may speculated that at high fibrinogen concentrations the elevated NO efflux from erythrocytes might be a balancing pathway to prevent too strong aggregation (of erythrocytes but also of thrombocytes, especially in veins).

All the results obtained until now and others to show in the future will contribute to understand the implications of the membrane components and second messengers like nitric oxide on the hemorheological properties of human erythrocytes.

5. Conclusions

We can conclude that the erythrocyte (i) CD47 ligands namely fibrinogen and 4N1K and the modulators of the membrane protein band 3 phosphorylation degree interferes in the NO efflux and NO derivatives molecules; (ii) protein band 3 phosphorylation status increases the levels of erythrocyte nitrite and nitrates when both CD47 ligands fibrinogen and 4N1K are present; in the *in vitro* model of hiperfibrinogenemia (iii) CD47 agonist peptide 4N1K induces erythrocyte NO mobilization in dependence of erythrocyte membrane protein band 3 phosphorylation status.

Acknowledgment

This study was supported by grants from the FCT—Fundação para a Ciência e a Tecnologia (project reference PTDC/SAU-OSM/73449/2006). The authors declare no conflict of interest.

References

Anong, W.A., T. Franco, H. Chu, T.L. Weis, E.E. Devlin, D.M. Bodine, X. An, N. Mohandas, and P.S. Low, 2009, *Blood* 114, 1904-1912.

Balagopalakrishna, C., P.T. Manoharan, O.O. Abugo, and J.M. Rifkind, 1996, *Biochem.* 35, 6393-6398.

Bordin, L., A.M. Brunati, A.D. Deana, B. Baggio, A. Toninello, and G. Clari, 2002, *Blood* 100, 276-278.

Brunati, A.M., L. Bordin, G. Clari, P. James, M. Quadroni, E. Baritono, L.A. Pina, and A.D. Deana, 2000, *Blood* 96, 1550-1557.

Campanella, M.E., H. Chu, and P.S. Low, 2005, *Proc. Natl. Acad. Sci. USA* 102, 2402-2407.

Carvalho, F.A., J.P. Almeida, I.O. Fernandes, T.F. Santos, and C. Saldanha, 2008, *Clin. Hemorheol. Microcirc.* 40, 207-227.

Carvalho, F.A., J.M. Silva, and C. Saldanha, 2004, *Biosens. Bioelectron.* 20, 505-508.

Carvalho, F.A., R. Mesquita, J.M.Silva, and C. Saldanha, 2004, *J. Appl. Toxicol.* 24, 419-427.

Cook, J.A., S.Y. Kim, D. Teague, M.C. Krishna, R. Pacelli, J.B. Mitchell, Y. Vodovotz, R.W. Nims, D. Christodoulou, A.M. Miles, M.B. Grisham, and D.A. Wink, 1996, *Anal. Biochem.* 238, 150-158.

Dahl, K.N., R. Parthasarathy, M. Westhoff, D.M. Layton, and D.E. Discher, 2004, *Blood* 103, 1131-1136.

de Almeida, J.P.L., T.F.Santos, and C. Saldanha, 2011, *Clin. Hemorheol. Microcirc.* 49, 407-416.

de Oliveira, S. and C. Saldanha, 2010, *Clin. Hemorheol Microcirc.* 44, 63-74.

de Oliveira, S., A.S.S. Herdade, and C. Saldanha, 2008, *Clin. Hemorheol. Microcirc.* 39, 363-373.

de Oliveira, S., V. de Almeida, A. Calado, H.S. Rosário, and C. Saldanha, 2012, *Biochem. Biophys. Acta* 1818, 481-490.

Galli, F., R. Rossi, P.D. Simplicio, A. Floridi, and F. Canestrari, 2002, *Nitric Oxide* 6, 186-199.

Gross, S.S., 2001, *Nature* 409, 577-588.

Guevara, I.I., J. Wanejko, A.D. Kieæ, J. Pankiewicz, A. Wanat, P. Anna, I. Go³abek, S. Bartucœ, M.M. Malec, and A. Szczudlik, 1998, *Clin. Chim. Acta* 274, 177-188.

Huang, K.T., T.H. Han, D.R. Hyduke, M.W. Vaughn, H. van Herle, T.W. Hein, C. Zhang, L. Kuo, and J.C. Liao, 2001, *Proc. Natl. Acad. Sci. USA* 98, 11771-11776.

Huie, R. and S. Padmaja, 1993, *Free Radic. Res. Commun.* 18, 195-199.

Ignaro, L.J., G.M. Buga, K.S. Wood, R.E. Byrns, and G. Chaudhuri, 1987, Endothelium-derived relaxing factor produced and released from artery and vein is nitric oxide, *Proc. Natl. Acad. Sci. USA* 84, 9265-9269.

Jiang, J., N. Magilnick, K. Tsirulnikov, N. Abuladze, I. Atanasov, P. Ge, M. Narla, A. Pushkin, Z.H. Zhou, and I. Kurtz, 2013, *PLoS One* 8, e55408.

Mallosi, C., M.A.D. Stasi, and M. Minetti, 2001, *Free Rad. Biol. Med.* 30, 108-117.

May, J.M., Z.C. Qu, L. Xia, and C.E. Cobb, 2000, *Am. J. Physiol. Cell Physiol.* 279, C1946-C1954.

McMahon, T.J., A.E. Stone, J. Bonaventura, and J.S. Stamler, 2000, *J. Biol. Chem.* 275, 16738-16745.

Murphy, M. and H. Sies, 1991, *Proc. Natl. Acad. Sci. USA* 88, 10860-10864.

Pawloski, R., D.T. Hess, and J.S. Stamler, 2005, *Proc. Natl. Acad .Sci.USA* 102, 2531-2536.

Possel, H., H. Noack, W. Augustin, G. Keilhoff, and G. Wolf, 1997, *FEBS Letters* 416, 175-178.

Rampling, M.W., 1998, *Clin. Hemorheol. Microcirc.* 19, 129-32.

Saldanha, C., T. Freitas, and de Almeida J.P.L., Program and Abstract Book of the XXIInd International Fibrinogen Workshop 4th - 6th July 2012, Brighton, 77.

Saldanha, C., A.S. Silva, S. Gonçalves, and J.M. Silva, 2007, *Clin. Hemorheol. Microcirc.* 36, 183-194.

Saldanha, C., 2013, *Clin. Hemorheol. Microcirc*. 53, 39-44.

Sargento, L., C. Saldanha, J. Monteiro, C. Perdigão, and J.M. Silva, 2005, *Thromb. Haemost.* 94, 380-388.

Stamler, J.S., L. Jia, J.P. Eu, T.J., McMahon, I.T. Demchenko, J. Bonaventura, K. Gernert, and C.A. Piantadsoi, 1997, *Science* 276, 2034-2037.

Wang, X.Q. and W.A. Frazier, 1998, *Mol. Biol. Cell* 9, 865-874.

Weber, R.E., W. Voelter, A. Fago, H. Echner, E. Campanella, and P.S. Low, 2004, *Am. J. Physiol. Regul. Integr. Comp. Physiol.* 287, 454-464.

Clinical & Experimental Pharmacology

Saldanha and Silva-Herdade, Clin Exp Pharmacol
2014, 4:3
http://dx.doi.org/10.4172/2161-1459.1000159

Commentary OpenAccess

The Ubiquity Nature of Acetylcholine

Carlota Saldanha* and Ana Silva-Herdade

Instituto de Bioquímica, Instituto de Medicina Molecular, Faculdade de Medicina da Universidade de Lisboa, Portugal

***Corresponding author:** Carlota Saldanha, Av Prof Egas Moniz 1649-028 Lisboa, Portugal, Tel: 351217922600; E-mail: carlotasaldanha@fm.ul.pt

Received: April 26, 2014; **Accepted:** May 27, 2014; **Published:** June 3, 2014

Background

Acetylcholine (ACh) was viewed as the "vagusstoff" after Loewi`s experiment with the frog heart [1]. In 1936 Otto Loewi, and Henry Dale were recipients of the Nobel Prize in Physiology and Medicine, by their contribution for the acetylcholine discover as a neurotransmitter [1]. So, ACh was regarded as a neurotransmitter during several decades [2]. After that it was evidenced a widespread expression of the cholinergic system within a variety of non-neuronal tissues. The "Non-Neuronal Cholinergic System" (NNCS) is well established as the extra-neural effects of acetylcholine [3]. Beyond these neural and non neuronal cholinergic systems there is another one named by Tracey et al. as the Cholinergic Anti-Inflammatory Pathway (CAIP) [4]. Afferent and efferent signals transmitted in the vagus nerve are components of a neural circuit that modulates the innate immune response. The CAIP could be considered as a liaison between the cholinergic neural system and NNCS.

The enzymes implicated in the synthesis and responsible for hydrolysis of ACh in different mammalian cells are isoenzymes of Choline-Acetyltransferase (ChAT), and Acetylcholinesterase (AChE) respectively [5]. ACh is synthesised in the nerve cell from choline and acetyl-CoA by a process mediated by choline acetyltransferase and is stored in vesicles in pre-synaptic neurons [2]. Upon arrival of the nerve impulse, a membrane depolarisation is induced and ACh is released to the synaptic cleft. At postsynaptic membrane, ACh binds to its cholinergic receptor, initiating a cascade of actions that are stopped by the enzyme AChE, which hydrolyses ACh to Choline (Ch) and acetic acid [2].

Non-Neuronal Cholinergic System (NNCS)

Circulating acetylcholine can be produced by T-lymphocytes and endothelial cells [6,7].

Lymphocytes express most of the cholinergic elements and upon interaction with the antigen presenting cells or the endothelial cells, T cells synthesize and release acetylcholine [8]. The autocrine ACh action depends on cell membrane receptor and in case of TCR/CD3 receptors for example enhances the expression of both ChAT and M5 mACh receptors [8].

At the vascular wall the ACh produced by the endothelium acts through the auto-paracrine fashion in the intrinsic intima, [5]. All the neuronal components, ACh, ChAT and VAChT and AChE above mentioned, are also present in the NNCS [9].

We are the first to perform the biochemical characterization of the AChE in endothelial cell membrane of human umbilical vein. We have identified, with C-terminal anti-AChE, the expression of one molecular form membrane with 70 kDa, (the molecular mass characteristic of the human monomeric form of AChE). When the N-terminal anti-AChE was used two molecular forms with approximately 66 kDa and 77 kDa are expressed at membrane bound level [10]. The molecular form of 70 kDa is also expressed at cytoplasm and nuclear compartments, where the latter also expressed an AChE isoform with approximately 55 kDa [11]. We verified that the nuclear expression is not endothelial cell-specific but is also evidenced in non-neuronal and neuronal cells [11].

The widespread expression of non-neuronal acetylcholine is accompanied by the ubiquitous presence of acetylcholinesterase and nicotinic/muscarinic receptors. Red blood cells account for the blood elements with highest expression of membrane-bound acetylcholinesterase [12]. The enzyme AChE has the particularity to be inhibited by high concentrations of its own substrate, ACh. So, different types of enzyme complexes may be presented namely, active, inactive and less active ones according the amount of ACh existent [13].

Fuji and co-workers quantified the levels of ACh in plasma and blood at normal physiological conditions, and verified differences of its amount among animal species [14].

The circulating ACh induces vasodilation in dependence of integrity of the endothelium via the Nitric Oxide (NO) synthesised and released to smooth muscle [15,16]. Also the NO released from endothelial cells can move to the lumen of the vessels where is scavenged by erythrocyte and free hemoglobin present in the blood circulation [17]. The NO-Heme Hemoglobin adduct (HbFe (II) NO) has been detected during NO inhalation therapy used for pulmonary hypertension relief, but it also occurs when deoxygenated blood enters into a vascular bed in which NO is produced such as the pulmonary circulation [18,19].

Low tissue oxygen tension is perceived by erythrocytes with induced hemoglobin structural allosteric transitions favouring the transfer of its NO bound molecule to band 3 that allow the NO efflux to the tissues in the capillary bed [20,21]. Among the heterotrophic effectors of oxygen binding hemoglobin, NO binds to the thiol group of cysteine β93 at high tissue oxygen tension. At low tissue oxygen tension there is a NO release from either S-nitrosothiol of the S-nitrosated hemoglobin or from the reduction of the anion nitrite to NO in a non exclusive way [22,23]. It is known that the T state of SNO-Hb promotes the transnitrosation by which NO groups are transferred to thiol acceptors biomolecules in RBCs [24]. One of these is the protein band 3 [25], but the exact mechanism by which NO escape from erythrocyte membrane still remain uncertain.

We have verified that in presence of ACh there is an increased of the erythrocyte deformability, of the nitrite and nitrate concentration and the oxygen hemoglobin affinity and a decreased of erythrocyte aggregation [26,27].

The lower erythrocyte deformability expressed in blood samples obtained from hypertensive, hypercholesterolemic and kidney

transplant patients was ameliorate when in presence of ACh as we verified by studies conducted *in vitro* [28].

Non-neuronal acetylcholine appears to be involved in the regulation of elementary cell functions such as cell mitosis, cell-cell interaction, cell automaticity, locomotion, ciliary activity, barrier function, resorption and secretion [29-33]. In the airways, for instance, the great majority of cells express the components of NNCS and it is documented that a substantial increase on ACh levels triggers the release of proinflammatory effectors [34]. In addition, the excitability of airway mast cells can be powerfully inhibited by acetylcholine [35].

The cholinergic Anti-Inflammatory Pathway (CAIP)

The vagus nerve innervates major organs, including the spleen and the gut, regulates physiological responses to stress, injury and infection. It was observed that the action potential transmitted in sensory nerve fibers to the brain reports the presence of inflammatory stimuli in peripheral issues [14].

The electric stimulation of the vagus nerve enhances the release of acetylcholine from the spleen [36]. Several studies using immumohistochemistry, electron micrsoscopy and neurophysiological techniques [37,38] demonstrate communication between the nerve endings and the T cells, B cells and macrophages that lead to anti-inflammatory signals through the efferent vagus nerve. Tracey et al. based on his work proposes the cholinergic anti-inflammatory pathway [39-41]. It consists in the activation of adrenergic neurons in the spleen that liberate nor- epinephrine near the T cell capable to secrete acetylcholine. This pathway plays a critical role in controlling the inflammatory response through ACh interaction with peripheral $\alpha 7$ subunit – containing nicotinic acetylcholine receptors expressed on macrophages which suppress the synthesis and secretion of inflammatory cytokines. Macrophages act as an interface between the brain and the immune system [4] by the participation of its JaK2/STAT3 signal pathway or via inhibition of the transcription factor NF-kB [42,43]. So, a crosstalk is established between the immune system and the central nervous system that contribute for the reposition of homeostasis in the former.

The activation of afferent vagus nerve by endotoxin or pro-inflammatory cytokines stimulates hypothalamic-pituitary-adrenal anti-inflammatory responses conducted by the efferent vagus nerve [44].

Acetylcholine is an anti-inflammatory molecule that suppresses the production of pro-inflammatory cytokines [3] suggesting that the neuronal activation of the adrenergic system, for example in spleen, release nor-epinephrine from the efferent fibers near T cells which became able to liberate non neuronal acetylcholine. In consequence this ACh interacts with $\alpha 7$ nAChR expressed on cytokine production macrophages. The extraneuronal cholinergic system in lymphocytes is responsible for the levels of acetylcholine in blood circulation [6]. In the case for example of nicotine application it generates complex effects in dependence of the route or local of its administration [45,46].

In vivo Experimental Studies of the Effects of ACh in Inflammatory Response

The study done by Silva-Herdade and Saldanha was conducted *in vivo* on an animal model of Lipopolysaccharide (LPS) induced inflammation aimed to evaluate the effects of ACh on the leukocyte-endothelial cells interactions and to quantify the concentrations of TNF-alpha in blood circulation. Using intravital microscopy the number of rolling and adherent leukocytes in post-capillary venules of Wistar rats was registered after the intravenously administration of LPS alone or with further addition of ACh. Those results evidenced the anti-inflammatory effect of ACh showed by a decrease in TNF-alpha plasma levels and by the decrease of the number of adherent leukocytes [47]. Taking in consideration the non neuronal origin of ACh that we mimesis in these *in vivo* studies we cannot exclude with sure the participation of the cholinergic anti-inflammatory pathway when LPS was administered.

In a previous study the same authors using the same animal model protocol but without induced inflammation showed decrease of the number of rolling and adherent leukocytes while the rolling velocity was reduced without changes in plasma levels of IL-1-beta [48].

We conclude that ACh has an anti inflammatory effect decreasing the concentration of TNF-alpha in plasma and the adhesion of the leukocytes to the endothelial cells that is one of the former steps in the inflammatory innate response. The acute inflammatory state implicated by the surgery show also the anti inflammatory action of ACh that left unchanged IL-1-beta.

Conclusions

Apart from the former discovers of the neuronal action of acetylcholine much more different cellular locals of synthesis of ACh are evidenced which implicate diverse biological effects conferring its ubiquitous molecular behavior. For instance its ubiquity is different from that of coenzyme Q which moves inside the inner mitochondrial membrane occupying diverse places closer or away from one complex of the electron chain but with the same oxi-reduction function.

Acetylcholine acts in the parasympathetic system, in the neuron muscle junction, in the T-lymphocytes, in endothelial cells, in erythrocytes demonstrate the ability to bind and be recognized by a different membrane cell types. ACh induces in the endothelium the NO synthesis; when within the airway epithelium ACh is involved in the regulation of water and ion transport; acts as anti inflammatory agent when liberate by T-cell activation increasing its concentration in blood circulation. In general terms, the biochemistry point of view that the structure of one biomolecule dictates its physiological function has been enlarged by a multitude of actions and effects resulting from the signal transduction pathway associated with their different kind of receptors or with the same type of receptors in distinct cells.

References

1. Wittaker VP (1963) Cholinergic neurohormones. Comp Endocr 2: 182-208.
2. Michelson MJ, Zeimal EV (1973) Acetylcholine An approach to the molecular mechanism of action. Pergamon Press, Oxford, USA.
3. Wessler I, Kirkpatrick CJ (2008) Acetylcholine beyond neurons: the non-neuronal cholinergic system in humans. Br J Pharmacol 154: 1558-1571.
4. Pavlov VA, Wang H, Czura CJ, Friedman SG, Tracey KJ (2003) The cholinergic anti-inflammatory pathway: a missing link in neuroimmunomodulation. Mol Med 9: 125-134.
5. Wessler I, Kirkpatrick CJ, Racké K (1999) The cholinergic 'pitfall': acetylcholine, a universal cell molecule in biological systems, including humans. Clin Exp Pharmacol Physiol 26: 198-205.
6. Kawashima K, Fujii T (2000) Extraneuronal cholinergic system in lymphocytes. Pharmacol Ther 86:29-48.

Clin Exp Pharmacol
ISSN:2161-1459 CPECR, an open access journal

Volume 4 • Issue 3 • 1000159

7. Kawashima K, Fujii T, Watanabe Y, Misawa H (1998) Acetylcholine synthesis and muscarinic receptor subtype mRNA expression in T-lymphocytes. Life Sci 62: 1701-1705.
8. Kawashima K, Fujii T (2003) The lymphocytic cholinergic system and its contribution to the regulation of immune activity. Life Sci 74: 675-696.
9. Grando SA, Kawashima K, Kirkpatrick CJ, Wessler I (2007) Recent progress in understanding the non-neuronal cholinergic system in humans. Life Sci 80: 2181-2185.
10. Carvalho FA, Graça LM, Martins-Silva J, Saldanha C (2005) Biochemical characterization of human umbilical vein endothelial cell membrane bound acetylcholinesterase. FEBS J 272: 5584-5594.
11. Santos SC, Vala I, Miguel C, Barata JT, Garção P, et al. (2007) Expression and subcellular localization of a novel nuclear acetylcholinesterase protein. J Biol Chem 282: 25597-25603.
12. Wright DL, Plummer DT (1973) Multiple forms of acetylcholinesterase from human erythrocytes. Biochem J 133: 521-527.
13. Saldanha C (1985) Acetylcholinesterase Contribution for the kinetic study of the human erythrocyte enzyme. PhD Thesis, Universidade Nova de Lisboa, Portugal.
14. Fujii T, Yamada S, Yamaguchi N, Fujimoto K, Suzuki T, et al. (1995) Species differences in the concentration of acetylcholine, a neurotransmitter, in whole blood and plasma. Neurosci Lett 201: 207-210.
15. Furchgott RF, Vanhoutte PM (1989) Endothelium-derived relaxing and contracting factors. FASEB J 3: 2007-2018.
16. Zhou Y, Varadharaj S, Zhao X, Parinandi N, Flavahan NA, et al. (2005) Acetylcholine causes endothelium-dependent contraction of mouse arteries. Am J Physiol Heart Circ Physiol 289: H1027-1032.
17. Vaughn MW, Huang KT, Kuo L, Liao JC (2000) Erythrocytes possess an intrinsic barrier to nitric oxide consumption. J Biol Chem 275: 2342-2348.
18. Ignarro LJ, Byrns RE, Buga GM, Wood KS (1987) Endothelium-derived relaxing factor from pulmonary artery and vein possesses pharmacologic and chemical properties identical to those of nitric oxide radical. Circ Res 61: 866-879.
19. Sonveaux P, Lobysheva II, Feron O, McMahon TJ (2007) Transport and peripheral bioactivities of nitrogen oxides carried by red blood cell hemoglobin: role in oxygen delivery. Physiology (Bethesda) 22: 97-112.
20. Lane P, Gross S (2002) Hemoglobin as a chariot for NO bioactivity. Nat Med 8: 657-658.
21. Han TH, Qamirani E, Nelson AG, Hyduke DR, Chaudhuri G, et al. (2003) Regulation of nitric oxide consumption by hypoxic red blood cells. Proc Natl Acad Sci U S A 100: 12504-12509.
22. Nagababu E, Ramasamy S, Abernethy DR, Rifkind JM (2003) Active nitric oxide produced in the red cell under hypoxic conditions by deoxyhemoglobin-mediated nitrite reduction. Journal Biological Chemistry 278: 46349-46356.
23. Stamler JS, Jia L, Eu JP, McMahon TJ, Demchenko IT, et al. (1997) Blood flow regulation by S-nitrosohemoglobin in the physiological oxygen gradient. Science 276: 2034-2037.
24. Jia L, Bonaventura C, Bonaventura J, Stamler JS (1996) S-nitrosohaemoglobin: a dynamic activity of blood involved in vascular control. Nature 380: 221-226.
25. Pawloski JR, Hess DT, Stamler JS (2005) Impaired vasodilation by red blood cells in sickle cell disease. Proc Natl Acad Sci U S A 102: 2531-2536.
26. Mesquita R, Pires I, Saldanha C, Martins-Silva J (2001) Effects of acetylcholine and spermineNONOate on erythrocyte hemorheologic and oxygen carrying properties. Clin Hemorheol Microcirc 25: 153-163.
27. Carvalho FA, Mesquita R, Martins-Silva J, Saldanha C (2004) Acetylcholine and choline effects on erythrocyte nitrite and nitrate levels. J Appl Toxicol 24: 419-427.
28. Carvalho FA, Maria AV, Braz Nogueira JM, Guerra J, Martins-Silva J, et al. (2006) The relation between the erythrocyte nitric oxide and hemorheological parameters. Clin Hemorheol Microcirc 35: 341-347.
29. Sastry BV, Sadavongvivad C (1978) Cholinergic systems in non-nervous tissues. Pharmacol Rev 30: 65-132.
30. Wessler I, Kirkpatrick CJ, Racké K (1998) Non-neuronal acetylcholine, a locally acting molecule, widely distributed in biological systems: expression and function in humans. Pharmacol Ther 77: 59-79.
31. Kirkpatrick CJ, Bittinger F, Unger RE, Kriegsmann J, Kilbinger H, et al. (2001) The non-neuronal cholinergic system in the endothelium: evidence and possible pathobiological significance. Jpn J Pharmacol 85: 24-28.
32. Wessler I, Kilbinger H, Bittinger F, Unger R, Kirkpatrick CJ (2003) The non-neuronal cholinergic system in humans: expression, function and pathophysiology. Life Sci 72: 2055-2061.
33. Grando SA, Kawashima K, Kirkpatrick CJ, Wessler I (2007) Recent progress in understanding the non-neuronal cholinergic system in humans. Life Sci 80: 2181-2185.
34. Wessler I, Bittinger F, Kamin W, Zepp F, Meyer E, et al. (2007) Dysfunction of the non-neuronal cholinergic system in the airways and blood cells of patients with cystic fibrosis. Life Sci 80: 2253-2258.
35. Wessler IK, Kirkpatrick CJ (2001) The Non-neuronal cholinergic system: an emerging drug target in the airways. Pulm Pharmacol Ther 14: 423-434.
36. Brandon KW, Rand MJ (1961) Acetylcholine and the sympathetic innervation of the spleen. J Physiol 157: 18-32.
37. Niijima A, Hori T, Aou S, Oomura Y (1991) The effects of interleukin-1 beta on the activity of adrenal, splenic and renal sympathetic nerves in the rat. J Auton Nerv Syst 36: 183-192.
38. Niijima A, Hori T, Katafuchi T, Ichijo T (1995) The effect of interleukin-1 beta on the efferent activity of the vagus nerve to the thymus. J Auton Nerv Syst 54: 137-144.
39. Borovikova LV, Ivanova S, Zhang M, Yang H, Botchkina GI, et al. (2000) Vagus nerve stimulation attenuates the systemic inflammatory response to endotoxin. Nature 405: 458-462.
40. Tracey KJ, Czura CJ, Ivanova S (2001) Mind over immunity. FASEB J 15: 1575-1576.
41. Tracey KJ (2002) The inflammatory reflex. Nature 420: 853-859.
42. de Jonge WJ, van der Zanden EP, The FO, Bijlsma MF, van Westerloo DJ, et al. (2005) Stimulation of the vagus nerve attenuates macrophage activation by activating the Jak2-STAT3 signaling pathway. Nat Immunol 6: 844-851.
43. Wang H, Liao H, Ochani M, Justiniani M, Lin X, et al. (2004) Cholinergic agonists inhibit HMGB1 release and improve survival in experimental sepsis. Nat Med 10: 1216-1221.
44. Watkins LR, Goehler LE, Relton JK, Tartaglia N, Silbert L, et al. (1995) Blockade of interleukin-1 induced hyperthermia by subdiaphragmatic vagotomy: evidence for vagal mediation of immune-brain communication. Neurosci Lett 183: 27-31.
45. Miao FJ, Jänig W, Levine JD (1997) Vagal branches involved in inhibition of bradykinin-induced synovial plasma extravasation by intrathecal nicotine and noxious stimulation in the rat. J Physiol 498 : 473-481.
46. Miao FJ, Benowitz NL, Levine JD (2001) Endogenous opioids suppress activation of nociceptors by sub-nanomolar nicotine. Br J Pharmacol 133: 23-28.
47. Silva-Herdade AS, Saldanha C (2013) Effects of acetylcholine on an animal mode of inflammation. Clin Hemorheol Microcirc 53: 209-216.
48. Silva AS, Saldanha C, Martins e Silva J (2007) Effects of velnacrine maleate in the leukocyte-endothelial cell interactions in rat cremaster microcirculatory network. Clin Hemorheol Microcirc 36: 235-246.

Biosensors **2014**, *4*, 1-17; doi:10.3390/bios4010001

OPEN ACCESS

biosensors

ISSN 2079-6374

www.mdpi.com/journal/biosensors/

Review

Application of a Nitric Oxide Sensor in Biomedicine

Carlota Saldanha [1,*], José Pedro Lopes de Almeida [1,2] and Ana Santos Silva-Herdade [1]

[1] Instituto de Bioquímica, Instituto de Medicina Molecular, Faculdade de Medicina de Lisboa, Edifício Egas Moniz, Av. Prof. Egas Moniz, 1649-028 Lisboa, Portugal; E-Mails: jpedro.gla@gmail.com (J.P.L.A.); anarmsilva@fm.ul.pt (A.S.S.-H.)

[2] Servico de Imunoalergologia, Centro Hospitalar Lisboa Norte-Hospital de Santa Maria, 1649-028 Lisboa, Portugal

***** Author to whom correspondence should be addressed; E-Mail: carlotasaldanha@fm.ul.pt; Tel.:+351-91-8985450; Fax: +351-21-7999477.

Received: 19 December 2013; in revised form: 21 January 2014 / Accepted: 23 January 2014 / Published: 4 February 2014

Abstract: In the present study, we describe the biochemical properties and effects of nitric oxide (NO) in intact and dysfunctional arterial and venous endothelium. Application of the NO electrochemical sensor *in vivo* and *in vitro* in erythrocytes of healthy subjects and patients with vascular disease are reviewed. The electrochemical NO sensor device applied to human umbilical venous endothelial cells (HUVECs) and the description of others NO types of sensors are also mentioned.

Keywords: endothelium erythrocyte nitric oxide; microelectrode

1. Introduction

Nitric oxide (NO) is a soluble gas synthesized from L-arginine by the enzyme nitric oxide synthase (NOS) [1]. Three isoforms of NOS have been described, namely the neuronal (nNOS or NOSI), the inducible (NOSII or iNOS), and the constitutive endothelial form (eNOS or NOSIII), which was the first to be discovered [1–3]. Both neuronal and endothelial enzymes are activated by the calcium and calmodulin complex, and the inducible form binds to calmodulin but is independent of intracellular calcium concentration [4]. These isoenzymes are flavoproteins that act on L-arginine, in the presence of oxygen and NADPH, and require tetrahydrobiopterin (BH4). In the absence of BH4, a superoxide

anion is formed instead of NO [5]. The isoform eNOS is also expressed in platelets and in cardiac myocytes [6,7].

NO produced in the endothelial cell diffuses to the lumen where it is captured by red blood cells (RBC) and transferred into muscle cells where it induces relaxation, eliciting vasodilation. In this mechanism, guanosine 3′,5′-cyclic monophosphate (cGMP), formed from guanosine 5′-triphosphate (GTP) by the action of guanylate cyclase (GC), is activated by NO [3]. cGMP modulates the myosin light chain (MLC) phosphatase positively and MLC kinase negatively, resulting in the dephosphorylation of MLC with subsequent muscle relaxation [3]. NO-induced vasodilation is dependent on hematocrit, blood flow and the hemoglobin free concentration in the circulation [8]. The presence of free hemoglobin reduces vasodilation in pig coronary arteries, induced previously by serotonin or by shear stress [8]. The increase in vascular permeability, inhibition of platelet aggregation, platelet adhesion, proliferation, and migration of smooth muscle cells are effects mediated by NO-dependent cGMP [9].

The intact vascular endothelium establishes a dynamic interface between blood and tissues, allowing gas and metabolites exchanges and participates in hemostasis, in thrombosis, and in inflammatory and anti-inflammatory mechanisms [10,11]. The phenotype of endothelial cells is dependent on the location in the vascular field and presents specific responses to various stimuli [11]. Endothelial cells of post capillary venules respond to inflammatory signals and those in the arterial vascular network release vasoactive substances into the blood [11]. Among the endogenous vasoactive compounds, acetylcholine (ACh) acts like an autocrine or paracrine signal in endothelial cells, stimulating eNOS, with the formation of NO [1,3].

The rapid time course of these events and the short half-life of NO includes several methods, based on electrochemical, chemiluminiscent, and spectrophotometric principles, which have been developed in order to measure NO or its derivative molecules. The method must be sensitive for *in situ* measurements. NO microsensors have been developed for real time assessment *in vivo* [12–14]. The real time measurement of NO, in response to stimuli and drugs, will contribute to therapeutic advances in endothelial dysfunction.

2. Nitric Oxide Sensors

The utilization of NO sensors allows the quantification of NO concentration ranging from subnamolar to micromolar values [15]. Usually, the biosensor consists of a biorecognition element, a signal transducer and a detector. The electrochemical sensors are, for now, the more reliable tool for NO detection in real time. They operate via the application of a potential at the electrode surface positive or negative to electrochemically oxidize or reduce NO. The resulting transfer of electrons is measured as a current proportional to the NO concentration.

Our studies of NO measurement in human erythrocytes suspensions were performed with the amiNO-IV sensor (Innovative Instruments Inc., Tampa, FL, USA) [16]. The figure of the electrode can be seen in the webpage: http://www.2in.com.

The sensor has a sharp metallic tip completely covered with a series of membrane, including a gas permeable membrane. The ―amiNO‖ series of nitric oxide sensors, with tip diameter ranges of 7 µm to 600 µm, do not require an external reference electrode has high sensitivity abolishing the errors due to baseline drift associated with temperature changes and they are shielded from electrical noise. They

were designed for *in vivo* and large surfaces (cultured cells), works with the inNO-T meter with easy calibration procedures. The inNO-Tcombine both a NO configured potentiostat and a software controlled data acquisition system included in one battery powered unit. The ─amiNO‖ series sensor is covered with a triplecoat gas permeable membrane to guarantee selectivity and fast response time. The NO diffuses through the membrane and is then oxidized at the working platinum electrode, resulting in an electric current. The redox current is proportional to the NO concentration outside the membrane and is continuously monitorized with an inNO-TM software (version 1.9 supplied by Innovative Instruments Inc.) installed on a PC computer. The calibration curve and its representative appear in Figure 1 of our published previous work [16]. Briefly, the sensor is calibrated by a simple, economical, and a reliable chemical reaction for NO production. This reaction is based on the conversion of nitrite to nitric oxide in acidic solution in the presence of iodide ion. The reaction has a ratio of one to one, meaning that the amount of NO produced in this reaction equal to the amount of nitrite added.

The amino-IV sensor with its NO-permeable membrane triplecoat avoid a broad range of interfering molecules forming during the electrochemical reaction of NO on metal surfaces at positive electrode potentials via electron oxidation mechanism: Alloys of platinum [17], carbon fibber [18], and glassy carbon [19] are materials additionally developed to cover the surface of the electrodes that show variable sensitivity, selectivity, and signal stability [20–23].

The most common modes of electrode operate are by electroreduction of NO, direct electrooxidation of NO and catalytic electrooxidation of NO [20–23]. The electroreduction has the advantage to eliminate the interfering molecules but, at variance, has low sensitivity and pH and electrode surface characteristics dependence [24–26]. In these types of electrode oxygen molecules interferes and is a problem in biological applications due to its scavenger properties as mentioned in the previous sections. In the electrode operate by electroreduction of NO the introduction of a transition metal or metalloproteins such as haemoglobin have proven to be useful to improve sensitivity and measurements of NO at low range of sub-micromolar concentrations [24,25].

In the electrode operate by the direct electrooxidation of NO there are broad types of sensors with different electrode material composition of NO-selective membranes, and diverse diameters originating a large variety of values of limit of detection ranging from 0.083 nM to 75 nM [27,28]. Thus, they are dependent on the permselective membrane. In the type of electrode that operates by catalytic electrooxidation of NO a redox mediator for example a metalloporphyrins immobilized on the electrode surface or incorporated in a polymer is utilized [18]. The function of the mediator is to acts as catalysts for the oxidation of NO. However, non-porphyrin complexes have showed also similar results [29].

The sensors descried in the literature to measure NO in solution are classified as belonging to three classes as follows: Shibuki-style; solid permselective; and solid catalytic and their characteristics and composition are summarized in the Table 1 [20,30]. The first one style of sensor determine NO by electrooxidation and the others two by electrooxidation or electroreduction [20,30]. All the three types of sensors integrate a reference electrode that is within the electrolyte filling solution in the Shibuki-style. The catalytic style comprise a mediator (metalloporphyrins or metal phtalocyanines) for catalyze the oxidation or reduction of NO.

While sensors applied to *in vivo*, NO measurements in blood has confined in humans [31] others for determinations of NO released in biological tissues like heart, brain, or lung are used only in animal

experimental models [32–34]. For example an electrochemical microsensor has been inserted into a human hand vein to detect NO in blood vessels of healthy persons [31]. It is confirmed *in vivo*, in human beings, that the endothelium derived relaxing factor is the NO from the stimulation with ACh [31].

Table 1. Characteristics and composition of nitric oxide sensors.

Sensor class	Internal filling solution	Composition	Sensitivity	Miniturization
Shibuki-style	Electrolyte	Platinum and silver	Variable over time and between sensors	Not possible
Solid permselective	Eliminated	Carbon	Multiple membranes discriminate interference molecules	Possible
Solid catalytic	Eliminated	Mediator incorporated in electrode surface or in permselective membrane	Minimize interference molecules	Possible

3. Nitric Oxide in Arterial Endothelium

The vasoactive function of ACh could be compromised by the erythrocyte aggregation tendency that is increased in a few vascular disorders including hypercholesterolemia, arterial hypertension, acute myocardial infarction, and diabetes [35–38].

The vascular endothelium is dysfunctional when it is not able to regulate its tone to maintain structural organization contributing to the installation and progression of hypertension and atherosclerosis [11,39]. These arterial diseases are considered cardiovascular risk factors and are associated with stimulation of NAPH oxidase and generation of reactive oxygen species [40,41]. Dismutation of the superoxide anion hydrogen peroxide is formed, stimulating the expression of eNOS that was verified to be associated with these two cardiovascular risk factors [42,43]. In this case, NO production is insufficient to overcome consumption by superoxide anion with the generation of peroxynitrite that deregulates (uncouples) eNOS, switching to the production of superoxide anion instead of NO [44].

Vasodilation of the vessels fails to appear by lower concentrations of NO, which support platelet and leukocyte adhesion stimulating the inflammatory response in the pathogenesis and progression of atherosclerotic disease [45]. Its etiology is recognized as complicated and multi-factorial [45]. Thus, any manipulations of the pathway of eNOS appear to be promising treatments [46,47].

In the composition of the atheromatous plaque there are muscle cells, macrophages that are in the apoptotic state and are ingested by phagocytes, which decrease the inflammatory response and plaque regression [48]. Pro-apoptotic functions and anti-atherogenic properties of NO are important, along with destabilization of the plaque, which could occur due to enhancement of muscle cell apoptosis induced by NO [48]. The most effective way to increase NO synthesis is by adaptation to hypoxia that is observed in hypertensive stage 1 patients characterized by decreased concentrations of NO [49,50]. Patients with grade 1 hypertension submitted to intermittent conditions of normobaric and hypoxia normalize blood pressure and NO synthesis [50].

The constant presence of hypoxia can lead to decreased synthesis of NO and in turn to the onset of pulmonary arterial hypertension. Inhaled ethyl nitrite has shown promising results in neonates with

pulmonary hypertension [51]. Inhibitors of the enzyme phosphodiesterase that catalyze the decomposition of cGMP may be an alternative therapy to the inhalation of NO applied in pulmonary hypertension [52,53]. Nitroglycerin (GTN) acts by inducing vasodilation independent of the endothelium and is used as a therapeutic agent in coronary artery disease with some conditions [54]. Chronic use of NTG regress NO levels and maintains endothelial dysfunction [54].

There are many exogenous compounds leading to nitric oxide availability including nitrite, S-nitrosothiols, N-nitroso-proteins, and iron nitrosyl complexes [55]. Nonsteroidal anti-inflammatory compounds (NSAID) related to derivatives of NO molecules have been synthesized to verify its effectiveness as NO donors and as cardioprotective agents [56]. Among the NSAIDs, aspirin derivatized with NO donors decreases intestinal toxicity and stimulates the eNOS enzyme in a pulsatile manner [56,57]. The statins, the type 1 receptor blockers of angiotensin II and estrogen, increase the synthesis of tetrahydrobiopterin. Statins also inhibit NADPH oxidase and protect the cofactor from oxidation induced by eNOS [58]. Polyphenols present in red wine, by inhibiting the overexpression of NAPH oxidase reduce oxidative stress and protect endothelial cells by maintenance of the basal level of NO, reducing the tendency of peroxinite formation [59].

Patients with depression have diminished levels of the natural substrate of NO, L-arginine; it is estimated that depression can lead to the onset of coronary artery disease (CAD) [60]. However, whether supplementation of L-arginine provides improvement for CAD is unknown [60]. It is known that a diet with high levels of black beans, endive, and spinach can be a source of nitrate that gives nitrites in the salivary-enteric circulation, following a sequence of catalysis reaction involving acidic oxides of nitrogen that lead to NO in the blood and tissues [61]. There is evidence that a diet rich in vegetables and supplements of nitrates decreases blood pressure and the risk of brain ischemic occurrences [62]. The risk of cardiovascular events in CAD is associated inversely with the catalytic activity of erythrocyte glutathione peroxidase [63]. In addition, published studies demonstrated the existence of NOS3 polymorphisms associated with some groups of patients with CAD and with groups of insulin-dependent diabetics who will develop CAD [64,65]. The implication of polymorphisms of NOS isoenzymes in the appearance of CAD requires further study.

Recently, measurements of NO *in vivo* and in humans directly using an electrochemical electrode sensor have been developed and applied in the coronary circulation [14]. The study was performed in patients with dilated cardiomyophaty and in healthy controls and NO was measured in the proximal great cardiac vein with a catheter-type sensor [14]. The authors give a contribute for the clinical quantification of endothelial dys(function) by measuring *in vivo* endothelium availability of NO [14]. The determination of NO associated with the evaluation of coronary diameter and coronary blood flow could give useful information for the application of adjusted therapeutics.

4. Nitric Oxide in the Venous Endothelium

Human umbilical vein endothelial cells (HUVECs) in the presence of ACh, the natural substrate of acetylcholinesterase (AChE), liberate higher values of NO than basal values [66]. Variance when velnacrine (AChE inhibitor) was added to the HUVECS lowers values of NO than those observed for ACh [66]. These results were obtained using the electrochemical sensor amino-IV NO [66]. Further studies are needed to clarify the signal transduction mechanisms in endothelial cells under the

influence of activators and inhibitors of acetylchonisterase. Others biosensors for NO evaluation are available as described above.

The appearance of structural changes in connective tissue, smooth muscle, and of functional changes in venous endothelium, defects in the microcirculatory network, and deficient supplies of nutrients in the venous sector are inducers of varicosity appearance [67,68]. In venous disease, the upright position originates a decrease of oxygen partial pressure in tissues, capillary stasis, and hypoxia that activates endothelial cells with increased cytoplasmic calcium. This is crucial for the release of proinflammatory factors (such as PAF, leukotriene B4, prostaglandins E2 and D2) [69–72]. The release of histamine and serotonin stimulate the migration of leukocytes to the endothelium and expression of adhesion molecules in both cells [73]. Moreover, endothelial cells produce cytokines (IL-1beta, IL-6, TNF alpha) and prothrombotic factors (von Willebrand factor) that elicit monocytes and activated T lymphocytes with the inflammatory response [73]. Inflammation does not occur only in the post-capillary venules, but also in the large veins which contributes to a better understanding of the etiology of venous thrombosis and pulmonary embolism [74]. Flow-mediated vasodilation is impaired in patients with spontaneous venous thromboembolism, which is an indicator of endothelial dysfunction [75].

In the venous endothelium of healthy individuals, as happens on the arterial side, there is release of nitric oxide which regulates and maintains venous tone [76]. The NO secretion by vascular endothelial cells is depending on shear stress [77]. In chronic venous insufficiency, the diameter of the vein is increased, decreasing shear stress and the production of NO by endothelial cells during the initial phase. After the expression of inducible nitric oxide synthase, higher amounts of NO are released that interact with the superoxide anion (produced by leukocytes and macrophages) producing peroxynitrite that causes tissue oxidation of chronic venous ulcers.

The restoration of basal levels of NO is a therapeutic target for the healing of ulcers [76]. The success of wound healing in patients receiving monocromatic infrared energy and submitted to stretching and resistance exercise may be associated with increases of NO in the blood [78].

If heart failure is accompanied with venous vascular dysfunction, it benefits from therapeutics that acts on restoring venous vascular function dependent on NO [76].

Application of an eNOS inhibitor on the venous network normalizes venous vascular resistance and blood pressure values in the lower limbs, although these results are still preliminary [79].

Hyperemia observed in the elderly with passive movement of the legs is absent in patients with peripheral arterial disease. This supports the hypothesis that NO is present in venous endothelial cells [80]. The results obtained with inhibitors of eNOS confirm this hypothesis [81]. The authors consider that the passive movement of the legs may become a noninvasive instrument for analyzing the function of the endothelial NO in venous tissue [80].

Endothelial function can be evaluated using non-invasive techniques including high-resolution ultrasonography that measures vasodilation in the radial, femoral, and brachial arteries [81]. The vasodilation resulting from the action of vasodilators is used as a benchmark. Nitroglycerin is used as a diagnostic test for portal hypertension (PHT) [82]. The extent of PHT is quantified in clinical practice by measuring the hepatic portal vein pressure gradient [83]. In PHT, the insufficient release of NO from endothelial cells influences the increase of vascular resistance at the level of the intra-hepatic microcirculation [84,85]. There is excessive production of NO in the splanchnic circulation that must be accounted for when NO donors are used to reduce portal pressure [86]. Many of the studies

regarding the influence of NO donors on the venous vascular sector are performed in experimental animal models, suggesting the best treatment strategies dependent on NO can function in the resolution of human venous disease.

5. Nitric Oxide in Erythrocytes

In physiological conditions, the erythrocyte senses oxygen partial pressure (PaO2) in the vasculature scavenging both oxygen and nitric oxide in higher PaO2 or delivering them in lower PaO2 (NO) [87]. The capture and donation of both gases is dependent on the haemoglobin (Hb) conformation states being its relaxed state is associate with scavenging and its tense state with both gases donation [88,89]. Erythrocytes mediate the availability of NO and collection to and from the endothelium [87]. This recruiting cycle, reservation and donation of NO by erythrocyte applies to both NO synthesized in the lung or inhaled [87].

Previous studies have demonstrated the presence of NO inside the erythrocyte using fluorescence microscopy [90].The influx of NO to red blood cells occurs through the band 3 protein also known by the chloride/bicarbonate anionic channel [91]. The influx depends on the tendency of the band 3 protein to adopt the structure of the dimer or the tetramer and on the degree of denaturation of hemoglobin, *i.e.*, the presence of Heinz bodies and methemoglobin [92]. The presence of tetramers or methemoglobin and Heinz bodies are unfavourable and blocks the entry of NO into erythrocytes [12]. The rate of influx in the erythrocytes is higher in the hemoglobin deoxygenated state than in the oxygenated state [93]. Conditions of increased hematocrit favor the influx in oxygenated RBCs [93].

The erythrocyte acts as a carrier and as a nitric oxide donor. The output of NO from the erythrocytes occurs through the band 3 protein dependent on its degree of phosphorylation [94]. The molecular forms of NO, namely the nitrosilhemoglobin (NO bound to heme iron of hemoglobin) the nitrosohemoglobin (NO bind to the thiol group of cysteine 93 of the beta chain of hemoglobin) and nitrosoglutathione regulate the availability of NO by erythrocyte [95].

Glutathione is an abundant molecule inside erythrocytes which has a thiol group that can react with nitric oxide, forming nitrosothiols such as S-nitrosoglutathione (GSNO) [96]. The NO reservoir attributed to glutathione could be influenced by the inactivation of glutathione reductase induced by oxidative stress [97]. The thiol/disulfide reagents such as reduced or oxidized gluthathione (which are present at high levels inside RBCs), have a suitable redox potential that is useful for protein regeneration. For instance, dithiothreitol (DTT) is a thiol-reducing agent capable of regenerating disulfide-containing proteins and also able to establish interchangeable thiol-disulfide reactions with glutathione [98]. The presence of DTT induces erythrocyte changes in enzymatic activity states for example in protein tyrosine phosphatase (PTP) and protein tyrosine kinase (PTK) [99,100]. DTT significantly mobilizes erythrocyte NO to generate nitrites/nitrates and SNOHb, thereby decreasing NO efflux [100]. Using the same experimental model, DTT was proven to enhance the levels of GSNO, nitrite/nitrate concentrations [101].

When auto-oxidation of hemoglobin occurs, it produces peroxide anion which generates peroxynitrite after reacting with NO [102]. The decomposition of peroxynitrite molecules yields nitrite and nitrate [103] and the reaction between peroxynitrite and hemoglobin generates SNOHb, which could decompose to nitrosothiol and nitrate [104]. However, NO may reduce oxyhemoglobin to

methemoglobin along with the formation of nitrate without any variation in the methemoglobin concentration [104,105]. This could be associated with the presence of hemoglobin reductase coupled with NADH that is produced in the glycolytic pathway [106]. *In vitro*, the NO donor, Spermine NONOate, induces an increase in the methemoglobin concentration and decreases the P50 values, which means that hemoglobin oxygen affinity increases [105].

An electrochemical method was described for quantification of the efflux of NO from erythrocytes using an NO electrode sensor in erythrocyte suspensions containing acetylcholine [16]. Further studies documented a signal transduction mechanism in erythrocytes involving the AChE-acetylcholine (active enzyme—substrate complex), the Gi protein, the band 3 protein—dependent of the degree of phosphorylation [107,108]. In the presence of velnacrine, an inactive enzyme complex is formed and lower levels of erythrocyte efflux were observed than those obtained in the presence of acetylcholine [107,108]. Timolol is an inhibitor of erythrocyte AChE [109] and does not change erythrocyte NO bioavailability in erythrocyte suspensions [110]. This can be considered an advantage if the vascular lumen is under high levels of reactive oxygen species, as the formation of peroxinitrite will not be favored. The antioxidant properties of timolol have been reported *in vivo* and *in vitro* [111–113].

The erythrocyte scavenging property of NO is preserved by fibrinogen binding to the RBC membrane [114]. The same was verified mimicking hiperfibrinogenemia conditions in the absence or presence of acetylcholine [115,116]. However, a reverse situation is obtained when higher fibrinogen concentrations are simultaneously present with phosphorylation of band 3 protein [115]. This result could be considered a useful therapeutic tool in blood storage for further transfusion. Fibrinogen binds to the erythrocyte membrane CD47 and when the agonist peptide of CD47 is added to erythrocytes, the same NO scavenging property was verified [117].

High NO release from RBC samples was observed *in vitro* from patients with hypoxia and inflammatory states, namely sickle cell disease, hypercholesterolemic, and hypertensive patients; also, impairment in erythrocyte deformability was documented [118].

Vasoconstriction and ischemia may occur when patients are submitted to blood transfusions originating from blood-bank-stored blood, which have a lower ability to release both oxygen and NO [119]. NO consumption by erythrocytes is regulated under hypoxic conditions by deoxygenated Hb that binds to iron heme (NO occupies the vacant site left by oxygen). The NO-heme hemoglobin adduct (HbFe (II) NO) has been detected during NO inhalation therapy used for pulmonary hypertension treatment, but it also occurs when deoxygenated blood enters a vascular bed in which NO is produced, such as the pulmonary circulation [120,121]. In situations of hyperemia, the nitrosylated hemoglobin recently measured *in vivo* by a modified subtraction method using electron paramagnetic resonance correlated with the endothelium function measured by tonometry [122]. Under hypoxic conditions established *in vitro* in segments of mesentery arteries of Wistar rats perfused with erythrocyte suspensions vasodilation occurs due to the liberation of NO from erythrocyte in dependence of the shear stress [123].

Inducible NOS expression in the endothelium increases in ischemia/hypoxia conditions or ischemia/reperfusion in which blood flow decreases, thereby favoring HbFe (II) NO formation [124]. From all these results, the use of NO donors must be accompanied by NO *in situ* monitoring with a microelectrode sensor.

6. Conclusions

Nitric oxide is a signaling molecule influential in several vascular diseases. By NOS uncoupling, NO lowers its levels and endothelial dysfunction is installed. The endothelial dysfunction generates reactive oxygen species that impair the NO concentration by its combination with superoxide anion. The tendency to apply NO donors seems to be the choice for monitoring the therapeutic option. However, care must be taken with NO measurements *in situ* resulting in the expression of the inducible NOS. The availability of erythrocyte to scavenge or release NO, measured using a microelectrode sensor, is a reflex also of the endothelium and recommended to monitor cardiovascular disease. The signal transduction mechanisms evidenced for the ACh–AChE active complex can be a routed for therapeutic control of NO bioavailability of the erythrocyte. The electrochemical sensors are well established class of *in vivo* sensors, which offer almost real-time NO determinations

Acknowledgments

This study was supported by grants from the FCT—Fundação para a Ciência e a Tecnologia (project reference EXCL/Mat-NAN/0114/2012).

Author Contributions

The co-authors contribute with their technical expertise on the research published papers here referenced and with the revision of this paper.

Conflicts of Interest

The authors declare no conflict of interest.

References

1. Palmer, R.M.J.; Ashton, D.S.; Moncada, S. Vascular endothelium cells synthesize nitric oxide from L-arginine. *Nature* **1988**, *333*, 664–666.
2. Michel, T.; Feron, O. Nitric oxide synthase: Which, where, how and why? *J. Clin. Invest.* **1997**, *100*, 2146–2152.
3. Ignarro, L.J. Nitric oxide as a unique signaling molecule in the vascular system: A historical overview. *J. Physiol. Pharmacol.* **2002**, *53*, 503–514.
4. Griffith, O.W.; Stuehr, D.J. Nitric oxide synthases: Properties and catalytic mechanism. *Ann. Rev. Physiol*. **1995**, *57*, 707–736.
5. Guzik, T.J.; West, N.E.J. Vascular superoxide production by NAD(P)H oxidase: Association with endothelium dysfunction and clinical risk factors. *Circ. Res.* **2000**, *86*, e85–e90.
6. Ramndriamboavony, V.; Fleming, I. Endothelial nitric oxide synthase (eNOS) in platelets: How is regulated and what is it doing there? *Pharmacol. Rep.* **2005**, *57 (Suppl.)*, 59–65.
7. Bloch, K.D.; Janssens, S. Cardiomyocyte-specific overexpression of nitric oxide synthase 3: Impact on left ventricular function and myocardial infarction. *Trends Cardiovasc. Med.* **2005**, *15*, 249–253.

8. Liao, J.C.; Hein, T.W.; Vaughn, M.W.; Huang, K.T. Intravascular flow decreases erythrocyte consumption of nitric oxide. *Proc. Nat. Acad. Sci. USA* **1999**, *96*, 8757–8761.
9. Lugnier, C.; Keravis, T.; Eckly-Mychel, A. Cross talk between NO and cyclic nucleotide phosphodiesterases in the modulation of signal transduction in blood vessel. *J. Physiol. Pharmacol.* **1999**, *50*, 639–652.
10. Pries, A.R.; Kuebler, W.M. Normal endothelium. *Hand. Exp. Pharmacol.* **2006**, *176*, 1–40.
11. Singh, D.K.; Winocour, P.; Farringhton, K. Endothelial cell dysfunction, medial arterial calcification and osteoprotegerin in diabetes. *Brit. J. Diab. Vasc. Dis.* **2010**, *10*, 71–77.
12. Wadsworth, R.; Stankevicius, E.; Simonsen, U. Physiologically relevant measurements of nitric oxide in cardiovascular research using electrochemical microsensors. *J. Vasc. Res.* **2006**, *43*, 70–85.
13. Hall, C.N.; Garthwaite, J. What is the real physiological NO concentration *in vivo*? *Nitric Oxide* **2009**, *21*, 92–103.
14. Takarada, S.; Imanishi, T.; Goto, M.; Mochizuki, S.; Ikejima, H.; Tsujioka, H.; Kuroi, A.; Takeshita, T.; Akasaka, T. First evaluation of real-time nitric oxide changes in the coronary circulation in patients with non-ischaemic dilated cardiomyopathy using a catheter-type sensor. *Eur. Heart J.* **2010**, *31*, 2862–2870.
15. Zang, X. Real time and *in vivo* monitoring of nitric oxide by electrochemical sensors—From dream to reality. *Front Biosci.* **2004**, *1*, 3434–3446.
16. Carvalho, F.A.; Martins-Silva, J.; Saldanha, C. Amperometric measurements of nitric oxide in erythrocytes. *Biosens. Bioelectron.* **2004**, *20*, 505–508.
17. Bogdan, C. Nitric oxide and the immune response. *Nat. Immunol.* **2001**, *2*, 907–916.
18. Malinski, T.; Taha, Z. Nitric oxide release from a single cell measured *in situ* by a porphyrinic-based microsensor. *Nature* **1992**, *358*, 676–678.
19. Casero, E.; Pariente, F.; Lorenzo, E.; Beyer, L.; Losada, J. Electrocatalytic oxidation of nitric oxide at 6,17-diferrocenyldibenzo[b,i]5,9,14,18-tetraaza[14]annulen-nickel(II) modified electrodes. *Electroanalysis* **2001**, *13*, 1411–1415.
20. Ciszewski, A.; Milczarek, G. Electrochemical detection of nitric oxide using polymer modified electrodes. *Talanta* **2003**, *61*, 11–26.
21. Bedioui, F.; Villeneuvre, N. Electrochemical nitric oxide sensors for biological samples-principle, selected examples and applications. *Electroanalysis* **2003**, *15*, 5–18.
22. Bedioui, F.; Trevin, S.; Albin, V.; Villegas, M.G.G.; Devynck, J. Design and characterization of chemically modified electrodes with iron(III) porphyrinic-based polymers: Study of their reactivity toward nitrites and nitric oxide in aqueous soulution. *Anal. Chim. Acta*. **1997**, *341*, 177–185.
23. Diab, N.; Schuhmann, W. Electropolymerized manganese porphyrin/polypyrrole films as catalytic surfaces for the oxidation of nitric oxide. *Electrochim. Acta.* **2001**, *47*, 265–273.
24. Liu, X.J.; Shang, L.B.; Pang, J.T.; Li, G.X. A reagentless nitric oxide biosensor based on haemoglobin/polyethyleneimine film. *Biotechnol. Appl. Biochem.* **2003**, *38*, 119–122.
25. Markus, M.; Pariente, F.; Wu, Q.; Toffanin, A.; Shapleigh, J.P.; Abruna, H.D. Electrocatalytic reduction of nitric oxide at electrodes modified with electropolymerized films of $[Cr(v\text{-}tpy)_2]^{3+}$ and their application to cellular NO determinations. *Anal. Chem.* **1996**, *68*, 3128–3134.

26. Meulemans, A. Continuous monitoring of N-nitroso-L-arginine using micro carbon electrode in rat brain. *Neurosci. Lett*. **1993**, *157*, 7–12.
27. Shin, J.H.; Privett, B.J.; Kita, J.M.; Wightman, R.M.; Schoenfisch, M.H. Fluorinated Xerogel-derived microelectrodes for amperometric nitric oxide sensing. *Anal. Chem*. **2008**, *80*, 6850–6859.
28. Kitamura, Y.; Uzawa, T.; Oka, K.; Komai, Y.; Ogawa, H.; Talizawa, N.; Kobayashi, H.; Tanishita, K. Microcoaxial electrode for *in vivo* nitric oxide measurement. *Anal. Chem*. **2000**, *72*, 2957–2962.
29. Mao, L.Q.; Yamamoto, K.; Zhou, W.L.; Jin, L.T. Electrochemical nitric oxide sensors based on electropolymerized film of M(salen) with central ions of Fe, Co, Cu, and Mn. *Electroanalysis* **2000**, *12*, 72–77.
30. Shibuli, K. An electrochemical microprobe for detecting nitric oxide release in brain tissue. *Neurosci. Res*. **1990**, *9*, 69–76.
31. Vallance, P.; Patton, S.; Bhagat, K.; Macallister, R.; Radomski, M.; Moncada, S.; Malinski, T. Direct measurement of nitric oxide in human beings. *Lancet* **1995**, *346*, 153–154.
32. Brovlkovych, V.; Stolarczyk, E.; Oman, J.; Tomboulian, P.; Malinski, T.J. Direct electrochemical measurement of nitric oxide in vascular endothelium. *Pharm. Biomed. Anal.* **1999**, *19*, 135–143.
33. Brown, F.O.; Finnerty, N.J.; Lowry, J.P. Nitric oxide monitoring in brain extracellular fluid: Characterization of Nafion®-modified Pt electrodes *in vitro* and *in vivo*. *Analyst* **2009**, *134*, 2012–2020.
34. Griveau, S.; Dumezy, C.; Seguin, J.; Chabot, G.G.; Sherman, D.; Bedioui, F. *In vivo* electrochemical detection of nitric oxide in tumor-bearing mice. *Anal. Chem*. **2007**, *79*, 1030–1033.
35. Dormandy, J.; Ernst E.; Matrai, A.; Flute, P.T. Hemorrheological changes following acute myocardial infarction. *Am. Heart J.* **1982**, *104*, 1364–1367.
36. Gaimi, G.; Serra A.; Presti, C.R.L.; Sarno, A.; Gerasola, G. Red cell metabolic parameters rheological determinants in essential hypertension. *Clin. Hemorheol.* **1993**, *13*, 35–44.
37. Jay, R.H.; Rampling, M.W.; Betteridge, D.J. Abnormalities of blood rheology in familial hypercholesterolemia: Effects of treatment. *Atherosclerosis* **1990**, *85*, 249–256.
38. Khodabandehlou, T.; Le Deveat, C.; Razavian, M.; Boynard, M. Functional capacity of fibrinogen and erythrocyte aggregation in the diabetic. *J. Mal. Vasc.* **1994**, *19*, 278–282.
39. Félétou, M.; Köhlerm, R.; Vanhoute, P.M. Endothelium-derived vasoactive factors and hypertension: Possible roles in pathogenesis and as treatment targets. *Curr. Hypertens.* **2010**, *12*, 267–275.
40. Vanhoute, P.M. Endothelial dysfunction the first step toward coronary arteriosclerosis. *Circ. J.* **2009**, *73*, 595–601.
41. Griendling, K.K.; Sorescu, D.; Ushio-Fucai, M. NAD(P)H oxidase: Role in cardiovascular biology and disease. *Circ. Res.* **2000**, *86*, 494–501.
42. Sorecu, D.; Weiss, D.; Lassegue, B.; Campus, R.E.; Szocs, K.; Sorecu, G.P.; Valppu, L.; Quinn, M.T.; Lambeth, J.D.; Veja, J.D.; Taylor, W.R.; Griendling, K.K. Superoxide production and expression of Nox family proteins in human atherosclerosis. *Circulation* **2002**, *105*, 1429–1435.

43. Li, H.; Wallerath, T.; Münze, T.; Förstermann, U. Regulation of endothelial-type NO synthase expression in pathology and I response to drugs. *Nitric Oxide Biol. Chem.* **2002**, *7*, 149–164.
44. Drummond, G.R.; Cai, H.; Davies, M.E.; Ramasamy, S.; Harrison, D.G. Transcriptional and posttranscriptional regulation of endothelial nitric oxide synthase expression by hydrogen peroxide. *Circ. Res.* **2000**, *86*, 347–354.
45. Ludewig, B.; Zinkernagel, R.M.; Hengar, T.H. Arterial inflammation and atherosclerosis. *Thends Cardiovasc. Med.* **2002**, *12*, 154–159.
46. Sogo, N.; Magid, K.S.; Shawca, C.A.; Webb, D.Y.; Meyson, I.L. Inhibition of human platelet aggregation by nitric oxide donor drugs: Relative contribution of cGMP-independent mechanism. *Biochem. Biophys. Res. Commum.* **2000**, *279*, 412–419.
47. Wang, B.Y.; Ho, H.K,; Lin, P.S.; Pollman, M.J.; Gibbons, G.H.; Tsao, P.S.; Cooke, J.P. Regression of atherosclerosis: Role of nitric oxide and apoptosis. *Circulation* **1999**, *99*, 1236–1241.
48. Kocks, M.M.; Knaapen, M.W. The role of apoptosis in vascular disease. *J. Pathol.* **2000**, *190*, 267–280.
49. Napoli, C.; Ignaro, L.I. Nitric oxide and pathogenic mechanisms involved in development of vascular disease. *Arch. Pharm. Res.* **2009**, *32*, 1103–1108.
50. Lyamina, N.P.; Lyamina, S.V.; Senchiknin, V.N.; Mallet, R.T.; Downey, H.F.; Manukhina, E.B. Normobaric hypoxi conditioning reduces blood pressure and normalizes nitric oxide synthesis in patients with arterial hypertension. *J. Hypertens.* **2011**, *29*, 2265–2272.
51. Moya, M.P.; Gow, A.J.; Califf, R.M.; Goldberg, R.N.; Stamler, J.S. Inhalated ethyl nitrite gas for persistent pulmonary hypertension of the newborn. *Lancet* **2002**, *360*, 141–143.
52. Wilkins, M.R.; Aldashev, A.; Morrell, N.W. Nitric oxide, phosphodiesterase inhibition and adaptation to hypoxic conditions. *Lancet* **2002**, *359*, 539–1540.
53. Gosh, R.; Sawant, O.; Ganpathy, P.; Pitre, S.; Kadam, V.J. Posphodiesterase inhibitors: Their role and implications. *Int. J. Pharm. Tech. Res.* **2009**, *1*, 1148–1160.
54. Herman, A.G.; Moncada, S. Therapeutic potential of nitric oxide donors in prevention and treatement of atherosclerosis. *Eur. Heart. J.* **2005**, *26*, 1945–1955.
55. Lundberg, J. Nitric oxide metabolites and cardiovascular disease markers, mediators, or both? *J. Am. Coll. Cardiol.* **2006**, *47*, 580–581.
56. Wallace, J.I.; Ignarro, L.J.; Fiorucci, S. Potential cardioprotective actions of NO-releasing aspirin. *Nat. Rev. Drug Discov.* **2002**, *1*, 375–382.
57. Lazzarato, L.; Donnola, M.; Rolando, B.; Chegaev, K.; Marini, E.; Cena, C.; Di Stilo, A.; Fruttero, R.; Biondi, S.; Ongini, E.; Gasco, A. Nitrooxyacyloxy methyl esters of aspirin as novel nitric oxide releasing aspirins. *J. Med. Chem.* **2009**, *52*, 5058–5068.
58. Förstermann, U. Nitric oxide and oxidative stressing vascular disease. *Pflügers Arch. Eur. J. Physiol.* **2010**, *459*, 923–939.
59. Dal-Ros, S.; Zoll, J.; Lang, A.L.; Auger, C.; Keller, N.; Bronner, C.; Geny, B.; Schini-Kerth, V.B. Chronic intake of red wine polyphenols by young rats prevents aging-induced endothelial dysfunction and decline in physical performance: Role of NADPH oxidase. *Biochem. Biophys. Res. Commun.* **2011**, *401*, 743–749.

60. Pinto, V.; Brunini, T.; Ferraz, M.R.; Okinga, A.; Mendes-Ribeiro, A.C. Depression and cardiovascular disease: Role of nitric oxide. *Cardiovasc. Hematol. Agents Med. Chem.* **2008**, *6*, 142–149.
61. Kapil, V.; Webb, A.J.; Ahluwalia, A. Iinorganic nitrate and the cardiovascular system. *Heart* **2010**, *96*, 1703–1709.
62. Tang, Y.; Jiang, H.; Bryan, N.S. Nitrite and nitrate: Cardiovascular risk-benefit and metabolic effect. *Curr. Opin. Lipid.* **2011**, *22*, 11–15.
63. Blakenberg, S.; Rupprecht, H.J.; Bickel, C.; Torzewski, M.; Hafner, G. Tiret, L.; Smieja, M.; Cambiem, F.; Meyer, J.; Lackner, K.J.; for the AtheroGene Investigators. Gluthathione peroxidase 1 activity and cardiovascular events in patients with coronary artery disease. *N. Engl. J. Med.* **2003**, *349*, 1605–1613.
64. Bhandary, U.; Tse, W.; Yang, B.; Knowles, M.R.; Demaine, A.G. Endothelial nitric oxide synthase polymorphisms are associated with hypertension and cardiovascular disease in renal transplantation. *Nephrology* **2008**, *13*, 348–355.
65. Mollsten, A.; Lajer, M.; Jorsal, A.; Tamow, L. The endothelial nitric oxide synthase gene and risk of diabetic nephropathy and development of cardiovascular disease in type 1 diabetes. *Mol. Gen. Metab.* **2009**, *97*, 80–84.
66. Carvalho, F.A; Saldanha, C.; Silva, J.M.E. Doseamento electroquímico do monóxido de azoto em células endotelias humans. *RFML* **2003**, *8*, 205–212.
67. Travers, J.P.; Brookes, C.E.; Evan, J.; Baker, D.M.; Kent, C.; Makin, G.S.; Mayhew, T.M. Assessment of wall structure and composition of varicose vein with reference to collagen, elastin and smooth muscle content. *Eur. J. Vasc. Endovasc. Surg.* **1996**, *11*, 230–237.
68. Venturi, M.; Bonavina, L.; Annoni, F.; Colombo, L.; Butera, C.; Peracchia, A.; Mussini, E. Biochemical assay of collagen and elastin in the normal and varicose vein wall. *J. Surg. Res.* **1996**, *60*, 245–248.
69. Michiels, C.; Arnould, T.; Knott, I.; Dieu, M.; Remacle, J. Stimulation of prostaglandin synthesis by human endothelial cells exposed to hypoxia. *Am. J. Physiol.* **1993**, *264*, C866–C874.
70. Michiels, C.; Arnould, T.; Remacle, J. Hypoxia-induced activation of endothelial cells as a possible cause of venous diseases: Hypothesis. *Angiology* **1993**, *44*, 639–646.
71. Michiels, C.; Bouaziz, N.; Remacle, J. Role of the endothelium and blood stasis in the development of varicose veins. *Int. Angiol.* **2002**, *21*, 18–25.
72. Michiels, C.; Renard, P.; Bouaziz, N.; Heck, N.; Eliaers, F.; Ninane, N.; Quarck, R.; Holvoet, P.; Raes, M. Identification of the phospholipase A_2 isoforms that contribute to arachidonic acid release in hypoxic endothelial cells: Limits of phospholipase A_2 inhibitors. *Biochem. Pharmacol.* **2002**, *63*, 321–332.
73. Schmid-Schönbein, G.W. Inflammation and the pathophysiology of chronic venous insufficiency. *Phlebolymphology* **2003**, *39*, 95–99.
74. Eriksson, E.E.; Karlov, E.; Lundmark, K.; Rotzius, P.; Hedin, U.; Xie, X. Powerful inflammatory properties of large vein endothelium *in vivo*. *Arterioscler. Thromb. Vasc. Biol.* **2005**, *25*, 723–728.
75. Migliacci, R.; Becattini, C.; Pesavento, R.; Davi, G.; Vedovati, M.C.; Guglielmini, G.; Falcinelli, E.; Ciabattoni, G.; Valle, F.D.; Prandoni Pagnelli, G.; Gresele, P. Endothelial dysfunction in patients with spontaneous venous thromboembolism. *Hemathology J.* **2007**, *92*, 812–818.

76. Blackman, D.J.; Morris-Thurgood, J.Á.; Atherton, J.J.; Ellis, G.R.; Anderson, R.A.; Cokcroft, J.R.; Frenneaux, M.P. Endothelium-derived nitric oxide contributes to the regulation of venous tone in humans. *Circulation* **2000**, *101*, 165–170.
77. Martini, J.; Carpentier, B.; Chávez Negrete, A.; Cabrales, P.; Tsai, A.G.; Intaglietta, M. Benefitial effects due to increasing blood and plasma viscosity. *Clin. Hemorheol. Microcirc.* **2006**, *35*, 51–57.
78. Ahmed, E.T.; Maayah, M.F.; Asi, Y. Anodyne therapy *versus* exercise therapy in improving the healing rates of venous leg ulcer. *Int. J. Res. Med. Sci.* **2013**, *13*, 198–203.
79. Foutaine, M.F.; Raduolovic M.C.; Cardozo, C.P.; Spungen, A.M.; DeMeersman, R.E.; Bauman, W.A. Effects of acute nitric oxide synthase inhibition on lower leg vascular function in chronic tetraplegia. *J. Spinal Cord. Med.* **2009**, *32*, 538–544.
80. Mortensen, S.; Askew, C.D.; Walker, M.; Nyberg, M.; Hellesten, Y. The hyperaemic response to passive leg movement is dependent on nitric oxide; a new tool to evaluate endothelial nitric oxide function. *J. Physiol.* **2012**, *590*, 4391–4000.
81. Esper, R.J.; Nordaby, R.A.; Vilarino, J.O.; Paragano, A.; Cacharrón, J.L.; Machado, R.A. Endothelial dysfunction: A comprehensive appraisal. *Cardiovasc. Diabetol.* **2006**, *5*, doi:10.1186/1475-2840-5-4.
82. Vujanac, A.; Jakovljevic, V.; Djordevic, D.; Zivkovic, V.; Stojlovic, M.; Celikovic, N.; Skevin, A.J.; Djuric, D. Nitroglycerine effects on portal vein mechanics and oxidative stress in portal hypertension. *World Gastroenterol.* **2012**, *18*, 331–339.
83. Burroughs, A.K.; Thalheimer, U. Hepatic venous pressure gradient in 2010: Optimal measurement is key. *Hepatology* **2010**, *51*, 1894–1896
84. Rockey, D.C. Hepatic fibrosis, stellate cells, and portal hypertension. *Clin. Liver Dis.* **2006**, *10*, 459–479.
85. Iwakiri, Y.; Groszmann, R.J. Vascular endothelial dysfunction in cirrhosis. *J. Hepatol.* **2007**, *46*, 927–934.
86. Zafra, C.; Abraldes, J.G.; Turnes, J.; Berzigotti, A.; Fernández, M.; Garca-Pagán, J.C.; Rodés, J.; Bosch, J. Simvastatin enhances hepatic nitric oxide production and decreases the hepatic vascular tone in patients with cirrhosis. *Gastroenterology* **2004**, *126*, 749–755.
87. MacMahomn, T.; Doctor, A. Extrapulmonary effects of inhalated nitric oxide. *Proc. Am. Thorac. Soc.* **2006**, *3*, 153–160.
88. Lane, P.; Gross, S. Hemoglobin as a chariot for NO bioactivity. *Nature Med.* **2002**, *8*, 657–658.
89. Jia, L.; Bonaventura, J.; Stamler, J.S. S-nitrosohaemoglobin: A dynamic activity of blood involved in vascular control. *Nature* **1996**, *380*, 221–226.
90. Mesquita, R.; Martins-Silva, J.; Saldanha, C. Acetylcholine induces nitric oxide production by erythrocytes *in vitro*. *Nitric Oxide Biol. Chem.* **2000**, *177*, 313–314.
91. Han, T.H.; Qamirani, E.; Nelson, A.G.; Hyduke, D.R.; Chaudhuri, G.; Kuo, L.; Liao, J.C. Regulation of nitric oxide consumption by hypoxic red blood cells. *Proc. Nat. Acad. Sci. USA* **2003**, *100*, 12504–12509.
92. Huang, K.T.; Han, T.H.; Hyduke, D.R.; Vaughn, M.W.; Herle, H.V.; Hein, T.W.; Zang, C.; Kuo, L.; Liao, J.C. Modulation of nitric oxide bioavailability by erythrocytes. *Proc. Nat. Acad. Sci. USA* **2001**, *98*, 11771–11775.

93. Azarov, I.; Huang, K.T.; Basu, S.; Gladwin, M.T.; Hog, N.; Kim-Shapiro, D.B. Nitric oxide scavenging by red blood cells as a function of hematocrit and oxygenation. *J. Biol. Chem.* **2005**, *280*, 19024–19032.
94. Pawloski, J.R. Hess, D.T. Stamler, J.S. Impaired vasodilation by red blood cells in sickle cell disease. *Proc. Nat. Acad. Sci. USA* **2005**, *10*, 2531–2536.
95. Chen, K.; Popel, A.S. Nitric oxide productions pathways in erythrocyte and plasma. *Biorheology* **2009**, *46*, 107–119.
96. Galli, F.; Rossi, R.; Di Simplicio, P.; Floridi, A.; Canestrari, A. Protein thiols and glutathione influence the nitric oxide-dependent regulation of the red blood cell F metabolism. *Nitric Oxide* **2002**, *6*, 186–199.
97. Fujii, T.; Hamaoka, R.; Fujii, J.; Taniguchi, N. Redox capacity of cells affects inactivation of glutathione reductase by nitrosative stress. *Archives Biochemical. Biophysica* **2000**, *378*, 123–130.
98. Rothwarf, D.M.; Scheraga, H.A. Equilibrium and kinetic constants for the thiol-disulfide interchange reaction between glutathione and dithiothreitol. *Proc. Nat. Acad. Sci. USA* **1992**, *89*, 7944–7948.
99. Zipser, Y.; Piade, A.; Kosower, N.S. Erythrocyte thiol status regulates band 3 phosphotyrosine level via oxidation/reduction of band 3-associated phosphotyrosine phosphatase. *FEBS Lett.* **1997**, *406*, 126–130.
100. Lopes de Almeida, J.P.; Carvalho, F.A; Silva-Herdade, A.S; Santos-Freitas, T. Saldanha, C. Redox thiol status plays a central role in the mobilization and metabolism of nitric oxide in human red blood cells. *Cell Biol. Inter.* **2009**, *33*, 268–275.
101. Lopes de Almeida, J.P.; Freitas-Santos, T.; Saldanha, C. Fibrinogen-dependent signalling microvascular erythrocyte function: Implications on nitric oxide efflux. *J. Membr. Biol.* **2009**, *231*, 47–53.
102. Balagopalakrishna, C.; Manoharan, P.T.; Abugo, O.O.; Rifkind, J.M. Production of superoxide from hemoglobin-bound oxygen under hypoxic conditions. *Biochemistry* **1996**, *35*, 6393–6398.
103. Pfeiffer, S.; Mayer, B. Lack of tyrosine nitration by peroxynitrite generated at physiological pH. *Biol. Chem.* **1998**, *273*, 27280–27285.
104. Gladwin, M.T.; Wang, X.; Reiter, C.D. SNitrosohemoglobin is unstable in the reductive erythrocyte environment and lacks O_2/NO-linked allosteric function. *J. Biol. Chem.* **2002**, *277*, 27818–27828.
105. Mesquita, R.; Pires, I.; Saldanha, C.; Martins-Silva, J. Effects of acetylcholine and spermineNONOate on erythrocyte hemorheologic and oxygen carrying properties. *Clin. Hemorheol. Microcirc.* **2001**, *25*, 153–163.
106. Inal, M.E.; Egüz, A.M. The effects of isosorbide dinitrate on methemoglobin reductase enzyme activity and antioxidant states. *Cell Biochem. Funct.* **2004**, *22*, 129–133.
107. Carvalho, F.A.; Almeida, J.P.; Fernandes, I.O.; Freitas-Santos, T.; Saldanha, C. Non-neuronal cholinergic system and signal transduction pathways mediated by band 3 in red blood cells. *Clin. Hemorheol. Microcirc.* **2008**, *40*, 207–227.
108. Carvalho, F.A.; Lopes de Almeida, J.P.; Freitas-Santos, T.; Saldanha, C. Modulation of erythrocyte acetylcholinesterase activity and its association with G protein band 3 interactions. *J. Membrane Biol.* **2009**, *228*, 89–97.

109. Zabala, L.; Saldanha, C.; Martins-Silva, J.; Souza-Ramalho, P. Red blood cell membrane integrity in primary open angle glaucoma: *ex vivo* and *in vitro* studies. *Eye* **1999**, *13*, 101–103.
110. Saldanha, C.; Teixeira, P.; Santos-Freitas, T.; Napoleão, P. Timolol modulates erythrocyte nitric oxide bioavailability. *J. Clin. Exp. Ophtalmol*. **2013**, *4*, doi:10.4172/2155-9570.1000285.
111. Izzotti, A.; Saccà, S.C.; Di Marco, B.; Penco, S.; Bassi, A.M. Antioxidant activity of timolol on endothelial cells and its relevance for glaucoma course. *Eye* **2008**, *22*, 445–453.
112. Djanani, A.; Kaneider, N.C.; Meierhofer, C.; Sturn, D.; Dunzendorfer, S. Allmeier, H.; Wiedermann, C.J. Inhibition of neutrophil migration and oxygen free radical release by metipranolol and timolol. *Pharmacology* **2003**, *68*, 198–203.
113. Ricci, B.; Minicucci, G.; Manfredi, A.; Santo, A. Oxygen-induced retinopathy in the newborn rat: Effects of hyperbarism and topical administration of timolol maleate. *Graefe's Arch. Clin. Exp. Ophthalmol.* **1995**, *233*, 226–230.
114. Lopes de Almeida, J.P.; Freitas-Santos, T.; Saldanha, C. Fibrinogen-dependent signaling in microvascular erythrocyte function: Implications on nitric oxide flux. *J. Membrane Biol.* **2009**, *231*, 47–53.
115. Lopes de Almeida, J.P.; Freitas-Santos, T.; Saldanha, C. Evidence that the degree of band 3 phosphorylation modulates human erythrocytes nitric oxide efflux—*In vitro* model of fibrinogenemia. *Clin. Hemorheol. Microcirc.* **2011**, *49*, 407–416.
116. Saldanha C; Freitas-Santos, T.; Lopes de Almeida, J.P. Fibrinogen effects on erythrocyte nitric oxide mobilization in presence of acetylcholine. *Life Sci.* **2012**, *91*, 1017–1022.
117. Saldanha, C.; Freitas-Santos, T.; Lopes de Almeida, J.P. CD47 Agonist Peptide Effects on Human Erythrocyte Nitric Oxide Mobilization in Presence of Fibrinogen Poster Presentation (P002). In *Program and Abstract Book*; In Proceedings of XXIInd International Fibrinogen Workshop, Brighton, UK, 4–6 July 2012; p. 77.
118. Carvalho, F.A.; Maria, A.V.; Braz Nogueira, J.; MGuerra, J.; Martins-Silva, J.; Saldanha, C. The relation between the erythrocyte nitric oxide and hemorheological parameters. *Clin. Hemorheol. Microcirc.* **2006**, *35*, 341–347.
119. Bonaventura, J. Clinical implications of the loss of vasoactive nitric oxide during red blood cell storage. *Proc. Nat. Acad. Sci. USA* **2007**, *104*, 19165–19166.
120. Ignarro, L.; Byrns, J.R.E.; Buga, G.M.; Wood, S.K. Endothelium-derived relaxing factor from pulmonary artery and vein possesses pharmacologic and chemical properties identical to those of nitric oxide radical. *Circ. Res.* **1987**, *61*, 866–879.
121. Cannon, R.R.O., III.; Schechter, A.N.; Panza, J.; Ognibene, F.P.; Pease-Fye, M.E.; Waclawiw, M.A.; Shelhamer, J.H.; Gladwin, M.T. Effects of inhaled nitric oxide on regional blood flow are consistent with intravascular nitric oxide delivery. *J. Clin. Invest.* **2001**, *108*, 279–287.
122. Lobysheva, I.; Biller, P; Gallez, B; Beauloye, C; Balligand, J. Nitrosylated Hemoglobin levels in human venous erythrocytes correlate with vascular endothelial function measured by digital reactive hyperemia. *PLoS One* **2013**, *8*, doi:10.1371/journal.pone.0076457.
123. Ulker, P.; Gunduz, F.; Meiselman, H. J.; Baskurt, O.K. Nitric oxidegenerated by red blood cells following exposure to shear stress dilates isolated small mesenteric arteries under hypoxic conditions. *Clin. Hemorheol. Microcirc.* **2013**, *54*, 357–369.

124. Battista, S; Mengozzi, G.; Bar, F.; Cerutti, E.; Pollet, C.; Torchio, M.; Biasi, F.; Cavalli, G.; Sallizoni, M.; Poli, G.; Molino, G. Nitric oxide level profile in human liver transplantation. *Digest. Dis. Sci.* **2002**, *47*, 528–534.

Clinical Hemorheology and Microcirculation 56 (2014) 47–56 47
DOI 10.3233/CH-121662
IOS Press

An *in vitro* study on the modulation of the neutrophil adhesive behavior by soluble fibrinogen

V. Vitorino de Almeida*, A. Calado, A.S. Silva-Herdade, H.S. Rosário and C. Saldanha
Unidade de Biologia Microvascular e Inflamação, Instituto de Medicina Molecular, Instituto de Bioqu´ımica, Faculdade de Medicina, Universidade de Lisboa, Portugal

Abstract. Fibrinogen constitutes an important plasma glycoprotein involved in hemostasis and in inflammation. Previously, we have shown that at physiological concentrations, soluble fibrinogen is able to modulate the pattern of neutrophil activation. This led us to propose that under these conditions, fibrinogen could as well interfere with the adhesive behaviour of circulating neutrophils which is of utmost importance in their recruitment to the vascular wall during inflammatory processes.

To address our working hypothesis, *in vitro* adhesion assays were here performed in a flow chamber by using primary cultures of human umbilical vein endothelial cells (HUVEC) and neutrophils isolated from peripheral venous blood of healthy human donors. In the presence of a physiological concentration of soluble fibrinogen (300 mg/dL), we observed that despite the number of neutrophils rolling on an activated endothelium was not affected, their rolling velocity was increased in comparison to that of non-activated neutrophils. Consequently as expected, the number of fibrinogen-treated neutrophils adhering to activated HUVEC monolayers was significantly diminished. Overall, we have here demonstrated that at least *in vitro*, soluble fibrinogen under physiological concentrations is able to modulate the interaction of neutrophils with the vascular endothelium. *In vivo* studies will enable us in the future to study the physiological relevance of these findings and further to understand the mechanisms underlying this function.

Keywords: Neutrophil recruitment, fibrinogen, flow chamber

1. Introduction

Inflammation triggers an extensive variety of physiological and pathological processes as a protective response to insult or injury. Acute inflammation is characterized by the recruitment of specific leukocyte populations, namely neutrophils and monocytes, from the blood circulation towards the affected area. Initially, neutrophils are predominantly recruited so as to eradicate the inflammatory agent. These leukocytes are later followed by monocytes that by maturing into macrophages further set the stage for inflammation resolution and subsequent tissue repair [16].

Targeting of leukocytes to sites of inflammation is a complex process that relies initially in a multistep recruitment cascade that enables leukocyte migration through an activated endothelium of postcapillary venules via cell-cell interactions [13]. In brief, this recruitment process comprises the following steps: “tethering”, rolling, slow rolling, arrest, post-adhesion strengthening, crawling, and paracellular or transcellular transmigration [2, 12].

*Corresponding author: V. Vitorino de Almeida, Unidade de Biologia Microvascular e Inflamação, Instituto de Medicina Molecular, Instituto de Bioqu´ımica, Faculdade de Medicina, Universidade de Lisboa, Portugal. Tel.: +351 217 999 479; Fax: +351 217 999 477; E-mail: vandaalmeida@fm.ul.pt.

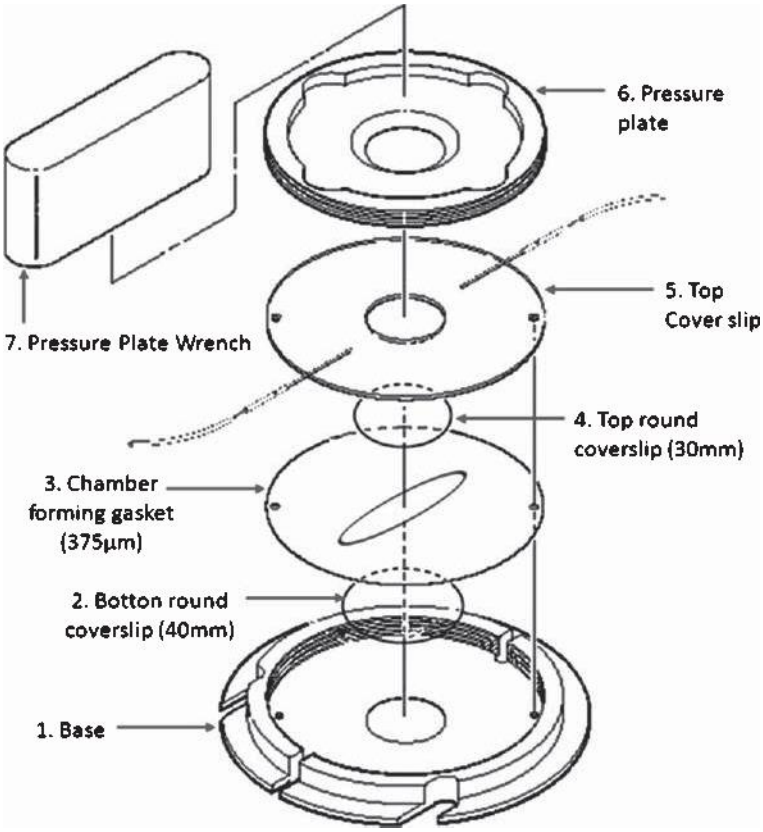

Fig. 1. Scheme illustrating the assembly of the flow chamber with the indication of the required components (herein numbered).

Distinct *in vitro* and *in vivo* methodologies have been pivotal in the study of leukocyte recruitment through the past decades. Among *in vitro* approaches, flow assays performed in specially devised chambers as that depicted in Fig. 1 have shown a potential application in this respect by more closely mimicking an *in vivo* situation than static assays. In fact, *in vitro* experimental systems have proven capable of generating controlled mechanical forces similar to those induced by hemodynamic forces *in vivo*. Among these, the most relevant mechanical force in leukocyte–endothelial cell adhesion is shear stress and normal time-averaged levels of venous shear stresses usually range *in vivo* between 1–5 dyn/cm^2. Assuming a unidirectional and laminar flow, the shear rate, γ, at the bottom surface of the flow chamber is given by $\gamma = \frac{6Q}{wh^2}$ (where Q is the volumetric flow rate; w, the width of the flow field; and h, the height of the flow field). As the shear stress, τ, is related to the shear rate by the equation $\tau = \gamma\mu$ (where μ is the viscosity of the fluid used in the experiments, typically 0.007 poise for a diluted saline solution at 37◦C), it can be represented by the expression, $\tau = \frac{6Q\mu}{wh^2}$. Ideally, any of these parameters could be changed to modulate shear stress. However as the geometry of the flow chamber is held constant, only the volumetric flow rate can be normally altered for such purpose. With this experimental design the shear stress exerted on the cells is assumed to be approximately equal to the chamber wall shear stress. Of utmost importance, flow chamber assays thus enable the study and visualization of the leukocyte recruitment cascade under well-defined wall shear stress conditions. In these assays, steps as rolling and cell adhesion can be quantified by selective image acquisition and subsequent image processing. In particular, these assays are especially

appropriate for addressing adhesive events which occur very rapidly in a short time scale. In addition, they also enable the study of initial events such as cell stabilization and spreading giving insight into the kinetics of particular cell-cell or cell-substrate adhesive behaviour [11, 18].

The different steps of the leukocyte recruitment cascade involve sequentially an array of specific factors among which stand distinct adhesion molecules expressed on the cell surface of leukocytes and endothelial cells, such as integrins. In steady state conditions, circulating leukocytes maintain their integrin receptors in a low affinity and non-adhesive state. But in response to local inflammatory stimuli, integrins are rapidly activated to bind specific ligands [6, 7]. Members of the β2 integrin family, such as Mac-1 (αMβ2, CD11b/CD18), play crucial roles in the particular case of neutrophil recruitment [6]

Among other ligands, Mac-1 serves as the receptor for fibrinogen, a large multidomain plasma glycoprotein consisting of two pairs of α, β and μ polypeptide chains organized into three major structural regions: A central E and two peripheral D regions held together by coiled-coil connectors [15]. Fibrinogen is synthesized by hepatocytes in the liver and further secreted into the circulating bloodstream. This protein is a crucial player in the coagulation cascade through which it polymerizes into fibrin, the major protein component of blood clots [1, 8, 17]. Moreover, fibrinogen is also known to constitute an acute phase protein involved in other biological responses, such as in inflammation [17]. This is due to its particular molecular structure which comprises binding sites for several receptors expressed on cells that act as central mediators of the inflammatory process. As a ligand for Mac-1, fibrinogen has been shown to play a role in neutrophil signalling by modulating the generation of second messengers, production of oxygen free radicals and cell adhesion in inflammatory conditions [7].

Previously, we have shown that at physiological concentrations, fibrinogen is able to modulate the pattern of neutrophil activation without interfering with the expression and activation of the Mac-1 integrin [3]. In fact, an increased free radical production was observed in neutrophils freshly isolated from peripheral blood of human healthy donors upon their incubation with physiological concentrations of fibrinogen. Interestingly however, both the membrane expression and the activation status of the Mac-1 integrin were not modified under these conditions. Overall, these results led us to suggest that fibrinogen could as well play a role in modulating the adhesive behaviour of the neutrophil towards the vascular endothelium under normal physiological conditions. In the present report, we aimed to address this issue by assaying neutrophil recruitment *in vitro* in flow assays performed under a physiological concentration of soluble fibrinogen (300 mg/dL). For such, we employed flow chambers and analysed the recruitment of neutrophils isolated from peripheral venous blood of healthy human donors onto monolayer of human umbilical vein endothelial cells (HUVEC).

2. Materials and methods

2.1. Human Umbilical Vein Endothelial Cells (HUVECs) monolayer preparation

Human umbilical vein endothelial cells (purchased from Invitrogen) were cultured in tissue culture dishes in Medium 200 supplemented according to manufacturer's instructions and maintained at 37°C in an atmosphere of 5% CO_2. HUVECs were used between passages 3 and 6. All supplements and media were purchased from Invitrogen.

For the flow assays, HUVECs were grown on 40 mm sterile round glass coverslip up to a cell confluence of around 80%. When required, HUVECs were activated in the presence of TNF-α (10 ng/mL) for 2 hour prior to the flow assay.

2.2. Isolation of human neutrophils

Human neutrophils were isolated from heparinised peripheral venous blood from healthy donors. After erythrocyte sedimentation in the presence of 6% of Dextran T500 (*Pharmacosmos*), the leukocyte-rich plasma was layered onto a Ficoll-Paque Plus (*Amersham Biosciences*) gradient and centrifuged at 400 g during 30 min at 4◦C. The pellet of neutrophils was collected and further washed in HBSS buffer (Hank's Balance salt solution, *Sigma*).

When required, neutrophils were incubated in 10 μM fMLP (N-formyl-methionine-leucine-phenylalanine, *Calbiochem*) or in 300 mg/dL fibrinogen (Sigma-Aldrich) for 15 min at 37◦C prior to being used in the flow assays.

2.3. Flow assay

The flow chamber and all the required components were purchased from Warner Instruments. This chamber was assembled according to the scheme presented in Fig. 1 and to the manufacturer's instructions. Briefly, the bottom round coverslip of 40 mm diameter (designated as component #2 in Fig. 1), over which a HUVECs monolayer was previously grown, was inserted into the base of the chamber (component #1). The chamber forming gasket (component #3) was further placed on the top of the culture. The 30 mm round coverslip (component #4) was inserted in the top cover slip (component #5) of the chamber and the pressure plate (component #6) tight.

The flow chamber was further assembled onto to the flow assay scheme presented in Fig. 2. In brief, a syringe filled with the neutrophil suspension at a concentration of 10^6 cells/mL in HBSS (purchased from Invitrogen) was placed onto a syringe pump and further connected to the outlet flow chamber at a shear stress of 1 dyn/cm^2. This flow chamber was then coupled onto the heated stage of a Fluorescence Inverted Microscope (Leitz Fluovert FU, objective 10×/0.30).

For the flow assay, neutrophils were initially allowed to flow for 5 minutes so as to ensure for flow stabilization and to attain an adequate number of cells interacting with the HUVECs monolayer. Image acquisition was then performed for up 10 to 25 min by employing a CCD-Iris color video camera (Sony). For each assay, images were collected at several locations on the dish but always concentrating in the middle of the flow chamber and avoiding its edges.

Acquired video sequences were further analysed with ImagePro-Plus software to quantify: (i) the number of rolling leukocytes (defined as the number of leukocytes moving at a low-velocity with a high-variance translation of 100 μm) as well as their rolling velocities (calculated by $v = d/t$, where d stands for the displacement of the leukocyte over a period of time, t) and (ii) the number of adherent leukocytes (defined as the total number of leukocytes adhering to the HUVEC monolayer per unit area for at least 30 sec). For this analysis, neutrophils were manually tagged and their movements on the monolayer monitored.

2.4. Statistical analysis

Data were obtained from six independent experiments and expressed as mean values ± standard error deviation (SD). Student's *t* test was used to determine the significance of differences between sample means. Statistical analysis was performed using Origin Pro8.

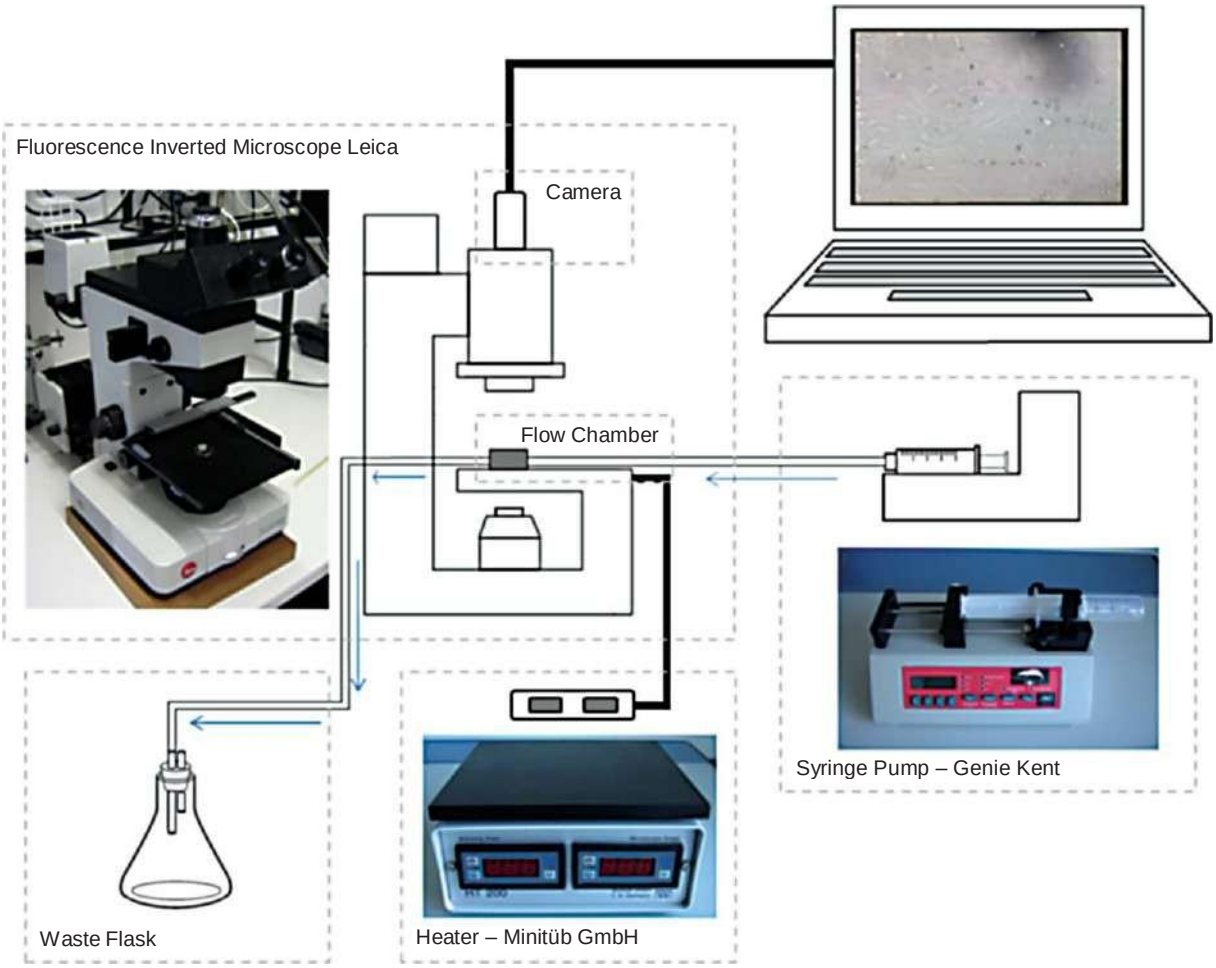

Fig. 2. Assembly of the flow chamber assays. Blue arrows depict the flow orientation.

3. Results

In this report, we made use of *in vitro* flow assays to understand whether soluble fibrinogen is able to interfere with the adhesive behaviour of the neutrophil in relation to an endothelial cell layer under physiological flow conditions. For such, we employed a flow chamber assay schematically depicted in Fig. 1 in which neutrophils isolated from peripheral blood of human healthy donors were flown over monolayers of HUVECs. In order to mimic more closely the *in vivo* situation, we used a constant wall shear stress of 1 dyn/cm^2, a value comparable to that found in postcapillary venules and that has been shown not to allow the direct adhesion of neutrophils to endothelial cells in the absence of an increased expression of selectins [11]. The neutrophil adhesive behaviour was further analysed by determining the following parameters: Number of rolling leukocytes; velocity of rolling and number of adherent leukocytes.

To ensure that the obtained neutrophils were not activated by our isolation procedure, fresh neutrophil isolates were first assayed on HUVEC monolayers previously activated or not. HUVEC activation was

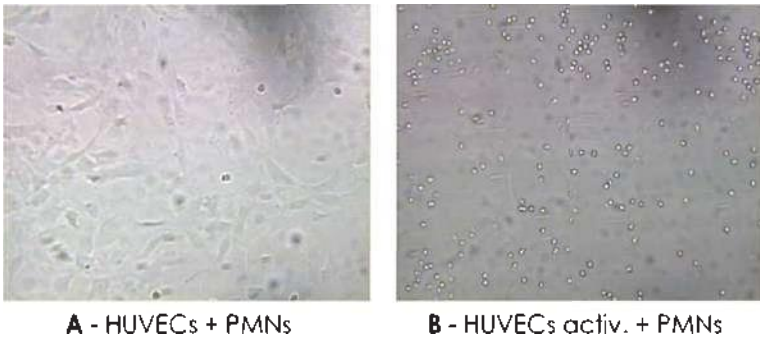

Fig. 3. Images acquired from the flow assays performed with non-treated neutrophils (here referred as PMNs) and HUVECs (panel **A**) or TNF-a-activated HUVECs, referred here as HUVECs activ (panel **B**). For each condition six assays were performed ($N = 6$). As depicted in the micrographs presented, an increased number of neutrophils were observed either rolling or adhering to the HUVEC monolayers in the assays shown in panel **B**.

performed by incubating the cell monolayer in the presence of a known inflammatory activator of endothelial cells, the tumour necrosis factor-alpha, TNF-a, at a concentration of 10 ng/mL for a period of 2 hours prior to use in the flow assay. In these assays, we observed a significantly smaller number of neutrophils either rolling on or adhering to a non-activated HUVEC monolayer in comparison to the numbers obtained when using a TNF-a-activated endothelial monolayer (Figs. 3 and 4 and Table 1). These results demonstrated that the isolated neutrophils were not able to bind spontaneously to the non-activated HUVECs and were not therefore activated during the isolation procedure used.

As a proof-of-concept of our flow assays, we further assayed the recruitment of neutrophils pre-treated with fMLP (a well-known neutrophil activator [10] onto TNF-a-activated HUVECs. In comparison with assays using non-treated neutrophils and activated HUVEC, we observed here a decreased number of rolling leukocytes (Fig. 4 and Table 1) with lower rolling velocities (Fig. 5 and Table 1) and an increased number of adherent neutrophils (Fig. 4 and Table 1). As discussed below, this scenario is consistent with that expected for an inflammatory situation [4].

Finally to address for a role for fibrinogen on the adhesive behaviour of neutrophils under normal conditions, neutrophils were pre-incubated with soluble fibrinogen at a concentration of 300 mg/dL for 15 min at room temperature prior to the flow assay. By probing these neutrophils on flow assays performed on activated HUVECs, we were able to observe that both neutrophil rolling as well as adhesion were differently affected when comparing to results obtained from flow assays using non-treated neutrophils and TNF-a-activated HUVEC (Figs. 4 and 5; Table 1). In fact, despite the number of rolling neutrophils was not affected in the presence of a physiological concentration of fibrinogen (Fig. 4 and Table 1), the rolling velocities of fibrinogen-treated neutrophils were significantly augmented (Fig. 5 and Table 1). Moreover, the number of adherent neutrophils was substantially diminished when these cells were pre-incubated with fibrinogen (Fig. 4 and Table 1).

4. Discussion

In a previous report, we demonstrated that soluble fibrinogen is able to modulate neutrophil activation when present at physiological concentrations [3]. This led us to propose that this plasma glycoprotein could as well modulate the adhesive behaviour of circulating neutrophils and therefore could modulate their recruitment towards the vascular endothelium.

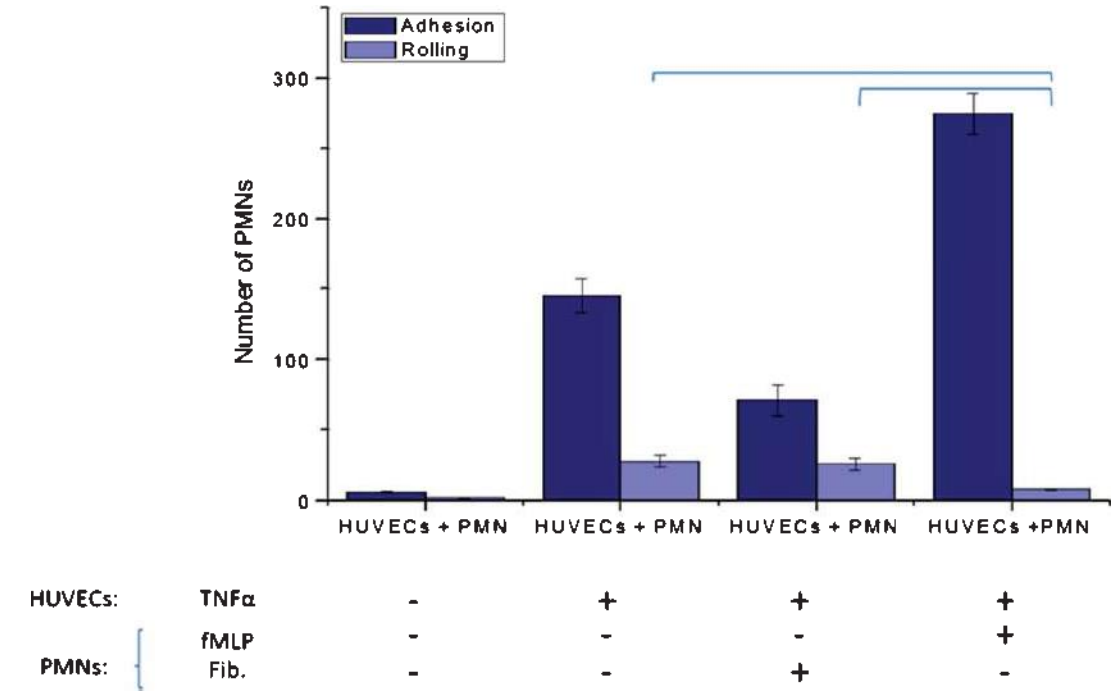

Fig. 4. Graphic representation of the mean values of the numbers of neutrophils (referred here as PMNs) rolling on HUVECs (labelled as Rolling in the Figure legend) or adhering to this endothelial cell layer (labelled as Adhesion in the Figure legend) determined in the distinct experimental conditions employed in the present manuscript. In the lower part of the figure, the treatments inflicted to HUVECs or neutrophils are indicated for each of the experimental conditions tested (Fib stands for fibrinogen). Error bars represent the standard error deviation obtained in a total of six experiments performed per experimental condition. In the presence of a physiological concentration of fibrinogen 300 mg/dL, the number of neutrophils rolling on an activated endothelium is not affected whereas the number of adherent neutrophils is substantially decreased ($p < 0.01$) when comparing to the recruitment data collected when using non-activated neutrophils and TNF-a-activated HUVECs.

Table 1

Summary of the results obtained for the neutrophil recruitment parameters determined in the flow assays performed in this study. For each condition six assays were performed ($N = 6$). Results are presented as mean values and the associated standard error deviations. PMN (abbreviated from polymorphonuclear cells) refers to the neutrophils; HUVECs activ stands for TNF-a-activated HUVECs; PMN Fib stands for neutrophils pre-incubated with fibrinogen (Fib) prior to the flow assay; PMN active stands for neutrophils pre-incubated with fMLP prior to the flow assay

	Number of adherent neutrophils	Number of rolling neutrophils	Rolling Velocities (μm/s)
HUVECs + PMN	6 ± 0.35	2 ± 0.35	0 ± 0
HUVECs activ + PMN	145 ± 12.21	28 ± 4.25	7,27 ± 2
HUVECs activ + PMN Fib	71 ± 10.79	26 ± 4.03	14 ± 1.48
HUVECs activ + PMN activ	275 ± 14.70	8 ± 0.50	4,1 ± 1.18

To address this working hypothesis, we made here use of *in vitro* flow assays by using (i) HUVEC monolayers and (ii) neutrophils freshly isolated from peripheral blood of human healthy donors. For the isolation of human neutrophils, we made use of a protocol shown previously to yield non-activated cells. Consistently, our neutrophil isolates did not bind spontaneously to non-activated endothelium under flow.

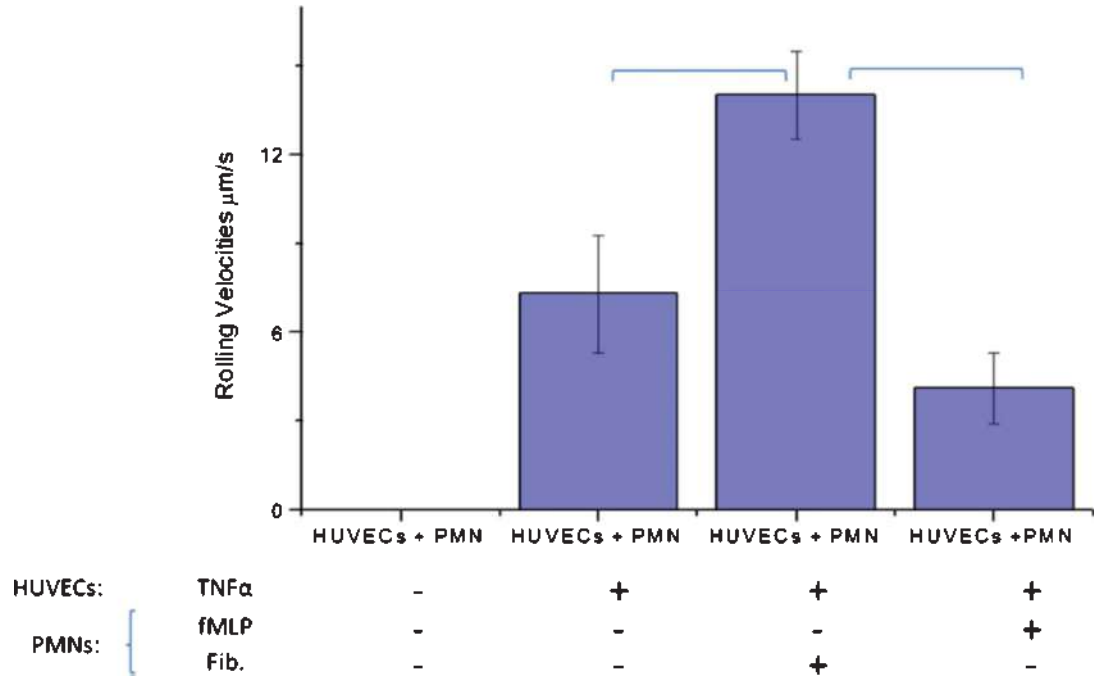

Fig. 5. Graphic representation of the mean values of the rolling velocities of neutrophils (referred here as PMNs) on HUVECs monolayers determined for the different experimental conditions employed in the present manuscript. In the lower part of the Figure, the treatments inflicted to HUVECs or neutrophils prior to the flow assays are indicated for each of the experimental conditions tested. Here (−) stands for absence of treatment and (+) for the incubation with the mentioned product (Fib stands for fibrinogen). Error bars represent the standard error deviation obtained in a total of six experiments performed per experimental condition. The rolling velocities of neutrophils increased significantly when the neutrophils were pre-incubated with soluble fibrinogen at 300 mg/dL in comparison to those measured for non-activated or fMLP-activated neutrophils ($p < 0.01$).

In vitro flow assays closely reproduce leukocyte recruitment under inflammatory conditions. In fact in these assays, activated neutrophils are expected to be significantly recruited towards an activated endothelium under flow. Accordingly, we were able to observe that neutrophils pre-incubated with fMLP, a known neutrophil activator [5, 9], adhered more extensively to the TNF-a-activated HUVEC monolayer in comparison to non-activated neutrophils. Additionally, rolling velocities for the former were also lower than those exhibited by non-activated cells. Altogether, these results are in agreement with the current knowledge on how leukocyte recruitment towards the vascular endothelial wall occurs in inflammation.

During the recruitment cascade, leukocytes are able to roll along the wall of inflamed post-capillary venules until they halt, adhere and then transmigrate. It is assumed that the recognition of endothelial-bound chemokines triggers the activation of particular leukocyte integrins which are responsible for the transition from rolling to adhesion. Depending on their conformational state, binding of an activated integrin to their specific ligands on the endothelium will lead either to a reduction of the rolling velocity or to the arrest of the leukocyte. Subsequent firm adhesion further will require additional activation of neutrophil integrins mediated via their binding to ligands expressed on the surface endothelial cell. Along this process, a slow rolling step will also contribute to the firm adhesion of the leukocyte to the vascular wall [12]. In fact at higher rolling velocities, strong leukocyte adhesion is not favoured and therefore a reduction in the rolling velocity must take place for a rolling leukocyte to adhere more firmly.

Having proven that our neutrophil isolates exhibited the expected adhesive behaviour in the used flow assays, we further assessed whether fibrinogen in a physiological concentration (300 mg/dL) could play a role in this respect. Under these conditions, we observed that the numbers of rolling neutrophils were not significantly affected when compared to those measured for non-activated neutrophils. Surprisingly however, rolling velocities measured for the former situation were significantly higher than those exhibited by the latter. As higher rolling velocities would predictably preclude neutrophil adhesion to the activated HUVECs, the number of adherent fibrinogen-treated neutrophils was consistently smaller than that determined for non-activated leukocytes.

Altogether, our current analysis of neutrophil recruitment under flow enabled us to conclude that at least *in vitro*, soluble fibrinogen at physiological concentrations is able to accelerate neutrophil rolling and consequently, to reduce their adhesion towards the vascular wall. Such reduction will necessarily translate into a decreased ability of the neutrophil to transmigrate towards an affected area and therefore into a diminished inflammatory response.

By combining these results with the published data [4, 14] where the authors suggested that leukocytes that engage fibrinogen molecules loosely bound to the surface of fibrin(ogen) matrix, we propose here that soluble fibrinogen at physiological concentrations is normally able to modulate the adhesive behaviour of the circulating neutrophil to activated endothelium. This action may reflect an ability of fibrinogen to shield the neutrophil from excessive adhesion towards the vascular wall. In other words, binding of soluble fibrinogen to the neutrophil membrane under normal conditions may loosen putative neutrophil-endothelium interactions so that the neutrophil may then be able to easily detach from the endothelial wall. Such a putative role for soluble fibrinogen could for instance be instrumental by preventing unwanted accumulation of neutrophils in the vasculature and subsequently, avoiding thrombus formation and growth.

Our future studies will address the *in vivo* functional relevance of such activity and importantly, the molecular mechanisms underlying this proposed shielding effect of soluble fibrinogen.

Acknowledgments

We would like to acknowledge FCT (Fundação para a Ciência e Tecnologia, Portugal) for funding this scientific project (PTDC/SAU-OSM/73449/2006) and VVA wishes to thank FCT for her Ph.D. Grant (SFRH/BD/30145/2006).

References

[1] S. Ahmadizad, M. El-Sayed and D. MacLaren, Effects of time of day and acute resistance exercise on platelet activation and function, *Clin Hemorheol Microcirc* **45**(2-4) (2010), 391–399.

[2] A. Atherton and G. Born, Quantitative investigations of the adhesiveness of circulating polymorphonuclear leucocytes to blood vessel walls, *J Physiol* **222** (1972), 447–474.

[3] V.V. de Almeida, A. Calado, H.S. Rosário and C. Saldanha, Differential effect of soluble fibrinogen as a neutrophil activator, *Microvascular Researche* **83**(3) (2012), 332–336.

[4] J.L. Dunne, C.M. Ballantyne, A.L. Beaudet and K. Ley, Control of leukocyte rolling velocity in TNF-alpha-induced inflammation by LFA-1 and Mac-1, *Blood* **99**(1) (2002), 336–341.

[5] D. Feng, J.A. Nagy, K. Pyne, H.F. Dvorak and A.M. Dvorak, Neutrophils emigrate from venules by a transendothelial cell pathway in response to FMLP, *J Exp Med* **187**(6) (1998), 903–915.

[6] M.J. Flick, X. Du, D.P. Witte, M. Jirousková, D.A. Soloviev, S.J. Busuttil, E.F. Plow and J.L. Degen, Leukocyte engagement of fibrin(ogen) via the integrin receptor aMb2/Mac-1 is critical for host inflammatory respose *in vivo*, *The Journal of Clinical Investigation* **113**(11) (2004), 1596–1606.
[7] M.J. Flick, D. Xinli and J.L. Degen, Fibrin(ogen)-alphaMbeta2 Interactions Regulate Leukocyte Function and Innate Immunity *In Vivo*, *Exp Biol Med* **229** (2004), 1105–1110.
[8] T. Gori, Viscosity, platelet activation, and hematocrit: Progress in understanding their relationship with clinical and subclinical vascular disease, *Clin Hemorheol Microcirc* **49**(1-4) (2011), 37–42.
[9] B. Heit, S. Tavener, E. Raharjo and P. Kubes, An intracellular signaling hierarchy determines direction of migration in opposing chemotactic gradients, *J Cell Biol* **159**(1) (2002), 91–102.
[10] T. Kinzer-Ursem, K. Sutton, A. Waller, G.M. Omann and J. Linderman, Multiple receptor states are required to describe both kinetic binding and activation of neutrophils via N-formyl peptide receptor ligands, *Cell Signal* **18**(10) (2006), 1732–1747.
[11] K. Konstantopoulos, S. Kukreti and L.V. McIntire, Biomechanics of cell interactions in shear fields, *Advanced Drug Delivery Reviews* **33** (1998), 141–164.
[12] P. Kubes and S.M. Kerfoot, Leukocyte Recruitment in the Microcirculation: The rolling paradigm revisited, *News Physiol Sci* **16** (2001), 76–80.
[13] K. Ley, C. Laudanna and M.N.S. Cybulsky, Getting to the site of inflammation: The leukocyte adhesion cascate update, *Nat Rev Immunol* **7** (2007), 678–689.
[14] V.K. Lishko, T. Burke and T. Ugarova, Antiadhesive effect of fibrinogen: A safeguard for thrombus stability, *Blood* **109** (2007), 1541–1549.
[15] V.K. Lishko, N.P. Podolnikova, V.P. Yakubenko, S. Yakovlev, L. Medved, S.P. Yadav and T.P. Ugarova, Multiple binding sites in fibrinogen for integrin alphaMbeta2 (Mac-1), *The Journal of Biological Chemistry* **279**(43) (2004), 44897–49064.
[16] R. Medzhitov, Origin and physiological roles of inflammation, *Nature* **454** (2008), 428–435.
[17] M. Mosesson, Fibrinogen and fibrin structure and functions, *Journal of Thrombosis and Haemostasis* **3**(8) (2005), 1894–1904.
[18] K. Urschel, A. Wörner, W. Daniel, C. Garlichs and I. Cicha, Role of shear stress patterns in the TNF-a-induced atherogenic protein expression and monocytic cell adhesion to endothelium, *Clin Hemorheol Microcirc* **46**(2-3) (2010), 203–210.

Hemorheological Effects of Valsartan in L-NAME Induced Hypertension in Rats

Ana Santos Silva-Herdade* and Carlota Saldanha

Instituto de Bioquímica, Unidade de Biologia Microvascular e Inflamação, Instituto de Medicina Molecular, Faculdade de Medicina de Lisboa, Portugal

Abstract: Animal models are a useful tool, for example, in the study of hypertension, but its use requires robust knowledge and well characterized models in order to extrapolate the obtained results. Nitric oxide is an important regulator of vascular function and blood pressure. The chronic administration of nitric oxide synthase (NOS) inhibitors provides an animal experimental model of hypertension. Our study aims to investigate the hemorheological effects of (i) N^{μ}-nitro-L-arginine methyl ester (L-NAME) added daily to Sprague-Dawley rats in drinking water and (ii) valsartan, an angiotensin II AT1-receptor antagonist, administration when the Sprague-Dawley rats acquired the hypertensive state. In three experimental groups (Control, Hypertensive and Valsartan) systolic blood pressure was measured and blood samples were collected for determination of erythrocyte membrane deformability and fluidity as well as blood and plasma viscosities.

L-NAME intake induces an increase in the systolic blood pressure indicating the development of systemic hypertension. Concerning the hemorheological parameters, the erythrocyte deformability is decreased in the hypertensive animal group and on contrary the erythrocyte membrane fluidity increased being both parameters values reverted after valsartan administration. Valsartan also decreases the plasma and blood viscosities values obtained in the animal group which have acquired systemic hypertension after L-NAME intake.

In conclusion, the angiotensin II AT1-receptor antagonist, valsartan, restores in hypertensive Sprague-Dawley rats L-NAME- dependent their systolic blood pressure to the physiological values, as well as, normalized their hemorheological parameters values; due to the similarity effects to human essential hypertension we conclude that this can be a suitable animal model for hemorheological studies in the field of hypertension.

Keywords: Hypertension, hemorheology, animal model, nitric oxide synthase.

1. INTRODUCTION

Hypertension is a common disease among adult populations and is a significant contributor to ill health, resulting in an excess of both morbidity and mortality. Moreover, hypertension is directly implicated in various cardiovascular disease states, including stroke, ischemic disease and peripheral vascular disease [1]. Studies in the area of hypertension showed that, an increase in arterial blood pressure leads to a decrease in the nitric oxide for the circulation, which reflects the role of the arginin-nitric oxide in the pathophysiology of hypertension [2].

Hypertension is an important risk factor for cardiovascular diseases and its treatment is essential for the prevention of those illnesses. Hemorheological properties are known to be associated with hypertensive states, although it is still not known if hemorheological abnormalities are the cause or the result of systemic arterial hypertension [2]. There is a significant positive correlation between blood pressure and hematocrit value [2, 3] and it has been shown that whole blood viscosity, plasma viscosity and red blood cell (RBC) aggregation tendency were increased, while erythrocyte deformability was decreased in hypertensive patients [2, 3]. On one hand, these hemorheological alterations may lead to an increased arterial blood pressure by altering the hemodynamic resistance [4, 5]. On the other hand, erythrocyte redox properties and hemorheological parameters are well known to be sensitive to the disturbances in local and general homeostasis in the living organism [6].

There is evidence that in human blood circulation, erythrocyte acts either as a donor or a scavenger of nitric oxide (NO) mediated by R (oxygenated) or T (deoxygenated) states of haemoglobin in dependence of tissues oxygen partial pressure [7, 8]. It has been also reported that NO modulated erythrocyte signal transduction mechanisms and deformability [9-13].

Animal models are important tools for the study of hypertension, but the use of laboratory animals implies a well characterized model in which it should be possible to generalize the findings and extrapolate them to other animal species or human [14]. This work aimed a hemorheological characterization and an erythrocyte nitric oxide efflux ability of an induced animal model of hypertension based on the chronic inhibition of NOS by the *N* -nitro-L-arginine methyl ester (L-NAME) and its response to the administration of an antagonist of AT1 receptors of angiontensin II, valsartan.

*Address correspondence to this author at the Instituto de Bioquímica, Unidade de Biologia Microvascular e Inflamação, Edíficio Egas Moniz, Faculdade de Medicina de Lisboa, 1649-028 Lisboa, Portugal;
Tel: +351217985136; Fax: +351217999477;
E-mail: anarmsilva@fm.ul.pt

1877-3826/11

2. METHODS

2.1. Animals

The animals used in this study received human care in accordance with the Directive of the European Community nº86/609/CEE that mentions the protection of animals used for economic ends and other scientific ends.

Sprague-Dawley male rats (N=30) (*Rattus norvegicus*, Sprague-Dawley, Harlan Iberica, Spain), with an average weight of 257±56g, were kept in an animal facility with a 12h light/dark cycle and housed in cages in a temperature controlled room. All animals were kept on a diet standard rat food and water *ad libitum*. Three groups of animals were considered: a Control group (N=10), a Hypertensive group (N=10) and the Valsartan group (N=10). The Hypertensive group (HTA) was obtained in rats to which was given 600mg/L of *N* -nitro-L-arginine methyl ester (L-NAME, Sigma, Fluka) in drinking water during 21 consecutive days, as in [15] and blood collections were performed at the end of this period. In the third group, valsartan group (HTA-VLT), rats were given 600mg/L L-NAME in drinking water during 21 consecutive days, as in the previous group, and an intravenous injection of 2mg/Kg of valsartan (Novartis, Germany), an antagonist of AT1-receptors of angiotensin II; in this group blood was collected 30 minutes after valsartan administration. Valsartan was administrated intravenous because it induces less stress and the dose administrated is comparable (dose/body weight) with the oral dose usually prescribed to humans.

2.2. Surgical Procedures

For the surgical procedures and microcirculatory measurements, the rats were anesthetized intraperitoneally with 1,5g/Kg body weight urethane (Sigma-Aldrich) and intramuscular 50mg/Kg body weight ketamine (Pfizer, Parke Davis) after 20 minutes. Body temperature was maintained between 35-37ºC with auto-regulable heating platform. A tracheostomy was performed to maintain the animal in spontaneous breath during all the experiment. For drug administration, the right jugular vein was cannulated with polyethylene tubing and the left carotid artery was cannulated for measurement of mean arterial pressure and cardiac frequency. Blood was also collected in the left carotid. At the end of the experiments the animals were euthanized with over-dosage of anaesthesia.

2.3. Systolic Blood Pressure

Arterial pressure was measured with a catheter connected to a pressure transducer TRANSPAC® (Abbot, Sligo, Ireland); being the cardiac frequency and the systolic and diastolic pressures measured and registered through hardware and software system PowerLab/400 (AD Instruments, Castle Hill, Australia).

2.4. Measurement of NO by an Amperometric Method Error! Reference source not found.

Erythrocyte suspensions were centrifuged and sodium chloride 0.9 % at pH 7.0 was added in order to reach a hematocrit of 0.05%. The suspension was gently mixed by tube inversion. For amperometric NO quantification, we used the amino-IV sensor (Innovative Instruments Inc. FL, USA), as previously described [11]. Briefly, after stabilization of the NO sensor immersed in erythrocyte suspensions (N = 5), the erythrocytes were stimulated with acetylcholine (ACh) 10 μM and changes in the electric current registered, the change being proportional to the amount of NO mobilized by ACh-stimulated erythrocytes.

2.5. Erythrocyte Deformability

The erythrocyte deformability for different shear stress (0.30, 0.60, 1.20, 3.00, 12.00, 30.00 and 60.00 Pa) was determined by using the Rheodyn SSD shear stress diffractometer from Myrenne GMBH (Roentgen, Germany) and erythrocyte deformability is expressed as the elongation index (EI) in percentage. The Rheodyn SSD diffractometer determines RBC deformability by simulating the shear forces exerted by the blood flow and vascular walls on the erythrocytes [16, 17]. Erythrocytes are suspended in a viscous medium and placed between a rotating optical disk and a stationary disk. A well defined shear force is exerted upon the suspension which forces the erythrocytes to deform to ellipsoids and align with the fluid shear stresses. If a laser beam is allowed to pass through the erythrocyte suspension a diffraction pattern appears on the opposite end. That diffraction pattern will be circular with resting erythrocytes, but becomes elliptical when the erythrocytes are deformed by shear. The light intensity of the diffraction pattern are measured at two different points (A and B), equidistant from the center of the image. The erythrocyte elongation index (EEI), in percentage, is obtained according the following formula: EEI(%)=A-B/A+B ×100.

2.6. Erythrocyte Membrane Fluidity

Erythrocyte membrane fluidity was assessed, as previously described [18]. using the lipophilic fluorescent probes DPH and TMA-DPH by fluorescence anisotropy measurements [19]. DPH fluorescence measurements were performed at an excitation wavelength (Z_{exc}) of 352 nm, an emission wavelength (Z_{em}) of 430nm and both bandwidths of 5 nm. TMA-DPH fluorescence measurements were carried out with Z_{exc}=340 nm, Z_{em}=425nm and both bandwidths of 5 nm. Results are expressed in fluorescence anisotropy values.

2.7. Plasma and Blood Viscosity

Blood samples treated with the anticoagulant K_3EDTA were centrifuged at 1200 rpm for 1 minute. The resulting plasma was collected for the determination of plasma viscosity by the Harkness method [20]. Whole blood viscosity (WBV) was determined in a Brookfield digital viscometer model LVTDV II cp., using native blood aliquots submitted at low (22.5 s^{-1}) and high (225 s^{-1}) shear stress forces.

2.8. Statistical Analysis

Data are expressed as means ± standard deviation. One-way ANOVA tests were used to compare values between different groups. Statistical analysis was conducted using the GraphPadPrism version 5.0. Statistical significance was set at $p < 0.05$.

3. RESULTS

Systolic blood pressure was measured in the three experimental groups - Control, HTA and HTA-VLT in order to analyse the hypertensive state of all the experimental

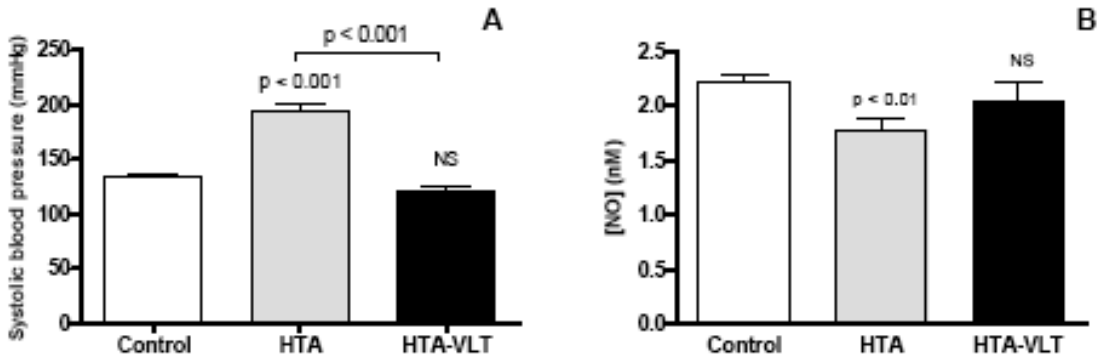

Fig. (1). (A) Mean ± standard deviation of systolic blood pressure values in Control, HTA and HTA-VLT groups. (B) Mean values ± standard deviation of NO concentrations in red blood cells in Control, HTA and HTA-VLT groups.

groups. Systolic blood pressure (Fig. **1**) is significantly increased ($p<0.001$) relatively to the control in the HTA group, as already shown in [14] and significantly decreased ($p<0.001$) when compared with HTA group after administration of the antihypertensive (HTA-VLT group).

The NO concentrations in the red blood cells in the three experimental groups are represented in Fig. (**1**) showing, as expected, that NO concentration is significantly decreased ($p<0.01$) in the HTA group. The intravenous administration of valsartan increases the NO concentrations when compared with HTA group, to values similar to the Control group.

The, already known, association of hemorheological parameters with hypertension lead us, in this animal model of hypertension, to study some of those properties, in order to characterize this model. Erythrocyte deformability (Fig. **2**) is, relatively to the normotensive, decreased in hypertensive rats (HTA), meaning that in this group the erythrocytes are less deformable, as already described by [14]. Analysing the values of EEI in the HTA-VLT group we observe that valsartan reverts the effect obtained in the hypertensive rats for higher values of shear stress, but maintained the deformability for lower shear stress levels in comparison with the HTA group.

The fluorescence anisotropy was determined in order to assess the erythrocyte membrane fluidity, high levels of fluorescence anisotropy represent low erythrocyte membrane fluidity. Therefore, hypertensive rats (HTA) have higher membrane fluidity when compared with the normotensive rats and after valsartan administration the erythrocyte membrane fluidity decreases to values similar with the control group (Fig. **3**).

Both plasma and blood viscosities (Fig. **4**) are significantly increased in the hypertensive rats group (HTA) and significantly decreased after valsartan administration. Althought not determined by us, L-NAME induced hypertension doesn't induce significant changes in hematocrit values [21], meaning that the changes in blood viscosity aren't a result of hematocrit changes.

4. DISCUSSION

Our results show that with this animal model of hypertension achieved by NOS inhibition, with L-NAME, leads to a hypertensive state, characterized by an increased systolic blood pressure, which is reverted by the antihypertensive – valsartan - administration.

Concerning erythrocyte NO efflux levels obtained in the induced – hypertensive animals there was a decrease in relation to the control group. There was NO efflux values reversion by administration of valsartan in that animal group after the installed hypertension leading to NO concentrations similar to normal levels. The decrease of erythrocyte NO efflux verified when hypertension was induced in the rats is not in accordance with our results obtained in blood samples of hypertensive humans [13]. The hypertension aetiology differences between human and L-NAME induced-hypertension animal model may be an explanation for the different compensatory mechanism of erythrocyte NO efflux. Valsartan is an angiotensin II type 1 (AT1) receptor blocker which doesn't reduce angiotensin II concentrations, in contrast with angiotensin converting enzyme inhibitors. Angiotensin II, by type 2 receptors, stimulates NO release by the endothelium [22-24], inducing vasodilation and decreasing the blood pressure. We may raise the hypothesis of a similar signal transduction mechanism induced by valsartan at erythrocyte level as we have demonstrated with

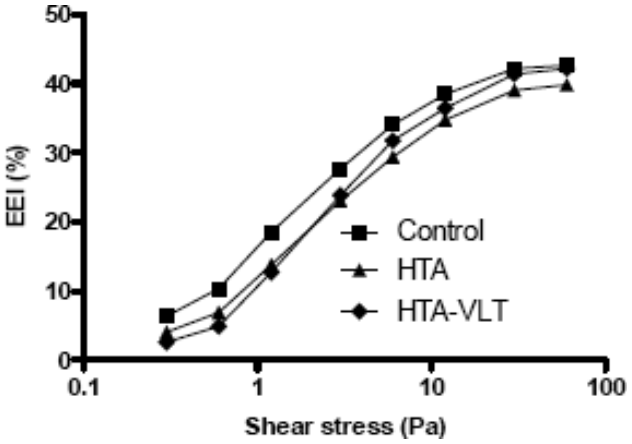

Fig. (2). Mean values of erythrocyte elongation index (EEI) in Control, HTA and HTA-VLT groups.

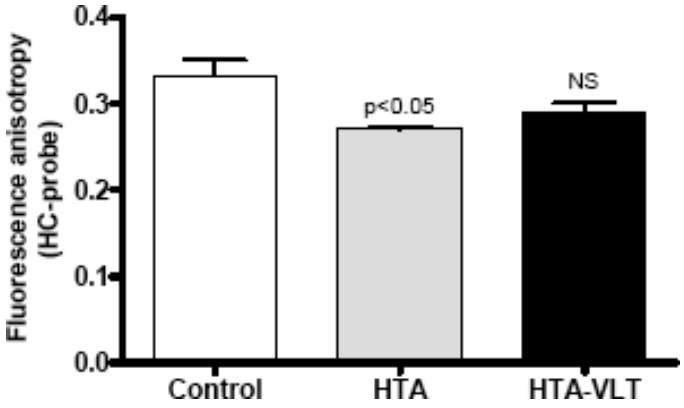

Fig. (3). Mean values ± standard deviation of fluorescence anisotropy (HC probe) in Control, HTA and HTA-VLT groups.

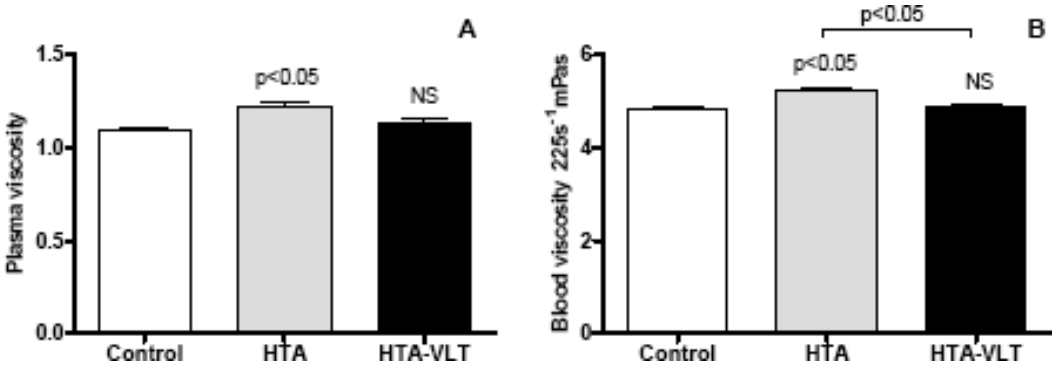

Fig. (4). Mean values ± standard deviation for plasma (A) and blood viscosity (B) in Control, HTA and HTA-VLT experimental groups.

acetylcholine also known as a vasodilator mediated by NO at intact endothelium [11].

Hypertension is an important risk factor for cardiovascular diseases and that its treatment is essential for the prevention of those diseases. The study of hemorheological properties is very important in cardiovascular diseases and alterations in some hemorheological parameters, as blood and plasma viscosity, red blood cells deformability and aggregation, are associated with hypertensive conditions [3].

Relatively to the hemorheological properties of the NOS inhibition-induced hypertensive animal model there have similar profile to the hemorheological properties evaluated in humans with hypertension. Red blood cells deformability is lower after NOS inhibition which is reverted, for higher shear stress values, after the administration of valsartan. As a compensatory mechanism for the decreased deformability, in the hypertensive group the red blood cells membrane fluidity is increased. We verified that Valsartan in turn decreases the red blood cells membrane fluidity in hypertensive rats recovering the mice normal values. The mechanism underlying the valsartan induced-erythrocyte membrane fluidity changes may be associated with several biochemical process involving external domains of the erythrocyte membrane near the lipid-water [19]. Concerning plasma and blood viscosities, we found similar alterations as has been observed in human hypertensive patients [5], namely they are increased in the studied animal model of hypertension but both parameters values are decreased after valsartan administration.

NOS inhibition-induced hypertension animal model has a hemorheological profile similar to human essential hypertension [5] and valsartan ameliorates the hypertensive state restoring the hemorheological modifications obtained. These results show that the NOS inhibition-induced hypertension animal model is a suitable model for hemorheological studies in the field of hypertension, because the alterations observed in this model are similar to the ones observed in human essential hypertension and the reversibility of the model can easily be achieved by the administration of an antagonist of AT1-receptor of angiotensin II, like valsartan.

ACKNOWLEDGEMENTS

We thank Mrs. Teresa Freitas (Faculdade de Medicina - Universidade de Lisboa) for the technical assistance in the hemorheological determinations.

REFERENCES

[1] Lip, G.Y.; Barnett, A.H.; Bradbury, A.; Cappuccio, F.P.; Gill, P.S.; Hughes, E.; Imray, C.; Jolly, K.; Patel, K. Ethnicity and cardiovascular disease prevention in the United Kingdom: a practical approach to management. *J. Hum. Hypertens.*, **2007**, *21*, 183–211.

[2] Kang, K.-T.; Sullivan, J.C.; Sasser, J.M.; Imig, J.D.; Pollock, J.S. Novel nitric oxide synthase–dependent mechanism of vasorelaxation in small arteries from hypertensive rats. *Hypertension*, **2007**, *49*, 893-901.

[3] Ross, R. Atherosclerosis – an inflammatory disease. *N. Engl. J. Med.*, **1999**, *340*, 115-126.

[4] Chae, C.U.; Lee, R.T.; Rifai, N.; Ridker, P.M. Blood pressure and inflammation in apparently healthy men. *Hypertension*, **2001**, *38*, 399-403.

[5] Meiselman, H.J. Hemorheologic alterations in hypertension: chicken or egg? *Clin. Hemorheol. Microcirc.*, **1999**, *21*, 195–200.

[6] Ajmani, R.S. Hypertension and hemorheology. *Clin. Hemorheol. Microcirc.*, **1997**, *17*, 395–484.

[7] MacMahon, T.; Doctor, A. Extrapulmonary Effects of Inhaled Nitric Oxide. *Proc Am. Thorac. Soc*., **2006**, *3*, 153-160.

[8] Pawloski, J. R.; Hess, D. T.; Stamler, J. S. impaired vasodilation by red blood cells in sickle cell disease. *PNAS* **2005**, *102*, 2531-2536.

[9] Mallozzi, C.; Di Stasi, A.M.; Minetti, M. Peroxynitrite modulates tyrosine-dependent signal transduction pathway of human erythrocyte band 3. *FASEB J*., **1997,** *11*, 1281-1290

[10] Carvalho, F.A.; Mesquita, R.; Martins-Silva, J.; Saldanha, C. Acetylcholine and choline effects on erythrocyte nitrite and nitrate levels. *J. Appl. Toxicol.*, **2004**, *24*, 419–427.

[11] Carvalho, F.A.; Martins e Silva, J.; Saldanha, C. Amperometric measurements of nitric oxide in erythrocytes. *Biosens. Bioelectron.*, **2004**, *20*, 505-8.

[12] Mesquita, R.; Pires, I.; Saldanha, C.; Martins-Silva, J. Effects of acetylcholine and spermineNONOate on erythrocyte hemorheologic and oxygen carrying properties. *Clin. Hemorheol. Microcirc*., **2001,** *25*, 153-163.

[13] Carvalho, F.A.; Maria, A.V.; Braz Nogueira, J.M.; Guerra, J.; Martins-Silva, J.; Saldanha, C. The relation between the erythrocyte nitric oxide and hemorheological parameters. *Clin. Hemorheol. Microcirc*., **2006,** *35*, 341-347.

[14] van Zutphen, L.F.M.; Baumans, V.; Beynen, A.C. Principles of laboratory animal science. New York: Elsevier; **2005**.

[15] Hacioglu, G.; Yalcin, O.; Bor-Kucukatay, M.; Ozkaya, G.; Baskurt, O.K. Red blood cell rheology properties in various rat hypertension models. *Clin. Hemorheol. Microcirc*., **2002**, *26*, 27-32.

[16] Starzyk, D.; Korbut, R.; Gryglewski, R.J.; Effects of nitric oxide and prostacyclin on deformability and aggregability of red blood cells of rats *ex vivo* and *in vitro*. *J. Physiol. Pharmacol.*, **1999,** *50*, 629-637.

[17] Schmid-Schönbein, H.; Ruef, P.; Linderkamp, O. The shear stress diffractometer Rheodyn SSD for determination of erythrocyte deformability, I. Principle of operation and reproducibility, *Clin. Hemorheol. Microcirc*., **1996**, *16*, 48-50.

[18] Saldanha, C.; Santos, N.C.; Martins-Silva, J. Fluorescent probes DPH, TMA-DPH and C17-HC induced erythrocyte vesiculation. *J. Membr. Biol*., **2002**, *190(1)*, 75-82.

[19] Lentz, B.R. Membrane 'fluidity' from fluorescence anisotropy measurements. Loew M Ed. Spectroscopic Membrane Probes, Volume I. Boca Raton (Florida): CRC Press; 1988.

[20] Harkness, J. A new instrument for measurement of plasma viscosity. *Lancet* **1963**, *16*, 280-281.

[21] Balaszczuk, A.M.; Tomat, A.; Bellucci, S.; Fellet, A.; Arrauz, C. Nitric oxide synthase blockade and body fluid volumes. *Braz. J. Med. Biol. Res*., **2002,** *35*, 131-134.

[22] Ruilope, L.M.; Rosei, E.A.; Bakris, G.L.; Mancia, G.; Poulter, N.R.; Taddei, S.; Unger, T.; Volpe, M.; Waeber, B.; Zannad, F. Angiotensin receptor blockers: therapeutic targets and cardiovascular protection. *Blood Pressure*, **2005**, *14*, 196-209.

[23] London, M. The role of blood rheology in regulating blood pressure. *Clin. Hemorheol. Microcirc.*, **1997**, *17*, 93–106.

[24] Mchedlishvili, G.; Tsinamdzvrishvili, B.; Beritashvili, V.; Gobejishvili, L.; Ilencko, V. New evidence for involvement of blood rheological disorders in rise of peripheral resistance in essential hypertension. *Clin. Hemorheol. Microcirc*., **1997**, *17*, 31–39.

Received: August 05, 2010 Revised: October 10, 2010 Accepted: October 16, 2010

Series on Biomechanics vol.25, No.1-2 (2010), 54-60

Erythrocyte deformability responses to shear stress under external and internal stimuli influences

C. Saldanha [a], J.P. Lopes de Almeida [b], T.Freitas [a], S. Oliveira [a], Ana S.Silva-Herdade [a]

[a] *IMM Faculdade de Medicina Universidade de Lisboa, ubimi@fm.ul.pt*
[b] *jpedro.gla@gmail.com*

Abstract

The degree of erythrocyte deformability (ED) changes as a consequence of alterations on either its membrane properties, or shape or internal composition may provide information about erythrocyte functional disturbances.

Several metabolic, cerebral and cardiovascular diseases are characterized by decreased ED that may compromise the blood flow in microcirculation.

"In vitro" effects of compounds on ED under different shear stresses may be studied using an ektacytometer apparatus which give us the erythrocyte elongation index (EEI) as a degree of the ED ability.

When phosphorylation level of erythrocyte band 3 protein was modified by specific PTK and PTP inhibitors, no ED changes were observed. Cytoskeleton protein phosphorlation levels modifications obtained with PKC inhibitor or activator decreased and increased EEI respectively.

When the thiol status of the erythrocyte were preserved with dithiothreitol (DTT), no alterations on EEI were verified. ED values increased for all shear stresses when in presence of the acetylcholine at variance when submitted to the Spermine NONOate that only at high shear stresses an EEI increase was observed.

Better understanding of those molecules on erythrocyte signal transduction mechanisms may bring potential targets for drug intervention on ED-dependent blood rheology.

Keywords: Erythrocyte deformability, acetylcholine, band 3 protein

1.Introduction

Erythrocytes are blood components in charge to tissue oxygenation, after hemoglobin (Hb) oxygen saturation at lung level, where a transition of a partial deoxygenated tense (T) form of Hb to a relaxed (R) conformation occurred with nitrosylation of cysteine 93 β-chain by nitric oxide (NO), resulting S-nitroso-hemoglobin (SNO-Hb)[1]. After the oxygen supply at tissue level Hb ferrous heme quenched NO, produced by vascular endothelial cells or platelets, with the formation at both α and β chains of ferrous heme –nitrosyl adducts. [2].Red blood cells (RBCs) act as oxygen and nitric oxide sensor in the systemic microcirculation, [3]. After the discovery of NO induced vasodilation on intact endothelium in dependence of acetylcholine (ACh) [4], the presence of this one in plasma was determined and the genes and proteins expression need for its synthesis and hydrolysis were confirmed in endothelial cells, and lymphocytes, [5, 6,7, 8]. Erythrocyte has at membrane level the enzyme acetylcholinesterase, (AChE) considered as a membrane integrity biomarker, [9], and among others proteins has also the integral protein "band 3", [10]. It was shown that band 3 may provide a route for both the NO influx and efflux to or from erythrocyte [11, 12]. A S- nitroso-Hb- band 3 complex was evidenced by Pawloski et all, [11] according to which, the NO leaves the SNO-Hb being capted by the thiol group of band 3 N-terminal cytoplasmic domain (cdb3). The NO mobilization inside erythrocyte was quantified by its derivatives molecules also named nitric oxide reactive species (NORS) such as nitrites, nitrates, S-nitroso-glutathione, peroxinitrite and the major binding protein complex the SNOHb, those being interrelated by chemical reactions in dependence of the thiol and the oxidative status of RBCs [13,14,15]. We have verified that when erythrocytes are incubated with ACh there is an increase in NO efflux and changes on nitrite and nitrate concentrations [16]. The signal

transduction mechanism proposed by us [16] to explain the relation between the chemical external signal ACh and its effect on the erythrocyte NO efflux and mobilization involving the intervention of the $G\alpha i\beta$ protein and the band 3 phosphorylation was further confirmed [17,18,19]. In vivo the band 3 phosphorylation and dephosphorylation states are in dynamic equilibrium maintained by proteins tyrosine kinase (PTK) of Src-family (lyn) and p72syk and by protein tyrosine phospatase (PTP) [20]. PTK and PTP may exist in active or inactive states under erythrocyte thiol status dependence, thereby meaning that oxidation of the thiol groups induce PTK activation and PTP inactivation [21]. The phosphorylation of p72syk and PTP serine/theonine residues by protein kinase C (PKC) induce enzyme activation in the former and inhibition in the second, [20].

The interactions established between erythrocyte membrane peripheral and cytoskeleton proteins are modulated by PKC activity [22] and the number and strength of those along with other kinds of membranes biomolecules interactions are responsible for the maintenance of erythrocyte deformability (ED) [23]. Beyond erythrocyte membrane properties the internal viscosity and the ratio between volume surface are crucial parameters on the erythrocyte ability to deform when in vivo pass thought capillaries of lower diameter that its own under blood flow shear stress [24]. Ektacytometer is an instrument developed initially by Groner et all, that allows in vitro quantification of the erythrocyte elongation index (EEI) as a degree of the ED ability subjected to different defined shear stresses, [25].

The aim of our work was to study the effects of internal and external chemical stimuli on ED under different shear stresses using an ektacytometer apparatus.

2. Methods

2.1 Chemical compounds – All the chemical compounds namely acetylcholine (ACh), SpermineNONOate, dithiothreitol (DTT), p72syk inhibitors namely (Syk) and aminogenistein (AMGT), PTP inhibitor calpeptin (Calp), chelerythrine chloride (Che), phorbol 12-myristate 13-acetate (PMA) used are purchased as indicated in our previously publications: [16,18,26,27].

2.2. Blood samples - Blood samples were supplied according protocol, with the Portuguese Institute of Blood, in Lisbon and it was collected into tubes BD Vacutainer ^{TM} with lithium heparin (17UI/ml) as an anticoagulant. All donors were males and duly informed.

2.3 Erythrocyte deformability - Erythrocyte deformability at different shear stress (0.30; 0.60; 1.20; 3.00; 12.00; 30.00; 60.00 Pa) was determined by using the Rheodyn SSD shear stress diffractometer from Myrenne GMBH (Roentgen, Germany) and erythrocyte deformability was expressed as the elongation index (EI) in percentage. Rheodyn SSD diffractometer determines RBC deformability by simulating shear forces exerted by blood flow and vascular walls on erythrocytes. Erythrocytes were suspended in a viscous medium and placed between a rotating optical disk and a stationary disk. A well define shear force is exerted upon the suspension witch forces the erythrocytes to deform to ellipsoids and align with the fluid shear stresses. If a laser beam is allowed to pass through the erythrocyte suspension a diffraction pattern appears on the opposite end. That diffraction pattern will be circular with resting erythrocytes, but becomes elliptical when these ones are deformed by shear. Light intensity of the diffraction pattern are measured at two different points (A and B), equidistant from the centre of the image. Erythrocyte elongation index (EEI), in percentage, is obtained according the following equation: EEI (%) = [(A-B)/ (A+B)] x 100.

2.4 Experimental design - Anticoagulated blood samples are divided in aliquots of 1mL., centrifuged at 11000 rpmh (Biofuge 15 centrifuge, Heraeus) during 1 minute at room temperature. 10µL of plasma is removed or not (aliquot control) and 10µl of the desired internal or external chemical stimuli is added in order to reach the desired final concentration as previously published, [16, 18, 26, 27]. Then the blood sample aliquots were homogenised by gently inversion and erythrocytes deformability was determined.

2.5 Statistical analysis - The results are presented as means ± standard deviation.
Student's *t*-test for paired observations was used to evaluate statistical significance of differences between the studied parameters. For every parameter all samples were tested against their respective control,and both

controls were tested against each other. Statistical significance was considered for values of $P < 0.05$. The statistical analysis was performed using the following software (for IBM PCs or compatible platforms):(i) SPSS 10 (SPSS Inc.), (ii) SYSTAT Version 9 (SPSS Inc.) and (iii) SigmaPlot 2000 version 6.0 (SPSS Inc.).

3. Results

3.1 Erythrocyte deformability under external stimuli influences

3.1.1 Acetylcholine dependence (16) - As show (see Fig. 1), RBC deformability increased slightly but significantly in the aliquots incubated with ACh 0.01 mM for low shear stress values (6 Pa) [37.0±1.4 vs. 36.5±1.6 (control), $P < 0.030$], and for higher shear stress values (30 Pa) [46.8±3.5 vs. 45.8±3.7 (control), $P < 0.041$]. RBC deformability in presence of acetylcholine 1mM showed no significant changes relatively to control.

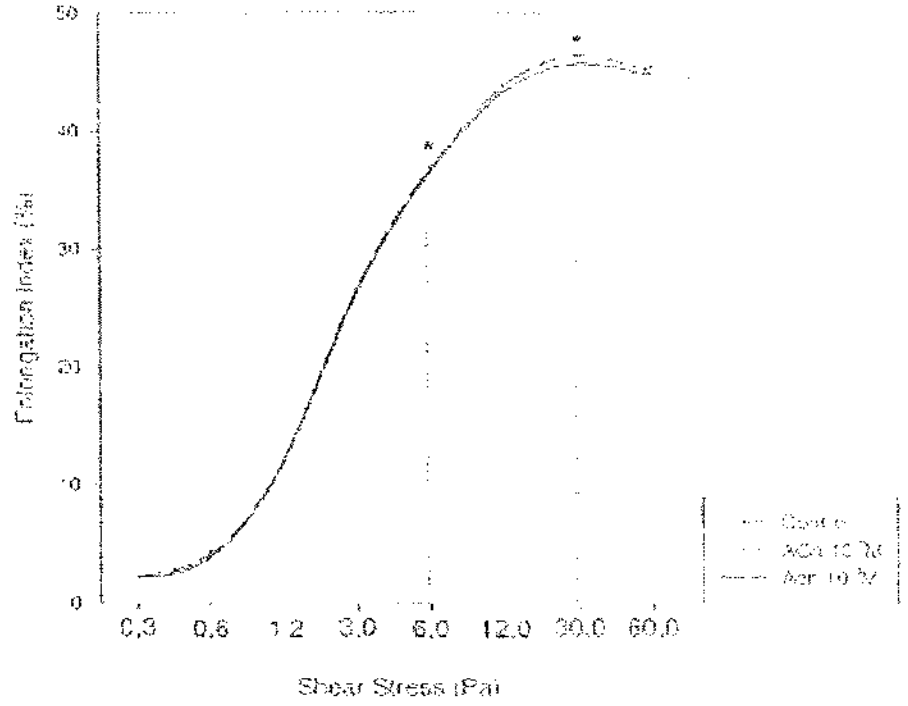

Fig.1. Effect of ACh on the erythrocyte deformability, [16]. * Indicates statistical difference as indicated in the text

3.1.2 NO donor SpermineNONOate dependence (16, 26) - In aliquots incubated with SpermineNONOate (see Fig. 2), 10−5 M we observed an increase in RBC deformability for shear stress values of 12 Pa [45.17 ± 3.3 vs. 43.66 ± 3.4, $P < 0.012$]; 30 Pa [48.38 ± 4.5 vs. 46.32 ± 4.4, $P < 0.008$] and 60 Pa [46.85 ± 4.2 vs. 45.16 ± 4.6, $P < 0.016$]. In presence of SpermineNONOate 10−4 M RBC deformability increased significantly for shear stress values of 30 Pa [47.81±4.4 vs. 46.32±4.4, $P < 0.023$] and 60 Pa [46.38±4.3 vs. 45.16 ± 4.6, $P < 0.019$]

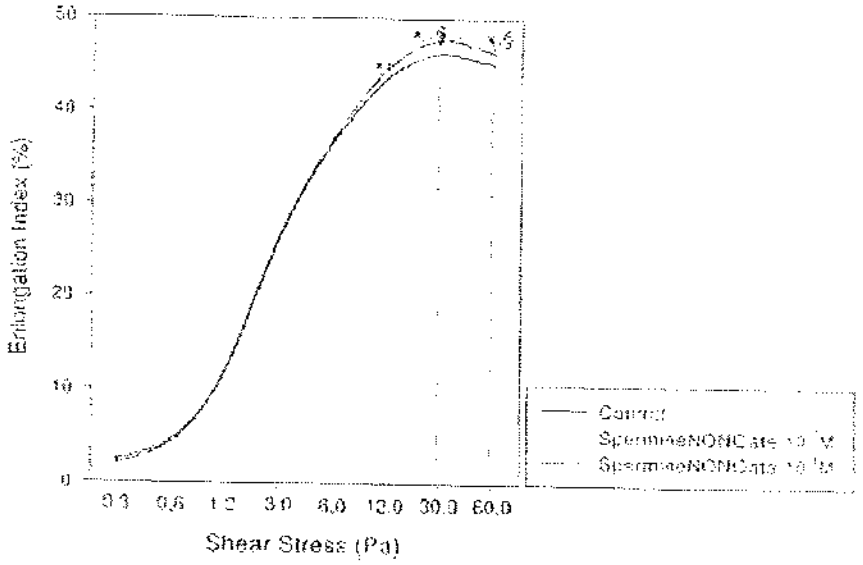

Fig.2 Effect of SpermineNoNoate on the erythrocyte deformability, [16]. * Indicates statistical difference as indicated in the text

3.1.3 *DTT dependence (18)* - The control erythrocyte samples showed an average elongation index of 4.41 ± 3.46% at low shear stress (0.6 Pa) and 51.36 ± 3.70% at high shear stress (60 Pa). The presence of DTT 1 μM decreases the elongation index at 0.6 Pa shear stress (4.11 ± 4.26% vs. control samples; $p > 0.05$), as well as at 60 Pa shear stress (48.24 ± 6.26% vs. control samples; $p > 0.05$).

3.2 *Erythrocyte deformability under internal stimuli influences*

3.2.1 Band 3 protein phosphorylation degree dependence (27) – The values of erythrocytes elongation indexes measured at different shear stresses did not significantly change in the presence of any of the inhibitors of band 3 phosphorylation enzyme PTK (Syk, and AMGT), and dephosphorylation enzyme PTP (Calp) in the blood samples aliquots when compared with the control aliquot.

3.2.2 PKC inhibition or activation dependence (28) - PKC inhibition promotes a significantly ($P < 0.01$) decreased on erythrocyte deformability when we compare the aliquot Che (PKC inhibitor) with the aliquot control (see Fig. 3). On the aliquots of AMGT+Che the values of erythrocyte deformability had significantly ($P < 0.01$) increased when we compared them with the values obtained in Che aliquot. For the aliquots with Calp + Che the EEI values were not significantly different in relation to the values obtained in Che aliquot.

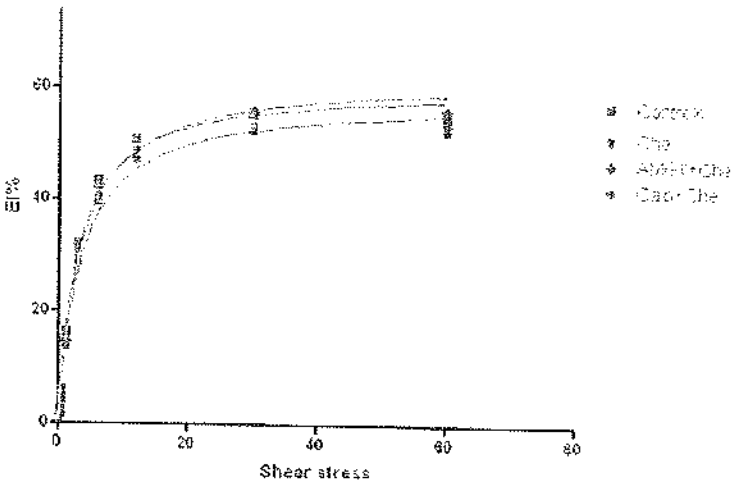

Fig.3. Effect of PKC inhibitor (Che) in absence and presence of PTK and PTP inhibitors

PKC activation with PMA promotes a significantly ($P < 0.01$) increased on erythrocyte deformability when compared with the values of erythrocyte deformability obtained for control aliquot. (see Fig.4). In the aliquots Calp+PMA the erythrocyte deformability values were significantly decreased ($P < 0.01$) when we compared them with PKC activation control aliquot and also with the control aliquot (see Fig.4).

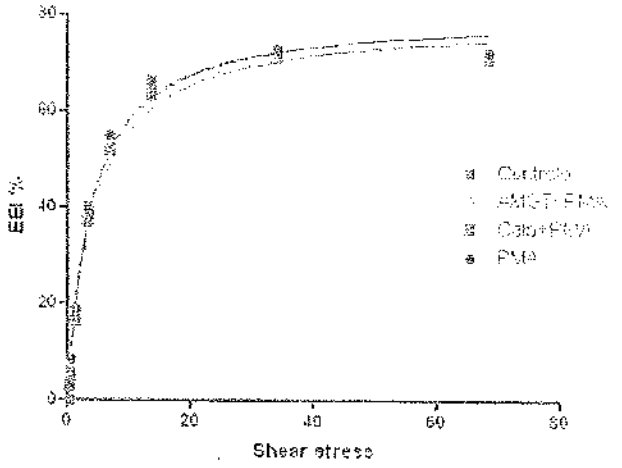

Fig.4. Effect of PKC activator (PMA) in absence and presence of PTK and PTP inhibitors' respectively AMGT and Calp on EEI values at all shear stress measured.

4. Discussion

The results obtained in our *in vitro* study, with the erythrocyte as an experimental model, showed that at physiological shear stress and above, ED is disturbed by internal and external chemical stimuli.
ACh 10-5 M induces significantly higher EEI values at 6 Pa and 30 Pa (see Fig. 1).Increasing acetylcholine concentrations blunt this effect in RBC deformability. The samples incubated with SpermineNONOate exhibited an increase in RBC deformability index for shear stress values of 12, 30 and 60 Pa (Fig.2). Accordingly the results of SpermineNONOate, and NO effects on RBC deformability are not dose-dependent and are more pronounced than acetylcholine's therby meaning higher EEI values obtained at high shear stress.
The ED modulation by external stimuli such as ACh and SpermineNONOate (NO donor) may be associated with the band 3 phosphorylation degree which is in accordance with the known (i) NO mediated passage from outside to inside erythrocytes and vice versa through band 3 and (ii) the occurrence of RBCs band 3 phosphorylation in the presence of the ACh [18]. Others observed a maintained dynamic equilibrium between the band 3 phosphorylation and dephosphorylation states[20] that may explain the absence of the RBCs deformability changes finding by us [27].

However, when those band 3 interferences in its phosphorylation state are in presence of PKC inhibitor or activator there are erythrocyte responses in terms of its ability to deform under the shear stresses applied, (see Fig. 3 and Fig. 4). As mentioned above PKC activate PTK and inhibits PTP as a result of the phosphorylation induced in both enzymes [20]. Our results showed higher and lower values of EEI when
PKC is activated in presence of PMA or inhibited with Che indicated a band 3 phosphorylation degree dependence (see Fig. 3 and Fig. 4). The phosphorylation of erythrocyte membrane cytoskeleton band 4.1 protein by PKC directly or cAMP dependent as previously demonstrated [29,30]decreased the interaction spectrin-band 4.1 [30] and may be a synergic factor to explanation of the EEI increase obtained when PKC is activated (see Fig. 4). A dissociation between band 4.1 phosphorylated by PKC and band 3 was described as a mechanism by which the RBCs membrane mechanical properties and proteins association may be modulated [31,32]. The erythrocyte membrane proteins phosphorylation levels are regarded by others as influencing factors of membrane mechanically stability in wich a higher deformability is associated with high phosphorylation degree [33]. We have previously assessed an increase of PKC enzyme activity, when erythrocyte are incubated in presence of ACh [34] and the PKC evidence effects on membrane proteins may be another explanation for the favourable ED obtained [16] (see Fig.1).

The maintenance of a normal erythrocyte thiol status at the expenses of DTT induces no variation for all the shear stresses studied on ED [18]. The presence of DTT avoiding possible reactions of the nitric oxide and oxygen reactive species within erythrocyte either with biomolecules or with organic metabolites may explain the absence of ED modifications.

In conclusion our work showed that erythrocyte deformability modifies at several shear stress under the influence of added chemical compounds with implications on signal transduction mechanism. This might open novel routes for further therapeutically avenues.

Acknowledgements

This work was supported by Fundação para a Ciência e a Tecnologia grant. We are grateful to Emília Alves for manuscript typewriting

References

[1] Brunori, M. Taylor, JF. Antonini, E. Wyman, J. Rossi-Fanelli, A., 1967. Studies on the oxidation-reduction potentials of heme proteins. VI. Human hemoglobin treated with various sulfhydryl reagents. J Biol Chem. 242, 2295-2300.

[2] Bonaventura, C. Ferruzzi, G. Tesh, S. Stevens, RD., 1999. Effects of S-nitrosation on oxygen binding by normal and sickle cell haemoglobin. J Biol Chem. 274, 24742-24748.

[3] Sonveaux, P. Lobysheva, II. Feron, O. McMahon, TJ., 2007. Transport and peripheral bioactivities of nitrogen oxides carried by red blood cell hemoglobin: role in oxygen delivery. Physiology 22, 97-112.

[4] Furchgott, RF. Vanhoutte, PM., 1989. Endothelium-derived relaxing and contracting factors. FASEB J 3, 2007-2018.

[5] Wessler, I. Kirkpatrick, CJ. Racké, K. 1998. Non-neuronal acetylcholine, a locally acting molecule, widely distributed in biological systems: expression and function in humans. Pharmacol Ther 77, 59-79.

[6] Wessler, I. Kilbinger, H. Bittinger, F. Kirkpatrick, CJ., 2001. The biological role of non-neuronal acetylcholine in plants and humans. Jpn J Pharmacol. 85, 2-10.

[7] Sergei A. Grando, Koichiro Kawashima, Ignaz Wessler. 2003. Introduction: The non-neuronal cholinergic system in humans. Life Sciences 72, 2009-2012.

[8] Carvalho, FA. Graça, LM. Martins-Silva, J. Saldanha, C., 2005. Biochemical characterization of human umbilical vein endothelial cell membrane bound acetylcholinesterase. FEBS J, 272, 5584-5594.

[9] Aloni, B. Livne, A., 1974. Acetylcholine esterase as a probe for erythrocyte-membrane intactness. Biochem Biophys Acta 339, 359-366.

[10] http://www.ruf.rice.edu/~bioslabs/studies/sds-page/rbcmembrane.html.

[11] Pawloski, JR. Hess, DT. Stamler, JS., 2005. Impaired vasodilation by red blood cells in sickle cell disease. PNAS 102, 2531-2536.

[12] Huang, KT. Han, TH. Hyduke, DR. Vaughn, MW. Van Herle, H. Hein, TW. Zhang, C. Kuo, L. Liao, JC., 2001. Modulation of nitric oxide bioavailability by erythrocytes. PNAS 98, 11771-11776.

[13] Pfeiffer, S. Mayer, B., 1998. Lack of tyrosine nitration by peroxynitrite generated at physiological pH. J Biol Chem. 273, 27280-27285.

[14] Vaughn, MW. Huang, KT. Kuo, L. Liao, JC., 2000. Erythrocytes possess an intrinsic barrier to nitric oxide consumption. J Biol Chem. 275, 2342-2348.

[15] Gladwin, MT. Wang, X. Reiter, CD. Yang, BK. Vivas, EX. Bonaventura, C. Schechter, AN., 2002. S-Nitrosohemoglobin is unstable in the reductive erythrocyte environment and lacks O_2/NO-linked allosteric function. J Biol Chem. 277, 27818-27828.

[16] Mesquita, R. Pires, I. Saldanha, C. Martins-Silva, J., 2001. Effects of acetylcholine and spermineNONOate on erythrocyte hemorheologic and oxygen carrying properties. Clin Hemorheol Microcire. 25, 153-163.

[17] Carvalho, FA. Mesquita, R. Martins-Silva, J. Saldanha, C., 2004. Acetylcholine and choline effects on erythrocyte nitrite and nitrate levels. J Appl Toxicol. 24, 419-427.

[18] Carvalho, FA. Almeida, JP. Fernandes, IO. Freitas-Santos, T. Saldanha, C., 2008. Non-neuronal cholinergic system and signal transduction pathways mediated by band 3 in red blood cells. Clin Hemorheol Microcire. 40, 207-227.

[19] Carvalho, FA. de Almeida, JP. Freitas-Santos, T. Saldanha, C., 2009. Modulation of erythrocyte acetylcholinesterase activity and its association with G protein-band 3 interactions. J Membr Biol. 228, 89-97.

[20] Bordin, L. Brunati, AM. Donella-Deana, A. Baggio, B. Toninello, A. Clari, G., 2002. Band 3 is an anchor protein and a target for SHP-2 tyrosine phosphatase in human erythrocytes. Blood, 100, 276-282.
[21] Omodeo-Salè, F. Cortelezzi, L. Riva, E. Vanzulli, E. Taramelli, D., 2007. Modulation of glyceraldehyde 3 phosphate dehydrogenase activity and tyr-phosphorylation of Band 3 in human erythrocytes treated with ferriprotoporphyrin IX. Biochem Pharmacol 74, 1383-1389.
[22] Manno, S. Takakuwa, Y. Mohandas, N., 2005. Modulation of erythrocyte membrane mechanical function by protein 4.1 phosphorylation. J Biol Chem. 280, 7581-7587.
[23] Low, PS. Willardson, BM. Mohandas, N. Rossi, M. Shohet, S., 1991. Contribution of the band 3-ankyrin interaction to erythrocyte membrane mechanical stability. Blood. 77, 1581-1586.
[24] Mohandas, N. Clark, MR. Jacobs, MS. Shohet, SB., 1979. Quantitative analysis of factors regulating erythrocyte deformability. Blood 54(Suppl. 1), 30a.
[25] Groner, W. Mohandas, N. Bessis, M., 1980. New optical technique for measuring erythrocyte deformability with the ektacytometer. Clin Chem. 26, 1435-1442.
[26] Mesquita, R. Piçarra, B. Saldanha, C. Martins e Silva, J., 2002. Nitric oxide effects on human erythrocytes structural and functional properties - An in vitro study. Clin Hemorheol Microcirc. 27,137-147.
[27] Saldanha, C. Silva, AS. Gonçalves, S. Martins-Silva, J., 2007. Modulation of erythrocyte hemorheological properties by band 3 phosphorylation and dephosphorylation. Clin Hemorheol Microcirc. 36,183-194.
[28] de Oliveira, S. Silva-Herdade, AS. Saldanha, C., 2008. Modulation of erythrocyte deformability by PKC activity. Clin Hemorheol Microcirc. 39, 363-373.
[29] Ling, E. Danilov, YN. Cohen, CM., 1988. Modulation of red cell band 4.1 function by cAMP-dependent kinase and protein kinase C phosphorylation. J Biol Chem. 263, 2209-2216.
[30] Manno, S. Takakuwa, Y. Mohandas, N., 2005. Modulation of erythrocyte membrane mechanical function by protein 4.1 phosphorylation. J Biol Chem. 280, 7581-7587.
[31] An, XL. Takakuwa, Y. Nunomura, W. Manno, S. Mohandas, N., 1996. Modulation of band 3-ankyrin interaction by protein 4.1. Functional implications in regulation of erythrocyte membrane mechanical properties. J Biol Chem. 271, 33187-33191.
[32] Danilov, YN. Fennell, R. Ling, E. Cohen, CM., 1990. Selective modulation of band 4.1 binding to erythrocyte membranes by protein kinase C. J Biol Chem. 265, 2556-2562.
[33] Yuthavong, Y. Limpaiboon, T., 1987. The relationship of phosphorylation of membrane proteins with the osmotic fragility and filterability of Plasmodium berghei-infected mouse erythrocytes. Biochim Biophys Acta. 929, 278-287.
[34] Almeida, JP. Carvalho, FA. Martins e Silva, J. Saldanha, C., 2008. The modulation of cyclic nucleotide levels and PKC activity by acetylcholinesterase effectors in human erythrocytes. Actas Bioq. 9, 111-114.